Vanderbilt University

2016-2017 NASA Student Launch

Critical Design Review

January 13, 2017

Contents

List of Figures

List of Tables

1 Summary

1.1 Team Summary

1.1.1 Project Title and School Name

Post-Boost Roll Control Using Cold Gas Thrusters

Vanderbilt University, Nashville, TN

Mailing Address:

Amrutur Anilkumar
Professor of the Practice of Aerospace and Mechanical Engineering
Director: Vanderbilt Aerospace Design Laboratory
Department of Mechanical Engineering
VU Station B # 351592
2301 Vanderbilt Place
Nashville, TN 37235-1592

1.1.2 Team Members

a. Team Advisor
Dr. Amrutur Anilkumar
Professor of the Practice of Aerospace and Mechanical Engineering
Department of Mechanical Engineering
Amrutur.V.Anilkumar@Vanderbilt.edu

b. Faculty Advisor for Control Systems
Dr. William Emfinger
Adjunct Assistant Professor of Mechanical Engineering
Department of Mechanical Engineering

c. Rocketry Mentor
Robin Midgett
Safety Officer and Rocketry Mentor
Senior Electronics Technician
NAR Level II Certified
Department of Mechanical Engineering
Robin.Midgett@Vanderbilt.edu

d. Graduate Student Mentors

(i) Dynamics Mentor
Brian
Postdoctoral Associate
Department of Mechanical Engineering
Brian.E.Lawson@Vanderbilt.edu

(ii) Instrumentation and Controls Mentor
Dexter
Graduate Student
Department of Mechanical Engineering
Dexter.A.Watkins@Vanderbilt.edu

(iii) Structures and Systems Integration Mentor
Ben
Graduate Student
Department of Mechanical Engineering
Benjamin.W.Gasser@Vanderbilt.edu

(iv) Fluids and Payload Mentor
Chris
Graduate Student
Department of Mechanical Engineering
Christopher.T.Lyne@Vanderbilt.edu

e. Senior Design Team

(i) Derek
Student Launch President, Fabrication Lead
Senior, Mechanical Engineering
Derek.J.Phillips@Vanderbilt.edu

(ii) Dustin
Student Launch Vice President, Payload Lead
Senior, Mechanical Engineering
Dustin.C.Howser@Vanderbilt.edu

(iii) Jimmy
Student Launch Treasurer, Payload Specialist and Systems Integrator
Senior, Mechanical Engineering
Jimmy.Pan@Vanderbilt.edu

(iv) Paul
Design Engineer, Student Safety Officer
Senior, Chemical Engineering and Physics
Paul.J.Register@Vanderbilt.edu

(v) Arthur
CFD Engineer
Senior, Mechanical Engineering
Arthur.T.Binstein@Vanderbilt.edu

(vi) Michael
Design Engineer, Controls Lead
Senior, Mechanical Engineering
Michael.G.Gilliland@Vanderbilt.edu

(vii) Brian
Design Engineer, CAD Lead
Senior, Mechanical Engineering
Brian.J.Ramsey@Vanderbilt.edu

(viii) Nina
Design Engineer
Senior, Mechanical Engineering
Nina.A.Campano@Vanderbilt.edu

(ix) Bradley
DAQ, Electrical Engineer
Senior, Electrical Engineering
Bradley.N.Bark@Vanderbilt.edu

(x) Grady
Design Engineer, Testing Lead
Senior, Mechanical Engineering
Grady.T.Lynch@Vanderbilt.edu

(xi) Paul
Design Engineer
Senior, Mechanical Engineering
Paul.R.Moore@Vanderbilt.edu

(xii) Ross
Design Engineer
Senior, Mechanical Engineering
Ross.M.Weber@Vanderbilt.edu

1.1.3 NAR Association

Music City Missile Club, NAR #589

Officers:
Chris Dondanville, President
Brian Godfrey, Vice President
Robin Midgett, Treasurer, treasurer@mc2rocketry.com
Chris Gill, NAR Advisor
Fred Kepner, Secretary

1.1.4 Vanderbilt Aerospace Design Laboratory

1.1.4.1 Preamble

The Vanderbilt Aerospace Design Laboratory www.vanderbilt.edu/usli was started as the Vanderbilt Aerospace Club in 2007 to meet the emerging needs of Vanderbilt engineering students aspiring to pursue careers and advanced studies in aerospace engineering. Its membership consists of engineering seniors who utilize this project to fulfill their senior design project requirements, engineering graduate students whose research is allied to aerospace engineering, and engineering underclassmen with a demonstrated interest in aerospace engineering. Its agenda is to design and analyze unique rocket-flyable payload systems that highlight major challenges in space exploration and energy conversion. It also has a robust outreach program that works to build STEM enthusiasm in aerospace engineering among primary and secondary school students in Tennessee. The Vanderbilt Aerospace Design Laboratory (VADL) traditionally competes in the NASA Student Launch Competition, and project results are presented at AIAA Conferences and in select AIAA Journals. VADL also hosts the AIAA student chapter at Vanderbilt University.

1.1.4.2 Vanderbilt AIAA Student Chapter

The Vanderbilt AIAA student chapter, sponsored by the Vanderbilt Aerospace Design Laboratory, is a volunteer student organization that promotes aerospace engineering activities at Vanderbilt. It also conducts aerospace educational outreach at Middle Tennessee elementary, middle, and high schools. The aerospace activities apply directly to the profession of Aerospace Engineering (AE) and its practice. Implementation of the outreach program is most relevant to undergraduate upperclassmen and graduate students studying engineering with an aptitude for AE and to undergraduate upperclassmen in the School of Arts & Sciences or the School of Education who may be interested in school science teaching. AIAA members actively participate in the NASA Student Launch Competition through the School of Engineering's capstone senior design project.

1.1.4.3 Constitutional Articles Vanderbilt AIAA

a. The AIAA must have a mechanical engineering professor who serves as the faculty advisor. In addition, the club must also have a financial advisor pursuant to Vanderbilt policy.

b. AIAA members must actively seek to promote aerospace and STEM education and outreach in the Nashville area.

c. The largest AIAA membership that can compete and be active in the NASA SL competition is 15 members. Preference for Student Launch Competition participation is given to Vanderbilt University School of Engineering (VUSE) seniors and graduate students with specific skill sets.

d. Students who are selected to compete in the NASA SL competition must demonstrate qualities that will contribute to the club's mission and success at the competition. Such qualities may include prior rocketry experience, interest in aerospace engineering or science teaching as a career, a good academic standing, and a very strong work ethic in a field that is of use to the team (particularly educational outreach or engineering).

e. The NASA SL Competition also serves as the senior design project for the VUSE Curriculum.

f. Any amendments to this Constitution can be made by a vote of the members and approved by the faculty advisor.

1.2 Launch Vehicle Summary

1.2.1 Rocket Specifications

Vanderbilt's full scale rocket will have a body diameter of 5.52", an overall length of 94.75", and an overall weight of 30.3 lbs (24.6 lbs w/o motor). The selected motor is a Loki L1400, which is an off-the-shelf re-loadable 54 mm motor. This specific motor has been chosen for its short burn time of 2.0sec allowing for higher initial vehicle velocity as the rocket departs the launch rail causing straighter flight while remaining subsonic throughout ascent. The predicted and targeted altitude of the rocket is 5280 ft AGL. The recovery system for this rocket is a dual deployment system comprised of a 24" drogue parachute deployed at apogee, and an 8 main parachute deployed at 600 ft AGL for a safe recovery of the rocket and payload. The recovery system is controlled by a redundant pair of barometric pressure based altimeters.

1.2.2 Recovery System Summary

Over the past years, Vanderbilt's NASA Student Launch Teams have focused their attention on contemporary aerospace issues with universal applications. For the 2016-2017 design year, VADL chose to direct its efforts on developing solutions for spacecraft attitude control. The need for fast-actuating, precise thrusters with robust control systems arises in countless applications ranging from satellite high-gain antenna aiming to spacecraft guidance. VADL will have the opportunity to use the rocket as a test bed for data gathering and as an extension to other applications. Additionally, rocket attitude control provides an intense challenge, as all sensing and actuating must be completed in the short time scale of 10 seconds of post-MECO, pre-apogee flight.

In terms of finite goals, VADL seeks to control rotation about the central axis of a flight vehicle, as described by NASA USLI. To accomplish this in a payload, an actuation system, a sensing suite, and a well-defined control algorithm are all necessary. After conducting the experiment and reaching apogee, the team will deploy its dual parachute system featuring a 24" drogue and an 8' main. The drogue will deploy immediately following apogee with the main being deployed at 600 ft. Parachutes are selected with a criteria to reduce landing speed and drift.

1.2.3 Milestone Review Flysheet

The Milestone Review Flysheet is included in the following pages.

Milestone Review Flysheet

Institution	Vanderbilt University

Milestone	Critical Design Review

Vehicle Properties	
Total Length (in)	94.75
Diameter (in)	5.5
Gross Lift Off Weight (lb)	30.3
Airframe Material	Carbon Fiber reinforced Blue Tube
Fin Material	Carbon Fiber
Drag	0.3

Motor Properties	
Motor Manufacturer	Loki
Motor Designation	L1400
Max/Average Thrust (lb)	428.6/319.5
Total Impulse (lbf-s)	2842.88
Mass Before (lb)/After Burn(lb)	5.59/3.08
Liftoff Thrust (lb)	428.6

Stability Analysis	
Center of Pressure (in from nose)	62.3
Center of Gravity (in from nose)	50.4
Static Stability Margin	2.16
Static Stability Margin (off launch rail)	2.29
Thrust-to-Weight Ratio	10.5
Rail Size and Length (in)	144
Rail Exit Velocity (ft/s)	90.4

Ascent Analysis		
Maximum Veloxity (ft/s)	626	
Maximum Mach Number	0.62	
Maximum Acceleration (ft/s^2)	444	
Target Apogee (From Simulations)(Ft)	5280	
Stable Velocity (ft/s)	45	
Distance to Stable Velocity (ft)	3	

Recovery System Properties				
Dogue Parachute				
Manufacturer/Model	Fruity Chutes			
Size	24"			
Altitude at Deployment (ft)	apogee			
Velocity at Deployment (ft/s)	30			
Terminal Velocity (ft/s)	70.4			
Recovery Harness Material	Kevlar			
Harness Size/Thickness (in)	0.5 (6000 lb)			
Recovery Harness Length (ft)	25(11/16 W; 3000lb)			
Harness/Airframe Interfaces	U-bolt and Quicklink			
Kinetic Energy of Each Section (Ft-lbs)	Section 1	Section 2	Section 3	Section 4
	901.3	906		

Recovery System Properties				
Main Parachute				
Manufacturer/Model	Fruity Chutes			
Size	96"			
Altitude at Deployment (ft)	600			
Velocity at Deployment (ft/s)	70.4			
Terminal Velocity (ft/s)	14.2			
Recovery Harness Material	Kevlar			
Harness Size/Thickness (in)	0.5 (6000 lb)			
Recovery Harness Length (ft)	36			
Harness/Airframe Interfaces	U-Bolt and Quick Link			
Kinetic Energy of Each Section (Ft-lbs)	Section 1	Section 2	Section 3	Section 4
	36.4	22	36.7	

Recovery Electonics	
Altimeter(s)/Timer(s) (Make/Model)	StratologgerCF
Redundancy Plan	Two altimeters will be used for both main and drogue deployments
Pad Stay Time (Launch Configuration)	>>2 hrs

Recovery Electonics	
Rocket Locators (Make/Model)	16mW Big Red Bee
Transmitting Frequencies	433.91 Mhz
Black Powder Mass Drogue Chute (grams)	1
Black Powder Mass Main Chute (grams)	3.52

Milestone Review Flysheet

Institution	Vanderbilt University

Milestone	Critical Design Review

Autonomous Ground Support Equipment (MAV Teams Only)	
Capture Mechanism	Overview
Container Mechanism	Overview
Launch Rail Mechanism	Overview
	Include Description of rail locking mechanism
Igniter Installation Mechanism	Overview

Payload	
Payload 1	Overview
	The payload for this year's rocket will be the integration of a dual thruster couple system in order to generate a torque on the rocket during ascent. One couple will be used to rotate the rocket two full rotations while the second couple will be used to reverse the rotation and return the rocket to its original position.
Payload 2	Overview

Test Plans, Status, and Results	
Ejection Charge Tests	Ground deployment tests were conducted prior to the subscale launch. In these tests, black powder charges are manually ignited to test shear pin breakage and parachute deployment. There were two charges placed in the subscale rocket: one which functioned as the main charge and the second which functioned as the backup charge. Each charge was rated with a minimal safety factor of 2. Each charge successfully separated the rocket. The altimeters were tested in a shocktube to confirm their proper functionality.
Sub-scale Test Flights	A subscale test flight took place on December 14, 2016. The launch was a complete success, and the rocket was successfully recovered. The subscale launch tested a single thruster couple via two methods: continuous and pulsed. Data shows that the thruster couple was able to successfully apply a torque to rotate the rocket during ascent overcoming the forces of friction and air resistance.
Full-scale Test Flights	One full scale flight will be completed prior to competition. This flight is expected to take place in February 2017. We will have integrated our dual thruster couple into this rocket in preparation for our payload experiment.

Milestone Review Flysheet

Institution	Vanderbilt University

Milestone	Critical Design Review

Additional Comments

1.3 Payload Summary

1.3.1 Cold Gas Thruster System

VADL's chosen payload this year for the NASA USLI consists of roll control during post-MECO and pre-apogee flight. After analyzing various possible design solutions, VADL has chosen to perform this payload experiment through the use of tangential cold gas thrusters. Two pairs of thrusters will be used, mounted to the rocket orthogonal to the main axis and as close to the center of gravity as possible. Each pair consists of two thrusters that are 180 degrees apart and facing the same angular direction with one pair aligned for counter-clockwise rotation and the other pair aligned for clockwise rotation. The system will actuate each pair independently, first inducing two full rotations about the rocket main axis then decelerating and reversing this rotation until the rocket is oriented back to its original angular position.

1.3.2 Control System

On a high level, the payload objective is simple: create a system that can control the roll orientation of the launch vehicle. VADL's design for this system consists of four main components - the plant (launch vehicle), the actuator (cold gas thrusters), the sensor (IMU) and the controller (microprocessor). A microprocessor outfitted with custom control logic recieves data from an IMU, and actuates the cold gas thrusters according to this data by routing current through a custom circuit board. As VADL seeks to couple IMU (Intertial Measurement Unit) data with the aforementioned cold gas thrusters, transfer functions must be characterized, control theories tested, and the best performing design ultimately chosen. This process is aided by the development of a ground-based test facility that allows for hardware-in-the-loop testing of several control schemes along with iterative testing of varied parameters within each scheme. Physically, this test facility consists of a vertical test stand isolating the full body of a launch vehicle in the primary rotation axis, with primary input from the internal thrusters as well as a disturbance input from the external motor for simulation of structurally induced rotation, side winds, jet-fin interaction, or other system disturbances. All of these components will be tied together through the ROSMOD distributed system software package developed at the Vanderbilt Institute for Software Integrated Systems (ISIS), which allows for online experiment development and data visualization.

2 Changes Made Since PDR

2.1 Changes to Vehicle Criteria

(i) Rocket length changes to 94.75" from 88.5", stemming from a motor selection change that increased tail section length by 6 in

(ii) Estimated mass increased to 30.3 lbs from 28.7 lbs, stemming from more realistic estimate after the completed subscale launch vehicle was weighed

(iii) Loki L1400 (2850 Ns impulse) motor instead of Cesaroni L1030 (2787 Ns) motor, stemming from a sudden unavailability from Cesaroni

(iv) Additional general safety information, environmental precautions, launch operation procedures, and checklists have been identified and added to increase the security of the team

2.2 Changes to Payload Criteria

2.2.1 Changes to Payload Thruster System

(i) Increase of desired nozzle thrust due to dampening effects of fins under high axial velocities through increase tank pressure in order to successfully complete flight experiment

(ii) Increase of desired nozzle thrust through using pressurized nitrogen in addition to air as propellant in order to successfully complete flight experiment

(iii) Design more efficient and practical means of diverting flow between forward and aft thrusters in order to achieve a balance between the most robust, simple, and compact design

2.2.2 Changes to Payload Electronics

(i) Payload electronics assembly should not require disassembly except for unplanned maintenance for damage. This will allow for more efficient testing and assembly.

(ii) The payload electronics assembly will be capable of charging while inside its coupler tube enclosure.

(iii) The payload electronics assembly will be capable of communication while inside its coupler tube enclosure.

(iv) Payload arming switches will now be integrated into auxiliary circuit board to save space and assebly time.

(v) Auxiliary circuit board will now be manufactured using a third party fabrication house to avoid reliablity problems experienced in earlier prototypes.

2.3 Changes to Project Plan

2.3.1 Changes to Team-Derived Requirements

Team-derived requirements can be found in Section 7.2.

2.3.2 Changes to Budget

The budget was reassessed after the subscale launch and slightly reallocated. The changes included decreasing the FRAME budget from $3,000 to $2,500 and the outreach budget from $1,000. These funds were reallocated to rocket fabrication, which increased from $3,500 to $4,500. The main reason for this is the ”hotbox” used funds from rocket fabrication, and it ended up costing approximately $1,000. VADL is on track to be under budget; the current spending is further explained in 7.3.1.

2.3.3 Changes to Timeline

(i) Full scale launch window has been planned for February 20th-24th (see Section 7.4).

(ii) We have planned seven outreach events this semester at elementary, middle, and high schools as well as at a local science museum.

(iii) Various items on the full scale fabrication on the timeline have been adjusted to conform with our test flight schedule.

2.3.4 Development of Testing Plans

We have added a number of testing operations to our project plan, including:

(i) Further thruster testing plans in order to obtain more thrust (see Section 7.1.1

(ii) Further controls and payload testing utilizing the FRAME (for a software perspective see Section 7.1.3; for a systems perspective see Section 7.1.4).

(iii) Hydraulic crush testing of carbon fiber reinforced blue tube with high stress concentrations representing venting holes (see Section 3.1.2) and planned tearout testing of body tubes.

3 Vehicle Criteria

3.1 Design and Verification of Launch Vehicle

3.1.1 Mission Statement & Mission Success Criteria

3.1.1.1 Mission Statement

The VADL 2016-2017 team mission is to successfully build, test, and fly a rocket carrying an attitude control payload which will enable valuable in-flight experimentation and data collection. The objective of this attitude control payload is to induce roll about the rocket's vertical axis post motor-burnout, rotating the rocket in one direction and then returning it back to the original position with a counter roll. After the experiment is completed, the launch vehicle will reach apogee (5280 ft) and land safely, ready to be launched again in the same day.

3.1.1.2 Mission Success Criteria

First and foremost, for the mission to be a success, it must be conducted in accordance with all NASA imposed requirements and regulations, from planning to construction to final execution. Beyond this however, the Vanderbilt Aerospace Design Lab has identified a list of additional requirements and mission success criteria. These mission success criteria are not exhaustive in nature, and only apply to the vehicle and recovery systems. The payload success criteria is addressed specifically in Section **??**. A fully exhaustive list of all requirements and mission objectives can be found in Section **??**.

Launch Vehicle Mission Success Criteria

1. The launch vehicle must attain an altitude of 5280 ft AGL +/- 150 ft
2. The launch vehicle must attain an altitude of 5280 ft AGL $\pm$ 150 ft
3. When fully assembled on the launch pad, the launch vehicle must be structurally stable once the nosecone and payload airframe are removed, so as to allow for payload manipulation
4. All sections of the post-chute deployed rocket must remain structurally stable when in free fall
5. All sections of the launch vehicle must be able to be assembled within 4 hours, from the time the Federal Aviation Administration flight waiver opens
6. The launch vehicle must be capable of remaining in launch-ready configuration at the pad for a minimum of 1 hour without losing the functionality of any critical on-board component
7. No structural vehicle failures across all launches
8. All parts of the rocket are recoverable and reusable (able to launch again on the same day without modifications or repairs).

Recovery System Mission Success Criteria

1. The recovery system must be designed to be armed at the launch pad.
2. The drogue/main chute must deploy within 2.0 sec after apogee is reached.
3. The landing energy of the heaviest section of the rocket must be less than 75 lbf-ft

3.1.2 Fullscale Launch Vehicle Overview

The Vanderbilt Aerospace Design Lab will present a fullscale launch vehicle that is 94.75" in total length, featuring a body diameter of 5.52". The assembled weight of the vehicle will be approximately 30.3 lbs with motor, or 24.6 lbs without the motor. The fullscale launch vehicle has a center of gravity of 50.4" and a center of pressure at 62.3". The static stability margin at rail exit is calculated to be 2.28. A CAD model of the fullscale launch vehicle can be found in Figure 1 accompanied by a dimensional breakdown of the length by section in Figure 2.

Figure 1: CAD Model of Full Scale Launch Vehicle

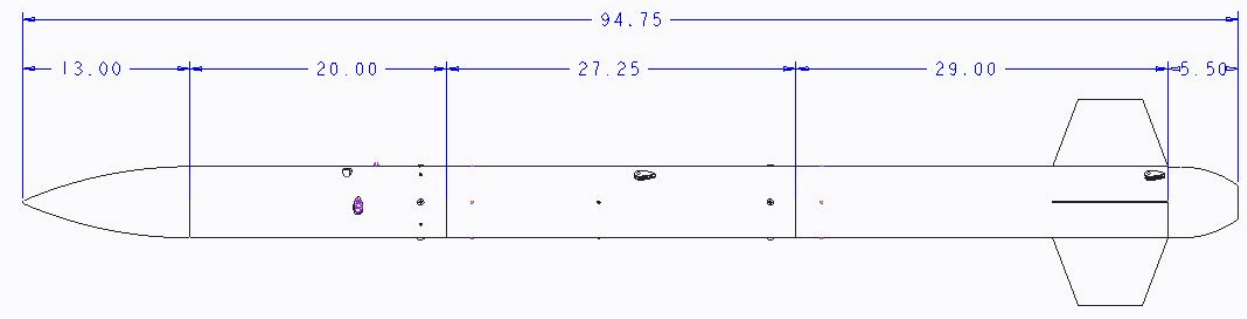

Figure 2: Dimensional Full Scale CAD Drawing (inches)

The launch vehicle will be split into three sections to allow for a dual parachute deployments. Deploying a smaller drogue parachute near apogee followed by a main at 600 ft will greatly reduce drift, and thus has become a NASA SL requirement for collegiate launch rockets (SL Req. 2.1). The three sections of our fullscale launch vehicle are the nose/payload section, the avionics section, and the tail section, shown respectively from left to right in Figure 3.

Figure 3: Fullscale CAD Model Split Into Sections

The vehicle design portion of these three sections will be detailed extensively in Section 3.1.3, below, while details of the components housed inside each respective section can be found elsewhere in the document. The leftmost nosecone/payload section will house all components relating to the thruster payload, which are further detailed in Section 5.1.1. The middle avionics section will house both parachutes and all avionics equipment, which are covered in-depth in Section 3.3.1. The rightmost tail section will house the motor, which is covered in Section 3.4. An analysis of percent weight by section can be found in Figure 4, while a breakdown of both masses and lengths of each section can be found in Figure 5.

Coupler tubes will be used to connect separation points of the launch vehicle, such as the nosecone/payload section to the avionics section and the avionics section to the tail section. These coupler tubes will be Blue Tube 8” in length, with 4” going into each side of the connection. The coupler tubes will have a diameter slightly smaller than the airframe to allow a precise fit. The motor tube will be constructed from Blue Tube with carbon fiber fillets securing the fins.

Broken down by section, the fullscale launch vehicle features a relatively even distribution of weight between the sections. The distribution of mass provides a favorable CP-CG relationship, with CP residing 11.11” behind the CG.

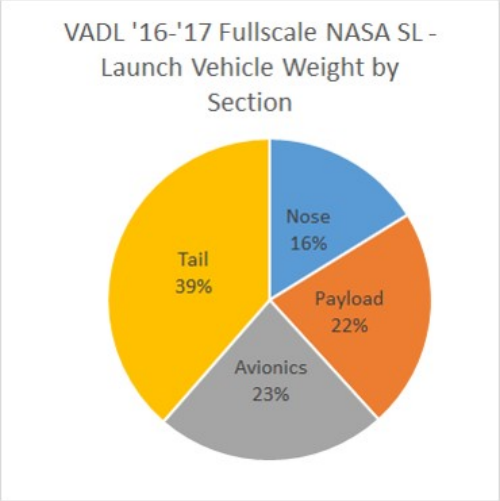

Figure 4: Fullscale Weight and Length Breakdown by Section

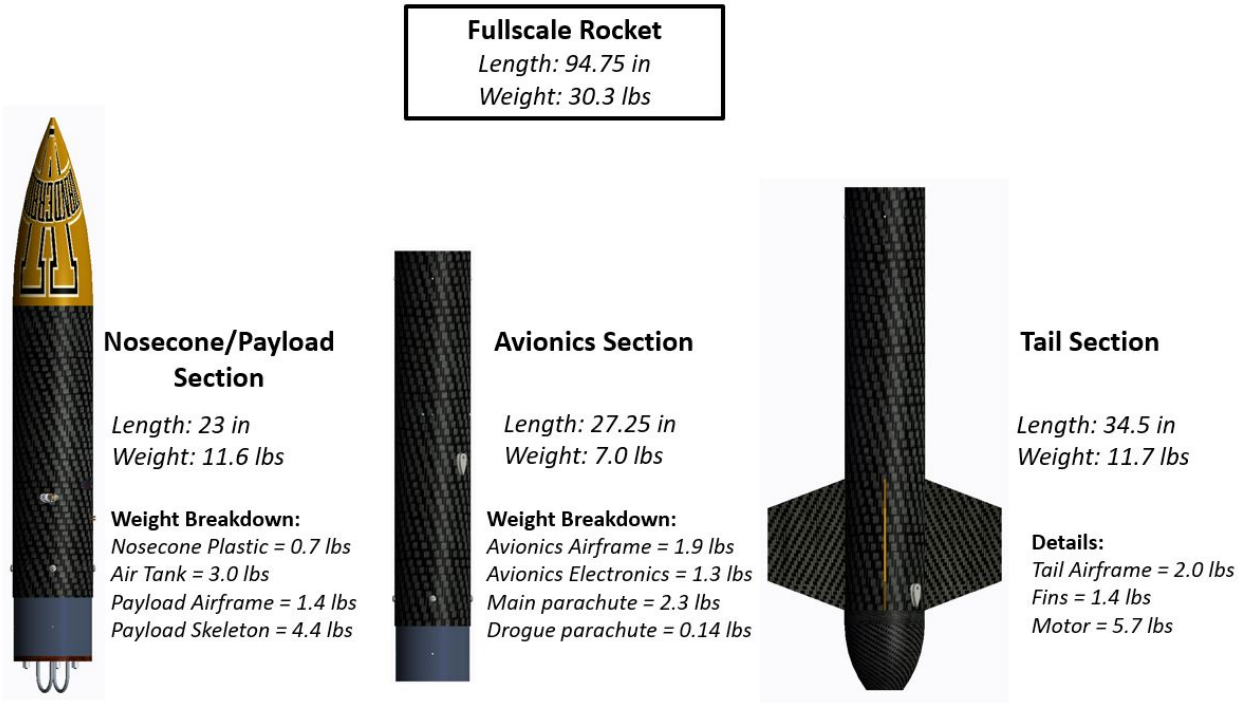

Figure 5: Fullscale Section Mass Breakdown

Material Selection and Corresponding Testing All vehicle airframe structures will be made out of carbon fiber reinforced Blue Tube. This combination of materials creates an ideal composite for model rocketry, as it is lower cost than pure custom carbon fiber while still maintaining a durable, high strength alternative to the phenolic tubing commonly used in rocketry. Using this carbon fiber reinforced Blue Tube for the airframe also moves manufacturing in-house, giving VADL undergraduates valuable experience.

To create the airframes, VADL will first order the appropriate sized Blue Tubes from Always Ready Rocketry. These Blue Tubes are cut to size and sanded to allow for adhesion to the carbon fiber. Next, a sheet of carbon fiber placed on a table and coated generously with epoxy resin. After the fibers are saturated with the epoxy, the carbon fiber is carefully rolled onto the Blue Tube. This epoxy only cures to their optimum properties when they are heated above room temperature, for about 120 minutes. To solve this problem, we built a ”Hotbox” - a large temperature-controlled curing chamber - to place the curing carbon fiber reinforced Blue Tube in while the epoxy sets. A picture of the Hotbox with a sample airframe can be found in Figure 6.

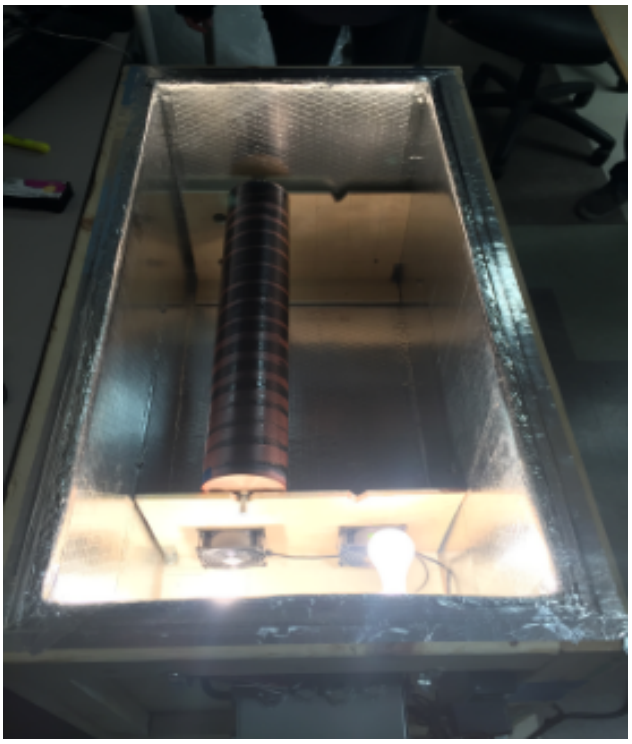

Figure 6: Hotbox Airframe Curing Chamber

To ensure the carbon fiber reinforced Blue Tube is an appropriate material, two compression tests were performed. The first tested the solid carbon fiber reinforced Blue Tube. The failure load of this airframe was 10,880 lbs force, which correlates to a stress of 6468 psi. Its stress-strain diagram is shown in Figure 7.

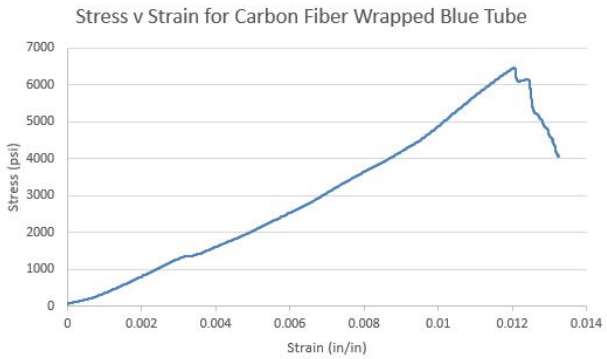

Figure 7: Stress-Strain Diagram for Solid Bodytube

The next crush test took into account airframes with holes in them. Holes will be drilled into the launch vehicle airframe for a variety of reasons, such as exhaust holes to prevent over-pressurization in the payload section, or access holes in the avionics section. An airframe was therefore tested to characterize the strength of the carbon fiber reinforced Blue Tube containing stress concentrations caused by the holes. As expected, the airframe failed along the lines of the holes. This is shown in Figure 8.

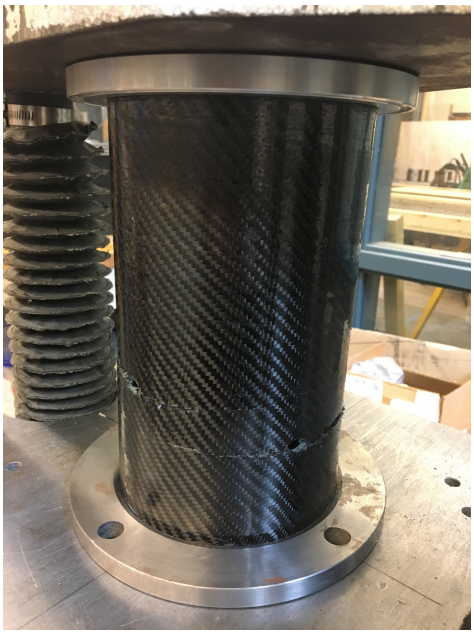

Figure 8: Failure Points for Bodytube with Stress Concentrations

The failure point of this tube is 9,790 lbs force, which correlates to a stress of 5827 psi. The stress-strain diagram is shown in Figure 9.

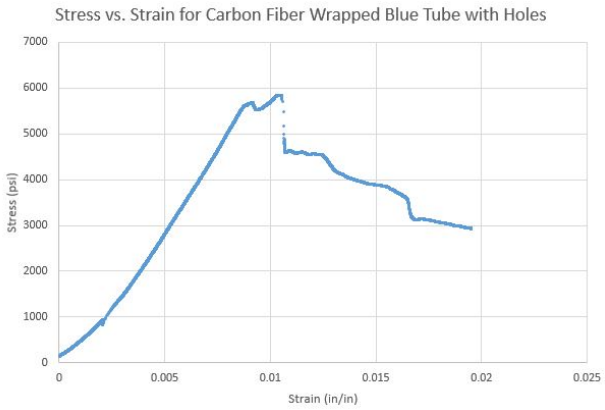

Figure 9: Stress-Strain Diagram for Bodytube with Holes

This test proved that holes in the airframe somewhat decrease the minimum failure load. In order to prove that the carbon fiber wrapped Blue Tube can stand up to inertial effects of rocket acceleration, a worst case scenario was analyzed. The acceleration of the rocket is greatest at takeoff. If the takeoff acceleration was 18g's, healthily above the predicted 15g's, and the isolated tail section instantaneously hit the rest of the rocket body, there would be an inertial force of 334 lbf. This is well below the experimental deformation value of 9,790 lbf. The airframe will withstand all inertial forces during takeoff and the duration of the launch, thereby making the carbon fiber wrapped Blue Tube an appropriate material choice for the airframe.

3.1.3 System Breakdown of Chosen Final Design and Integrity

As mentioned previously in Section 3.1.1.1, the primary objective of VADL's launch vehicle is to allow an environment for this year's roll control payload to tested post-MECO, while remaining recoverable and reusable. As such, each system in the fullscale launch vehicle was designed with the success of this goal in mind. A conceptual overview of the mission statement can be found in Figure 10. It should be noted the purpose of the visual is to convey the order of events on the fullscale launch, and not to display the physical orientation of the rocket.

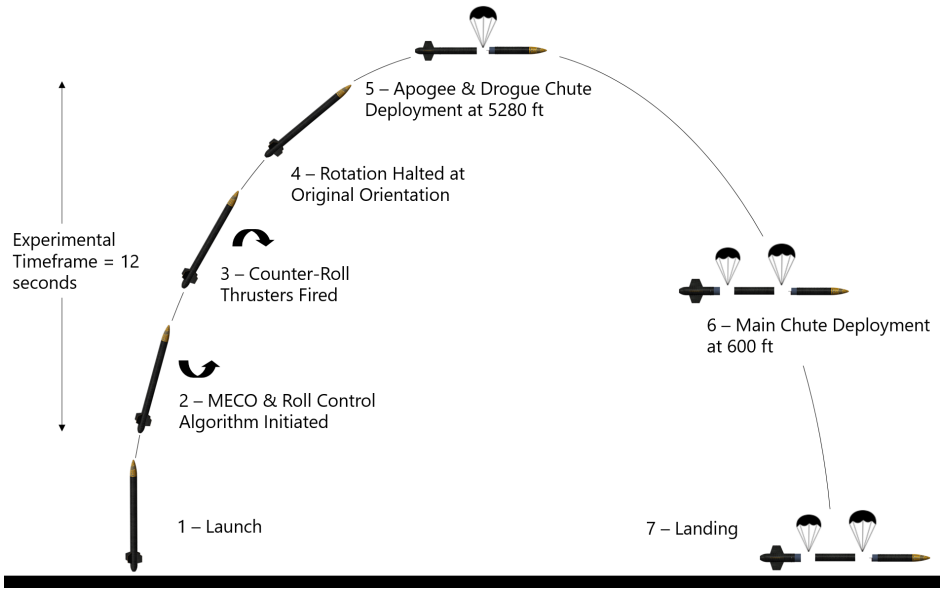

Figure 10: Concept Of Flight Operations

Each launch vehicle system will be described in detail along with its specific (1) requirements as they pertain to the launch vehicle, (2) chosen alternative design from PDR, and (3) integrity in relation to the launch vehicle.The systems are as follows:

1. Nosecone
2. Payload Section
3. Avionics Section
4. Tail Section

3.1.3.1 Nosecone

Requirements The purpose of the nosecone is to add an aerodynamic shape to the forward end of the rocket, reducing drag. It is also beneficial for the nosecone to have sufficient volume so as to allow rocket components to be housed inside. This brings the CG of the rocket forward, making the rocket more stable, and also eliminates unused space. Lastly, the nosecone must be structurally stable and able to provide both itself and the components inside of it the ability to survive many launches.

Chosen Design The chosen nose cone for the VADL '16'17 SL vehicle is the PNC - 5.38" - Short poly-propylene plastic nose cone from Apogee Rockets. The nose cone weights 12.6 oz, has a nose length of 13", and a shoulder length of 4". As noted previously, a parabolic, dense polystyrene design was chosen over alternatives in order to maximize internal volume relative to nose cone length for the fitting of an internal pressure vessel sabot and to meet safety and price constraints. This sabot will be rigidly constrained by expanding foam applied to the interior of the nose cone.

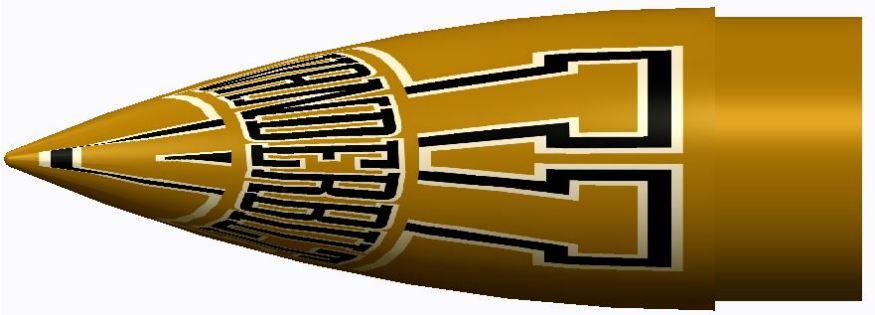

Figure 11: CAD Model of Nosecone

Since the fullscale launch vehicle will be flying well below the speed of sound (Mach 0.6), the nose cone pressure drag is essentially zero and the majority of the drag comes from the friction drag. The friction drag is dependent upon the whetted area, surface roughness, and discontinuities in shape. For this reason, a short, blunt nose cone like the one selected is preferred. In addition, in order to minimize drag, VADL will be careful to maintain a smooth surface and minimize the diameter transition from nosecone to payload airframe, as the carbon fiber adds a non-negligible amount of thickness to the Blue Tube.

Directly below the nose cone rests the payload section, which holds the cold gas thruster assembly. This thruster assembly necessitates a compressed air tank to offer a supply of gas throughout flight for actuation. In a space-saving measure, it was decided to place the compressed air tank inside the hollow nose cone. Supporting the compressed air tank is a layer of foam at the top end of the nose cone, and bulkheads at the bottom end of the nose cone. The first bulkhead will be made of 1/2" high-strength plywood, laser-cut to the correct dimensions. This wooden bulkhead will rest against the body of the compressed air tank. The next bulkhead will be thinner, .0565" metal piece manufactured to size. These two bulkheads are supported by threaded rods running through the course of the payload

section of the rocket, in an assembly referred to as the ”payload skeleton”. This skeleton adds additional structural stability to the system, as it is comprised of many bulkheads and three threaded rods. A diagram of the nosecone and the components resting inside can be seen in Figure 12, below.

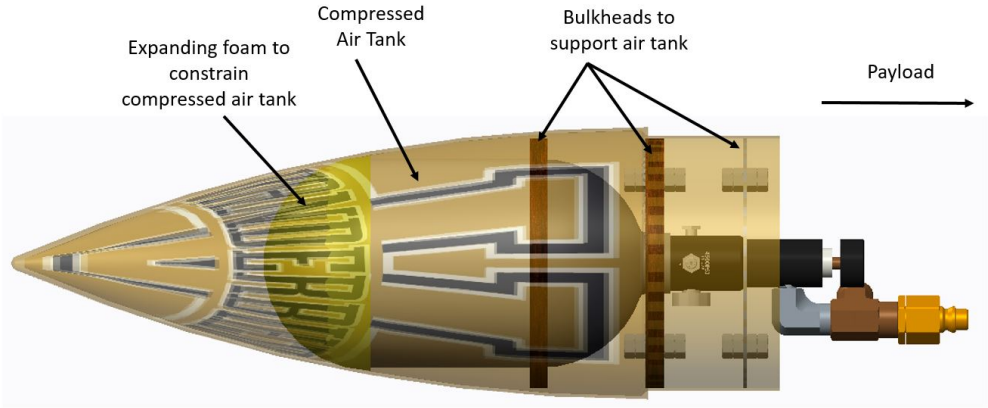

Figure 12: CAD Diagram of Nosecone

A CAD dimensional drawing of the nosecone and the components resting inside of the nosecone can be seen in Figure 13. The individual pieces making up the payload skeleton and their interaction with the launch vehicle design will be further detailed in the **??** section.

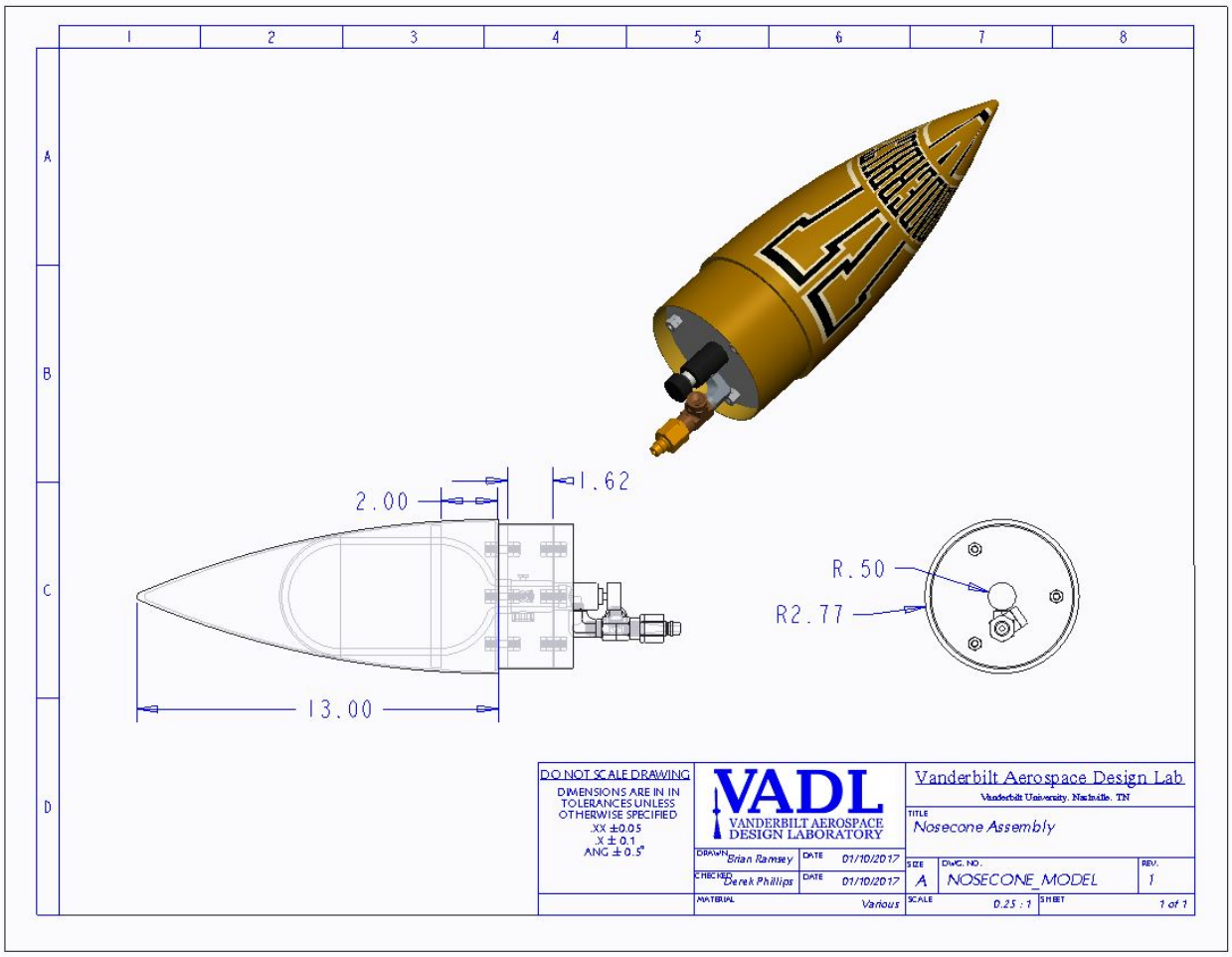

Figure 13: Dimensional Drawing of Nosecone and Components

Integrity The nosecone is technically part of the nosecone/payload section. All integrity tests and considerations will be addressed in the following Section 3.1.3.2.

3.1.3.2 Payload Section

Requirements The purpose of the payload section is to support and give structure to the payload experiment inside. For this specific team's mission, this means providing a way to house the thruster system and to constrain the rotation of the thruster system inside so that it translates rotational acceleration onto the remaining launch vehicle body. Additionally, this means that the payload airframe must give sufficient structural support to allow holes to be cut, allowing air to escape into the atmosphere. Lastly, the payload section must be able to interface effectively with the rest of the launch vehicle, providing high ease-of-assembly and practical integration between components.

Chosen Design The chosen payload system design for the VADL '16'17 SL vehicle will feature a 20" carbon fiber reinforced Blue Tube airframe with a rigid payload skeleton to support the thruster experiment housed inside. As noted in Section 3.1.2, the airframe material was chosen over other alternatives because of the substantial decrease in production costs compared to pure carbon fiber while retaining sufficient strength properties to withstand several dynamic launches and landings.

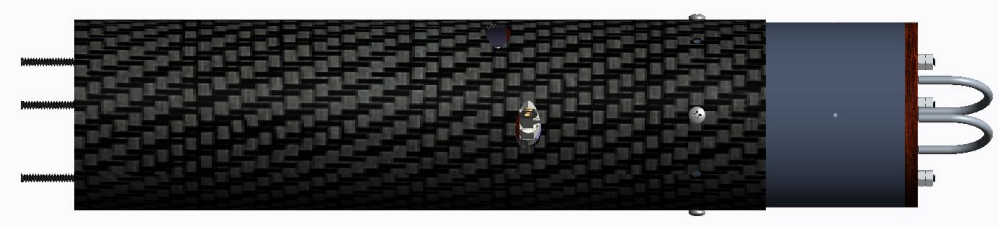

Figure 14: CAD Model of Payload Section

The two thruster couples will sit near the middle of the payload section, each with its own solenoid. The payload electronics will be housed in the coupler tube, at the bottom of the payload section. A CAD model with the inside components visible can be seen in Figure 15.

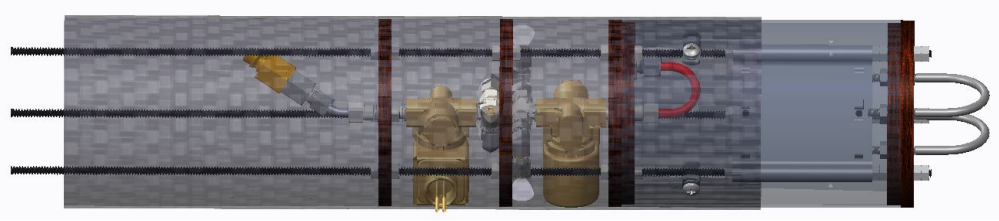

Figure 15: CAD Model of Payload Section with Inside Components

As previously noted, a "payload skeleton" will run through the inside of this section of the rocket to offer additional support and mounting capabilities to the inside experiment. The payload skeleton is comprised of a series of bulkheads and threaded rods that support everything from the compressed air tank, to the cold gas air thrusters, to the payload electronics. The payload airframe will be epoxied to the nosecone and will also bolted to the coupler tube connecting the nosecone/payload section to the avionics section using 4x 1/4" - 20 button head bolts into 1/4" - 20 weld nuts. This payload skeleton will be detailed further in Section **??**, however a conceptual view can be seen below, in Figure 16. It is worth noting that if the fullscale launch vehicle weighs less than expected, ballast can be mounted to the payload skeleton on top of the first bulkhead. This would add more weight aft of the CG, creating a higher static stability margin.

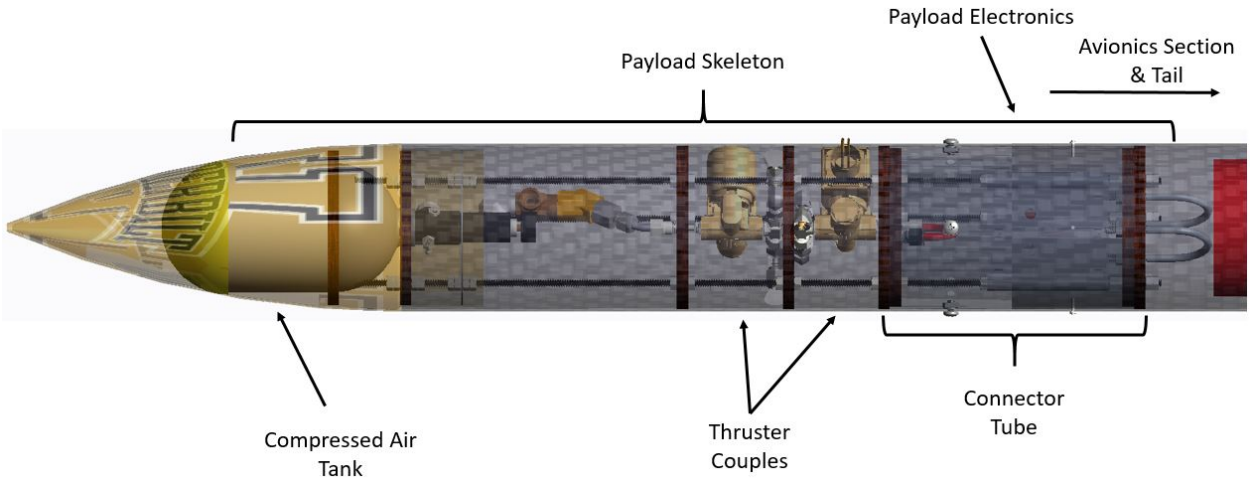

Figure 16: CAD Diagram of Payload Section

One of the reasons this of the payload skeleton design was chosen is that when the entire launch vehicle is assembled, complete removal of the nosecone/payload airframe is possible, leaving the payload skeleton assembly freestanding and easily accessible. This design will allow easy, 360 degree access to the entire payload skeleton on launch day, enabling payload operations such as pressurization of air tank or arming of electronics to be completed. On launch day, the bolts on the connector tube will be removed, the nosecone/payload airframe will slide off, and the team will be able to manipulate the payload skeleton freely. After adjustments, the nosecone/airframe will slide back on, the bolts will be re-screwed, and the launch vehicle will be ready for take-off. This concept can be seen in Figure 17.

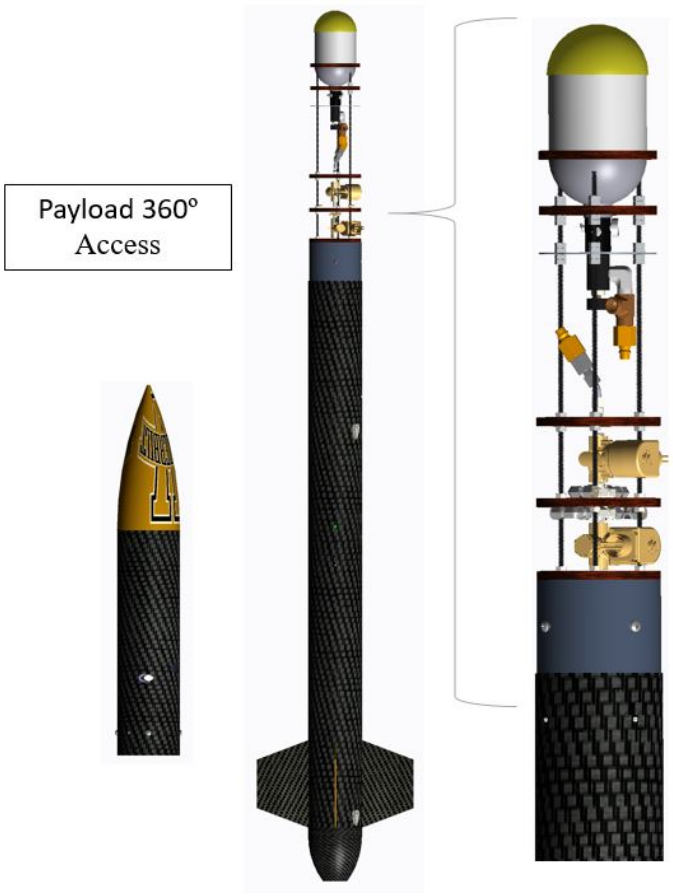

Figure 17: Launch Day Payload Access Diagram

A CAD dimensional drawing of the payload and the components resting inside of the payload can be seen in Figure 18. The individual pieces making up the payload skeleton and their interaction with the launch vehicle design will be further detailed in Section 3.1.3.2.

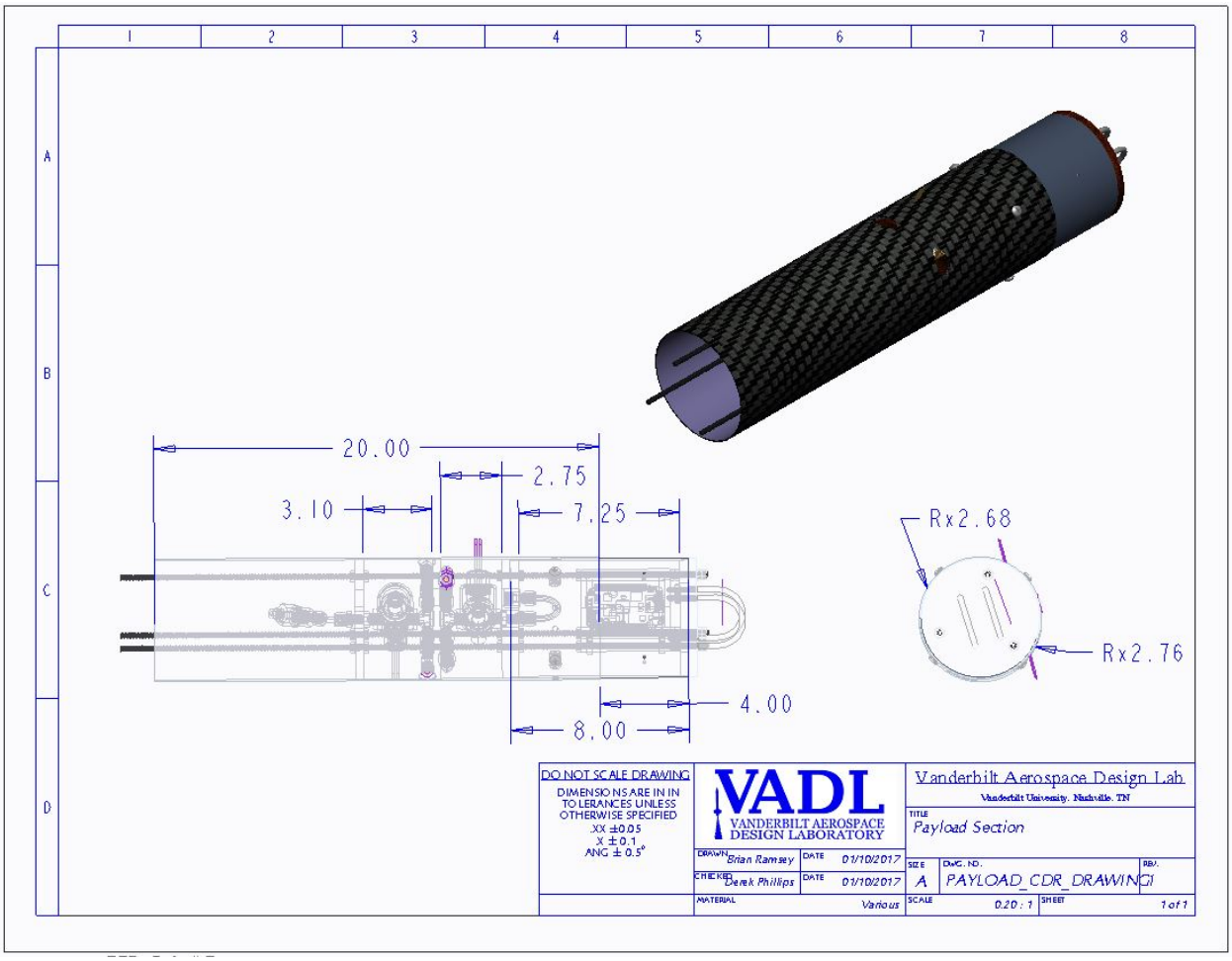

Figure 18: Dimensional Drawing of Nosecone and Components

Integrity The first integrity consideration analyzed is the constraining of the payload thrusters against the rest of the launch vehicle. The 1/4" - 20 weld nuts that affix the payload skeleton to the nosecone/payload airframe are attached using JB-Weld. The bonding area of the weld nuts is 2.53 in$\hat{2}$. JB-Weld's published Tensile Lap Shear strength is 1040 psi, giving a load capacity of 2,600 lbs. This is well below the force experienced by the skeleton during blast charge detonation (570 lb.) and validates the integrity of the weld nuts and use of JB-Weld epoxy. This skeleton blue tube, also functioning as a coupler and held in compression by the payload skeleton, transfers the rotation of the skeleton to the body of the rocket. While this compression has held the skeleton in place during testing, in order to further ensure that the skeleton does not slip inside the rocket body, we plan to use two wood screws that screw through the airframe and into the plywood bulkhead at the top of the coupler tube. Alternatively, if more mass is needed to achieve a 5280 ft altitude, a fourth aluminum bulkhead (similar to that described in 3.1.3.3 could be fabricated and tapped, replacing the wood screws with steel bolts.

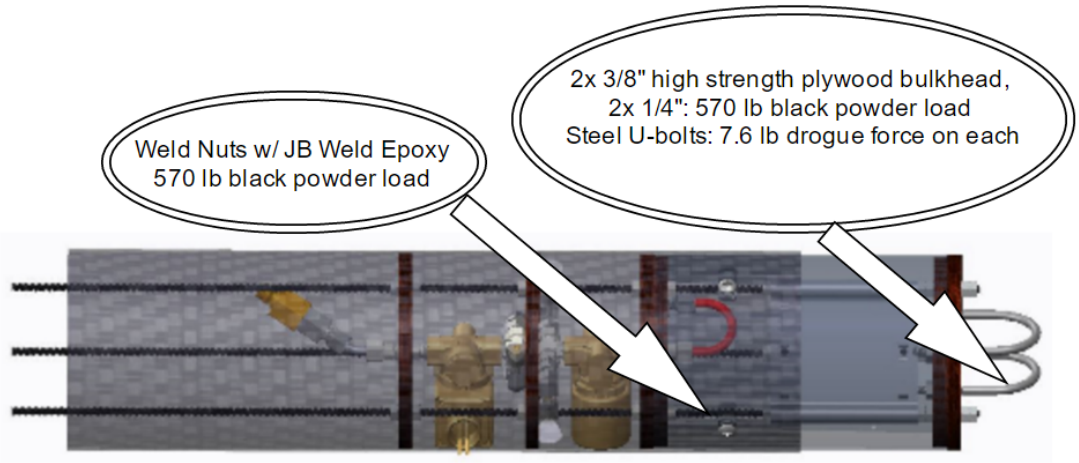

Figure 19: Concentrated Forces on Payload

The next integrity consideration analyzed are the forces the payload section experiences during flight. The payload section experiences two major forces, the force of the black powder explosion and the force of the drogue parachute deployment. These forces and the major components on which they act are illustrated in Figure 19.

In order to experimentally test this two U-bolt, two wooden bulkhead configuration, the configuration was replicated in the Vanderbilt material science load frame. The bulkhead was secured on one side with three steel threaded rods that simulate the actual configuration of the bulkhead within the rocket. The two U-bolts on the other side of the bulkhead was attached by one triangular quick link to replicate the drogue parachute attachment. The set up of the tension test is shown in Figure 20.

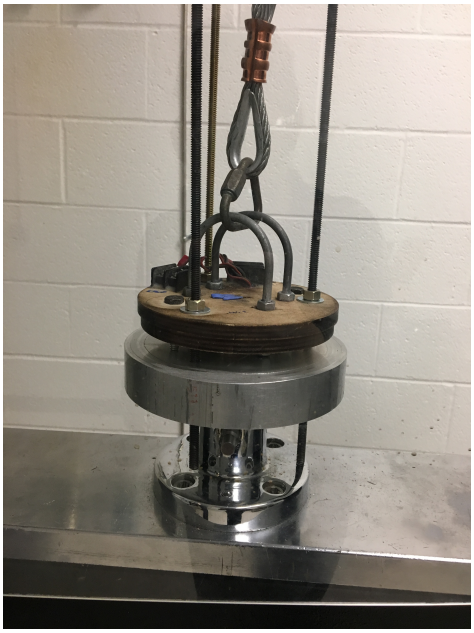

Figure 20: Wooden Bulkhead Test Set-up

A constant tensile force was applied to the bulkhead until it was permanently deformed. The point where the U-bolts began to deform occurred at 1,235.4 lbs, which is much higher than their rated failure load of 850.0 lbs. This

deformation continued until 2,221.0 lbs, which is the official failure point of the configuration as defined by the point that the bulkhead is deformed so much that the rocket will not be able to launch again. The bulkhead at this point is shown in Figure 21.

Figure 21: Wooden Bulkhead Failure Point at 2,221 Pounds

The tensile force was continued to be applied until the bulkhead reached an ultimate failure point where the plywood separated completely. This occurred at 4,353.6 lbs. An image of the bulkhead at this point is shown in Figure 22.

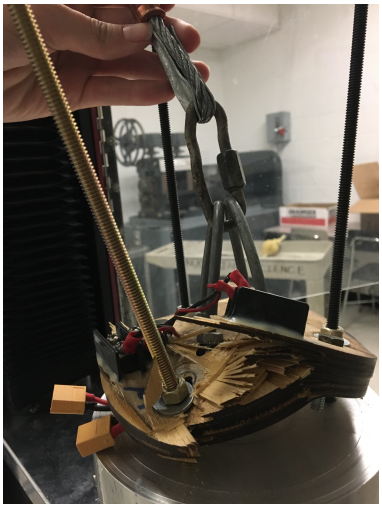

Figure 22: Wooden Bulkhead Ultimate Failure at 4,335 Pounds

This test proved that both the U-bolts and wooden bulkheads could withstand the force of 15.15 lbs of the drogue parachute deployment with a safety factor of over 15. Furthermore, this test proved that the wooden bulkhead could withstand the distributed load of 570 lbs of the black powder explosion. In this test, the load was applied at two

points on the bulkhead. In the case of the black powder explosion, the force on the bulkhead will be evenly distributed. Because the bulkhead can withstand much greater forces when the force is evenly distributed, the bulkhead will be able to withstand the force of the black powder explosion easily.

3.1.3.3 Avionics Section

Requirements The purpose of the avionics section is to support and give structure to the parachutes and avionics electronics inside. The avionics airframe must give sufficient structural support to allow holes to be cut, allowing arming holes to be drilled. Lastly, the avionics section must be able to interface effectively with the rest of the launch vehicle, providing high ease-of-assembly and practical integration between components.

Chosen Design The chosen payload system design for the VADL '16'17 SL vehicle will feature a 27.25" carbon fiber reinforced Blue Tube airframe with an avionics skeleton to support the the avionics electronics housed inside. As noted in Section 3.1.2, the airframe material was chosen over other alternatives because of the substantial decrease in production costs compared to pure carbon fiber while retaining sufficient strength properties to withstand several dynamic launches and landings.

Figure 23: CAD Model of Avionics Section

The avionics airframe houses the drogue parachute (attached via Shock Cords to U-bolts on the bottom payload bulkhead and top avionics bay bulkhead) along with the avionics bay and the main parachute (attached via Shock Cords to U-bolts on the bottom avionics bulkhead and top tail bulkhead). This avionics airframe is connected to the payload coupler tube by 4x 4-40 nylon shear pins, allowing complete separation at apogee between the nosecone/payload section and the rest of the rocket. The avionics airframe is connected to the tail airframe by using 4x 1/4" - 20 button head bolts into 1/4" - 20 weld nuts, allowing the coupler tube to remain with the avionics section while the tail section completely separates at 600ft AGL. The components resting inside of the avionics bay can be seen in Figure 24.

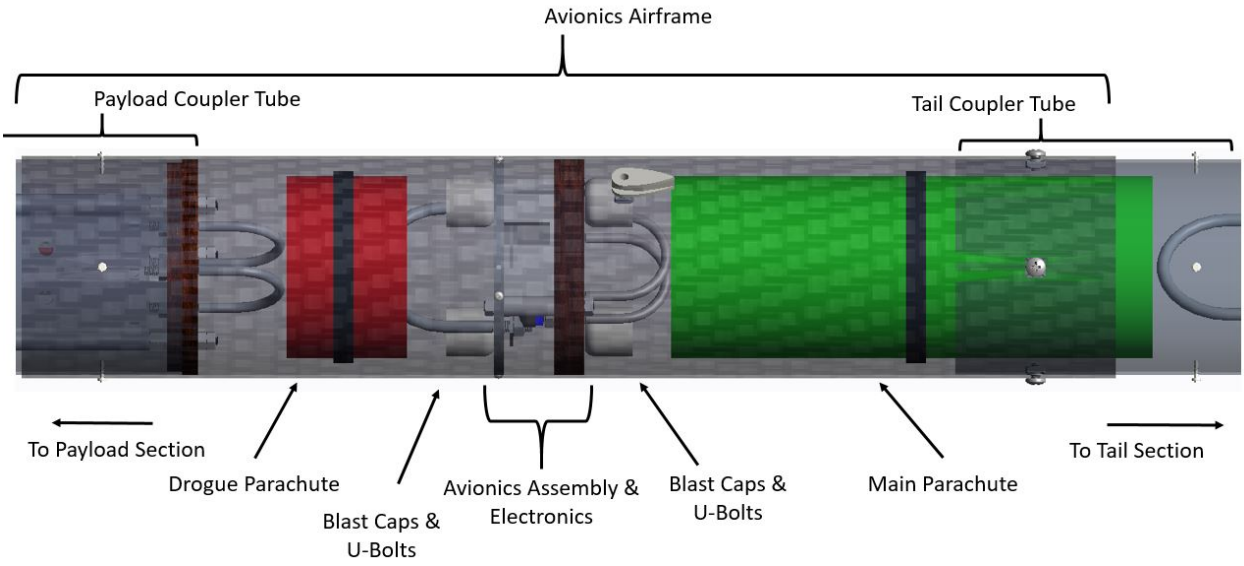

Figure 24: CAD Diagram of Avionics Section

A CAD dimensional drawing of the avionics section and the components resting inside can be seen in Figure 25. Additional details on the avionics and the recovery system housed inside the avionics section further detailed in Section **??**.

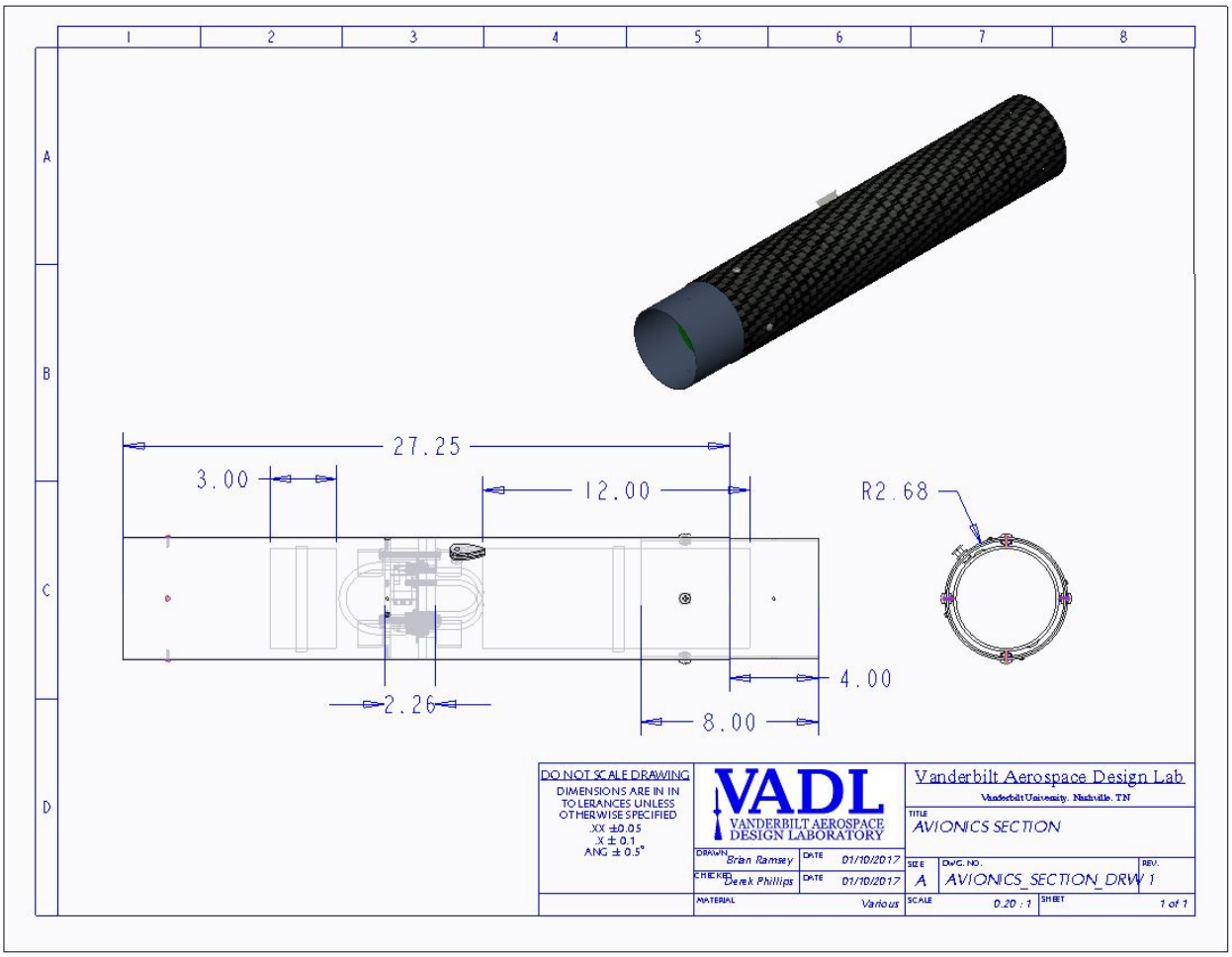

Figure 25: Dimensional Drawing of Avionics Section

Integrity The avionics section experiences three major forces, the force of the black powder explosion and the forces of the drogue and main parachute deployments. These forces and the major components on which they act are illustrated in Figure 26.

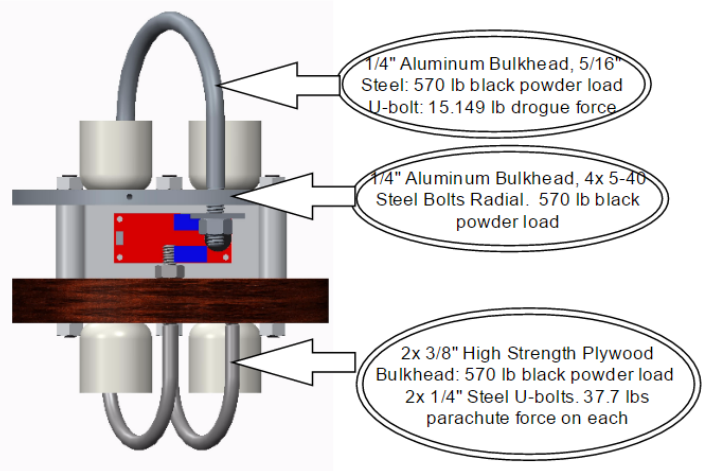

Figure 26: Concentrated Forces on Avionics

ANSYS was used to analyze the total stress and deformation on the avionics aluminum bulkhead as a result of the black powder ignition force, 570.0 lbs. The total equivalent stresses and deformation is shown in Figure **??** and 28.

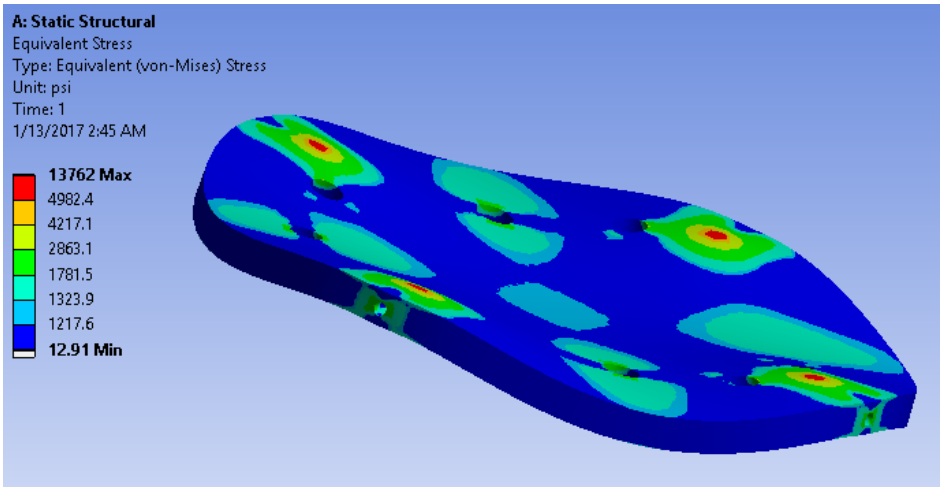

Figure 27: Equivalent Stresses Due to Black Powder Ignition

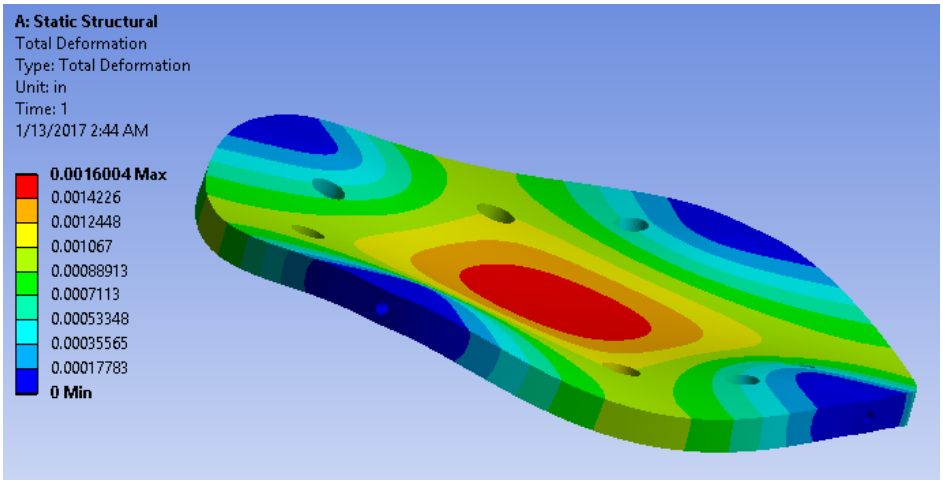

Figure 28: Bulkhead Deformation Due to Black Powder Ignition

These models show that the bulkhead can withstand the black powder ignition force with a safety factor of 2.95. As can be seen in Figure 27 and 28, the areas around the four fixed supports deform the least and experience the maximum stress of about 13.7 ksi. This analysis shows that aluminum is an appropriate material selection for this bulkhead.

The wooden bulkhead in this section must withstand the black powder ignition force as well. The forces and wooden bulkhead/U-bolt configuration are the same as in Section 3.1.3.2, and therefore the wooden bulkhead analysis can be applied here to show plywood as an appropriate material.

One additional test was done to ensure the aluminum bulkhead can withstand the forces acting upon it during flight. The design of the custom machined 1/4" Aluminum 6061 bulkhead (seen in Figure 29) at the top of the avionics bay allows an elegant solution to affix the avionics bay inside the avionics body tube. Four 5-40, 1/2" length steel bolts insert through the airframe and into the tapped bulkhead, effectively constraining the avionics bay from the forces induced by blast charge detonation and parachute deployment. In order to validate the design of this bulkhead, a quick structural analysis of tearout through the aluminum plate follows.

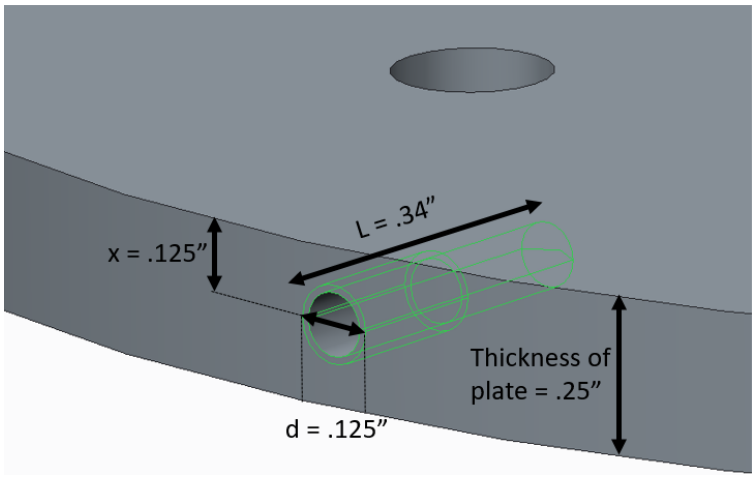

Figure 29: Custom Machined Avionics Aft Bulkhead

The length L that the bolt goes into the bulkhead is 0.50" (the length of the bolt) minus 0.16" (the thickness of the Carbon Fiber reinforced Blue Tube). This gives an effective length of 0.34". Because the bolts are steel and

embedded in the aluminum plate, the plate will fail in bearing failure. This is also referred to as tear-out because the bolts are tearing out the plate material. We use the shear strength of the aluminum plate in the max force calculation performed in Figure 30.

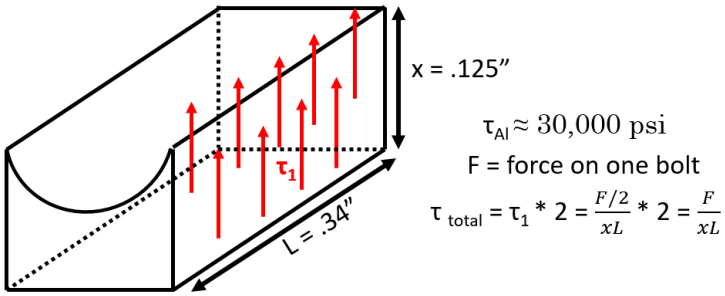

Then $F_{max} = \tau_{Al} * x * L *$ number of bolts

So that $F_{max} = 30{,}000\ psi * \frac{1}{8}\ in. * .34\ in. * 4$ bolts

F_{max} = 5100lb.

Figure 30: Custom Machined Avionics Aft Bulkhead Analysis

As seen above, the max axial force that the plate can withstand is 5100 lbs. Since this is well below the forces that the plate will experience (570 lbs during blast charge detonation), the design and materials chosen for the bulkhead and avionics bay are validated. In a test-to-failure, the carbon fiber blue tube will likely shear out first. In order to test this, a tear-out test can be performed to further characterize the carbon fiber blue tube. This is further covered in in 7.1.5.

3.1.3.4 Tail Section

Requirements The tail section of the launch vehicle has many purposes. First and foremost, the tail section must sufficiently retain the motor during propulsion and transfer the force behind the propulsion throughout the launch vehicle. Next, the tail section must house the fins of the rocket, providing the launch vehicle with stability and lowering the center of pressure. Lastly, the tail must end in a favorable airfoil, minimizing pressure drag on the rocket. Additionally, like all other sections, the tail must be able to interface effectively with the rest of the launch vehicle, providing practical integration between components.

Chosen Design The chosen payload system design for the VADL ’16’17 SL vehicle will feature a 29” carbon fiber reinforced Blue Tube airframe ending in a 5.5” boattail, bringing the tail to a total of 34.5” in length. The tail section was designed to appropriately transfer propulsion from the Loki L1400 motor throughout the launch vehicle, a journey that is detailed in Figure 31, below. As noted in Section 3.1.2, the airframe material was chosen over other alternatives because of the substantial decrease in production costs compared to pure carbon fiber while retaining sufficient strength properties to withstand several dynamic launches and landings.

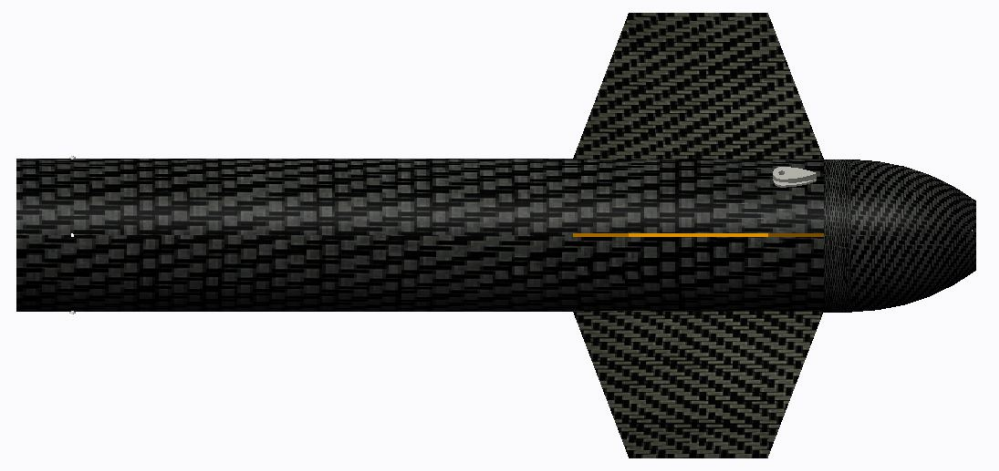

Figure 31: CAD Model of Tail Section

The tail will be comprised of the airframe, four fins, motor tube, motor, boattail, and the necessary assemblies to hold the tail together. At the front of the tail is the connection to the avionics section via a Blue Tube coupler tube and 4x 4-40 nylon shear pins. Next is a 1/4" aluminum custom-machined bulkhead, epoxied into the airframe. A 5/16" diameter steel U bolt will be mounted on this bulkhead, with a 600 lb force capacity to take the force of the parachute deployment. The 2.26" diameter motor tube begins at this bulkhead, epoxied into an 1/8" slot in the bulkhead. Near the middle of the tail section is a second 1/4" aluminum bulkhead which will act as a centering ring for the four Dragonplate fins. At the end of the motor tube is an aluminum retaining ring/ring cap combination, epoxied onto the motor tube to ensure proper transfer of propulsion force. Connecting the boattail to the tail section is a 2" Blue Tube connector tube. A schematic of these components can be seen in Figure 32, as well as dimensions in Figure 35.

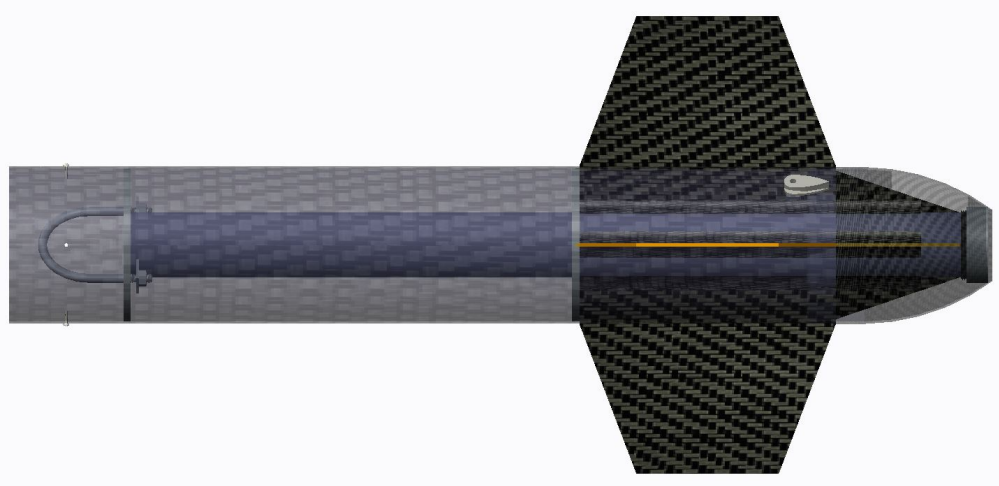

Figure 32: CAD Diagram of Tail Section

After review of possible fin designs, VADL decided to select a trapezoidal fin shape with non-tapered edges. The trapezoidal shape was chosen to for maximal stability and minimal trailing edge contact with the ground after landing, thereby lengthening the life of the fins. VADL will use 1/8" quasi-isentropic Dragonplate carbon fiber sheets, cut with a high-pressure water system. The material was selected for its strength rigidity, precision when forming, and its light weight. These fins are dimensioned to meet the specified center of pressure for the rocket, as calculated from flight simulations. They feature a 5" tip chord, a 9" root chord, and a 5.25" semi span protruding from the rocket. The fins will rest on the surface on the motor tube, held in place by epoxy and carbon fiber fillets that are adhered onto the top of the motor tube. One improvement that this year's team will implement is an 18.7 degree angle

on the trailing edge of the fin, maximizing the surface area of the fin in contact with the motor tube of the rocket. This elongation will transfer the thrust seen by the motor more effectively. Details of the fin can be seen in Figure 33.

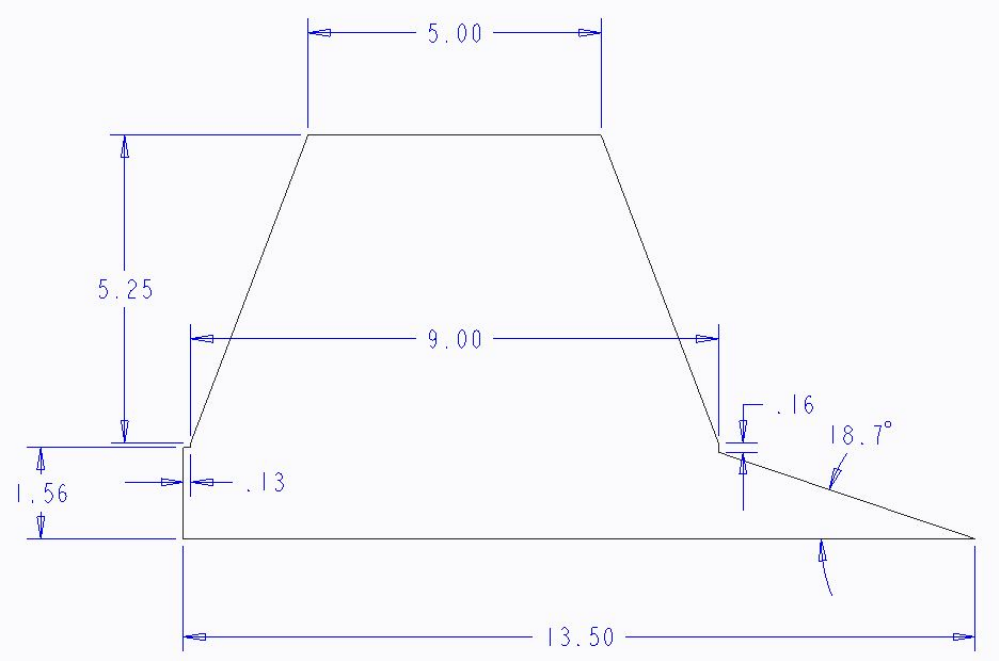

Figure 33: Dimensional Drawing of Fin

The final part of the launch vehicle, the boattail, was designed to cover the remainder of the motor while coming to a gradual stop in an effort to minimize pressure drag. This boattail will be manufactured in-house using a custom fiberglass mold. The boattail will be connected to the tail section via the connector tube and 4x 4-40 nylon shear pins. Details of the boattail can be seen in Figure 34.

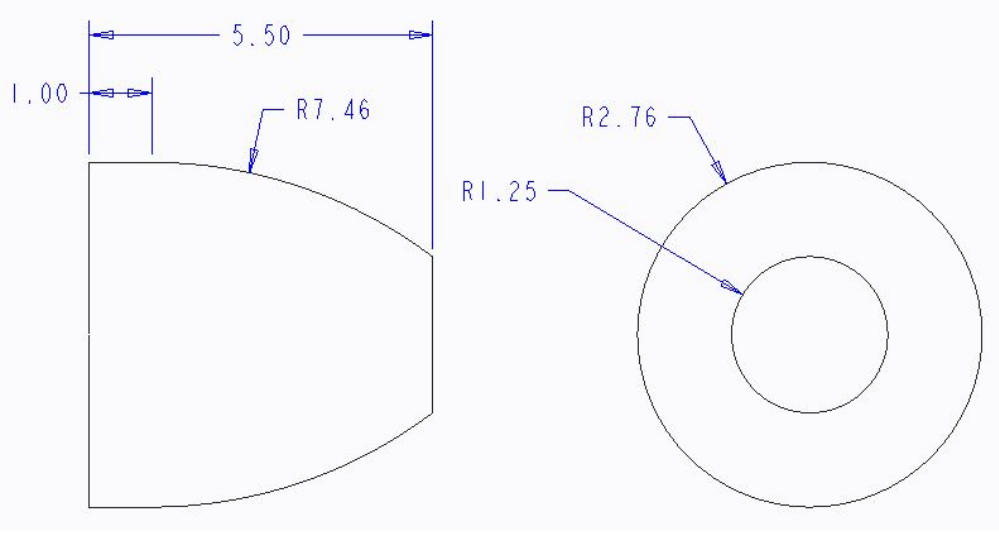

Figure 34: Dimensional Drawing of Boattail

A CAD dimensional drawing of the tail section and the components resting inside can be seen in Figure 35, below.

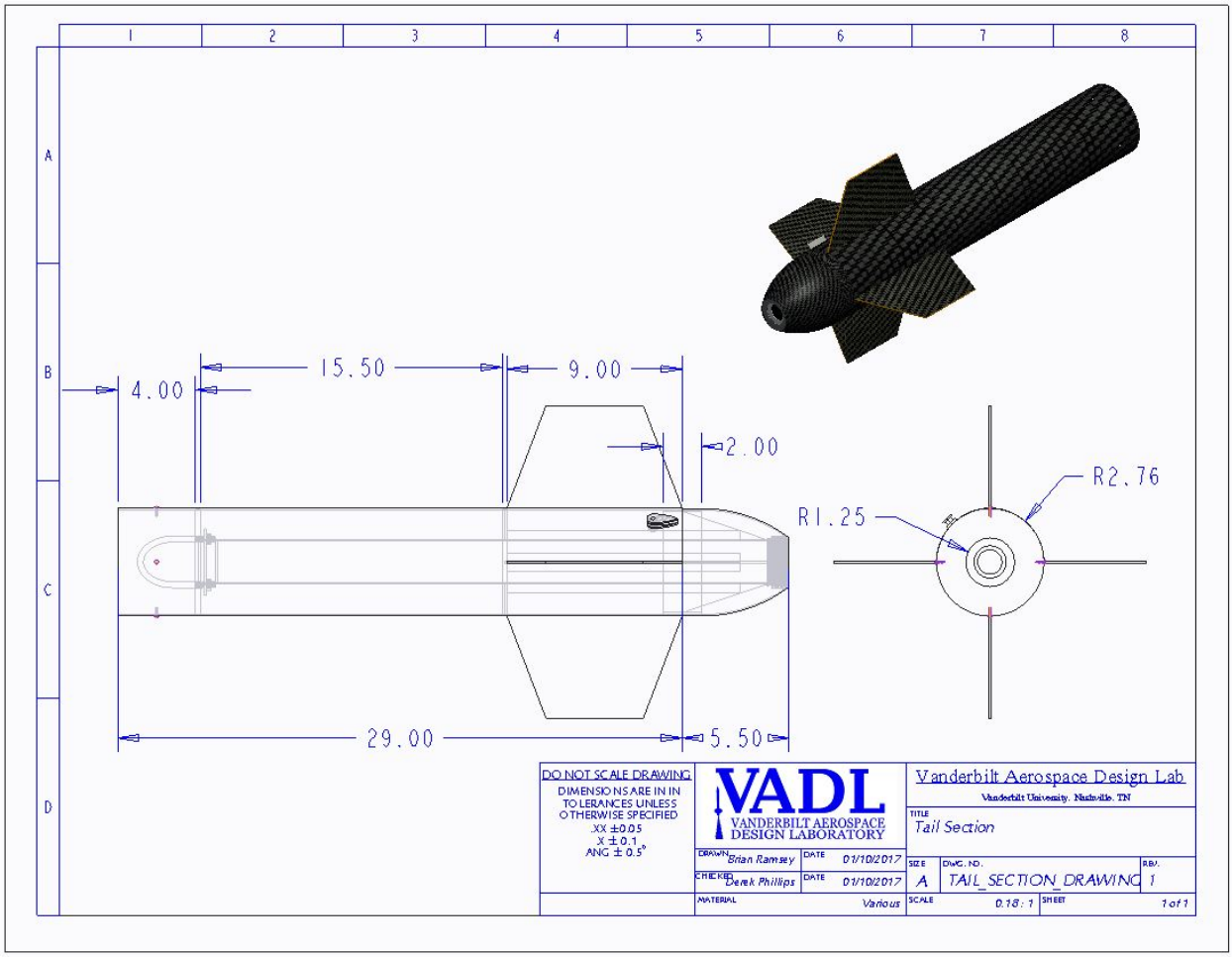

Figure 35: Dimensional Drawing of Tail Section

Integrity The tail section experiences three major forces, the force of the black powder explosion, the forces of the main parachute deployment, and the force of the motor. These forces and the major components on which they act are illustrated in Figure 36.

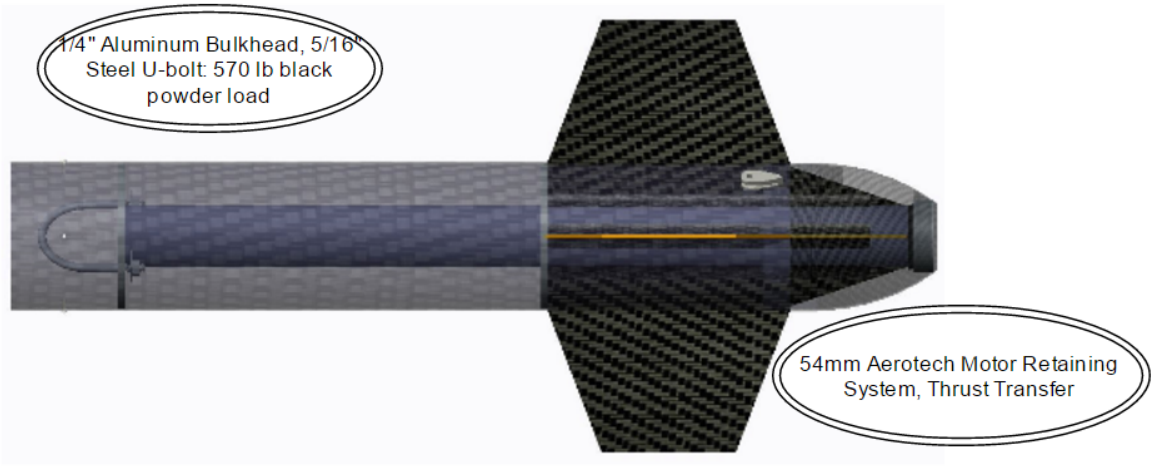

Figure 36: Concentrated Forces on Tail Section

The substantial force of the rocket motor on the rocket body (resultant from 11-12 g's) necessitates a very robust motor retention system. This system not only has to withstand tremendous amounts of force, but also must resist off-axis vibration to ensure straight flight. The following diagram shows how the force of the motor is transmitted throughout the rocket body.

Figure 37: Block Diagram Force Transmission

Further into the tail section, the 6061 aluminum bulkhead that separates the motor tube from the avionics bay undergoes the force of the main parachute deployment, the force of the motor, and the force of the black powder ignition. This bulkhead was analyzed similarly to the aluminum bulkhead in Section 3.1.3.3 to ensure it could withstand the force of the black powder ignition. This bulkhead was analyzed using FEA to ensure that it could withstand the other two forces. Figures 38 and 39 show the ANSYS generated equivalent stresses and deformation that the aluminum bulkhead endures as a result of the main parachute deployment force, 75.7 lbs, concentrated at the washers of the U-bolt. In these figures, the areas of red show the highest concentration of stress or deformation.

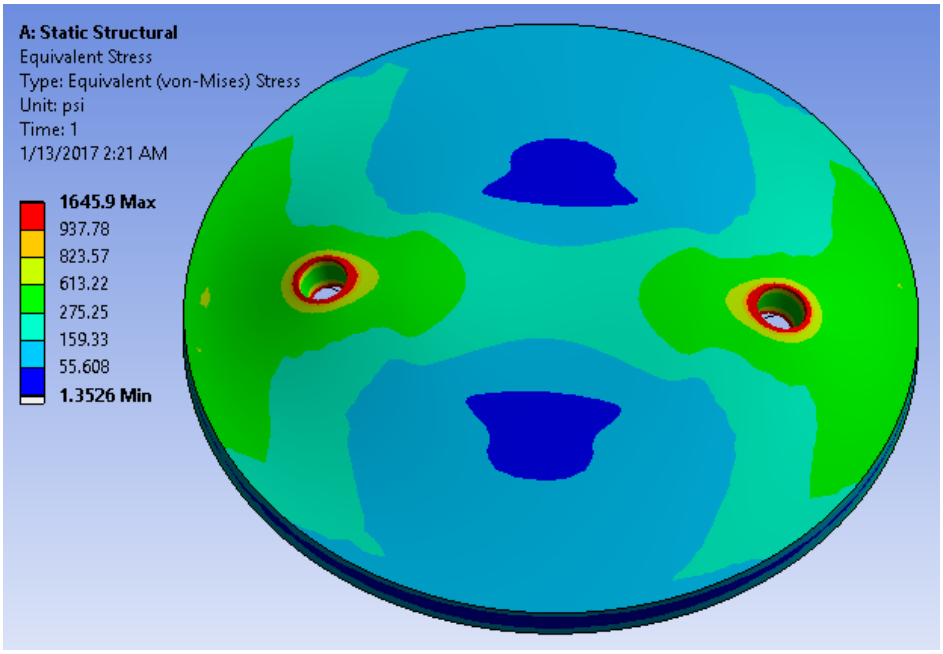

Figure 38: Equivalent Stresses Due to Main Parachute Deployment

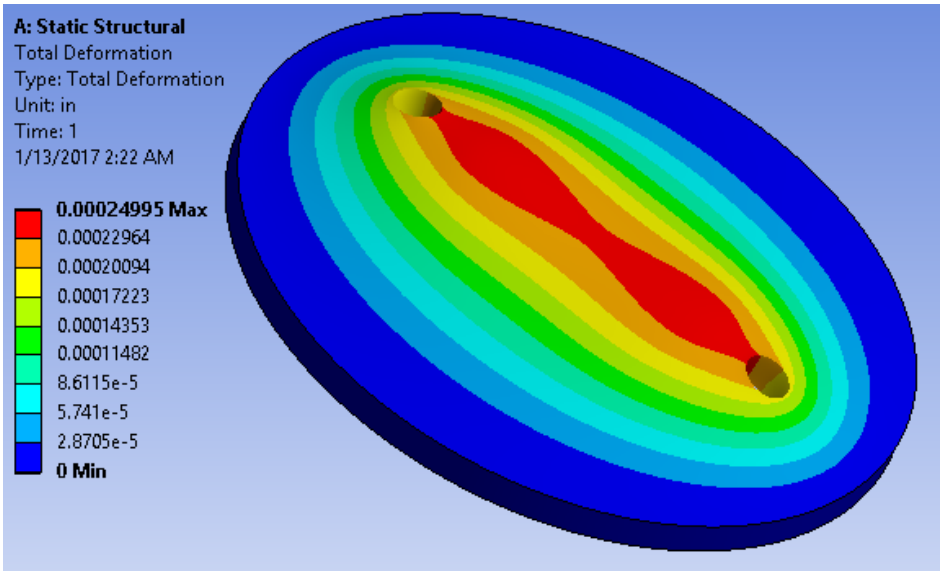

Figure 39: Bulkhead Deformation Due to Main Parachute Deployment

In these figures, the areas of red show the highest concentration of stress or deformation. The maximum von-Mises stress that acts on this bulkhead is approximately 1.6 ksi, and the maximum deformation the bulkhead will experience is .0002 inches, a negligible value. This analysis proves that the aluminum bulkhead can withstand the main parachute deployment force with a safety factor of 15 and minimal deformation.

Similar analysis was performed on this bulkhead to prove it can withstand the maximum motor force of 428.5 lbs. Figures 40 and 41 show the ANSYS generated models of this bulkhead when the rocket takes off.

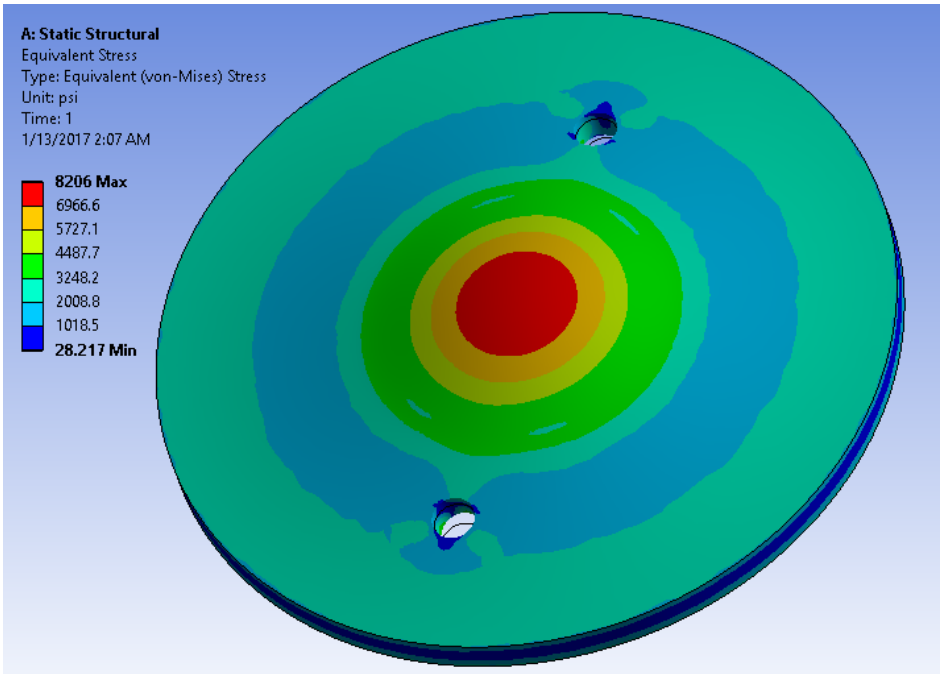

Figure 40: Equivalent Stresses Due to Motor Thrust

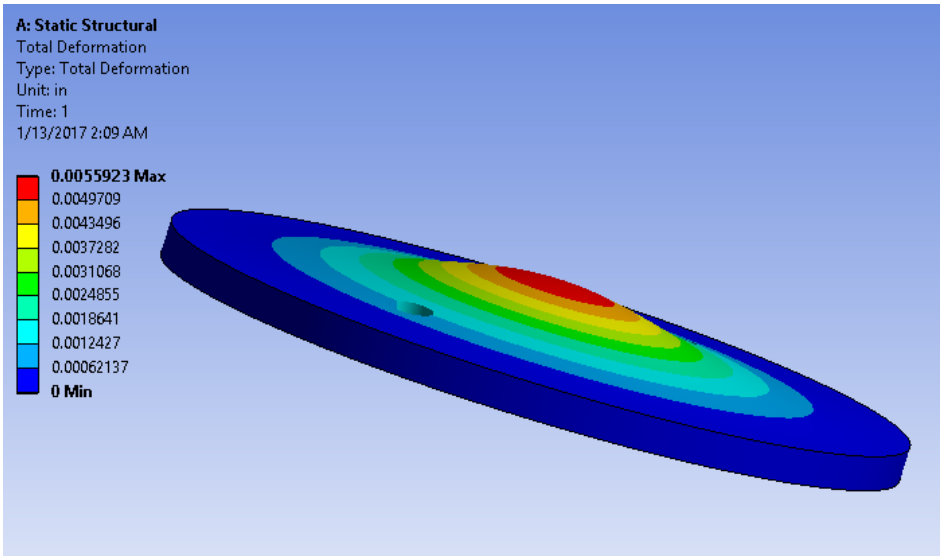

Figure 41: Bulkhead Deformation Due to Main Parachute Deployment

The force of the motor thrust is much greater than the force of the main parachute deployment, as can be seen in these figures. The maximum von-Mises stress that acts upon the bulkhead is approximately 8.2 ksi, and the maximum deformation this bulkhead will experience is 0.0056 inches. The choice of aluminum as the material for this bulkhead is appropriate because, even with this larger motor force, the bulkhead can withstand the von-Mises stress with a safety factor of 4.95. Furthermore, the total deformation of the bulkhead from both the motor thrust and main parachute deployment is acceptable.

In addition to ensuring the bulkhead will not fail as a result of these forces, it is also necessary to ensure that the epoxy bond between the bulkhead and the airframe does not fail. The bonding area of the epoxy is 2722.2 mm^2, and the epoxy's lap shear strength is 13.7 N/mm^2. Therefore, this epoxy can withstand up to 37,294 N or 8,384 lbs,

which is much greater than the maximum force that will act on this bulkhead.

One last possible point of failure is the U-bolt during main parachute deployment. This U-bolt is rated up to 600 lbs, so it will be strong enough to withstand the deployment force.

3.2 Subscale Flight Results

3.2.1 Launch Day Simulation and Recorded Data

3.2.1.1 Altitude

Mathematical modeling produced a predicted apogee altitude of 1366 ft. Two altimeters were flown on the subscale test rocket. The two altitudes recorded by the altimeters were 1393 and 1395 feet. It shall be noted that the variation between predicted and experimental values could be due to a 1.5% variance in motor thrust or a 5% variance in coefficient of drag, these two components being the least certain variables in the model. Some variation was seen between the projected parachute opening height and the actual opening height, but this was an artifact of blast charge location on the subscale launch vehicle. The full size vehicle design has been modified to improve deployment expedience. A plot of altitude over the duration of the flight can be seen below in Figure 42. The quantitative results are summarized in Table 1.

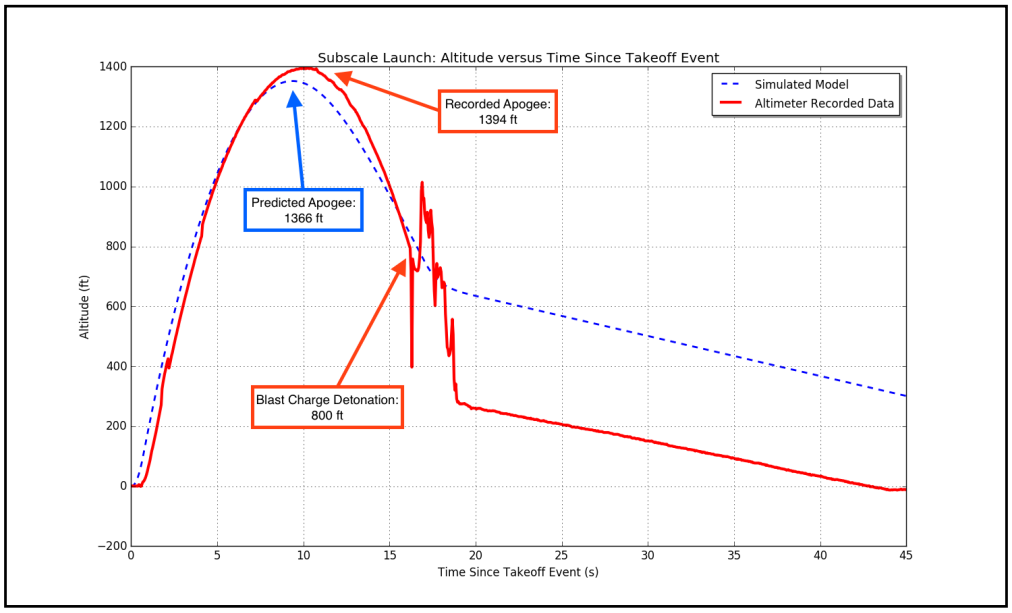

Figure 42: Simulation and Experimental Data for Subscale Apogee Altitude

Instance	Maximum Altitude (ft)
Matlab Simulation	1366
Avionics Recorded	1394 (avg)

Table 1: Subscale Launch Altitude Statistics

3.2.1.2 Drift

Drift was factored into a simulated trajectory of the subscale launch vehicle. Drift was predicted to be 500 ft launching into a 3 mph headwind with 5 degrees of cant off of the launch rail. True launch day wind conditions were not quantified while on site, but the rocket was indeed launched at five degrees into an intermittent headwind of indeterminate strength. Actual post-launch drift was paced to be approximately 200 feet. A simulated trajectory can been seen below in Figure 43. Quantitative results are summarized in Table 2.

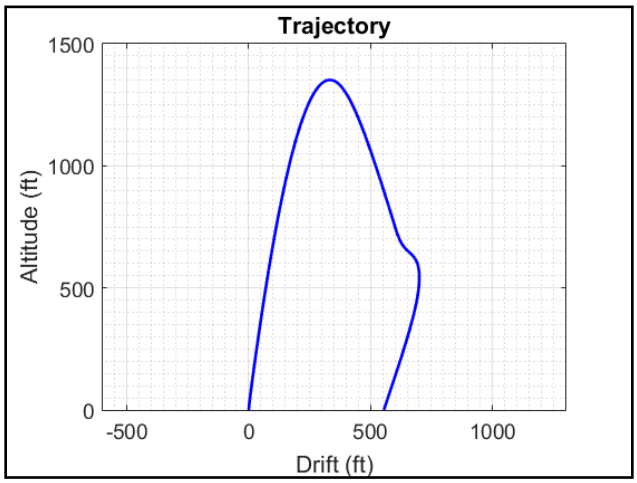

Figure 43: Simulation for Subscale Drift

Instance	Drift (ft)
Matlab Simulation	∼500
Actual Launch	∼200

Table 2: Subscale Launch Drift Statistics

3.2.1.3 Axial Acceleration (Vertical, Z Axis)

Acceleration in the vertical direction (along the vehicle's central axis) was simulated pre-flight and was recorded during the flight experiment by the on board IMU. Modeling proposed a maximum expected acceleration of 14.75g (14.75 times the acceleration of gravity on Earth at sea level). The experiment showed a maximum acceleration of 14.6g. It is important to know that this is the acceleration of the flight vehicle, and that it discounts the acceleration due to gravity, meaning that the true acceleration acting on the vehicle in the axial direction, when oriented vertically, is and additional 1g. The acceleration profile of the main engine burn (the period of maximum acceleration) can be seen for both simulation and subscale flight in Figure 44 below. Quantitative results are summarized in Table 3.

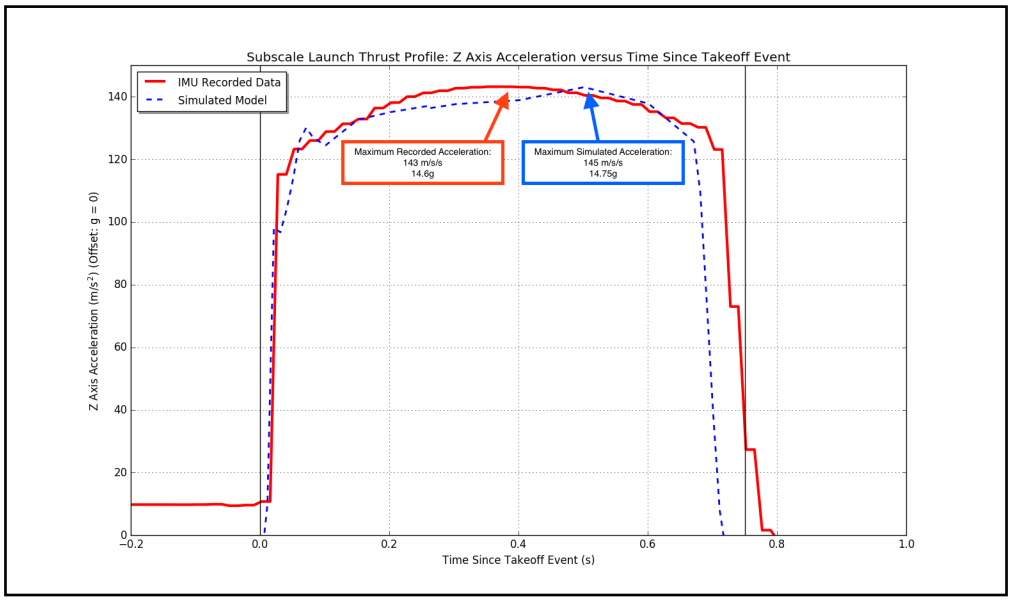

Figure 44: Simulation for Subscale Axial Acceleration

Instance	Axial Acceleration (g's)
Matlab Simulation	14.75
Actual Launch	14.6

Table 3: Subscale Launch Axial Acceleration Statistics

3.2.1.4 Roll (About Central Axis)

Arguably most central to the subscale flight was the payload experiment. As VADL is attempting the roll induction directive, the subscale flight experiment sought to validate the roll induction system and characterize its dynamics. The fundamental quantitative characteristic of this rotation is angular displacement about the central axis. This was simulated before the subscale flight and also experimentally determined through roll data provided by the Vectornav VN-100 IMU. It should be noted that the model can be viewed as relatively valid, but there are intrinsic difficulties and inaccuracies when modeling fluid effects on a complex body. Herein, a rough drag estimation ($C_d = 0.27$) is used to encapsulate pressure and skin drag. That said, the model predicted 18.8π radians of rotation; subscale flight saw 2.74π radians of rotation. A discussion of this discrepancy may be found in Section 3.4.3.2. After an improvement of the model, results fell neatly in line with predictions, as seen in Figure 46 Plots of rotation, both simulated and experimental, may be seen in Figure 45. A quantitative summary may be seen in Table 4.

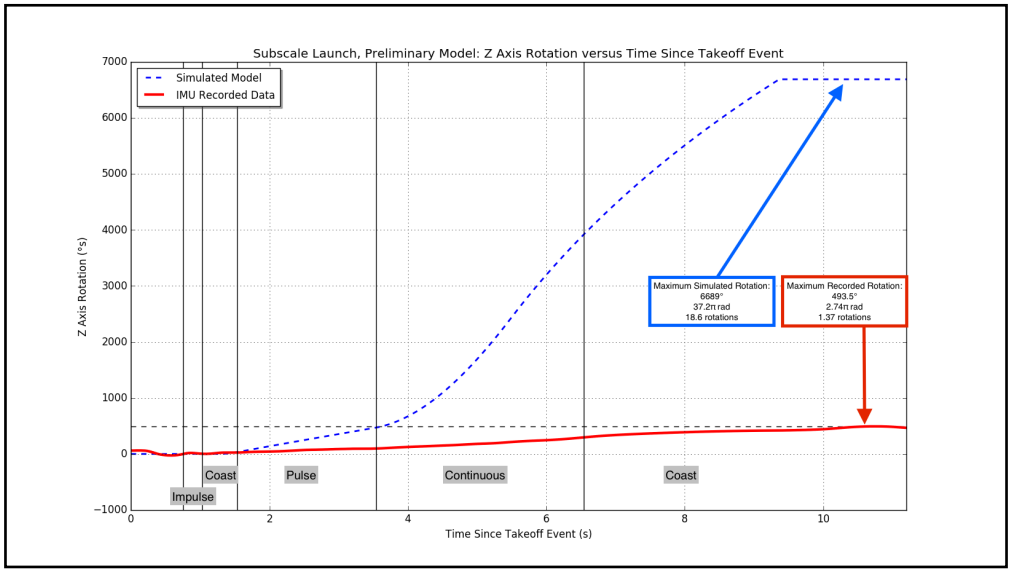

Figure 45: Simulation and Experimental Data for Subscale Angular Displacement

Instance	Angular Displacement (rad)
Matlab Simulation	18.8π
Actual Launch	2.7π

Table 4: Subscale Launch Angular Displacement Statistics

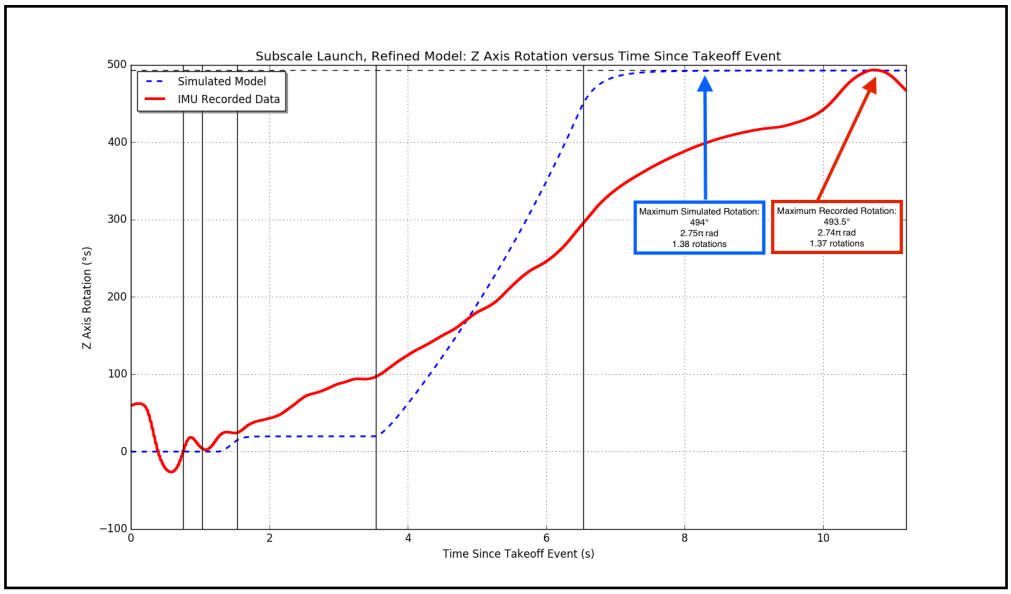

Figure 46: Simulation and Experimental Data for Subscale Angular Displacement, With Modeling Improvements

3.2.2 Impacts On Full Scale Design

December's subscale flight gave the team valuable data as well as considerations to keep in mind as the full scale vehicle and payload designs were finalized. Many features from the subscale design were proven functional and fit for the full scale design. For example, the subscale design feature of a bolted and fully removable forward section for 360 degree payload access was highly useful in both ease of assembly and safety checklist assurance. Other observations, like the analysis of IMU flight data, led the team to begin the process of payload design modifications.

The subscale flight was fully recoverable and, after analyzing the key parts of the launch vehicle for damage and not finding any, determined to be reusable. Thus, our vehicle design was validated. In addition to vehicle design features, the flight data obtained gave highly valuable information in relation to changes moving forward with the full scale design and build. While the altitude and drift results from the VADL subscale flight helped validate the simulations corresponding to these variables respectively, the angular displacement achieved during the flight experiment was lower than both the roll simulation and ground-based testing experiment results (see the **??** section for the latter results). After analyzing the IMU roll data from both the FRAME testing and the subscale launch in comparison with the simulations and research literature, the team feels an unaccounted for and significant resistive torque was present during flight that led to this lower roll value. Various possible causes of this resistive torque (or other possible reasons for the lower roll value) have been analyzed along with testing strategies to verify the presence of each.

1. During the axial air flow of flight, the dynamic pressure of the flow surrounding the fins resisted the rotation in a manner surpassing the assumptions of the current vehicle model.

2. As the thruster exhaust jet naturally spread out to a larger diameter, slow stream tube during actuation (observed from thruster tests on the ground), the presence of axial flow caused a jet-fin interaction that resisted axial rotation. The cross-flowing free stream around the vehicle reoriented the exhaust from the nozzles, and once this exhaust reached the downstream fins, the pressure field of these control surfaces was influenced to change the force generated [1].

[1] Beresh, S. J., Heineck, J. T., Walker, S. M., Schairer, E. T., & Yaste, D. M. (2007). Planar Velocimetry of Jet/Fin Interaction on a Full-Scale Flight Vehicle Configuration. AIAA Journal

3. A leak in an upstream component of the thruster system led to a lowered thrust value during actuation.
4. Thruster couple misalignment with exhaust ports occurred during launch and prior to the roll experiment.

These possible causes were ranked by the team based on plausibility (i.e. axial flow-introduced causes offer a much higher plausibility than mechanical failures and leaks occurring from team negligence in assembly and testing). Testing or mitigation strategies for each of these possible causes were also prepared and this information can be seen synthesized in Table 5.

Table 5: Plausibility and Testing of Possible Low Roll Causes

Possible Causes of Low Roll	Plausibility Rating	Testing/Mitigation Strategy
Dynamic pressure from flow around fins offered a resisting torque.	9	Place subscale vehicle on the FRAME and introduce damping from attached motor to simulate flight resistive torque while inducing roll via thrusters. Compare angular displacement with and without motor actuation.
A jet-fin interaction offered a resisting torque to the fins during thruster actuation.	7	Place subscale vehicle on the FRAME and introduce damping from attached motor to simulate flight resistive torque while inducing roll via thrusters. Compare angular displacement with and without motor actuation.
A leak in the upstream components of the thruster assembly led to a lowered delivered thrust.	3	Perform thorough system leak test prior to FRAME testing or launch.
Thrusters became misaligned with vehicle body exhaust ports during flight and exhausted propellant into rocket body.	2	Make sure to rigorously verify structural connections on all thruster system components prior to FRAME testing or launch.

Moving forward with fullscale build and testing, the team will test these possible causes using the protocols described in Table 5. In regards to possible solutions to this issue, VADL feels a higher output thrust for each couple in the fullscale design is of paramount importance. The team will begin testing the thruster system under various conditions including higher tank pressure, higher regulator pressure, and N2 addition to the air in the tank to achieve a higher output value (see the 3.4.5.6 section for more information on required thrust). This analysis will begin with extended tests on the thruster test stand and continue with ground-based tests on VADL's custom test facility (FRAME). The FRAME tests will also incorporate our active control system to make sure the full scale design meets our roll requirements while accurately taking into account the extra variables affecting vehicle attitude during a launch scenario that were discovered from our subscale flight experiment. For detailed information on how these flight damping conditions were analyzed and how the ground based testing protocol will simulate these conditions, see the 3.4.3.2 and 7.1.4.5 sections.

3.2.3 Scaling Factors

The subscale launch serves as a testing ground for the fullscale vehicle. The test launch allows the team to learn what works and what needs improvements and incorporate this knowledge into the fullscale vehicle. When translating from subscale to fullscale, there are many aspects of the rocket that can be held constant, and some that must be scaled for the higher apogee target, more comprehensive flight experiment, and dual-deployment recovery system.

The shape of the nose cone and the diameter of the rocket are held constant, which also leads to an equivalent coefficient of drag. The boat tail also affects the drag coefficient, and is also held constant. There was no requirement to increase the strength of the rocket, and for this reason there was no effort to scale the strength of the airframe components.

Figure 47 shows the various aspects of the rocket that will see a scaling from subscale to fullscale. Included is the increase in length, mass, and motor impulse, which causes an increase in rail exit velocity, altitude, and landing drift.

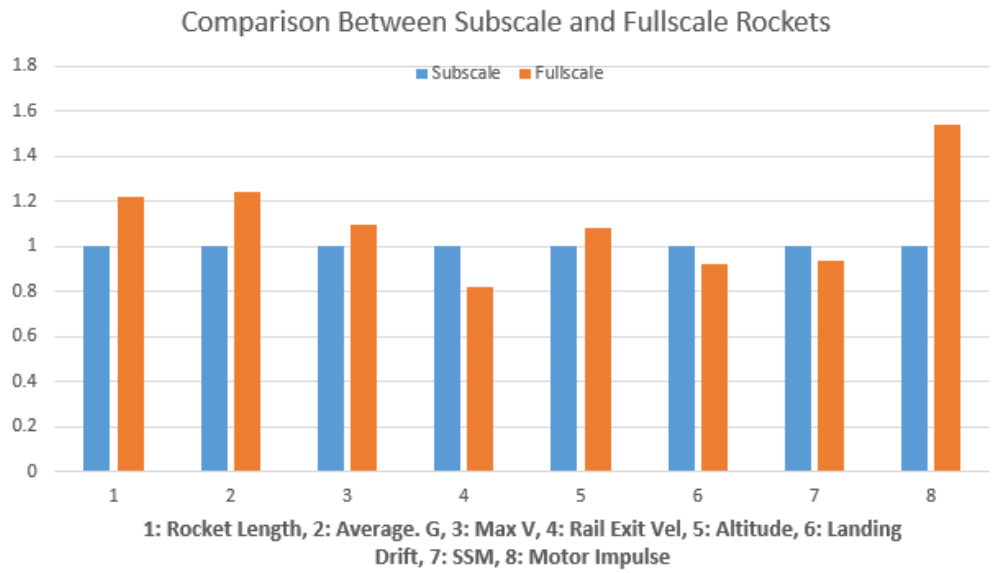

Figure 47: Scaling Factors From Subscale and Fullscale

3.3 Recovery Subsystem

3.3.1 Recovery System Motivation

The VADL recovery system is designed entirely with safety, reliability, and mission success in mind. All design selections are: 1. Simple 2. Reliable 3. Proven 4. Driven by Calculation. The system of a drogue parachute deployed at apogee by redundant altimeters and a main parachute deployed at a lower altitude out of independent compartments has been proven not only by years of use in this program but by hundreds of rocket enthusiasts around the world. Every component in our recovery system from the parachutes to the altimeters is entirely necessary and any unnecessary components whose failure could risk loss of vehicle have been unquestionably removed. Every component of the recovery system was validated by successful recovery of the subscale launch vehicle. Altimeters are fully redundant, and have been fully tested on the ground and in the test flight. Parachutes have been sized to minimize drift while meeting landing energy requirements.

3.3.1.1 Recovery System Overview

It is not considered a successful flight if the rocket is not recoverable. A safe landing includes proper deployment of the team's parachute in order to land at a reasonable velocity to not only minimize drift but ensure landing under the landing energy requirement of 75 lbf-ft. A flow chart of the recovery system plan can be seen in figure 48.
The system will include two StratologgerCF altimeters where one will serve as the main altimeter and the second as the backup to ensure a redundancy in the recovery system, one of the most important systems in the rocket. The altimeters will sense altitude in order to deploy the dual parachute system on the team's full scale rocket. The team will deploy a 24" drogue one second after apogee with the 8ft main being deployed at 600 ft. Each altimeter will be power by it's own battery to ensure redundancy in the system and prevent failure. Each altimeter will be connected to an e-match which will ignite a black powder blast charge. This charge pressurizes the rocket section and causes it to separate in order for the parachute to release and open. Attached to the shock cord will be a Big Red Bee radio transmitter which has a transmitting range of 10 miles. This will allow the team to find the rocket after it's safe return back to the ground. The rocket will drift on it's return path thus the radio transmitter will play a vital role in rocket location if the rocket lands out of eye sight.

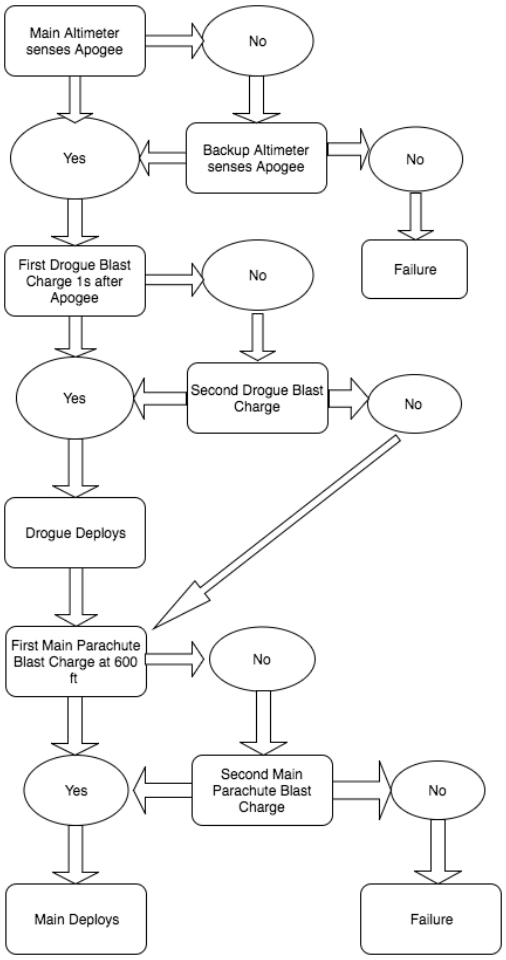

Figure 48: Recovery System Flowchart

3.3.1.2 Recovery System Testing

A complete test of the deployment system on the rocket is carried out before each launch. The test consists of two different aspects: testing the deployment charges / rocket separation, and testing the altimeters. Pictured in figure 49, the StratologgerCF altimeters work up to 100,000 ft. Each altimeter stores 16 flights of 18 minutes each. They have the ability to record altitude, temperature, and battery voltage at 20 samples per second. The device has a precision down to 1 foot increments which is sufficient enough for the team's flight to 5200 feet. Each altimeter beeps to indicate if it is on and it's target altitude. This is important when ensuring proper functionality of the altimeters before launch. The team tested the altimeters in the Vanderbilt shock tube. Two altimeters were placed in the tube, one main and one backup. The main was set to 800 ft and the backup to 600 ft. The results of the testing can be viewed in figure 50.

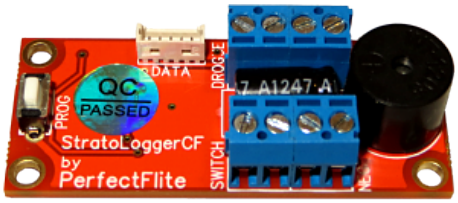

Figure 49: StratologgerCF Altimeter

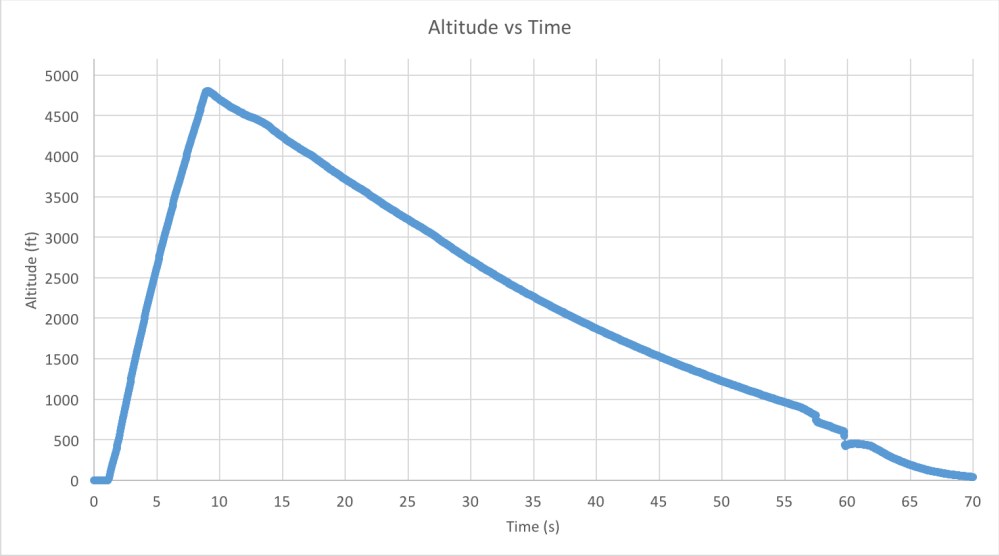

Figure 50: Altimeter Testing

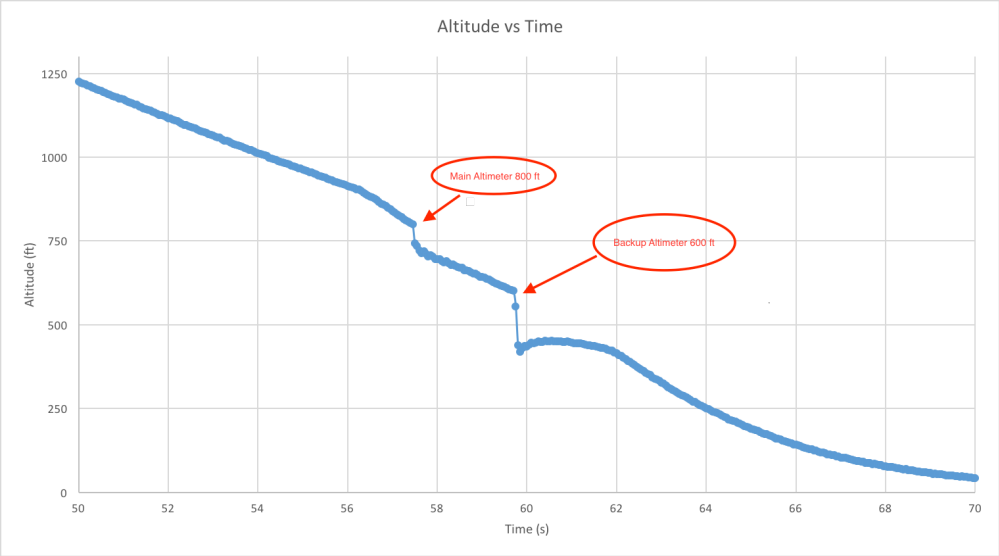

Figure 51: Altimeter Testing Zoom

The graphs confirmed that the altimeter would function and ignite the e-match at the proper altitude.

3.3.1.3 Deployment Testing

A complete, ground-based test of the launch vehicle recovery system is performed prior to each launch (subscale and full scale). The second phase of testing is ground-based deployment/separation event testing to assure that the electric matches, altimeter firing mechanisms, and drogue and main parachute deployment charges meet safety and operational standards.

To test the deployments, the launch vehicle is assembled in the horizontal position using mass simulators for excluded payload components. During assembly, 4F Black Powder charges are carefully placed in the designated blast locations. The avionics bay is secured in the forward section of the vehicle, as it would be for a true launch. The edges of the bay are sealed with putty to protect the internal instrumentation from forces experienced during the black

powder ignition. Parachutes are packed and placed in their correct positions. Igniters are connected to a custom electrical relay control mechanism that allows for remote, manual ignition. The area is cleared for obstructions and personnel as verified by Safety Mentor Robin Midgett and Student Safety Officer Paul Register. Subsequently, the drogue blast charges are fired manually. Next, the main blast charges are fired manually. After verifying both separation events, the Safety Officers assure there is no un-ignited black powder in the launch vehicle which could cause a safety hazard. Once this is verified, the test of the rocket separation is complete and equipment is transported back to the laboratory for manual inspection for damage. A successful deployment test was conducted before the subscale launch in December.

3.3.1.4 Rocket Separation

Rocket separation will occur in two events: the forward event and the aft event. The two separation events will occur (1) at the joint between the upper body tube and the coupler tube and (2) at the joint between the coupler tube and the aft section. One side of the coupler tube will house the drogue parachute while the other side will house the main parachute. The avionics bay will be house between the two parachute sections sandwiched between two bulkheads. A schematic of the full scale rocket can be seen in figure 52

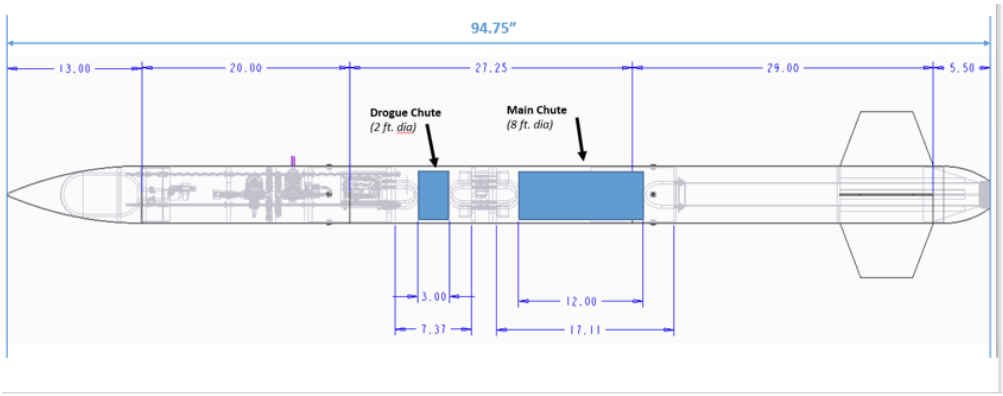

Figure 52: Full Scale Schematic

Physical separation will be achieved via controlled detonation of pyrotechnic charges located on the avionics bay bulkheads to create positive pressure inside the parachute bays. The pyrotechnic charges selected for both deployment events are 4F black powder charges specifically sized to create at least 283 lbs of separation force per charge. For each deployment event both a primary and a backup charge, each capable of independently forcing separation and controlled by their own altimeters, will be detonated to ensure rocket separation. The maximum shear strength of #4-40 nylon screws is 71 lb per screw. Nylon screws will be used to hold the rocket sections together.

$$F = \sigma A = 10,000 \frac{lb}{in^2} * \frac{\pi}{4} * (.095in)^2 = 70.88lb \tag{3.1}$$

$$Area = \frac{\pi * d^2}{4} = \frac{\pi * 5.36^2}{4} = 22.56in^2$$

$$4 \frac{screws}{junctions} * 70.88 \frac{lb}{screw} = 283.52lb$$

$$P = \frac{F}{A} = \frac{283.52lb}{22.56in^2} = 12.57psi \tag{3.2}$$

Black powder exhaust gases behave as ideal gases. The black powder exhaust gases can be simplified to do work only on the rockets bulkheads

$$PV = nRT$$

$$R = 266 \frac{lb - in}{lbm * R}$$

$$T = 3300R$$

The volume of the parachute, shock cord, u-bolts, and blast caps can be ignored. (This leads to a conservative answer). Therefore volume is a function of area and chamber length only. For the full scale launch, calculations for the black powder ejection charges can be found below. The volumes for both the main and drogue chambers can be calculated.

$$V_{drogue} = A * L_{drogue} = 22.56in^2 * 3in = 67.78in^3 \tag{3.3}$$

$$V_{main} = A * L_{main} = 22.56in^2 * 12in = 270.72in^3 \tag{3.4}$$

The figures below display the allotted space for the avionics and parachute sections of the rocket. The red shorter space represents the housing for the drogue while the green longer space represents the main parachute. One can also see the avionics support backing alongside the bulkheads, u-bolts, and blast caps.

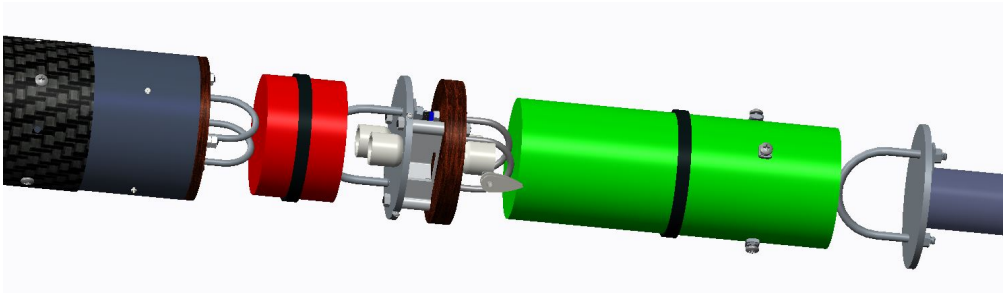

Figure 53: Avionics Assembly

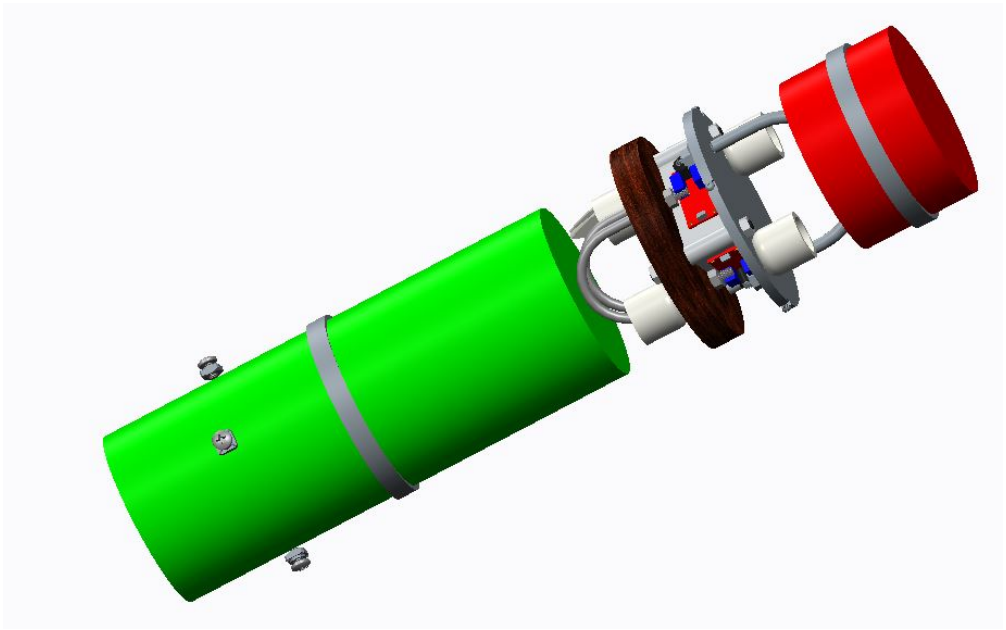

Figure 54: Parachute Bay Assembly

The mass of 4F black powder needed for each chamber can then be calculated using the ideal gas law

$$12.57\frac{lb}{in^2} * 67.78in^3 = n * 266\frac{lb-in}{lbm*R} * 3300R$$
$$n_{drogue} = .000971lbm = .44g$$
$$12.57\frac{lb}{in^2} * 270.72in^3 = n * 266\frac{lb-in}{lbm*R} * 3300R$$
$$n_{main} = .00388lbm = 1.76g$$

In order to assure the safe landing of the launch vehicle, the team decided to use a factor of safety of 2. The backup charge for each parachute was set to have a safety factor near 2.5 to ensure separation of the rocket. Drogue deployment in this launch vehicle is of utmost importance because without the reduced descent velocity, deployment of the main parachute may not occur in time for landing, or may cause damage to the launch vehicle itself. The masses of the deployment charges are shown below.

$$n_{drogue} = 1.0gram \tag{3.5}$$

$$n_{drogue_backup} = 1.5grams \tag{3.6}$$

$$n_{main_backup} = 3.52grams \tag{3.7}$$

$$n_{main_backup} = 4.0grams \tag{3.8}$$

3.3.1.5 Subscale Flight

On December 14th, the team flew the subscale rocket and collected data during the experiment. The altimeter data from the launch is displayed in figure 55

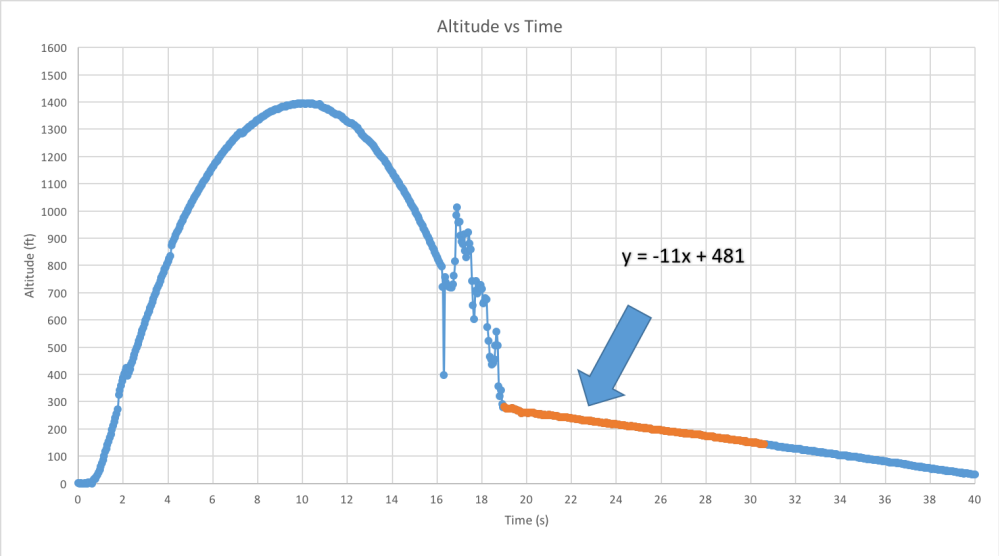

Figure 55: Subscale Launch 12/14/16 Altimeter Data

The rocket reached apogee at 1395 feet and began it's descent back to the ground. The altimeter ignited the blast charge at 800 ft as expected. The rocket drops many feet after parachute deployment because it was traveling 120 ft/s. The team used an 8 ft iris ultra parachute which has a cd value of 2.2. Fruity Chutes is the manufacturer of the parachute. The parachute had a two second opening time and opened in a way that was hard to mathematically model. But after fully opening, the rocket descended at about 11 ft/s.

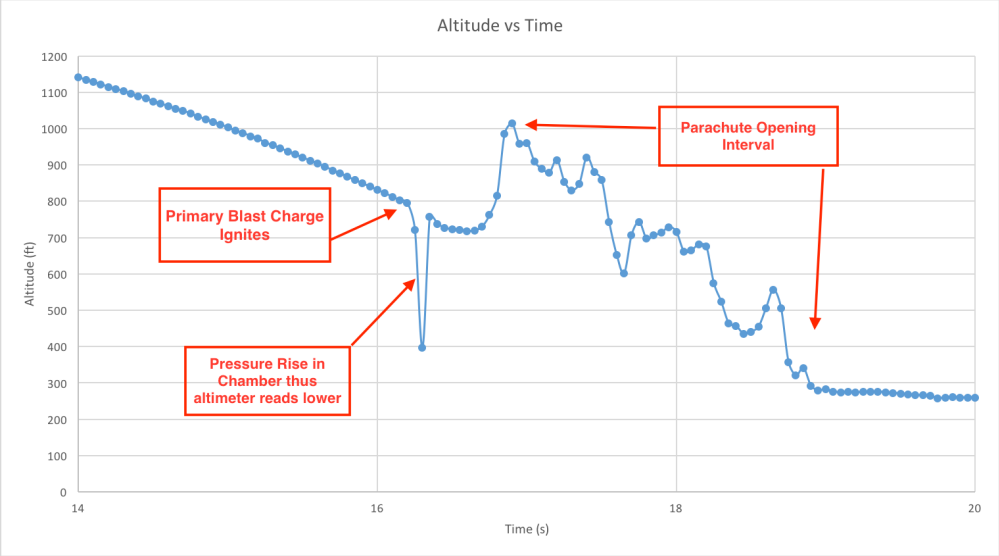

Figure 56: Subscale Launch 12/14/16 Altimeter Data Zoom

3.3.1.6 Avionics Bay

The avionics bay is designed to house all of the electronics required for activation of the recovery system. It must protect these electronics from many things including but not limited to: the explosive forces experienced during black powder ejection charge ignition and the vibrations during rocket flight. Because the PerfectFlite StratoLoggerCF altimeters in this rocket use barometric sensing to determine altitude AGL, the avionics bay must provide exposure to the atmosphere. This will allow the altimeters to sense external pressure such that they may accurately record altitude, trigger the drogue parachute deployment at apogee and the main parachute deployment at the desired altitude. Furthermore, the avionics bay must allow for altimeter activation on the launch pad once the rocket is fully assembled.

The team rapid prototyped an avionics backing support using Vanderbilt's 3-D printers. The design minimizes size while providing adequate space for the various components. A high level schematic of the recovery system can be viewed in figure 57. The design flown in our subscale rocket can be viewed in figure 58.

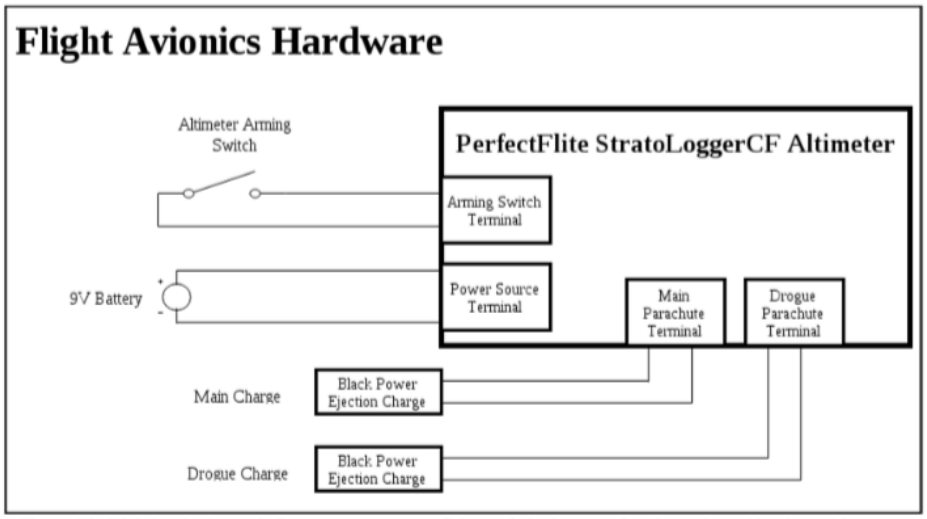

Figure 57: High Level Schematic Recovery System

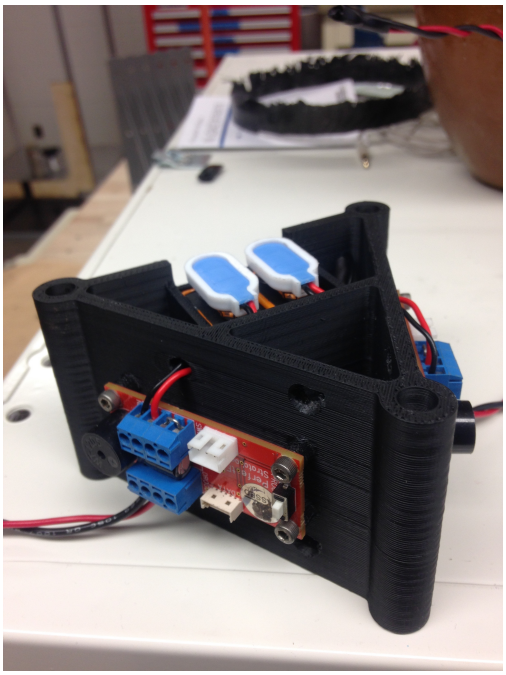

Figure 58: Avionics Support Subscale

The triangular design allows for the backing to be constrained on the team's threaded rod skeleton. It features a slot for two 9 V batteries. Each altimeter is powered by its own 9 V battery. Each altimeter sat on a separate face of the triangle and were mounted to the support backing. Two arming switches were mounted so that the altimeters could be armed last things before launch.
For ease of access and use, the team decided to use screw switches on the subscale and will continue to do so on the full scale rocket. Screw switches are less likely to not accidentally change state to the off position due to vibrations and high-g takeoff conditions. The performance of these switches is validated by years of experience and successful recoveries.

3.3.1.7 Parachute Selection

Vehicle	Subscale	Full Scale	
Parachute	Main	Drogue	Main
Diameter	96"	24"	96"
Shape	Iris Ultra	Elliptical	Iris Ultra
Cd	2.2	1.5	2.2
Source	Fruity Chutes	Fruity Chutes	Fruity Chutes
Deployment Altitude	800'	~5200'	600'
Descent Speed	11 fps	70.1 fps	14.2 fps
Shock Cord Length	20 ft	30 ft	15 ft
Shock Cord Material	Kevlar	Kevlar	Kevlar
Kinetic Energy of Heaviest Section	28 lbf-ft	906 lbf-ft	36.7 lbf-ft
4F Black Powder Charge Mass	3.52 grams	1.0 gram	3.52 grams
Fire Retardant Blanket	Nomex	Nomex	Nomex

Figure 59: Summary Parachte Parameters

Figure 59 shows the differences in the main and drogue parachutes. The first separation event occurs immediately after the rocket reaches apogee and initiates the drogue recovery process. Drogue recovery will use an 24 diameter

fruity-chute elliptical parachute. This will provide a stabilized descent at approximately 70.4 ft/sec for a rocket of weight 27.1 lb. after motor burn off. When calculating the descent velocity under the drogue parachute, the drag coefficient of both the chute and the rocket body itself must be taken into account. Falling speed with an 24 drogue from 5200 ft. to 600ft is calculated as follows:

$$V_d = \sqrt{\frac{mg}{.5\rho(C_D A_P + C_D A_R)}} = \sqrt{\frac{27.1lb * 32.17ft/s^2}{.5 * .0765lb/ft^3 * (1.5 * 3.1 + 1.2 * .0008)}} = 70.1ft/s^2 \tag{3.9}$$

A Nomex/Kevlar parachute protection pad will surround the parachute to prevent it from being burned by hot ejection gasses. For moderate to high wind conditions an 24 drogue chute is ideally suited to forestall excessive wind drift. The drogue parachute will attach to a 30ft. Kevlar 12 shock cord via quick link. The shock cord connects to a short 12 wide Kevlar harness near the ejection charges where fireproof material is needed. The shock cord, rated minimally at 3000lb, will tether the drogue parachute to the upper body tube and to one end of the avionics bay, again using quick links. Furthermore, nine 43 nylon shroud lines (86 continuous) will attach the parachute to the shock cord. A cross stitch seam type using #400 flat line threads will connect the nylon parachute sections. These parachute materials will be lightweight but also strong enough to safely return the rocket to the ground. Using quick links, the shock cord will tether the parachute to the coupler tube and the forward section (rigidly bolted to the body tube) via two 14 galvanized steel U bolts. These U bolts will be bolted to bulkheads within the rocket. These U bolts are rated to 425 lbs. The team will also make use of 5/16" black-oxide steel U-bolts which are rated to 600 lbs. The same attachment method will be used for the payload chute shock cord on the payload section side.

The second separation event occurs at 600ft. and initiates the payload recovery process. Payload recovery will use a 8 ft. diameter iris ultra parachute. This will provide a stabilized descent at approximately 14.2 ft. /sec. These parachutes were both purchased from Fruity Chutes, a reliable parachute maker. They have been selected for its consistent success in deployment and minimization of failure modes and risk to recovery. The landing speed of the rocket after main parachute deployment was calculated as follows:

$$V_d = \sqrt{\frac{mg}{.5\rho(C_D A_P + C_D A_R)}} = \sqrt{\frac{27.1lb * 32.17ft/s^2}{.5 * .0765 * (2.2 * 50.25 + 1.2 * .0008)}} = 14.2ft/s^2 \tag{3.10}$$

The heaviest section is the tail/payload section weighing in at 11.7 lb. The landing energy of the heaviest section is:

$$KE_{landingenergy} = \frac{\frac{W}{g} * V^2}{2} = \frac{11.7 * 14.2fps^2}{2 * 32.17} = 36.7lbf - ft < 75lbf - ft$$

Where KE is kinetic energy, W is weight, g is gravity, and V is velocity of descent. The landing energy assumes absolutely no ground wind; however, our experience has been that the ground wind speed contributes to lofting and the actual landing speeds with the main are substantially lower. These calculations give confidence in the design of the main parachute for the full scale design and will be fully vetted and scrutinized in the full scale test launch.

3.3.1.8 Full Scale Design Considerations

Many of the designs from the team's subscale launch will be carried over into the full scale design process. The team will make use a similar avionics support backing. The support will be designed smaller to get rid of wasted volume to ensure optimization of space inside the rocket. Two altimeters will be used to ensure redundancy in the system. Each altimeter will be powered by its own 9 V battery. PVC pipping will be used to house the blast charges will be located on both sides of the avionics bulkheads. Arming switches will be located on the avionics support backing with access holes to be drilled into the rocket. These holes will not compromise the structural integrity of the rocket. Pictured in figure 60 is the radio transmitter which will be securely fastened to the shock cord in order locate the rocket after touchdown. The transmitter will be fastened to the cord because the carbon fiber affects it's ability to transmit, i.e. it diminishes its range.

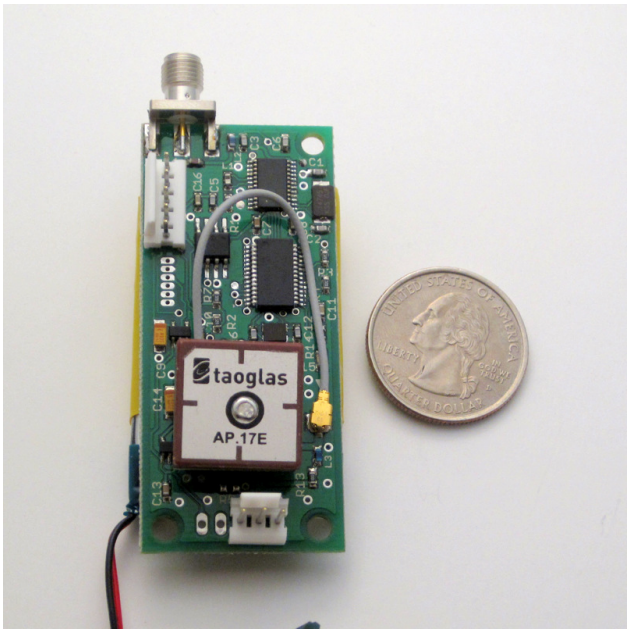

Figure 60: Big Red Bee Transmitter

3.4 Mission Performance Predictions

3.4.1 Mission Performance Criteria

The rocket and payload performance should be indicative of successful implementation of the design, build, and test process. The team understands that a safe and stable rocket flight is a prerequisite to any innovation in payload design. The following are quantitative requirements that must be met in simulation and testing to signify a safe competition flight:

- The rocket should attain a target altitude of 5,280 ft.
- The final drift of the rocket should be kept to a minimum to facilitate fast and simple recovery.
- The launch vehicle shall accelerate to a minimum velocity of 52 fps at rail exit.
- Each independent section of the rocket shall land with a kinetic energy of less than 75 ft.-lb$_f$.
- The launch vehicle shall have a minimum static stability margin of 2.0 at the point of rail exit.
- Following main engine cutoff and prior to apogee, the rocket should roll a minimum of 2 times around its main axis before performing a counter-roll and stopping in its initial rotational position.

3.4.2 MATLAB Flight Simulation

Production of an overall flight profile is crucial in understanding the role various launch conditions play on the flight targets. Theoretical results can be used to validate design choices and provide a benchmark for comparison with experimental data. For these reasons, a MATLAB script was created to simulate the entire rocket flight from launch to touchdown. The following sections detail the important components of the flight simulation.

3.4.2.1 Rocket Equations

The simulation numerically integrates the standard set of flight equations with thrust and drag to determine acceleration, velocity, and position over the course of the rocket's trajectory. For simplicity, only two dimensions are modeled–vertical (z) and horizontal (x)–though a third dimension could be readily added if needed. Table 6 defines the variables in Equation (3.11).

Table 6: Rocket Equations Symbol Definitions

Symbol	Definition
a_z	Vertical acceleration (m/s$\{2\}$)
a_x	Horizontal acceleration (m/s$\{2\}$)
v_j	Velocity in either the z or x direction (m/s)
v_d	Drag velocity (differs from total velocity due to wind)
j	Position in either the z or x direction (m)
ϕ	Angle of rocket axis relative to vertical (rad)
T	Thrust (N)
D	Drag (N)
W	Weight (N)
m	Rocket mass (kg)
w	Side wind velocity (m/s)
dt	Time step (s)
i	Index variable

$$a_{z,i} = \frac{(T - D)\cos\phi - W}{m_{i-1}} \tag{3.11a}$$

$$a_{x,i} = \frac{(T - D)\sin\phi}{m_{i-1}} \tag{3.11b}$$

$$v_{j,i} = v_{j,i-1} + (a_{j,i-1})(dt) \tag{3.11c}$$

$$j_i = j_{i-1} + (v_{j,i-1})(dt) + \frac{1}{2}(a_{j,i-1})(dt)^2 \tag{3.11d}$$

$$\cos\phi = \frac{v_z}{v_d} = \frac{v_z}{\sqrt{v_z^2 + (v_x + w)^2}} \tag{3.11e}$$

$$\sin\phi = \frac{v_x + w}{v_d} = \frac{v_x + w}{\sqrt{v_z^2 + (v_x + w)^2}} \tag{3.11f}$$

3.4.2.2 Drag

Drag force, D, is calculated as the sum of two separate sources of resistance: pressure drag, D_p, and skin friction, D_s (Equation (3.12)).

$$D = D_p + D_s; \tag{3.12}$$

Pressure Drag Pressure drag is given as Equation (3.13), where C_D is the drag coefficient, A is the largest cross-sectional area of the rocket, and the remaining variables are as described in Section 3.4.2.1. For a cylindrical rocket with a nose cone such as fabricated by VADL, the drag coefficient typically has a value close to 0.35; the apogee altitude of the subscale launch was found to be best approximated with a C_D of 0.27 (section 3.2.1).

$$D_p = \frac{1}{2}C_D\rho A v_d^2 \tag{3.13}$$

Skin Friction The equation for skin friction follows the same form as for pressure drag (Equation (3.14)), except the friction coefficient is generally much smaller than the drag coefficient. In which C_f is the friction coefficient and

A is the rocket's total surface area parallel to the flow[2],

$$D_s = \frac{1}{2} C_f \rho A v_d^2 = \frac{1}{2} C_f \rho (A_{cyl} + 4A_{fin}) v_d^2 \tag{3.14}$$

The value of the friction coefficient varies as a function of the Reynold's number and the state of the boundary layer. The Reynold's number for a flat plate is defined as in Equation (3.15), where L is the length of the rocket and ν is the kinematic viscosity of air[3.4.2.2]:

$$Re = \frac{v_d L}{\nu} \tag{3.15}$$

For Reynold's numbers less than 2×10^5, the flow is laminar, and the mean friction coefficient over the length of the plate is given by Equation (3.16)[3.4.2.2]:

$$C_f = \frac{1.328}{\sqrt{Re}}, Re < 2 \times 10^5. \tag{3.16}$$

For turbulent flow ($Re > 2 \times 10^5$), many correlations have been developed to approximate the skin friction coefficient; the simulation here uses the Prandtl-Schlichting formula[3]. Equation (3.17) is only valid for Reynold's numbers up to 10^7; while the fullscale vehicle will reach a maximum Reynold's number of $Re \approx 2 \times 10^7$, the correlation is assumed to hold for the entire simulation.

$$C_f = \frac{0.455}{[\log_{10}(Re)]^{2.58}}, 2 \times 10^5 < Re < 10^7 \tag{3.17}$$

The kinematic viscosity of air at 277K is about $1.36 \times 10^{-}5 \frac{m^2}{s}$, and the length of the fullscale rocket is around $2.5m$, leading to a laminar boundary layer only for velocities less than $\approx 4 \frac{m}{s}$. Therefore, the majority of the rocket's flight occurs with a turbulent boundary layer and augmented skin friction coefficient, though skin friction contributes about two orders of magnitude less than pressure drag to the overall drag force felt by the rocket.

3.4.2.3 Side Wind

Another consideration when evaluating the rocket's trajectory is the effect of a side wind. The simulation assumes a constant ground wind velocity acting in only the horizontal (x) direction. Wind enters the simulation in two ways: weathercocking or weathervaning, and drift from the parachute.

The wind is input as its speed at a reference height of 10 meters, high enough to ignore the boundary layer on the ground. A wind amplification scheme is followed that increases the velocity of the wind by Equation (3.18) based on altitude. Where w is wind velocity, z is height above ground level, and α is the wind speed amplification constant[4],

$$w = w_{ref}(\frac{z}{z_{ref}})^{\alpha} = w_{ref}(\frac{z}{10m})^{\frac{1}{7}} \tag{3.18}$$

With wind amplification established, the effect of weathercocking becomes apparent. The term "weathercocking" refers to a slow turning of the rocket into the wind as a result of a positive stability margin. While the fins are present to correct for any pitching motion of the launch vehicle, only very large axial velocities can prevent a gentle angling in the direction of the side wind. Weathercocking is important primarily during the motor burn phase of the launch because any angling of the motor tube causes the rocket to acquire an extra velocity in the direction opposite the wind. It is counterintuitive that the rocket would speed up when traveling into the wind, but acceleration generated by thrust is much greater than the resistive acceleration of the wind. As was discussed in Section 3.4.2.2, the wind does factor into calculation of the drag velocity. Refer to Figure 61 for a visual depiction of weathercocking; the black triangle represents the velocity vectors at the beginning of a time step, and the red lines show the resultant angle and drag velocity.

[2] Welty, J. R., Wicks, C. E., & Wilson, R. E. (1969). Fundamentals of Momentum, Heat, and Mass Transfer. New York: J. Wiley.

[3] https://www.cfd-online.com/Wiki/Skin_friction_coefficient

[4] Elliott, D.L., C.G. Holladay, W.R. Barchet, H.P. Foote, and W.F. Sandusky, 1986, Pacific Northwest Laboratory, Richland, WA. Wind Energy Resource Atlas of the United States

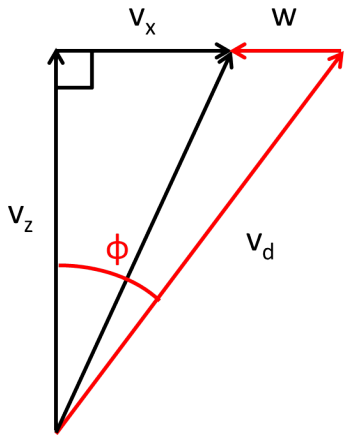

Figure 61: Instantaneous Flight Velocity Component Diagram

3.4.2.4 Standard Atmosphere Model

While the Earth's atmosphere varies little throughout the first mile of altitude, it is good practice to include an atmosphere model applicable to much greater altitudes. Therefore, the International Standard Atmosphere[5] is used in the simulation, the main output of which is air density (though temperature and pressure are also calculated in the process). The launch pad elevation, z_0, is taken as an input, and the 1976 U.S. Standard Atmosphere is interpolated to estimate the initial density ρ_0[6]. The ambient ground air temperature is also an input and varies with altitude as Equation (3.19a), where T_0 is the ground temperature, z is the altitude, and β is a constant. At altitudes below the tropopause (11 km), temperature decreases linearly by 6.5°C for every 1000 meters in altitude[3.4.2.4]. The local pressure is then calculated from Equation (3.19b), where R is the gas constant ($286.9 \frac{J}{kg-K}$ for air), and the local air density comes from Equation (3.19c).

$$T = T_0 - \beta \frac{z}{1000}, \quad \beta = 6.5 \tag{3.19a}$$

$$p = p_0 (\frac{T}{T_0})^{\frac{g}{R\beta}}, \quad g = g_0 (\frac{r_0}{r})^2, \quad r = r_0 + z_0 + z \tag{3.19b}$$

$$\rho = \frac{p}{RT} \tag{3.19c}$$

3.4.2.5 Compressibility

Compressibility effects on air density are assumed to be negligible under Mach 0.3[7]. The maximum fullscale launch velocity approaches Mach 0.55, so compressibility must be considered. The stagnation equations for isentropic flow could be employed to deduce the effective change in air density[8]. However, because the effective density is only used for the pressure drag calculation (Section 3.4.2.2, a correction for the drag coefficient will be used instead[9]. In Equation (3.20a), $C_{d,0}$ is the drag coefficient at zero velocity, M is the Mach number (Equation (3.20b), with a the local speed of sound, γ the specific heat ratio, and T the local temperature).

$$Cd = \frac{C_{d,0}}{\sqrt{1 - M^2}} \tag{3.20a}$$

$$M = \frac{v_d}{a} = \frac{v_d}{\gamma RT} \tag{3.20b}$$

[5] M. Cavcar, The International Standard Atmosphere (ISA), Anadolu University, Turkey, 2000.
[6] U.S. Standard Atmosphere, 1976, U.S. Government Printing Office, Washington, D.C., 1976
[7] https://www.grc.nasa.gov/www/k-12/airplane/machrole.html
[8] https://www.grc.nasa.gov/WWW/BGH/isentrop.html
[9] Cramer M.S. (2002) Foundations of fluid mechanics. Cambridge University Press.

3.4.2.6 Motor Burn Profiles

The launch is dictated by the published thrust and mass profile for the Loki Research L1400 motor[10]. Figures 62a and 62b display the experimental data input to the simulation.

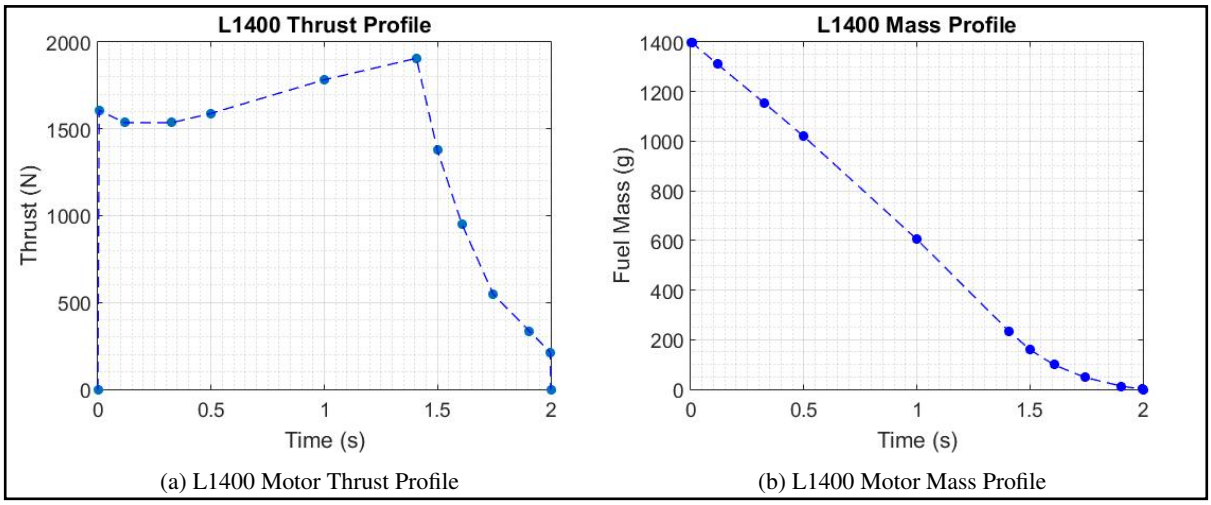

(a) L1400 Motor Thrust Profile (b) L1400 Motor Mass Profile

Figure 62: Loki Research L1400 Motor Data Profiles

The published data features points spaced by time periods greater than the time step of the model, and the points do not correspond exactly to times that occur during the simulation. Therefore, as shown by the dashed lines in Figure 62, the data is linearly interpolated to determine thrust and fuel mass values at times between two given points.

3.4.2.7 Parachute Deployment

The fullscale flight features the deployment of two parachutes: a drogue with diameter of 2 ft. and a main with diameter of 8 ft. The drogue is released soon after apogee to decrease the launch vehicle's terminal velocity; this reduces the force on the U-bolts upon main parachute deployment. The simulation accepts either a time-after-apogee or an altitude input to initiate drogue deployment. Main parachute deployment is signaled by an altitude input, likely near 800-1000 ft to minimize drift but still allow the system to achieve its terminal velocity. Neither parachute opens instantly, so an opening time for each is factored into the simulation as well. During this time period, the parachute diameter is assumed to expand linearly so that the drag area increases quadratically.

The same equations as in Section 3.4.2.1 are used to track the system's acceleration, velocity, and position over time. However, because of the relatively slow velocity, the parachute is assumed to remain in an upright position such that horizontal and vertical movement can be treated independently. A separate drag coefficient is applied to the x- and z-components, and the drag area can be calculated simply from the hemispherical shape of the parachute. While separating the components may not exactly describe experimental results, any deviations are overwhelmed by the unpredictable motion generated as the parachute deploys. The latter is not simulated; overall effects are instead captured empirically by the chosen drag coefficients.

3.4.3 MATLAB Payload Experiment Simulation

The payload experiment performed for the 2016-2017 launch is also capable of being simulated. The roll control experiment is modeled simultaneously with the rocket's trajectory. The cold gas thruster system was designed to not interfere with the rocket's flight, so the two simulations are treated independently despite happening concurrently. All of the rolling and counter-rolling of the launch vehicle occurs following a specified time after MECO and before the rocket reaches apogee.

[10] http://www.thrustcurve.org/motorsearch.jsp?id=403

3.4.3.1 Rotation Equations

Standard Newtonian physics are employed to simulate the rotation of the rocket. The equations in Equation (3.21) are numerically integrated at the same time as Equation 3.11 with an identical time step. Only a single rotational dimension is examined (see Figure 63[11]); perturbations in the pitch and yaw directions are ignored but may factor into empirically determined drag coefficients. Table 7 defines the variables in Equation 3.21.

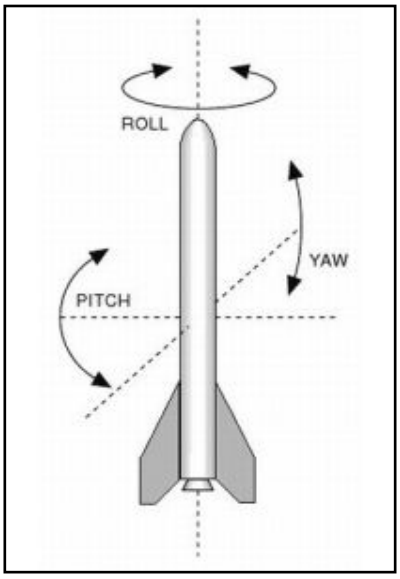

Figure 63: Roll, Pitch, and Yaw of a Rocket

Table 7: Rotational Equations Symbol Definitions

Symbol	Definition
α	Angular acceleration (rad/s^2)
ω	Angular velocity (rad/s)
θ	Angular position (rad)
τ	Net torque (N-m)
τ_{cg}	Thrusting torque (cold gas thrusters, N-m)
τ_d	Resistive torque (drag, N-m)
F	Force (N)
r	Length of moment arm (m)
I	Rotational inertia (kg-m^2)
dt	Time step (s)
i	Index variable

[11] http://sciencelearn.org.nz/Contexts/Rockets/NZ-Research/Rocket-control

$$\tau = Fr = I\alpha \tag{3.21a}$$

$$\alpha_i = \frac{\tau_{cg} - \tau_d}{I} \tag{3.21b}$$

$$\omega_i = \omega_{i-1} + (\alpha_{i-1})(dt) \tag{3.21c}$$

$$\theta_i = \theta_{i-1} + (\omega_{i-1})(dt) + \frac{1}{2}(\alpha_{i-1})(dt)^2 \tag{3.21d}$$

3.4.3.2 Resistive Torque

Rotation of the rocket is opposed by three different forces, mostly involving resistance to fin movement: pressure drag (τ_q), skin friction (τ_s), and jet-fin interaction ($\tau_j f$), and the total resistive torque (τ_d) is the sum of the individual torques (Equation (3.22).

$$\tau_d = \tau_q + \tau_s + \tau_{jf} \tag{3.22}$$

Pressure Drag Of the three torques, pressure drag is the most obvious resistance and is significant because of the large axial velocity of the launch vehicle. The side wind can be ignored as it net effect is zero for a rocket with symmetrical fins. As the rocket rolls, a resistive moment acts on the fins, the value of which increases radially outward on the fin. An integration must be performed across the height of the fin to calculate the total torque based on the dynamic pressure. The fin is assumed to be a flat plate with dimensions given in Figure 64.

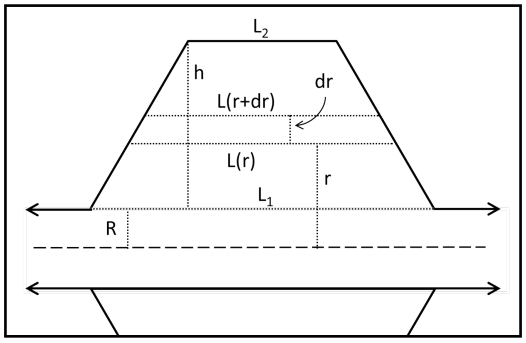

Figure 64: Trapezoidal Fin Schematic

Following the procedure outlined in the OpenRocket documentation[12], we begin with the definition of pressure drag and prepare an integral for the resistive torque, where η is the instantaneous angle of attack of the fin into the flow ($\eta = 0$ for non-rotating, vertically-aligned fins), v_0 is the total velocity of the fin v_d is the axial velocity, and v_ω is the horizontal velocity:

$$\begin{aligned}
\tau_q = Fr &= \frac{1}{2}C_{d,fin}\rho A v_0^2 \eta = \frac{1}{2}C_{d,fin}\rho\left(\sqrt{v_d^2 + v_\omega^2}\right)^2 rA(r)\frac{v_\omega}{v_d} \\
&= \frac{1}{2}C_{d,fin}\rho v_d^2 rA(r)\frac{\omega r}{v_d}, \qquad v_d \gg v_\omega \Rightarrow v_0 \approx v_d \\
&= \frac{1}{2}C_{d,fin}\rho\int_R^{R+h}(v_d)(\omega r)r[L(r)]dr \\
&= \frac{1}{2}C_{d,fin}\rho v_d\omega\int_R^{R+h} r^2\left[\frac{(L_1 - L_2)(r-R)}{-h} + L_1\right]dr
\end{aligned}$$

[12] S. Niskanen, OpenRocket technical documentation, for version 13.05, 2013.

The magnitude of τ_q varies linearly with both angular velocity and axial velocity and depends on the geometry of the fin, which arises as the constant Z_{fin}. Equation (3.23) describes the total pressure drag acting on four fins that opposes the torque from the cold gas thrusters.

$$\tau_q = (4 \text{ fins}) \left[\frac{1}{2} C_{d,fin} \rho v_d \omega Z_{fin} \right] \tag{3.23}$$

$$Z_{fin} = \int_R^{R+h} \left[\frac{(L_1 - L_2)(r - R)}{-h} + L_1 \right] r^2 dr$$

$$Z_{fin} = \frac{1}{4} \frac{L_2 - L1}{h} \left[(R+h)^4 - R^4 \right] + \frac{1}{3} \left(L_1 - \frac{L_2 - L1}{h} \right) \left[(R+h)^3 - R^3 \right]$$

Skin Friction Skin friction is calculated in the same manner with the same friction coefficient as in Section 3.4.2.2, though the area relevant solely to resistive torque excludes the fins. The viscous drag occurs on the body of the cylinder, so the moment arm length is the radius of the rocket. Equation (3.24) is used.

$$\tau_s = F_s R = \frac{1}{2} C_f \rho A_{cyl} v_d \omega R \tag{3.24}$$

Jet-Fin Interaction The final source of resistive torque, jet-fin interaction, refers to aerodynamic effects from vortices created by interference between the cold gas thruster stream and the axial flow. The magnitude of the effect is not well understood, but it has been approximated for a certain set of conditions through experiment[13]. Just as in other forms of drag, jet-fin interaction is characterized by a coefficient, C_{CT}. The countertorque coefficient is defined by Equation (3.25), where τ_{jf} is the countertorque due to the interaction vortices, A is the cross-sectional area of the vehicle, and d is the vehicle diameter[13].

$$C_{CT} = \frac{\tau_{jf}}{q_\infty A d} \tag{3.25}$$

However, if the countertorque coefficient is known from other methods, the torque can be computed directly from Equation (3.25). A correlation between the coefficient and the jet-to-freestream dynamic pressure ratio, J, has been established for $J < 40$[13]. In Figure 65, the solid blue curve best approximates the conditions of the VADL rocket, namely its subsonic nature and the fins' uncanted alignment.
Unfortunately, the launch vehicle operates at values of $J > 40$ for all but the first 2 seconds of the experiment, so Figure 65 cannot be used without extrapolation. Instead, a factor F_{jf} is applied to the resistive torque, in which F_{jf} accounts for all jet-fin interaction and any other inconsistencies in drag. As a result, Equation (3.22) becomes the following:

$$\tau_d = \tau_q + \tau_s + \tau_{jf} \approx F_{jf}(\tau_q + \tau_s) \tag{3.22}$$

[13] S. Beresh, et al., Planar Velocimetry of Jet/Fin Interaction on a Full-Scale Flight Vehicle Configuration, AIAA Journal (45-8), 2007.

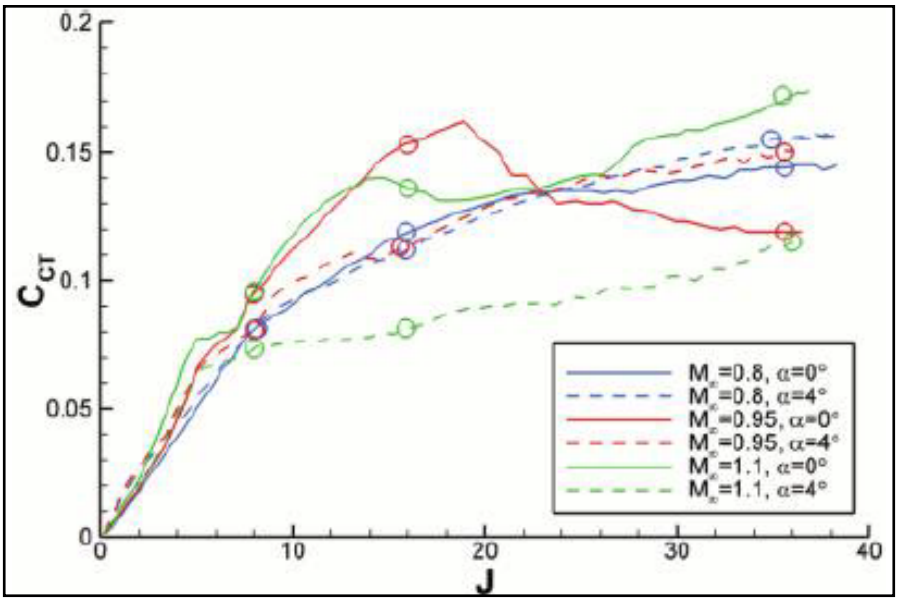

Figure 65: Jet-Fin Interaction Countertorque Coefficient

3.4.3.3 Computational Modeling

The results of subscale flight allowed VADL to realize the significance that the axial flow plays in the damping of roll induction. To better characterize these effects, Computational Fluid Dynamics (CFD) models were run using ANSYS Fluent, a popular modeling software. The goal of these simulations was to visualize the resistive torque on the fins via a pressure distribution plot, and to verify the mathematical models that VADL used to estimate the resistive torque as a function of angular velocity.

Pressure Distribution To visualize the resistive torque caused by the axial flow, it was necessary to visualize the pressure distribution across a plane perpendicular to the main axis of the rocket that passes through the fins. Figure 66 shows the distribution on this plane at varying angular velocities. The simulation was run with a fluid rotating at a varying angular velocity and a constant axial velocity of 100 m/s.

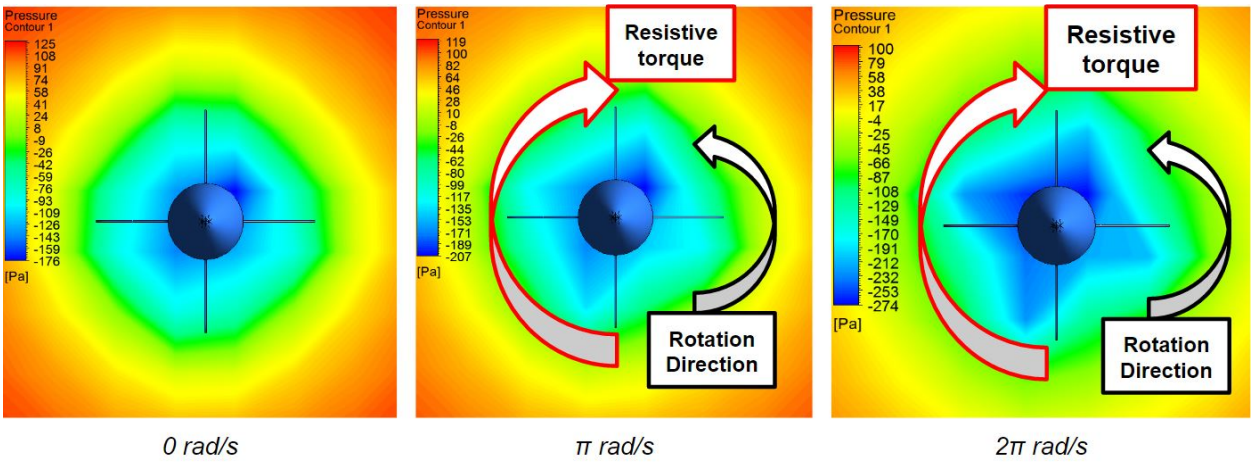

Figure 66: Pressure Distribution at Fins for Various Angular Velocities

As discussed in Section 3.4.3.2, the dynamic pressure on either side of the fins has a significant effect on the ability of the rocket to rotate. This CFD analysis shows the pressure difference that forms across the fins of the rocket during

rotation which adds to this resistive torque. To quantify this effect, a moment analysis was performed on the rocket about its main axis for various angular velocities. The results were compared to the damping coefficient calculated from Equation (3.23), which found a relationship between the damping torque and the angular velocity. The resistive torque is a function of both angular and axial velocity, so to describe the torque as a function of angular velocity alone, an axial velocity of 100 m/s was used in all calculations. The damping coefficient was found to be $T_d = .16\omega$. Figure 67 shows the results of the torque analysis from ANSYS, which produced a damping coefficient of .15, which supports the mathematical model and therefore the team's justification for the unsuccessful roll experiment.

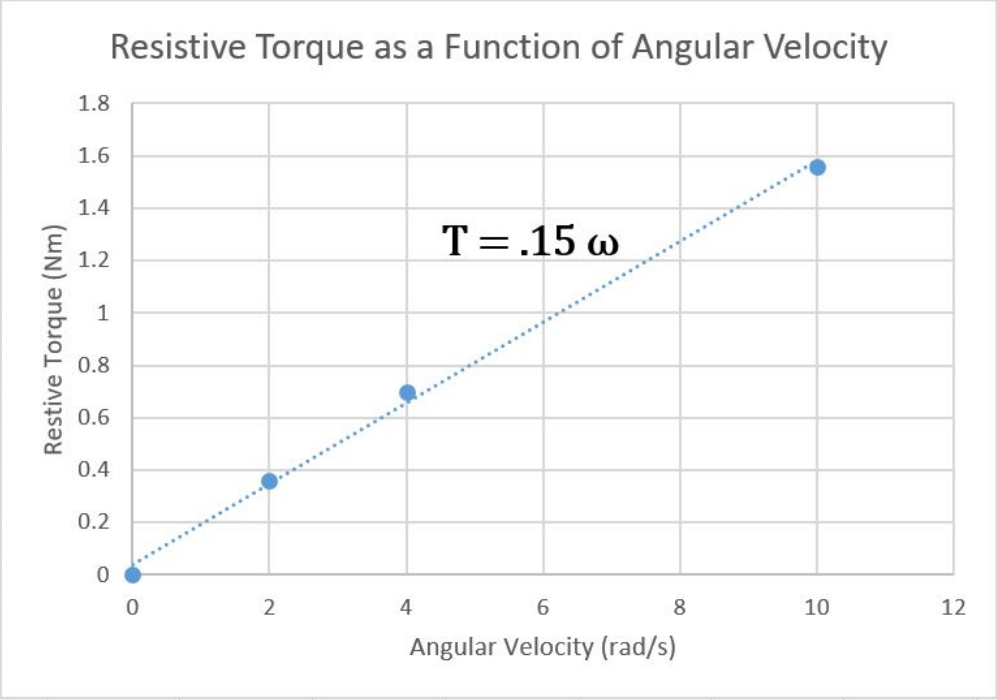

Figure 67: Damping Coefficient at an Axial Speed of 100 m/s

3.4.3.4 Pulsing Thrust

The payload experiment can be completed with the application of two different thrust conditions: pulsed and continuous, where continuous thrust refers to a single pulse applied for any extended period of time. Pending design of a control scheme and rigorous ground-based testing, as well as results from additional flight of the payload, non-continuous thrust must be able to be simulated. Therefore, the simulation has the capability for any number of consecutive pulse conditions; a duty cycle is carried out until a condition is met (e.g. time period, angular velocity, angular position, etc.), a second duty cycle is applied until a second condition is met, and so on. The process continues until all specified cycles are completed or the launch vehicle reaches apogee.

Whenever the cold gas thrusters are activated, the solenoid valve must be actuated at least twice-at the beginning and end of the pulse. Actuation of the solenoid valve is not an instantaneous event, so the mass flux and thrust should not be instantly toggled between zero and full output. The valve is therefore assumed to open and close quadratically such that the mass flux and thrust are directly proportional to the second power of the time since actuation:

$$T, \dot{m} \propto (t - t_{actuation})^2 \tag{3.26}$$

A different function may better capture the boundary properties of the solenoid valve performance, but a linear approximation is sufficient for the short time scale of actuation. A fast-actuating solenoid was chosen specifically to avoid the variable and unknown flow properties involved with a valve in between states.

3.4.4 Example Simulation

To illustrate the type of results generated by the simulation, a case study is presented here. Table 8 shows the input parameters to the example simulation.
The flight conditions are intended to be representative of a typical fullscale flight under moderate conditions; however, no conclusions regarding future success or failure of the competition launch should be drawn from this example. Analysis of the subscale launch is also omitted from this section in favor of the previous analysis in Section 3.2.1.

Table 8: Example Simulation Input Parameters

Input Parameter	**Value**	**Notes**
Flight Parameters		
Diameter	5.5 in	
Length	94.75 in	
Mass	30.3 lb	13.7 kg
Side wind	10 mph	
Launch angle	5°	Into wind
Drag coefficient	0.27	See Section 3.2.1
Motor	Loki L1400	See Section 3.4.2.6
Single fin area	0.0237 m^2	
Launch rail length	12 ft	
Elevation	600 ft	Huntsville, AL
Temperature	74°F	April in Huntsville
Drogue parachute	2 ft elliptical	
Drogue C_D	1.5/0.3	Vertical/horizontal
Drogue deploy	1 s after apogee	
Drogue opening time	1 s quadratically	
Main parachute	8 ft toroidal	
Main C_D	2.2/0.3	Vertical/horizontal
Main deploy	600 ft altitude	
Main opening time	3 s quadratically	
Payload Parameters		
Thrust	15 N	7.5 N $\times$ 2 thrusters
Moment arm	2.13 in	
1st pulse cycle	500 ms on, 500 ms off	Clockwise
1st cutoff condition	$\theta = 4\pi$	2 rotations
2nd pulse cycle	250 ms on, 250 ms off	Counterclockwise
2nd cutoff condition	$\theta = \frac{\pi}{8}$	Positive value close to zero chosen arbitrarily for simulation purposes
3rd pulse cycle	Continuous thrust	Clockwise
3rd cutoff condition	$\lvert\omega\rvert < 0.05$ rad/s	Rotation nearly stopped
Solenoid actuation time	30 ms	
Z_{fin}	5.04×10^{-4}	
Fin drag coefficient	1.28	Flat plate[14]
Air tank mass loss	22.24 g/s	Based on regulator and nozzle

As the simulation runs, milestones along the flight path are indicated on the display screen to give the user a sense of the progress of the simulated launch vehicle. A time stamp is printed with each event to facilitate analysis involving initial conditions, completion of the payload experiment, and the final state of the rocket. Figure 68 illustrates the simulation output.

```
Wind velocity = 10 mph
Launch angle = 5 degrees
Mass = 30.3 lb


0.00 s, Liftoff

0.27 s, Launch rail cleared; Rail exit velocity = 90.36 fps

2.00 s, MECO; Velocity at MECO = 626.74 fps

2.50 s, Roll initiated

9.00 s, Counter-roll initiated

13.25 s, Stopping mechanism initiated

13.43 s, Roll stopped; All thrusters off

17.03 s, Apogee; Altitude at apogee = 4735 ft

18.03 s, Drogue parachute deployed

83.49 s, Main parachute deployed, Drogue velocity = -58.59 ft/s

86.49 s, Parachute fully opened

135.52 s, Touchdown!, Main velocity = -14.01 ft/s

Apogee = 4735 ft
Final drift = 554 ft
Max velocity = 627 ft/s
Max acceleration = 13.84 g's
```

Figure 68: MATLAB Simulation Output

In addition to real-time output of launch checkpoints, the simulation environment stores all flight variables over the duration of the flight so that they can be accessed following completion of the simulation. Figure 69 shows examples of the post-flight analysis that can be performed on each simulation.

The trajectory plot is the most intuitive output from the flight simulation (Figure 69a); both axes are position, so the curve represents the expected path of an associated rocket launch. Regarding this particular set of conditions, it is clear that the side wind has decreased the potential apogee through weathercocking. Furthermore, the drift is relatively sensitive to the main parachute deployment altitude in that the system drifts about 150 feet for every 100 feet above ground level that parachute is released. Drift correlated with deployment altitude will be explored in Section 3.4.5.3. The second plot (Figure 69b), the acceleration of the launch vehicle, showcases four clear milestones during the flight. The thrust profile manifests itself within the first two seconds of flight; at MECO, drag force adds 20% to the acceleration of gravity. Deployment of the drogue parachute at 18 seconds puts little stress on the recovery subsystem, and the system reaches steady quickly. Significant stress is applied to the U-bolts constraining the main parachute during deployment at 85 seconds, but the system is able to withstand the load and ensure survivability of the launch vehicle and IMU data (see Section 3.1.3.4 for a stress analysis on the recovery system U-bolts).

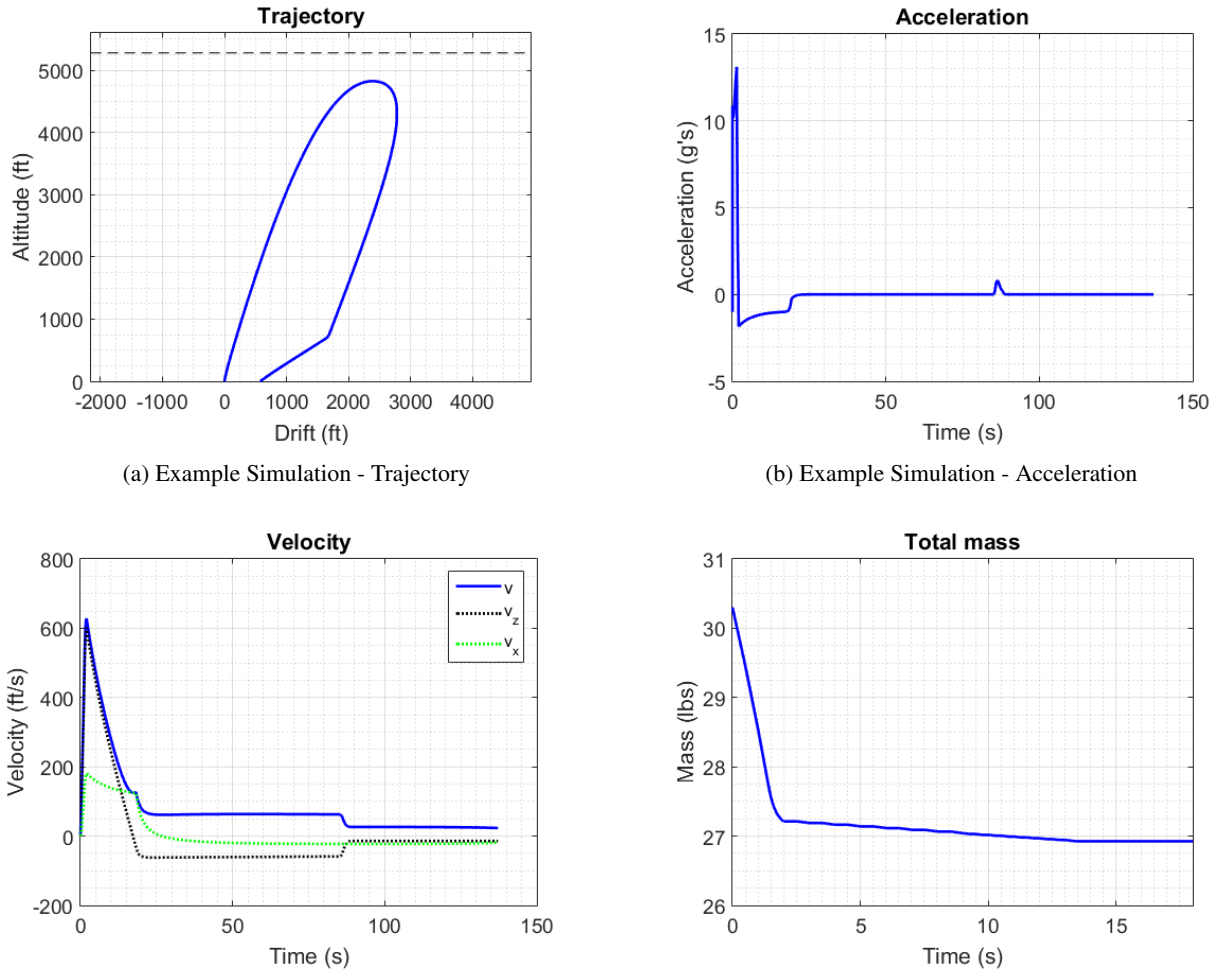

(a) Example Simulation - Trajectory

(b) Example Simulation - Acceleration

(c) Example Simulation - Velocity

(d) Example Simulation - Mass

Figure 69: Example Simulation - Rocket Flight

Figure 69c in the lower left simply mirrors the acceleration profile. Both the vertical and horizontal components of velocity are depicted, and one can see the reduction in terminal velocity from the drogue to the main parachute. In addition, the contribution of wind becomes clear, as the sideways velocity rapidly decreases post-apogee to match the wind speed. Finally, the mass profile in Figure 69d shows only pre-apogee flight as the total mass remains constant following completion of the payload experiment. Throughout the motor burn phase, the launch vehicle exhausts nearly 3.1 lbs of solid fuel, causing the center of gravity to move towards the nose. During the time period in which the cold gas thrusters fire, mass is lost from the air tank as well, though the exact amount is undetermined and will vary based on flight conditions and control capabilities. The air tank holds 0.76 lbs of air and nitrogen at 4000 psi, so the rocket mass should not decrease by more than about 0.5 lbs, assuming not all the air is needed to successfully achieve the desired roll and counter-roll.

As was previously mentioned in Section 3.4.3, the roll control experiment is modeled in parallel with the rocket flight. Figure 70 illustrates the effects of various pulse conditions performed within the constraints of the experiment goal. While ideally the rocket would achieve two rotations and return to its original angular position, the MATLAB simulation is employed only to guide the control system programming and should not be analyzed literally. In other words, the simulation is a tool used to suggest control parameters and predict feasibility of the experiment.

This example simulation uses three different pulse conditions: 0.5 second pulses to roll the vehicle two rotations, 0.25 second pulses to perform a counter-roll until the vehicle approaches its initial position, and continuous thrust to

negate the angular momentum of the rocket within a given tolerance. The varying pulse duration is clear in Figure 70a, which reports the angular acceleration of the rocket as it responds to torque applied by the cold gas thruster system. The angular velocity (Figure 70b increases accordingly with the angular acceleration; when the thrusters are off (in between pulses), the angular velocity drops significantly due primarily to the large dynamic pressure of the air surrounding the fins (Equation (3.23)). During the counter-roll (9-13 seconds), the ”minimum” angular speed in between pulses is much greater than during the first phase of the experiment. This is because the axial velocity of the launch vehicle has decreased substantially 7 seconds post-MECO, resulting in smaller resistive torque and an easier return to initial angular position. Regardless of the decrease in pressure drag, less than a quarter-second of continuous thrust is required to stop all rotation. Angular position (Figure 70c) is shown to increase and decrease in a stair-step manner with each pulse. It is important to note that attaining exactly 2 rotations is quite difficult–in fact, the mark will likely occur during the middle of a pulse. While the simulation is built to only allow full pulse lengths, the actual control scheme applied in flight may cut a pulse short once the required rotation is detected. In a situation such as this, the simulation serves more as a guide than the rule.

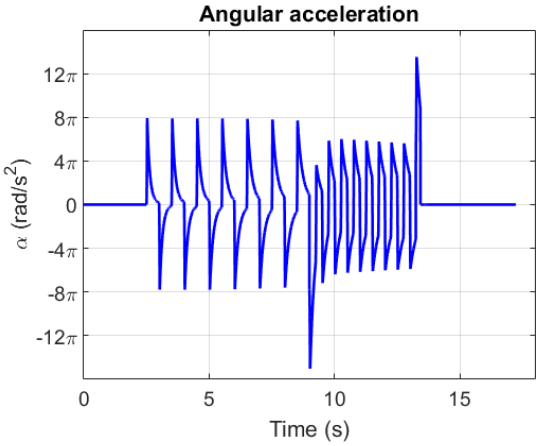

(a) Example Simulation - Angular Acceleration

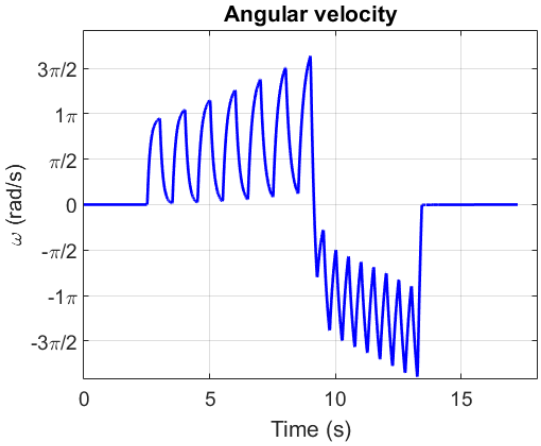

(b) Example Simulation - Angular Velocity

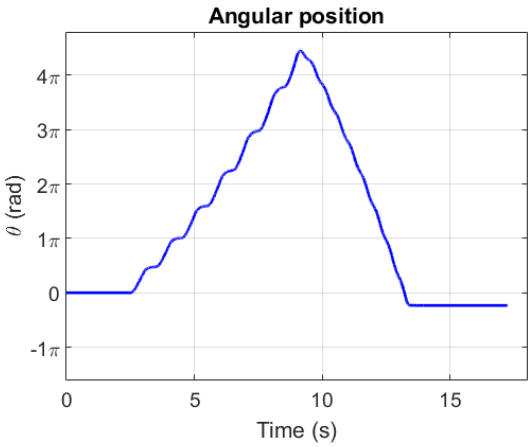

(c) Example Simulation - Angular Position

Figure 70: Example Simulation - Payload Experiment

3.4.5 Fullscale Flight Predictions and Sensitivity Analysis

The simulation described in Section 3.4.2 was validated by the subscale flight results (see Section **??**) and can therefore be used to predict performance of the fullscale flight vehicle. A supplemental simulation was employed to obtain information regarding the stability margin and to verify the relatively straight flight of the rocket. Parameters

such as side wind velocity, exact motor output, and mass, however, will not be known exactly until final rocket assembly or after launch, but they factor into important design choices. Therefore, ranges of these parameters and their effects on the flight must be explored to validate the chosen design and verify that the launch and payload experiment can be completed successfully.

3.4.5.1 Landing Kinetic Energy

One of the mission requirements, defined in Section 3.4.1, is that the landing kinetic energy of all independent and tethered components must not exceed 75 ft-lbs. The VADL rocket has three sections: nosecone/payload (forward), avionics, and tail, all of which are tethered together. With the 8-foot Iris Ultra main parachute, the terminal velocity of the rocket is approximately 14 fps, based on the expected mass of 30.3 lbs. Table 9 details the landing kinetic energy of each of the three sections. Even if the launch mass is significantly greater than anticipated, none of the sections will land with more than 75 ft-lbs of energy.

Table 9: Landing Kinetic Energy of Components

Component	**Estimated Mass (lb)**	**Landing Energy (ft-lb)**
Nosecone/Payload	11.6	36.4
Avionics	7.0	22.0
Tail	11.7	36.7

3.4.5.2 Center of Gravity, Center of Pressure, and Stability Margin

Calculations of the static stability margin arise from simulation in Rocksim and CFD. Figure 71 shows the estimated locations of the center of gravity and center of pressure. With the CG at 50.4 inches and the CP at 62.3 inches from the nose, the static stability margin on the launch pad is 2.16 ($(62.3 - 50.4)/5.5 = 2.16$). Following motor burn on the launch rail, the stability margin increases to 2.29 at rail exit. Figure 72 describes the variation in stability margin as the launch vehicle travels from the pad to apogee.

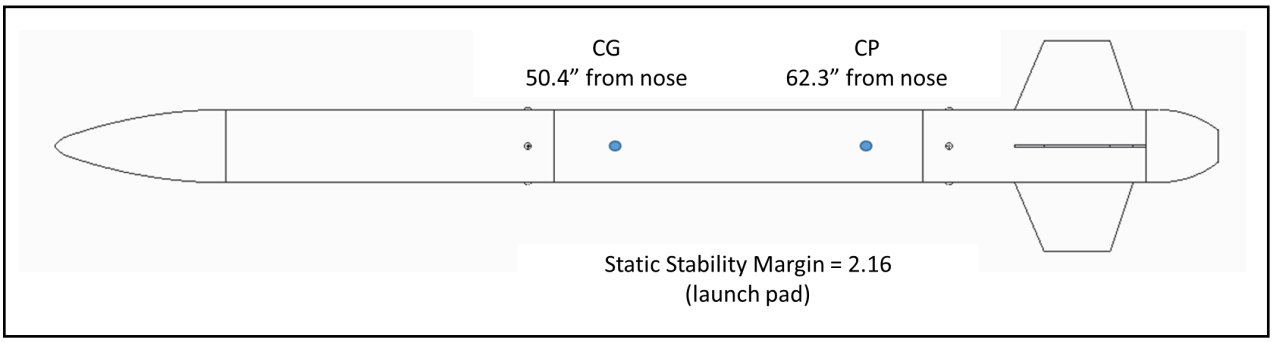

Figure 71: Effect of Thrust on Experiment Time

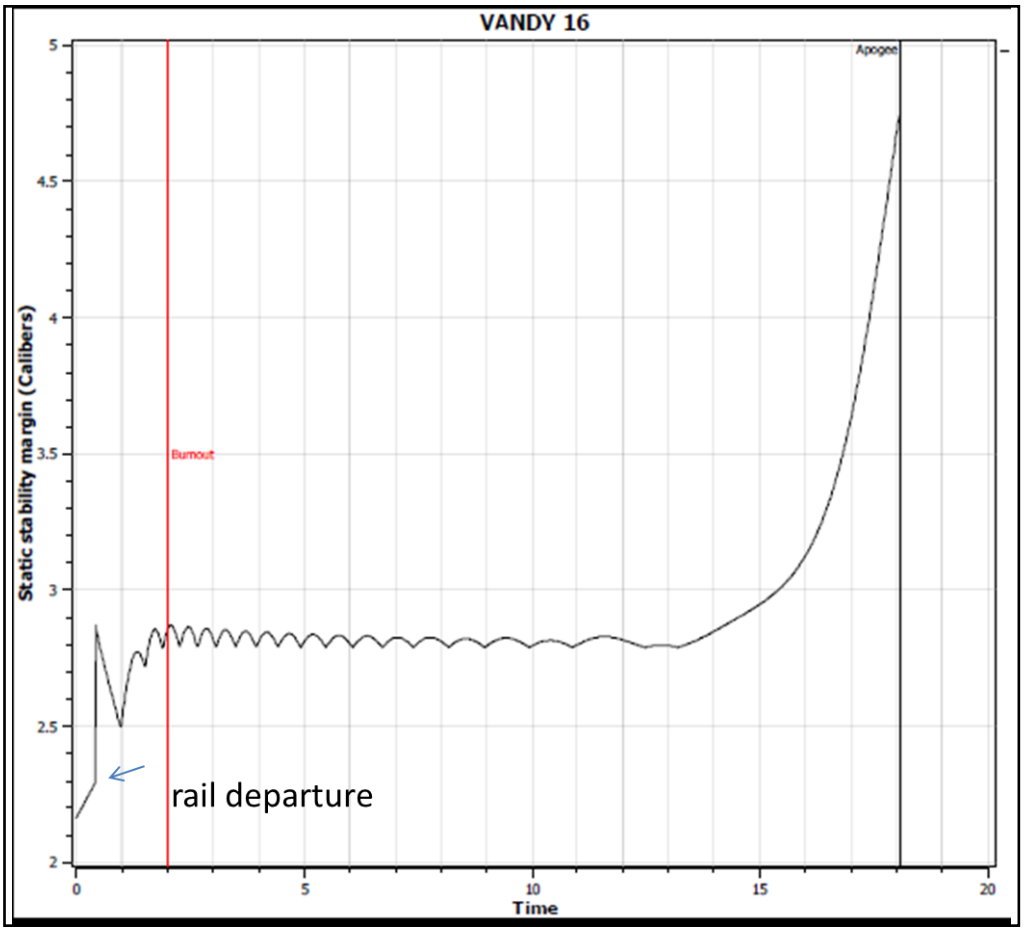

Figure 72: Variation in Static Stability Margin

3.4.5.3 Side Wind

Side wind is notably one of the most difficult aspects of the launch for which to prepare, and little can be done to mitigate process hazards arising from non-steady and non-uniform wind. The launch vehicle must be robust enough to deal with a range of wind conditions, and a wind speed ceiling must be established at which the launch is canceled. Historically, the maximum wind speed for launch in the NASA Student Launch competition has been 20 mph, and VADL will adhere to this limit in all test and competition launches. Assuming the launch vehicle is able to near its targeted apogee in any wind speed (this is not strictly true, but it is a reasonable assumption for the argument), the primary hazard posed by side wind is the extreme drift conditions. Parachutes are chosen for the rocket to minimize drift and landing speed under moderate weather conditions, a strategy that backfires with large wind speed. Table 10 indicates the final values of drift for winds of 0, 5, 10, 15, and 20 mph for both vertical launches and launches angled 5 degrees into the wind, and Figure 73 graphically demonstrates the effect of the side wind on drift. Furthermore, apogee altitude is affected by the magnitude of the side wind as well; simulation results are shown in Figure 74. The launch angle will be chosen anywhere between 0 and 5 degrees depending on the wind conditions on launch day.

Table 10: Drift for Various Wind Conditions

Wind speed (mph)	Drift (ft) - vertical launch	Drift (ft) - 5 degree launch
0	0	-1948
5	-188	-1419
10	328	-792
15	869	-188
20	1388	379

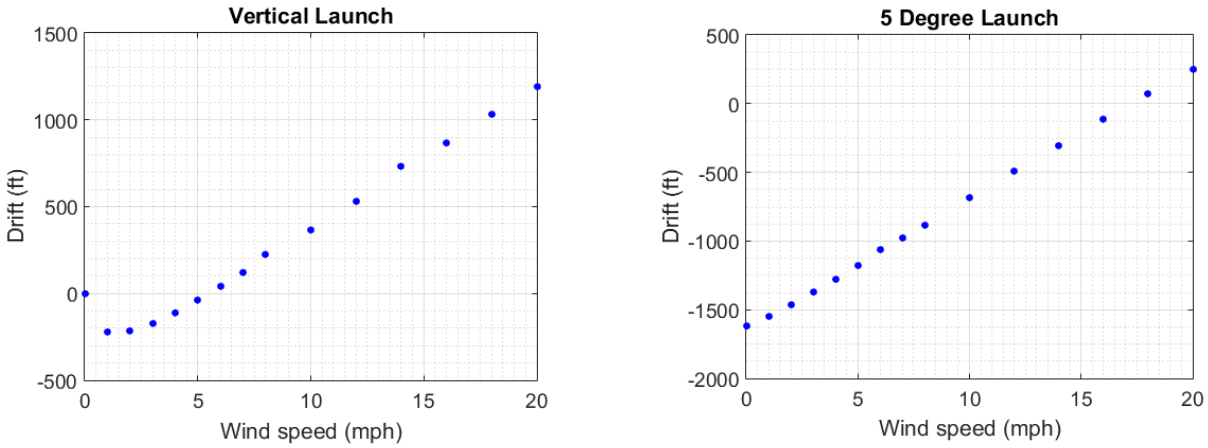

(a) Drift versus Side Wind - Vertical

(b) Drift versus Side Wind - 5 Degrees

Figure 73: Effect of Side Wind on Drift

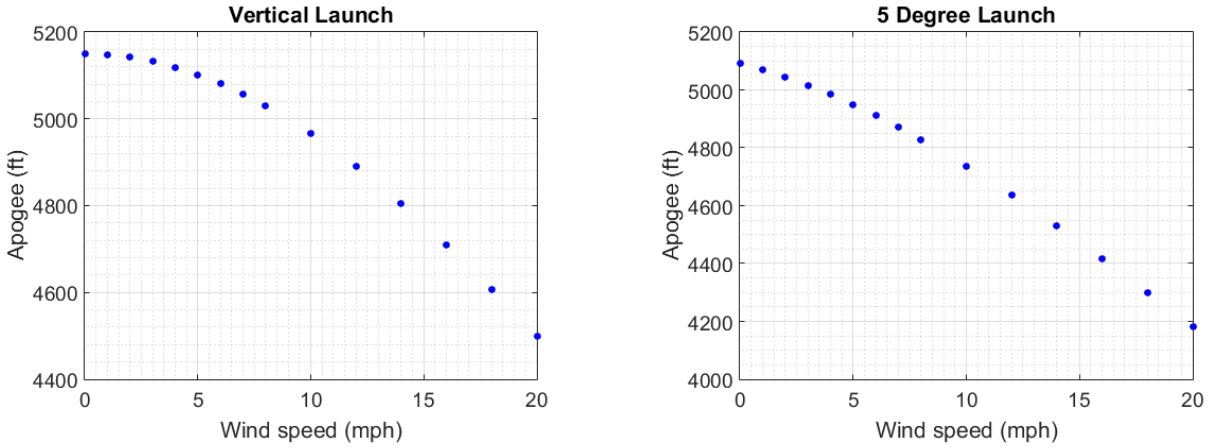

(a) Apogee versus Side Wind - Vertical

(b) Apogee versus Side Wind - 5 Degrees

Figure 74: Effect of Side Wind on Apogee

3.4.5.4 Motor Thrust Variability

Another parameter that is unknown prior to launch is the thrust output by the motor. While the published data for the motor must be taken at face value in the absence of statistical testing, knowledge of the sensitivity of the flight to the motor output is important. In particular, because a target altitude exists and overshooting the target by a few hundred feet is not allowed by competition rules, a plot of altitude based on actual thrust is useful. Figure 75 shows the expected apogee versus the percentage difference in thrust compared to the published data (Section 3.4.2.6). These data were produced for a vertical simulation with no wind, so they represent ideal launch conditions. The maximum

altitude of the launch vehicle varies approximately 80 feet for each 1% increase or decrease in thrust compared to published values. Assuming the actual thrust profile falls within 5% of expected thrust under moderate weather conditions, the flight should be considered a success in terms of the target altitude.

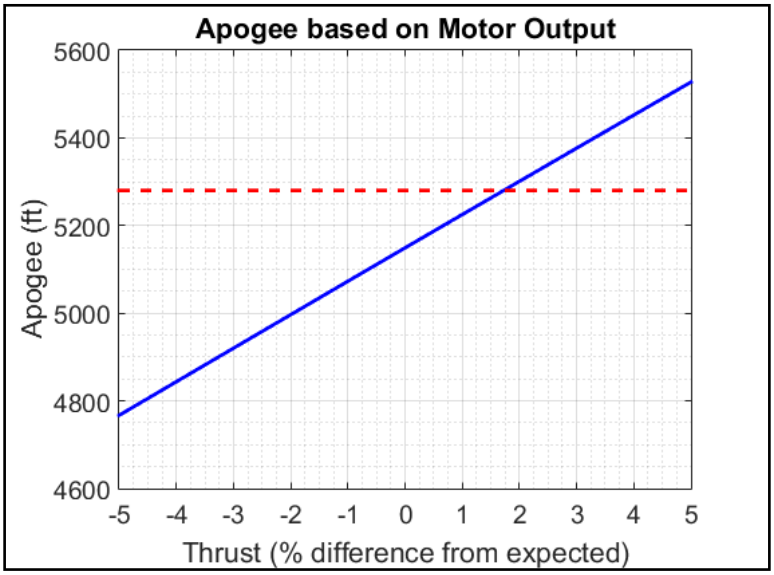

Figure 75: Variation in Apogee due to Non-Ideal Thrust

3.4.5.5 Launch Mass Variability

Finally, a parameter that will be known in the field prior to launch is the exact mass. The apogee altitude is quite sensitive to launch mass, and the capability to add a ballast near the center of gravity is designed into the vehicle. Figure 76 illustrates the variation in apogee with total mass. The mass range explored is centered around the expected mass of 30.3 lb, and the simulations are run with a vertical launch and no wind.

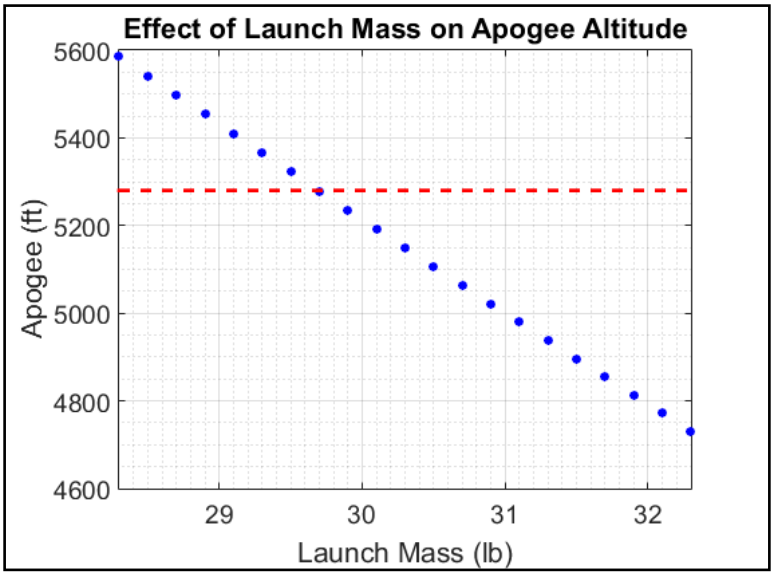

Figure 76: Variation in Apogee due to Changes in Launch Mass

3.4.5.6 Cold Gas Thruster Variability

In addition to flight variables, the amount of thrust produced by the cold gas thrusters cannot not characterized easily for in-flight application. Consequently, the design thrust must be greater than the required thrust in order to complete the payload experiment between MECO and apogee. The experiment window is approximately 15 seconds (Figure 68), but a short time should be reserved immediately after MECO to ensure temporal separation of the motor burn and the experiment. Moreover, the rocket slows down and pitches as it approaches apogee, rendering the last few pre-apogee seconds unusable in terms of roll control. As a result, the experiment window is actually around 11 or 12 seconds instead of 15. Figure 77 was produced to get an idea of the thrust needed to comfortably complete the experiment; 15 N, or 7.5 N per cold gas thruster appears to be sufficient.

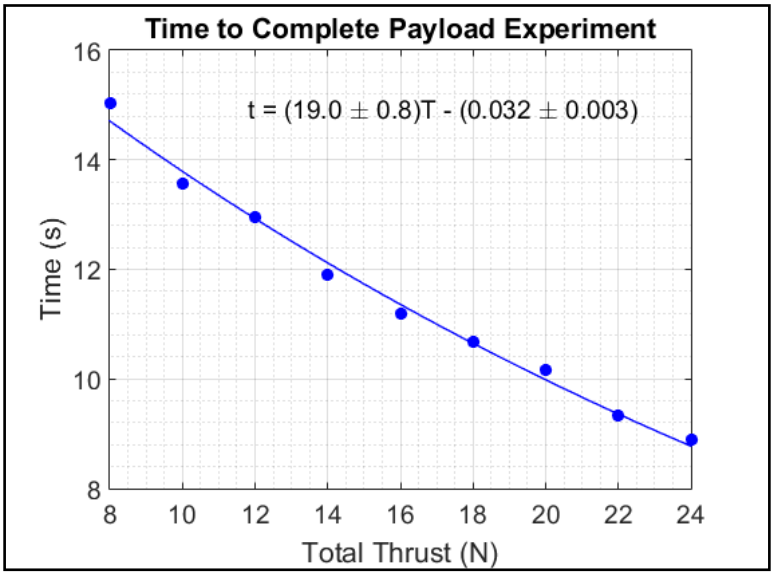

Figure 77: Effect of Thrust on Experiment Time

4 Safety

4.1 Team Safety Structure

The Vanderbilt SL rocketry team takes individual, group, and project safety seriously. The team is continuing to follow ideologies implemented in past years to establish a functional set of safety protocols and to foster safety-focused growth of the VADL members. The team's safety hierarchy is graphically depicted in Figure 78.

The top level consists of both the Safety Administration and the Safety Documents. Four individuals are responsible for management of the safety materials and maintain the authority to make substantive changes to the protocols and safety documentation as needed. In addition, they are vested with the power to make go and no-go decisions for the team when new processes or procedures are required. The Safety Administration consists of the following people: Robin Midgett (Safety Mentor), Paul Register (Student Safety Officer), Dexter Watkins (Assistant Safety Officer), and Ben Gasser (Assistant Safety Officer). Robin is a member of the National Association of Rocketry and holds NAR Level 2 certification. Paul is a senior undergraduate student in Chemical Engineering and Physics; he will oversee the rocketry team to ensure safety precautions are taken during the design, construction and testing of all rocket materials and equipment (see Section 4.2). In this, he will also be assisted by Dexter Watkins (NAR Level 1), a graduate student in Mechanical Engineering and a five-year veteran of the Student Launch program, and Ben Gasser, the 2015-2016 Student Safety Officer. These four individuals will be informed by and will enforce the Safety Documents.

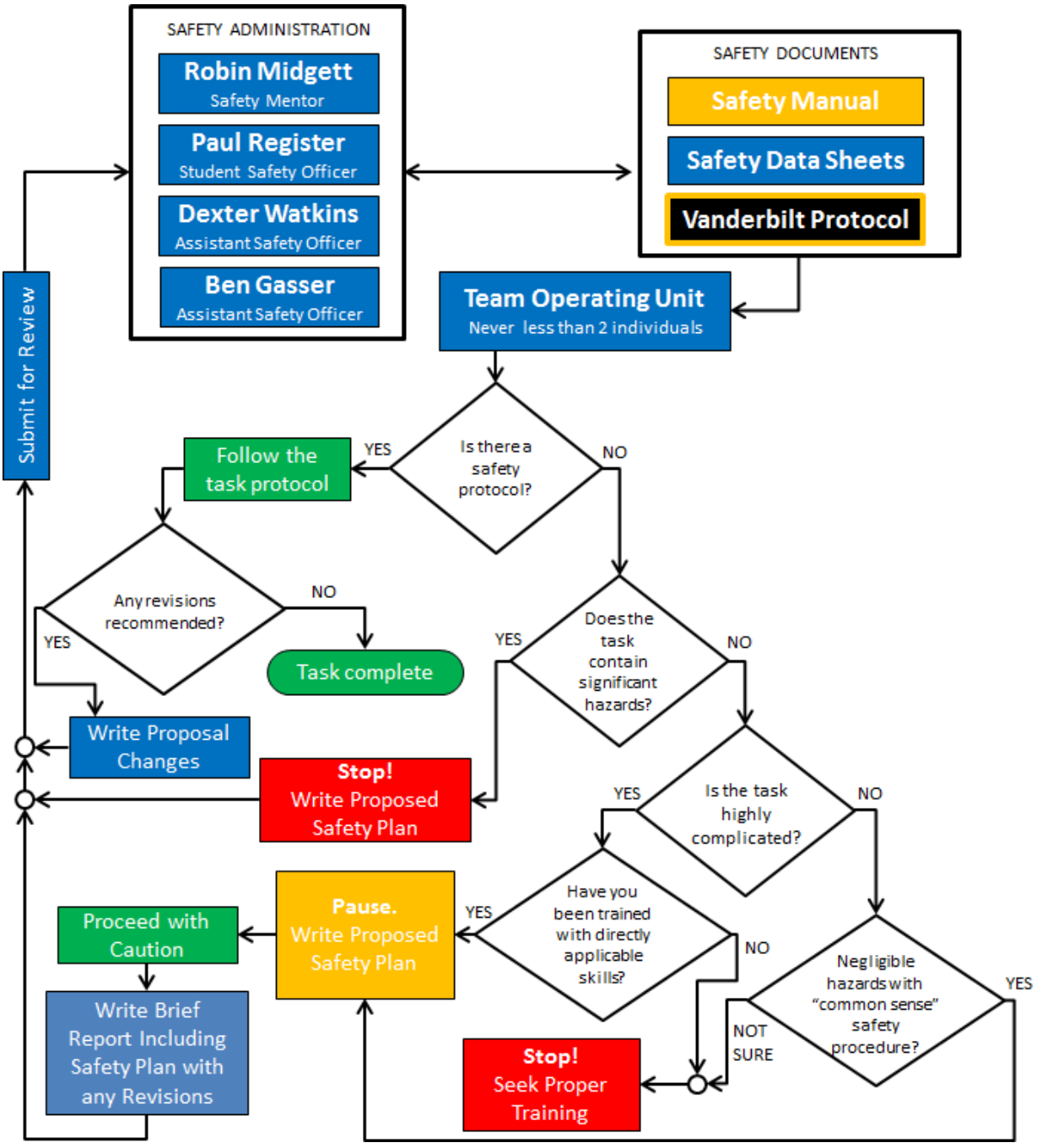

Figure 78: Vanderbilt Aerospace Design Laboratory Safety Protocol

At the core of the construction and launch procedures will be a Team Operating Unit (TOU). This is a subset of the team who have been assigned a specific task (by leadership, their peers, or via volunteering) to be accomplished. For the purpose of safety and accountability, this group will never consist of less than two individuals. All TOUs are informed by the Safety Administration and Safety Documents and are expected to pause prior to beginning any task to ask a few basic questions outlined in Figure 78. First, does a protocol exist? If yes, follow it and give feedback for future improvement. If there is no protocol, does the task contain significant hazards to either person or property? If yes, write a protocol and obtain approval prior to execution of the task. For tasks with no significant hazards, it is permissible for the members of the TOU to write a safety plan and then execute the task without administration

approval, provided that the members of the TOU have appropriate training with directly applicable skills. Furthermore, the TOU must generate a report following completion of the task that includes the safety plan and the members' relevant skills and training.

This team structure offers a significant safety net while also encouraging safety-oriented thinking in each individual. In addition, the common objective of safety fosters team unity, creative thinking, and problem solving skills that will promote individual and team success throughout both the Student Launch competition and in students' future careers.

4.2 Student Safety Officer

Paul has been designated as the Student Safety Officer. He will oversee the overall safety and launch procedures of the team and will work to fulfill the requirements listed in the SL Handbook:

- Monitor team activities with an emphasis on Safety during:
  - Design of vehicle and launcher
  - Construction of vehicle and launcher
  - Assembly of vehicle and launcher
  - Ground testing of vehicle and launcher
  - Sub-scale launch test(s)
  - fullscale launch test(s)
  - Launch day
  - Recovery activities
  - Educational Engagement Activities
- Implement procedures developed by the team for construction, assembly, launch, and recovery activities.
- Manage and maintain current revisions of the teams hazard analyses, failure modes analyses, procedures, and MSDS/chemical inventory data
- Assist in the writing and development of the teams hazard analyses, failure modes analyses, and procedures.

4.3 Written Safety Statement

- Compliance with Huntsville Area Rocketry Association range safety inspection of rocket.
- Admission of the fact that the HARA Range Safety Officer has the final say on all rocket safety issues.
- Any team that does not comply with the safety requirements will not be allowed to launch their rocket.

A written safety statement to this effect is on the VADL website at www.vanderbilt.edu/usli and has been signed by all members of the Vanderbilt Aerospace Design Laboratory team who will be participating in rocket design and fabrication.

4.4 Safety Officer/LEUP Holder

Through outreach projects in the past, the team has made several useful contacts at a variety of local, regional, and national organizations. Robin Midgett, a Mechanical Engineering Technician at Vanderbilt, serves as the rocketry and safety mentor. Paul Register, a senior undergraduate in Chemical Engineering serves as the Student Safety Officer. Dexter Watkins and Ben Gasser, Mechanical Engineering graduate students, serve as Assistant Safety Officers.

4.5 Facilities

All facilities to be used by the team for the fabrication and assembly of rocket components and systems will be supervised by qualified personnel during the times of operation. These facilities are equipped with shop tools (both power- and hand-operated) that are commonly used by students. University personnel familiar with safe shop practices will supervise students and ensure proper operation of all equipment. All students using the machine shops at Vanderbilt will abide by the codes and rules outlined in the shop safety guidelines (see the VADL website at www.vanderbilt.edu/usli).

4.6 Safety Equipment

Disposable gloves, face shields, goggles, shop aprons, and other safety apparel will be made available for use during fabrication. When applicable, SDS data will be referenced for the safe handling and storage of materials.

4.7 Injury/Emergency Situations

In the event of personal injury during the fabrication process, first aid kits are readily available in the club shop. The location of all first aid kits, fire extinguishers, and exits will be presented to all team members prior to their use of the facilities. Emergency personnel are available on campus at all hours. Fire extinguishers are located in shop areas and are inspected for readiness periodically in accordance with local fire protection regulations. Fire sprinklers and alarm systems are installed in areas where fabrication will occur.

4.8 Purchase, Storage, Transport, and Use of Rocket Motors

The design will include APCP motors. Robin Midgett, the rocketry and safety mentor, and Paul Register, the Student Safety Officer, will oversee the purchase and safe storing of these motors. The team will follow the recommendations of the local NAR chapter concerning the capability to purchase, store, transport, and use rocket motors. Necessary equipment will be purchased or built in accordance with applicable regulations regarding the handling, storage, and transportation of rocket motors. In particular, all motors, black powder, and electric matches will be purchased with the assistance of Robin Midgett. He will store these hazardous materials until the team is able to use them, at which point they will be transported in a suitable explosives magazine to the Vanderbilt University campus. Then, under Robin's supervision, the hazardous materials will be transferred to the Vanderbilt SL team's Magloc Explosives Storage Magazine, where they will remain until use. All usage of motors, black powder, and electric matches will be conducted exclusively under the supervision of the team's Safety Administration.

4.9 Transportation of Other Hazardous Materials

All hazardous materials will be handled in a fashion that is consistent with the pertinent Material Safety Data Sheet (see the VADL website at www.vanderbilt.edu/usli), as well as with all federal, state, and local safety, regulatory, and environmental laws and guidelines.

4.10 NAR High Power Rocket Safety Code

The NAR High Power Rocket Safety Code was presented, discussed, and explained to all team members at a team meeting prior to initial design and is being referenced throughout design, construction, test, and launch processes. The Music City Missile Club, NAR Charter #589, advises the team regarding NAR safety requirements, the performance of hazardous materials, handling and hazardous operations, and issues pertaining to environmental laws and regulations. The Performance Guidelines for NAR personnel, along with the rest of the NAR High Power Rocket Safety Code requirements, are attached (see the VADL website at www.vanderbilt.edu/usli). A copy of the Safety Code is kept in the club shop and will be referenced continuously throughout the course of the project.

4.11 Cognizance of Federal, State, and Local Laws and Regulations

The Safety Officer has briefed the team in a meeting regarding Federal Aviation Regulations 14 CFR, Subchapter F, Part 101, Subpart C; Amateur Rockets, Code of Federal Regulation 27 Part 55: Commerce in Explosives; and fire prevention, NFPA 1127 "Code for High Power Rocket Motors." Furthermore, environmental regulations will be consulted throughout the design and fabrication processes in order to ensure the team's compliance with all federal, state, and local laws. The Tennessee State Environmental Laws can be found at nasda.org. The Safety Officer has been tasked with recognizing all pertinent environmental regulations and recommendations for the handling of harmful or potentially hazardous materials and distributing this information to the team.

4.12 Safety Data Sheets

For the various potentially harmful materials that will be used in the design and construction of the rocket, Safety Data Sheets (see the VADL website at www.vanderbilt.edu/usli) detail the proper handling and disposal of their associated materials. A summary of the SDS information included in the shop is provided on the VADL website at www.vanderbilt.edu/usli. The Student Safety Officer will seek out and provide the team with additional relevant regulatory or safety information for materials lacking a Safety Data Sheet and will educate all team members about proper handling and disposal of these materials.

4.13 Final Assembly and Launch Procedures

The VADL team will review system preparation requirements well in advance of the launch. Safety oversight and launch procedures are managed by the launch leader. The student safety officer, Paul, will oversee all hazardous operations involving people or the rocket. Team leaders will supervise the preparation of their respective areas. Formal integration of systems requires the launch leader's oversight. A member of NAR with appropriate certifications will oversee the assembly of the motor system. This is a quality control measure to ensure that mission-critical systems are properly prepared for launch. All launch procedures are divided into systems along with the personnel required.

4.13.1 Launch Pad, Launch Rail, and Ignition System

Launch Platform The Vanderbilt Aerospace Design Laboratory will use a standard NAR launch pad that will be constructed this year based on the specifications set forth by NAR. The launch pad is an improvement from the previous launch pad that had been in use since 2007 with its reduction in weight, increase in mobility and launch angle control, and increase in stability.

Key features of the launch platform include:

- 1/8" x 2" square aluminum tube legs and mast; aluminum base plates, stainless steel mast plate
- Stainless steel nuts and bolts to improve corrosion resistance
- Two legs that fold out from a central leg at 120° angles
- Launch rail mast that rotates on a pivot and is pinned into the stainless steel mast plate
- Rocket loaded with rail in the horizontal and then righted and pinned before launch
- Slotted hole for pin allows launch angle to be adjusted 5° in either direction from vertical
- Rail is made of two 8020 aluminum removable rails, joined together by a custom steel joint to provide straight guided path for rocket

Launch Rail The launch rail will utilize 1.5" I-shaped launch lugs that slide onto the launch rail. These will be purchased from Giant Leap Rocketry, are manufactured by Acme Conformal Rail Guides, and are made out of 6061-T6 aircraft aluminum. The base of the rail guide that interfaces with the rocket body tube will follow a 6.0" curvature (this has been shown to work for the 5.5" diameter rocket body tubes because the difference in arc length is not significant for the relatively small chord length covered by the launch lugs). The launch lugs will be permanently joined to the rocket body tube with JB weld after both the rocket body tube surface and the rail guides have been treated with 220 grit sand paper. This will ensure the JB weld has better penetration and bonding between the body tube and the launch lug. JB weld is chosen for its flexibility relative to epoxy, which will ensure resistance to small torsional loads applied while mounting the rocket to the launch rail. The launch lugs will be spaced approximately 24" apart. The tail fin section launch lug will be installed with precise measurements that guarantee the launch lugs are located halfway in between two fins. Then, two aluminum L-rods will be held in place that give machined straight lines for insertion of the second launch lug which is located on the payload section. This rig will help verify that a straight line connects both launch lugs and that there will not be misalignment issues.

Ignition System The launch ignition system consists of a 12V battery connected to 500 foot leads. The leads go through a safety switch system to the motor igniter. The safety switch ensures that no voltage differential is delivered to the electric match igniter until a key is inserted into the safety switch and a button is pressed.

4.14 Launch Operations Procedures

Launch operations procedures for all aspects of the launch preparation, vehicle assembly, and ignition are located in Section **??**. Safety warnings and troubleshooting protocols are provided along with the operation procedure for each component of the launch.

	Consequence					
Likelihood		Trivial	Minor	Moderate	High	Critical
	Rare	A1	B1	C1	D1	E1
	Unlikely	A2	B2	C2	D2	E2
	Moderate	A3	B3	C3	D3	E3
	Probable	A4	B4	C4	D4	E4
	Very Likely	A5	B5	C5	D5	E5

Figure 79: Risk Assessment Matrix

4.15 Hazard Analysis

4.15.1 Risk Assessment Matrix

In order to fully assess the risks associated with the rocket and all its payloads, a risk assessment matrix (see Figure 79) is used that categorizes and ranks all risks according to the likelihood of occurrence and severity of consequence. An event's likelihood of occurrence is assigned a rating of 1, 2, 3, 4, or 5, corresponding to the designation of rare, unlikely, moderate, probable, and very likely, respectively. Similarly, an event's severity of consequence is given a rating of A, B, C, D, or E, corresponding to the designation of trivial, minor, moderate, high, or critical, respectively. When these two scales are crossed in a matrix, the resulting combinations provide enlightening information in terms of the risk level. In general, low alphanumeric combinations represent typically negligible risk, while high alphanumeric combinations tend to indicate much larger risks. Color-coding has also been included in the matrix to visually depict extent of risk. Events that fall within squares highlighted in green are considered low risk and require no mitigation or have no reasonable means of mitigation. In other words, "green" risks either occur infrequently or assume low consequence, such that serious consideration to mitigate the risk is not necessary. Similarly, squares highlighted in yellow contain events with moderate risk that should be mitigated, but the overall risk posed to the mission and general safety has been deemed acceptable. "Yellow" risks are more serious than "green" risks and could result in nontrivial consequences in terms of the success of the mission or to the safety of those involved; however, this category of risk does not necessarily represent no-go situations, assuming that potential mitigation strategies have been evaluated and implemented. The third and most critical category is highlighted in red, signifying events that pose hazardous and unacceptable risks to either mission success or personal safety. Without exception, "red" risks must be mitigated to a "yellow" or "green" level before the rocket and payload are considered safe for launch.

The explicit meanings of each of the rating designations are outlined as follows:

Likelihood of Occurrence

- 1 (Rare) - Probability of occurrence is almost non-existent. Mitigation need only exist for the most critical risks.
- 2 (Unlikely) - Probability of occurrence is very low but does exist. Mitigation should exist for high-risk consequences.
- 3 (Moderate) - Probability of occurrence is moderate. Mitigation efforts should exist for all risks resulting in greater than minor consequence.

- 4 (Probable) - Occurrence is more likely than not. Mitigation efforts should occur for all but the most trivial consequences.
- 5 (Very Likely) - Occurrence is to be expected. Mitigation is required for all but the most trivial consequences.

Severity of Consequence

- A (Trivial) - Occurrence of risk results in no effect on rocket/payload performance or safety of all persons involved. No mitigation is needed.
- B (Minor) - Occurrence of risk results in minor damage that is either easily reparable or has no effect on rocket/payload performance. No risk for injury to persons involved. Mitigation efforts should exist for the most likely risks.
- C (Moderate) - Occurrence of risks results in some damage to rocket/payload that could negatively affect performance and/or result in minor injury to persons involved. Mitigation efforts should exist for most risks.
- D (High) - Occurrence of risk results in major damage to rocket/payload that will negatively affect performance and/or result in serious injury to persons involved. Mitigation efforts should exist for all but the rarest risks.
- E (Critical) - Occurrence of risk results in catastrophic damage to rocket/payload that will eliminate performance capability and/or result in serious injury/death to persons involved or bystanders. Mitigation is necessary.

Combined Rating

- Green (Low) - Risk falls within an acceptable range of probability and consequence. Mitigation strategies should be implemented if possible but are not mission critical.
- Yellow (Moderate) - Risk may or may not be acceptable. Risk should be evaluated thoroughly for potential mitigation strategies.
- Red (Critical) - Risk has an unacceptable level of likelihood and consequence. Mission should not proceed until viable mitigation strategies are created and implemented.

All risks recognized by members of the team have been recorded and evaluated by the safety officer. Though not all risks have been encountered at the current stage of the design and fabrication process, each risk has been given an expected risk assessment rating both prior to mitigation efforts (RR) and post-mitigation (PMRR) in order to signify the safety- and reliability-oriented focus of the team. In all following risk assessment tables, each risk has been outlined along with possible causes, overall effect to the rocket/payload, mitigation strategy, verification plan of the mitigation, and risk assessment ratings for pre- and post-mitigation that have been color-coded by level of risk for easy comparison. Hazard analyses relating to the current competition has been broken into the following sections: personnel (Section 4.15.2); project management (Section 4.15.8); vehicle failure modes (Section 4.15.6); propulsion failure modes (Section 4.15.3); recovery system failure modes (Section 4.15.5); design of rocket/payload and launch (Section 4.15.4); and environmental concerns (Section 4.15.7).

4.15.2 Personnel Hazard Analysis

Table 11 indicates possible hazards to personnel working in the shop, including risks posed by chemicals and machinery.

Table 11: Personnel Hazard Risk Assessment

Personnel Hazard Risk Assessment						
Risk	**Cause**	**Effect**	**RR**	**Mitigation Strategy**	**Verification**	**PMRR**
Shop Safety						

Table 11: Personnel Hazard Risk Assessment

Personnel Hazard Risk Assessment						
Risk	**Cause**	**Effect**	**RR**	**Mitigation Strategy**	**Verification**	**PMRR**
Electric shock	Static build-up on equipment handler	Destruction of electrical components; black powder explosion	E3	Handlers of sensitive equipment will ground themselves to discharge static build- up. Furthermore, all high voltage components will be properly marked as ”HIGH VOLTAGE” and locked while in use.	Consultation of shop safety guidelines	E1
Lacerations or cuts from machines and tools	Improper use of machines/ equipment	Injury potentially requiring medical attention	E3	All team members performing potentially hazardous operations will be properly trained. At least two members must be present for hazardous operations.	Consultation of safety protocol flowchart	D2
Black powder explosion/ ignition while handling	Accidental connection to voltage source; Static discharge	Hearing damage; Dis-orientation; Personal injury	E3	Black powder handlers will only work with small amounts at a time and ground themselves prior.	Consultation of SDS	E1
Getting caught in a machine	Loose fitting clothing or jewelry; long hair not tied back	Potential for serious injury or death	E3	Those performing machining operations will never wear loose fitting clothing or jewelry. All long hair must be tied back.	Consultation of shop safety guidelines and safety protocol flowsheet	E1
Eye contact with chemicals or particulates; Exposure to arc from arc-weld	Improper handling of chemicals	Discomfort and/or vision impairment	D3	Appropriate eye protection will be worn for all activities involving machinery, chemicals, and welding	Consultation of SDS, PPE: eye protection	D1
Prolonged exposure to loud machinery	Prolonged operation of heavy machinery	Disorienta-tion and/or hearing loss	D3	Hearing protection will be worn when operating heavy machinery.	PPE: hearing protection	D1
Physical contact with hot surfaces	Leaving soldering iron on; touching welded parts immediately after welding	Burns	D3	All heat- producing tools will be turned off when not in use. Heat- resistant gloves will be worn when handling hot parts. Chemicals will be stored and handled safely.	Consultation of shop safety guidelines	D2
Inhalation of chemical fumes	Improper handling of chemicals	Discomfort and/or damage to lungs	D2	Volatile chemicals will only be handled in well-ventilated rooms and under a fume-hood when possible.	Consultation of SDS before use; PPE: eye protection	D1

Table 11: Personnel Hazard Risk Assessment

Personnel Hazard Risk Assessment						
Risk	**Cause**	**Effect**	**RR**	**Mitigation Strategy**	**Verification**	**PMRR**
Contact with flying debris from machining operations	Standard or improper tool use	Burns, abrasions, irritation of eyes or skin	C3	Closed-toed shoes and long pants will be worn at all times in the shop. All members present during cutting operations will wear eye protection.	PPE: clothes that cover the body, eye protection	C2
Contact with falling tools/parts	Improper storage of tools/parts	Personal injury	C3	All team members will wear closed toed footwear and long pants while machining in the shop.	Consultation of shop safety guidelines involving cleanup; PPE: clothes that cover the body	C2
Tripping over loose cords	Long power cords/wires being run across the shop floor	Personal injury	C3	Power strips have been installed near all machines/workspaces that may require a power outlet.	Consulation of shop safety guidlines	C1
Exposure to chemicals/allergens	Improper handling of chemicals and known allergens	Chemical burns, irritation of skin, allergic reaction	C2	Latex or vinyl gloves will be worn when handling chemicals or known allergens.	PPE: chemically resistant gloves	C1
Testing on the FRAME (formerly Ground-Based Test Facility)						
Catastrophic failure of air tank and regulator	Accidental overpressurization while refilling tank	Potential for serious injury or death	E3	Installment of 6 kpsi burst disc on air tank; air tank refilled by trained personnel under supervision of safety officer; large refill tank only pressurized to the design pressure (1/2 of air tank pressure rating)	PPE: eye protection and clothes that cover the body; consultation of safety protocol for refilling pressure tank	E1
Rocket dislodged	Improper axial constraint	Potential for serious injury	D3	Ensure tight compression fit of top and bottom mounts; be ready to adapt setup to different vibrational situations	Design analysis of FRAME; following of testing procedure	D1
Structural failure	Excessive vibration; joint failure	Potential for injury to operating personnel	D3	Monitor construction; ensure proper joint tightness; maintain safe distance from test facility during tests	Design analysis of FRAME; following of testing procedure to ensure structural stability of system prior to experiment deployment	B2

Table 11: Personnel Hazard Risk Assessment

Personnel Hazard Risk Assessment						
Risk	**Cause**	**Effect**	**RR**	**Mitigation Strategy**	**Verification**	**PMRR**
Runaway thruster input	Control anomaly; runaway motor input	Rocket dislodged; potential for serious injury	D2	Incorporation of a hard off switch on the motor input	Design analysis of FRAME, including ease of access to manual override switch	C2
Hotbox						
Electric shock	Improper shielding of control system	Potential for serious injury or death	E4	Follow electrical codes in wiring; maintain safe distance from hotbox while in use. Furthermore, the compartment containing high voltage electronics is marked with a warning sign and locked while the hotbox is in use.	Consultation of safety guidelines for handling high voltage components	E2
Shop fire	Runaway heating	Potential for serious injury or death	E3	PTC Thermistor used to cut off power to hotbox; webcam to monitor progress; digital thermometer included for redundancy in measurement; fire extinguishers kept in shop.	Design analysis of Hotbox prior to use; visual monitoring during initial uses	D1
Shop fire	Improper wiring or mounting of light bulbs	Potential for serious injury or death	E2	High power circuitry completed with safety officer present; fire extinguishers kept in shop	Design analysis of Hotbox prior to use; visual monitoring during initial uses	D2
Shop fire	Overheating of components	Potential for serious injury or death	E2	Maximum temperature possible greater than temperature ratings of every part exposed to heat; fire extinguishers kept in shop.	Design analysis of Hotbox; consultation of SDS for components to be heat-treated	D1
Thruster Test Stand						
Loose pressure vessel in shop	Accidental and uncontrolled thruster firing	Potential for serious injury	E2	Select normally-closed solenoid; hardwire manual power switch to test stand; clamp system to table	Consultation of safety protocol; design analysis of test stand; PPE: eye protection and clothing that covers the body	C1

Table 11: Personnel Hazard Risk Assessment

Personnel Hazard Risk Assessment						
Risk	**Cause**	**Effect**	**RR**	**Mitigation Strategy**	**Verification**	**PMRR**
Thruster rupture in shop	Over-pressurization of thruster components	Potential for serious injury	E2	Hydrostatic testing with a safety officer present	Consultation of safety protocol flowchart; PPE: eye protection and clothing that covers the body	D1

4.15.3 Propulsion Failure Modes

Table 12 displays modes of failure primarily concerning the rocket motor and propellant.

Table 12: Propulsion Failure Modes

Propulsion Failure Modes and Risk Assessment						
Risk	**Cause**	**Effect**	**RR**	**Mitigation Strategy**	**Verification of Mitigation**	**PMRR**
Propellant fails to ignite	Improper motor packing; faulty propellant grain; damage during transportation	Live situation; rocket does not launch; necessary replacement	E3	Proper ignition setup; safety advisor oversees motor packing by student safety officer	Consultation of strict safety protocol regarding motor and propellant issues	D1
Premature propellant burnout	Improper motor packing; faulty propellant grain	Altitude estimate not reached; main parachute may not deploy	E3	Proper motor assembly; obtain motor only from reputable source	Static fire testing; consultation of safety protocol	E1
Improper assembly of motor	Incorrect spacing between propellant grains; motor case improperly cleaned; end caps improperly secured	Motor failure; unstable flight; target altitude not reached; damage or loss of rocket	E3	Ensure proper training and supervision by safety advisor for motor assembly by student safety officer	Consultation of strict safety protocol regarding motor and propellant issues	E1
Motor mount fails	Insufficient mount strength; damage during previous launch or transportation	Motor launches through rocket; damage to/loss of rocket; unstable flight	E3	Proper motor mount construction; load verification testing; test launches	Load verification testing; design analysis of motor mount; pre- and post-flight inspections of motor mount	E1
Transporta-tion/ handling damage	Improper protection during transportation/ handling	Unusable motor; incapable of safe launch; potential damage to/loss of rocket	E3	Proper storage overseen by safety advisor and student safety officer; certified member handling	Consultation of strict safety protocol regarding motor and propellant issues	E2
Center ring failure	Unable to withstand motor force during launch; weak ring; poor seal to body and motor tube	Reduced stability; damage to/loss of vehicle	E3	Proper ring size and construction; sufficiently strong materials used(6061-T6 aluminum); redundant load path design that can sustain failure of fins or centering rings and still retain motor	Finite element modeling to verify rings to hold conservative thrust loads using von Mises failure criterion	E2

Table 12: Propulsion Failure Modes

Propulsion Failure Modes and Risk Assessment						
Risk	**Cause**	**Effect**	**RR**	**Mitigation Strategy**	**Verification of Mitigation**	**PMRR**
Propellant explodes	Improper motor packing; faulty propellant grain; damage during transportation	Destruction of motor casing; catastrophic failure of rocket; potential injury to personnel	E2	Proper motor assembly; safety advisor oversees motor packing by student safety officer	Consultation of strict safety protocol regarding motor and propellant issues	E1
Propellant burns through casing	Improper motor packing; faulty propellant grain; damage during transportation	Loss of thrust; loss of stability; catastrophic failure of rocket	E2	Proper motor assembly; safety advisor oversees motor packing by student safety officer	Static fire testing to verify proper motor assembly	E1
Motor tube dislodges from rocket body during launch	Failure of fin attachment, exposing motor tube connection	Catastrophic launch failure, uncontrolled flight	E2	Thorough construction of motor tube mounting through fins. For the motor tube to tear out, the fins would have to tear through the carbon fiber and blue tube body	Design analysis of tail section structure; visual inspection of tail section pre-flight	E1
Motor is misaligned	Centering rings misaligned; fins assembled to motor tube at an angle	Unexpected flight trajectory; unstable flight	C4	Careful machining of center rings on lathe with order of magnitude higher tolerance than laser cut plywood; proper assembly of tail section using centering rings and fin alignment jig	Design analysis of motor alignment equipment; pre-flight visual inspection of motor alignment	C1
Motor igniter fails	Faulty/incorrect igniter	Live situation; rocket does not launch; necessary replacement	C2	Proper igniter selection setup; proper power source	Adherence to safety protocol	C1

4.15.4 Payload/Control Failure Modes

Table 13 describes possible modes of failure of the cold gas thruster payload system and associated electronics and controls.

Table 13: Payload and Related Control Failure Modes

Cold Gas Thruster System Risk and Mitigation						
Risk	**Cause**	**Effect**	**RR**	**Mitigation Strategy**	**Verification of Mitigation**	**PMRR**
Insufficient space between parachute and blast charge installment	Designing to save mass and space without consideration of the recovery system integration into the vehicle body	Severe damage to recovery system	E3	Ensure proper parachute installment practices are followed per manufacturer instructions and testing	Design analysis; deployment testing	E1
Avionics power loss	Disconnec-tion in cables or wiring	Loss of competition-required data, failure to actuate parachutes	E2	Thorough testing on the ground will help to reduce doubts about the reliability of the power supply	Testing on the FRAME proves the reliability of the payload electronics	E1
IMU dislodged	Improper connection of IMU to payload sled; heavy vibration of vehicle during flight	Catastrophic disturbance to guidance algorithm, loss of control of rocket	E1	Secure attachment of the IMU should be taken as a serious priority. Failure here would prove disastrous. Additionally, software lockouts could be introduced for scenarious like this in which IMU data is wildly off of predicted values	Design analysis to verify the IMU is securely attached	E1
Thruster chain failure	Improper fitting of joints	Air stream leakage, possible damage flight vehicle	D3	Care in assembly and pressure testing to safety factor prior to use will help to ensure safety and reliability of the thruster chain	Design analysis of safety measures built in to regulator and pressure assembly; PPE: eye protection during testing	D2

Table 13: Payload and Related Control Failure Modes

Cold Gas Thruster System Risk and Mitigation						
Risk	**Cause**	**Effect**	**RR**	**Mitigation Strategy**	**Verification of Mitigation**	**PMRR**
Regulator failure	Improper fitting of joints; unexpected structural failure; defective part	Catastrophic loss of pressure; potential damage to flight vehicle	D2	Keeping the regulator operating at safe pressures as stated in its datasheet will mitigate possibiity of failure. Employ burst discs of appropriate ratings and venting holes on the airframe to rapidly depressurize in the event of overpressurization failure.	Design analysis of safety measures built in to regulator and pressure assembly; adherence to safety protocol, stand at safe distance; PPE: eye protection during testing	D1
Air tank fracture	Overuse; impact history; defective part	Catastrophic loss of pressure. Potential damage to flight vehicle	D2	While highly unlikely, air tank cracks could indeed prove catastrophic. Visual monitoring of the tank prior to use in launch activities and careful regulation of witnessed pressure will be the best measures taken to guarantee success and safety here.	Design analysis of safety measures built in to regulator and pressure assembly; adherence to safety protocol, stand at safe distance; PPE: eye protection during testing	D1
Failure of NASA marked altimeter	Improper handling of altimeter; dead battery	Inability to report official flight altitude for competition	D2	Test and verify proper altimeter operation before each test flight. Assure robustness of electronics configuration and avionics bay pre-flight.	Testing of the altimeter in the field before launch	C1
Thruster misalignment	Thrust torquing the nozzle about fittings	Thrust vector is not fully tangential to rocket. In the severe case, exhaust is cut off at the thruster portholes and is not fully ejected into the atmosphere. Both cases result in lost torque.	D2	Crimp compression fittings as tightly as possible without deforming rigid tubing. Secure thruster chain (particularly at the nozzle) to the bulkhead.	Design analysis to verify alignment of thrusters; test data on the FRAME confirms the desired thrust output	D1

Table 13: Payload and Related Control Failure Modes

Cold Gas Thruster System Risk and Mitigation						
Risk	**Cause**	**Effect**	**RR**	**Mitigation Strategy**	**Verification of Mitigation**	**PMRR**
Excess pitch and yaw	Heavy gusting; understability or overstability in terms of stability margin	Potential instability introduced to flight vehicle. If moved far past vertical, loss of control possible	C3	While gusting is out of control of the launch team, testing of the launch vehicle control system on the ground and CFD simulations will help to characterize this type of behaviour	Testing of the launch vehicle on the FRAME with application of simulated resistive torque	B3
Thruster structural failure	Unexpected structural failure; defective part	Loss of directional stability	C2	Pressure testing to safety factor and care in assembly will help to mitigate risk here	Testing of pressure apparatus; adherence to safety protocol	C1
Blue Tube expansion/-contraction from moisture	Excess humidity	Debonding of flight vehicle body, rapid unplanned disassembly of body components under launch/flight loading	C2	Thorough studies will be completed of moisture cycling of carbon fiber reinforced Blue Tube materials in order to characterize performance. If stabilizing chemical agents can be added to reduce any expansion effects, these measures will be taken.	Compression testing	B2
Flight computer power loss	Disconnec-tion in cables or wiring	Loss of control, interruption of control algorithm	C2	Thorough testing on the ground will help to reduce doubts about the reliability of the power supply	Testing on the FRAME proves the reliability of the payload electronics	D1
One or more thruster nozzles become clogged	A small amount of dirt or debris is sufficient to plug up the nozzles	Roll control is unsuccessful and in the case of a single nozzle, the unbalanced couple could alter flight path	C2	Care will be taken in thruster system assembly to ensure no contaminants are introduced to any part in the flow path of the propellant	Consultation of launch operations procedure to ensure nozzles are clear prior to launch	C1
Wildlife interference	Launch vehicle flies through a flock of birds	Catastrophic disturbance to flight vehicle	D1	One of the most unpredictable failure events, little can be done to mitigate this risk during flight	Consultation of launch operations procedure to ensure clear launch field prior to flight	D1

Table 13: Payload and Related Control Failure Modes

Cold Gas Thruster System Risk and Mitigation						
Risk	**Cause**	**Effect**	**RR**	**Mitigation Strategy**	**Verification of Mitigation**	**PMRR**
Solenoid stuck open	Electronics or physical failure	Continuous thrust, loss of roll control	B3	Thorough testing prior to launch will help to ensure proper functioning of solenoid valves	Testing on the thrust stand and FRAME	B2
Solenoid stuck closed	Electronics or physical failure	No roll induction or roll control possible	B3	Thorough testing prior to launch will help to ensure proper functioning of solenoid valves	Testing on the thrust stand and FRAME	B2
Air leak in hosing or fittings in thruster system	Improper fitting of joints; unexpected structural failure; defective part	Roll control is unsuccessful and air buildup could cause failure of other payload skeleton components	B2	Ground-based testing of all pressurized components will verify proper sealing. Venting holes will also be placed in all bulkheads and rocket exterior.	Testing on the thrust stand and with hydrostatic pressure testing	B1
Loss of thrust control	Empty air tank	Thruster use no longer possible	A4	This failure will not cause drastic issues with the mission unless rotation of the rocket is still necessary. Fueling the tank to maximum safe levels before flight will be the best mitigation strategy	Design analysis to verify the quantity of air in the tank is sufficient to complete the experiment	A2

4.15.5 Recovery System Failure Modes

Table 14 indicates hazards associated with failure of the parachute and recovery systems. All mitigations of risk are verified by consultation of launch operations procedure and testing through the subscale flight.

Table 14: Recovery System Failure Modes

Recovery System Failure Modes and Risk Assessment					
Risk	**Cause**	**Effect**	**RR**	**Mitigation Strategy**	**PMRR**
Deployment failure	Putty not added to seal bulkhead holes	Parachute chamber artifically large	E4	Backup charges; consultation of launch operations procedures	C2
Rocket ripped apart upon chute deployment	Zippering effect of parachute harness	Catastrophic failure of recovery system; damage to/loss of rocket and payload	E3	Use Fireball anti-zippering device to distribute load to body	E1
Low battery of avionics electronics power supplies	Old, untested batteries used in avionics bay assembly	Failure to power flight altimeters throughout flight; failure to fire drogue and/or main ejection charges	E3	Pre-launch checklist assures battery testing and replacement if necessary	E1
Parachute sections come apart	Inadequate parachute design; poor stitching between sections	Catastrophic failure of recovery system; damage to/loss of rocket and payload	E3	Use semi-flat felled seam between sections; verification testing of recovery system	E2
Shroud lines become unattached	Weak stitching or materials	Catastrophic failure of recovery system; damage to/loss of rocket and payload	E3	Sew reinforcement onto shroud lines	E2
Parachute breakaway	Harness failure; weak mounting of recovery system to rocket body	Loss of parachute; catastrophic damage to/loss of rocket/payload; potential damage/injury to property/persons on ground	E3	Design strong retention system with shock absorption; load testing; multiple body attachment points	E2
Drogue parachute deployment failure	Drogue parachute fails to eject upon separation event; weak/failed blast charges do not eject parachute	High descent rate from apogee; unlikely successful main parachute deployment; damage to/loss of launch vehicle	E3	Ground-based deployment testing; backup drogue chamber ejection charge firing with a 1 second apogee delay	E2
Main parachute deployment failure	Parachute fails to eject from nosecone upon separation event; weak/failed blast charges do not eject parachute	Excessive landing energy for successful recovery; damage to or loss of launch vehicle	E3	Ground-based deployment testing; backup drogue chamber ejection charge firing at a slightly reduced altitude from desired main deployment altitude	E2

Table 14: Recovery System Failure Modes

Recovery System Failure Modes and Risk Assessment					
Risk	**Cause**	**Effect**	**RR**	**Mitigation Strategy**	**PMRR**
Separation failure	Excessive shear pin holding strength; inadequate/failed ejected charge; altimeter failure	Damage to or loss of the launch vehicle; potential damage/injury to property or personnel on the ground	E3	Ground-based deployment testing; proper shear pin sizing/strength and blast charge calculations ground and flight based altimeter testing; redundant charges for both separation events; factor of safety application for blast charge size	E2
Altimeter failure	Circuitry failure due to wiring failure; loss of or insufficient power to operate altimeters and fire ejection charges; arming switch failure	Failure to ignite drogue and/or main ejection charges; deploy parachutes at undesired altitudes or lack of deployment altogether; damage to/loss of launch vehicle	E3	Main-backup altimeter scheme; individual power supply module for each redundant altimeter; fully ground-based altimeter testing before each flight	E2
Arming switch failure	Faulty screw-switch component; miswiring of power supply, switch, and altimeter; short-circuit condition; switch changes out of NO state before or during flight; insecure soldering of wires to screw switches	Failure to activate the altimeters pre-launch	E3	Ground-based testing of each arming switch; ground-based deployments tests; flight test of altimeter arming switch; securing solder with small amounts of epoxy	E2
Shock cord failure	Faulty shock cord	Parachute disconnect from rocket; catastrophic damage to/loss of rocket	E3	Inspect shock cord before packing parachutes	E2
Shroud lines or shock cords tangle after deployment	Shock cords too long	Potential for parachute to not fully deploy; catastrophic damage to/loss of rocket	E3	Maximize cord length to tail section; flight testing	E2
Shroud lines or shock cords tangle after deployment	Excess rocket rotation	Potential for parachute to not fully deploy; catastrophic damage to/loss of rocket	E3	Minimize shock cord length to nose cone; flight testing	E2
Parachute or shroud line tangle	Improper transportation, storage, or packing	Decreased parachute performance leading to potential damage to or loss of rocket	D4	Proper packing of recovery system; proper and consistent method of folding and storing after each use	C2

Table 14: Recovery System Failure Modes

Recovery System Failure Modes and Risk Assessment					
Risk	**Cause**	**Effect**	**RR**	**Mitigation Strategy**	**PMRR**
Parachute melts	Improper separation of/insulation between charges and parachute; improper storage	Decreased parachute performance leading to potential damage to/loss of rocket	D4	Proper shielding from ejection charges; ground-based testing	D2
Lack of adequate space for parachutes	Improper budgeting of rocket space; poor translation of requirements to rocket design	Incapable of safe launch	E2	Clear outline of rocket design; verification of design needs met	D1
Parachute tear	Parachute snags upon separation; improper transportation/storage	Decreased parachute performance leading to potential damage to/loss of rocket	D3	Inspect material for defects; proper and consistent packing technique; removal of potential snags within parachute compartment	C2
Avionics bay not properly sealed	Holes in rocket body or avionics bay; gaps between sections	Incorrect detonation of drogue and/or main ejection charges; failure to reach desired altitude; damage to/loss of launch vehicle; errored altitude sensing	D3	Putty used to seal edges between avionics bay bulkheads and airframe; putty used to seal holes used for wiring	D2
Descent rate too fast	Parachute C_d too low; cross-sectional area too small	Potential damage to or loss of rocket or payload	D3	Verification testing of recovery system	D2
Onboard fire in parachute compart-ments	Combustible material near separation charges	Potential damage to or loss of launch vehicle and internal components; failure to deploy parachutes	D2	Isolation of ejection charges from flammable material; ground-based deployment testing and subscale flight	D1
Descent rate too slow	Parachute C_d too high; cross-sectional area too large	Potential to land outside of authorized zone	C3	Verification testing of recovery system	C2

4.15.6 Miscellaneous Failure Modes

Table 15 shows modes of failure relating to the rocket body and its components that do not fall into the other hazard analyses.

Table 15: Miscellaneous Failure Modes and Hazard Analysis

Vehicle Failure Modes and Risk Assessment						
Risk	**Cause**	**Effect**	**RR**	**Mitigation Strategy**	**Verification of Mitigation**	**PMRR**
Premature rocket separation	Faulty separation charge wiring; shear pins too small; altimeter malfunction	Unstable flight; recovery failure; unable to reach target altitude; potential loss of vehicle	E3	Proper shear pins selection; ground-based deployment and altimeter testing	Design analysis of shear pins; testing on the FRAME; altimeter testing	E2
Buckling or shearing of airframe	Shear pins do not shear; bulkheads unable to withstand force from motor during launch; poor seal to rocket body and/or motor tube	Unstable flight; potential loss of vehicle	E3	Selection of strong airframe materials; proper manufacturing techniques; finite element stress analysis modeling	Design analysis of airframe components under high stress; testing of body tube material	E1
Bulkhead failure	Unable to withstand motor force during launch; weak ring; poor seal to body and motor tube	Damage to/loss of avionics, payload, or rocket; unstable flight	E3	Aluminum and steel bulkheads for critical components; proper construction; test for stability	Design analysis of bulkhead selection; finite element modeling; failure testing	E2
Structural failure despite stress modeling	Stress model underesti-mates true flight stress and overestimates factor of safety	Damage to vehicle or components; flight failure	E3	Verify the model with multiple experimental tests; use conservative design safety factors; use model uncertainty factors	In addition to finite element analysis, compression testing and validation from test launches	E1

Table 15: Miscellaneous Failure Modes and Hazard Analysis

Vehicle Failure Modes and Risk Assessment						
Risk	**Cause**	**Effect**	**RR**	**Mitigation Strategy**	**Verification of Mitigation**	**PMRR**
Rocket comes loose from launch pad	Rail buttons not securely mounted to rocket; extreme wind; team error in aligning rocket while attaching to pad	Rocket breaks free during initial phase of launch; potential damage to rocket, bystanders, and property; potential loss of vehicle and payload	D4	Rail buttons used on rocket for secure attachment; careful precision of alignment while guiding rocket on launch rail	Design analysis to align rail buttons; validation from subscale flight	C2
Premature section separation	Failure of shear pins	Deploy at incorrect altitude; potential damage to/loss of vehicle	E2	Proper shear pin sizing/strength	Design analysis of shear pin selection; deployment testing prior to launch	D1
Vehicle component not brought to launch site	Component not packed	Rocket does not launch	E1	Follow launch inventory and checklist; bring duplicates of smaller components like fasteners	Consultation of launch operations hardware checklist	D1
Carbon fiber joint failure	Weak adhesion; loss of material strength	Unstable flight; damage to/loss of vehicle	D3	Follow proper procedure for applying carbon fiber joints, including proper surface preparation, epoxy selection, and vacuum bagging technique	Consultation of fabrication protocol for rolling carbon fiber	B2
Fin failure or weakness	Damage in landing of previous launches or during travel; improper sealing from environmental hazards	Unstable flight	D3	Correct construction techniques; evaluate structural integrity after and before each launch; protective epoxy coating	Design analysis of fin choice; testing of carbon fiber strength	D2
CG is too far aft	Poor overall rocket and section design; unnecessary weight	Insufficient stability for reliable flight	C3	Proper simulation of rocket characteristics using RockSim; add ballast to forward section of rocket if needed	Design analysis with simulation environment	B2

Table 15: Miscellaneous Failure Modes and Hazard Analysis

Vehicle Failure Modes and Risk Assessment						
Risk	**Cause**	**Effect**	**RR**	**Mitigation Strategy**	**Verification of Mitigation**	**PMRR**
CP is too far forward	Poor overall rocket and section design; fin area too small	Insufficient stability for reliable flight	C3	Proper simulation of rocket characteristics using RockSim; increase fin size to move CP further back.	Design analysis with simulation environment	B2
Nosecone damage	Damage in landing of previous launches or during travel; improper sealing from environmental hazards	Unstable flight; unstable nosecone structure	C3	Strong nose cone selection; evaluate structural integrity after and before each launch; protective paint coating	Design analysis in choice of nose cone; validation from subscale launch	B2
Excess friction between rocket and launch rail	Misalignment or poor installation of launch lugs; misalignment of launch rail; improper lubrication or debris on launch rail	Rocket does not reach desired altitude	A3	Use of jig to align launch lugs; follow rail assembly procedures, checking for correct alignment and using acceptable lubrication	Verification from subscale launch; pre-flight inspection of alignment of rail buttons	A2

4.15.7 Environmental Effects Analysis

Tables 16 and 17 show interactions between the rocket and the environment during launch. While many of the risks listed are potentially hazardous to personnel at the launch sight, this section focuses on the interplay between weather, wildlife, and other environmental hazards with the rocket.

Table 16: Environmental Impact on Rocket

Environmental Impact on Rocket						
Risk	**Cause**	**Effect**	**RR**	**Mitigation Strategy**	**Verification of Mitigation**	**PMRR**
Structural failure; launch pad fire	High temperature or exposure to sunlight	Overheating of electronics; warping of body tube or structural components	E3	Prior to placement on launch pad, rocket assembled in tent-shaded area; time from setup on pad to launch minimized if possible	Study of launch operations procedure to minimize field time; body tube integrity verified by previous exposure to Hotbox during curing process; battery temperature tested on pad prior to launch. NO-GO IF BATTERIES ARE OVERHEATED	C1
Extreme weathercock-ing	Excessive wind	Unexpected vehicle trajectory; vertical launch compromised	D4	Vehicle has a stability margin that minimize risk of both understable and overstable flight	Design analysis of fins and mass distribution to procure favorable stability margin; consultation of launch operations procedure to verify SSM on launch pad; subscale flight test validates choice of SSM. NO-GO IF STEADY WIND SPEED EXCEEDS 20 MPH	B1
Structural or component damage; misalignment of rocket axis; unintended ignition of vehicle	Contact with animals, particularly cows in a farm setting	Unexpected vehicle trajectory; damage to vehicle components or launch pad	E2	All structural and electrical components located internal to rocket body; launch pad leveled immediately prior to launch; ignition actuator not located within distance specified by minimum distance table	Design analysis of structural components; adherence to launch procedures; visual monitoring of launch pad area from final setup until launch. NO-GO IF ANIMALS TAMPER WITH LAUNCH PAD SETUP	C1

Table 16: Environmental Impact on Rocket

Environmental Impact on Rocket						
Risk	**Cause**	**Effect**	**RR**	**Mitigation Strategy**	**Verification of Mitigation**	**PMRR**
Damage to rocket body; parachute destruction	Excessive wind; nearby obstacles in field	Vehicle drags along ground due to large horizontal velocity; components may snag on obstacles; drift exceeds size of launch field	D3	Launch vehicle body kept void of protuberances; launch only occurs in field clear of destructive obstacles	Design analysis of external vehicle profile; certification of robustness of external components; consultation of launch operations procedure in choosing launch location. NO-GO IF STEADY WIND SPEED EXCEEDS 20 MPH OR LAUNCH FIELD NOT CLEAR OF OBSTACLES	B2
Launch pad not level	Pad sinks due to soft ground conditions; pad not leveled properly upon setup	Unexpected vehicle trajectory	D3	Plywood boards to prevent the launch pad legs from sinking into the ground; level brought to launch site	Consultation of launch operations procedure, which incorporates multiple verifications of the launch pad condition. NO-GO IF LAUNCH PAD IS NOT LEVEL	B2
Difficulty assembling vehicle components in the field	Excess humidity	Swelling or warping of body tube and internal components, particularly wooden bulkheads	D2	Inner surface of body tube and internal components weatherproofed with polyurethane spray; sandpaper taken to launch field as potential minor resizing tool	Adherence to fabrication design; consultation of launch hardware list. NO-GO IF VEHICLE ASSEMBLY NOT POSSIBLE WITHOUT MAJOR MODIFICATIONS	A1
Ice buildup on vehicle body; sealing of vent holes	Below freezing temperatures and precipitation	Increased vehicle mass; uncharacter-ized changes in aerodynamic drag; pressure buildup inside rocket body	D2	Final assembly performed under tent; vehicle wrapped in blanket until immediately prior to launch; sandpaper taken to launch field to scrape off ice buildup	Visual inspection of vehicle prior to launch. NO-GO IF ICE VISIBLE ON VEHICLE BODY	C1
Launch pad fire	Wet conditions compromise integrity of the electronics or wiring	Electronics short circuit	C3	Electronics enclosures sealed with putty to prevent water exposure; weatherproofing of inner surface of body tube	Consultation of launch operations procedure; adherence to fabrication design. NO-GO IN CONDITIONS OF HEAVY PRECIPITATION	B2

Table 16: Environmental Impact on Rocket

Environmental Impact on Rocket						
Risk	**Cause**	**Effect**	**RR**	**Mitigation Strategy**	**Verification of Mitigation**	**PMRR**
Untethered hardware blown around	Excessive wind	Final vehicle assembly made more difficult; personnel hazard	B2	Minimization of hardware requirement on launch day; securement of hardware in labeled boxes	Design and consultation of launch hardware list. NO-GO IF WIND PREVENTS SAFE VEHICLE ASSEMBLY	A1
Excessive launch rail friction	High temperatures or exposure to sunlight, low humidity; misalignment of rail buttons	Unexpected vehicle trajectory	B2	Rail coated in Vaseline; rail buttons aligned properly	Design analysis and testing confirms alignment of rail buttons; consultation of launch operations procedure with inspection of rail condition prior to launch. NO-GO IF LAUNCH RAIL NOT IN PROPER CONDITION FOR LAUNCH	A1

Table 17: Rocket Impact on Environment

Rocket Impact on Environment						
Risk	**Cause**	**Effect**	**RR**	**Mitigation Strategy**	**Verification of Mitigation**	**PMRR**
Unsuccessful parachute deployment; parachute failure	Insufficient or excessive parachute deployment charges and/or shear pins	Destruction of launch vehicle upon ground impact; scattering of foreign debris; potential cratering	E4	Recovery system extensively ground-tested to validate deployment charge calculations, parachute wrapping technique, and deployment method	Design analysis to verify expected deployment of parachute; consultation of launch operations procedure while packing parachute	E1
Launch pad fire	Heat from main engine ignites dry vegetation surrounding the launch pad	Damage to vegetation and potential hazard to nearby team members	E2	Launch conducted in area clear of excess underbrush and vegetation; launch aborted in extremely dry conditions; fire extinguisher taken to launch site	Consultation of launch operations procedure during launch. NO-GO IF DRY CONDITIONS PRESENT FIRE HAZARD	D1

Table 17: Rocket Impact on Environment

Rocket Impact on Environment						
Risk	**Cause**	**Effect**	**RR**	**Mitigation Strategy**	**Verification of Mitigation**	**PMRR**
Mid-air explosion of rocket or components	Internal failure of payload or main engine	Widespread scattering of vehicle debris	E1	All payload components with explosive potential rated with a safety factor of 4; motor is sourced from a reliable, commercial supplier	Design analysis of components seeing pressure; hydrostatic testing of house-made nozzles	B1
Vehicle strikes people or structures outside planned launch area	Excessive wind; improper timing of main parachute deployment, possibly due to buildup of pressure near avionics bay	Vehicle drifts outside launch field	C2	Vent holes cut in bulkheads and vehicle body to eliminate pressure buildup; large launch field chosen in case of early parachute deployment	Design analysis to verify pressure venting and reduce pressure leaks from thruster system; simulation testing to predict drift under non-ideal conditions; launch operations procedures followed in choosing launch field. NO-GO IF WIND SPEED EXCEEDS 20 MPH	B1
Harm to environment from litter	Improper disposal of trash; failure to setup up designated trash bag	Poisoning, strangulation, or suffocation of wildlife	B5	Deployment of trash bags at launch site; documentation of hardware taken to site	Adherence to launch operations procedure; consultation of launch hardware checklist	B2
Injury to wildlife	Animals contact launch pad or vehicle; rocket impacts wildlife during flight or upon landing	Animal wounds, contusions, or death	D1	Launch conducted in area clear of wildlife or obstacles	Adherence to launch operations procedure; visual monitoring of launch pad from setup until launch	A1
Chemical poisoning of ponds or ground water	Leakage of battery fluid or excess fuel	Electrical components leech toxic chemicals into water if water landing	D1	Electrical components provided extra separation from environment within body tube; rocket recovered quickly to minimize exposure time; launch site chosen away from bodies of water	Consultation of launch operations procedure before and after launch. NO-GO IF BODY OF WATER WITHIN 2500 FEET OF LAUNCH PAD	B1

4.15.8 Project Management

Table 18 details difficulties that may be encountered while the team attempts to meet both self-imposed and NASA criteria/deadlines.

Table 18: Project Management Risk and Mitigation

Project Management Risk and Mitigation				
Risk	**Consequences**	**RR**	**Mitigation Strategy**	**PMRR**
Vehicle testing failure	Vehicle parts are destroyed or damaged during ground testing or flight testing. Could lead to ordering new materials late in the year and running the risk of not completing the project on time.	E3	Design the vehicle components after extensive mathematical and physics analysis in order to ensure that a damaging failure will not occur. Only conduct tests with the potential to cause damage once a robust design has been developed and implemented. Set up an inventory of spare parts and components for building a second rocket within a week	E1
Weather launch delays	Inability to meet CDR and FRR timelines and obligations	D4	Have multiple possibilities for launch by working with launch clubs in the Tri-State area of TN, AL, and KY.	C2
Rushed timeline	Low quality in manufacturing, vehicle safety, payload safety, and risks to mission success in all aspects	D3	Well defined component verification metrics and workmanship standards, internal launch readiness reviews, no culture of go fever	D1
Communication breakdown between team members	Failure to meet deadlines; failure to show results	D2	Frequent meetings to improve team morale and stress the importance of timelines, and chain of command. Recalibration of deliverables based on progress.	B1
Delays in critical path	If a portion of the project that is necessary to complete the next portion takes longer to complete than expected, there could be delays in project development.	C3	Make sure that realistic expectations are set for completion of elements along the critical path.	B2
Ambiguous product lead time	If the amount of time it takes for parts to ship is ambiguous or unknown, there could be unexpected delays in project development.	C3	Ensure somebody is responsible for knowing the lead times on all parts, and trying to eliminate all the ambiguity.	B1
Excessive academic responsibility	Fabrication, testing, or launch deadlines would be compromised	C2	Weekly team meetings cover individual availability to ensure adequate personnel are available for each scheduled task	C1
High budget costs	Could threaten the feasibility of the project, as well as a violation of the rules of the competition.	C2	Keep a detailed budget and projected budget to minimize the chance of overspending. Make sure that every purchase is justified.	C1

Table 18: Project Management Risk and Mitigation

Project Management Risk and Mitigation				
Risk	**Consequences**	**RR**	**Mitigation Strategy**	**PMRR**
Misplaced or lost component	Cause delays in construction of the rocket and payload. Loss of time in searching for misplaced component. Incurs redundant cost in the event of reordering.	B4	Routinely organize shop. Delegate sections of the shop for components/equipment of various sections of the rocket (i.e. mechanical payload section, payload electronics section, recovery section, etc.). Order in excess when fiscally reasonable for vital components. Take care to place vital components in designated, labeled areas.	A4
Equipment breakdown	Machine shop or laboratory equipment breakdown could cause a slowdown in production and threaten the timely completion of the project.	C1	Ensure that the team has access to multiple machine shops in case equipment in one place fails. Also, ensure that equipment is used and stored properly to minimize the likelihood that such a failure will occur.	B1
Unavail-ability of parts or delays in parts delivery	Delays in construction of the rocket and payload attachment scheme; rushing through work or settling with parts that are not compatible with the ideal design	B3	Start the design process very early, and allow room in the design for the use of parts other than those initially selected: flexibility in design without the compromise of safety or science value	A2
Limited access to machine shops	Delays in fabrication of various parts or rushed work. Impact on timely completion of the project.	B2	Ensure that contact with the machine shop operators is constant, and that available times for access are established.	B1
Personnel shortage	Student or faculty members could be unavailable, which can lead to higher workloads for others, or the lack of technical knowledge of some system aspect.	B2	Make sure that the knowledge of rocket construction and testing techniques is known by the entire team. Make sure that the schedule is known by everyone so that people are not voluntarily absent/unavailable at inopportune times.	B1
School holidays	Slows down the project and threatens timely completion and available times for testing.	A2	Ensure that the schedule for work and testing is designed with school holidays in mind, such that the team does not expect to have full access to equipment or personnel during those times.	A1

5 Payload Criteria

??

5.1 Design of Payload Equipment

5.1.1 Design Alternatives and Chosen Design

5.1.1.1 Design Selection

When approaching the flight experiment of roll control, VADL analyzed various actuator design solutions such as tangential thrusters, magnetic torque application, gravity-gradient torque, aerodynamic torque, solar radiation pressure, mass movement, momentum wheels (MWs), control moment gyroscopes (CMGs), as well as many others.

[15] Several of these were eliminated given that they are more suitable for use in high altitude flight, specifically those solutions of magnitudes suitable for satellite or long-distance spacecraft positioning over long time periods. These solutions include solar radiation pressure, gravity-gradient torque, and external magnetic torque. Other alternatives such as MWs and CMGs were eliminated due to the fact that the size of component needed for these two methods to produce adequate torque violated the size constraints of our launch vehicle. [16]

Furthermore, mass movement devices were eliminated due to their inherent characteristics such as mechanical complexity, single-use application, and low compatibility with an active control scheme. [17] Also eliminated after consideration were the aerodynamically induced applications of fin-based rotation control (i.e.thruster vanes and aerodynamic control surfaces) for many reasons, the most pressing of which were the high cost of construction and a needed active burn scenario for the case of thruster vanes and the difficulties in ground-based testing and mechanical complexity for the case of control surfaces.

Lastly, VADL analyzed the use of tangential cold gas thrusters. Despite the drawbacks of needing to carry compressed propellant within the flight vehicle, VADL feels that the high impulse and short time frame of the post-MECO and pre-apogee flight for USLI make this the best option for our roll control payload experiment. Additionally, the ground-based testability of this method offers superior characterization abilities for the system in terms of control and this ground-based analysis reduces the costs of relying on full scale launches alone for testing purposes. Figure 80 shows a summary of the weighted evaluation of the attitude control alternatives. More detailed information on the analysis of these alternatives can be found in the VADL Preliminary Design Review 2016-2017.

Attitude Control Method	Torque Potential	Ground-Based Testability	Ease of Manufacture	Verdict
Thruster	10	8	8	Proceed
Magnetic Torque	1	5	4	Abandon
Gravity-Gradient Torque	1	3	4	Abandon
Aerodynamic Torque	10	3	8	Abandon
Solar Radiation Pressure	1	1	2	Abandon
Mass Movement	5	3	7	Abandon
Momentum Wheel	3	5	5	Abandon
Control Moment Gyroscope	3	5	5	Abandon

Figure 80: Weighted Evaluation of Attitude Control Alternatives

For these reasons, VADL has chosen to move forward with the use of a tangential cold gas thruster system to induce and control our roll and counter roll during launch.

5.1.1.2 Design Criteria

The cornerstone of the cold gas thruster system is the converging-diverging nozzle which accelerates the propellant flow from stagnation conditions at the outlet of the air tank regulator to supersonic speeds at the nozzle exit, providing the thrust required to achieve the scientific payload objective.

For full scale, the team plans to use identical nozzles as used in subscale (albeit machined again from the same 12L14 steel stock given that four nozzles are now needed vs two for both roll and counter roll thruster couples). The nozzle design was determined through an analysis of isentropic flow equations and various design constraints (such as perfectly expanded conditions at 3000 ft and stagnation conditions equal to tank pressure and temperature values). The design also took into account aspects such as machinability, consistent geometry, pressure rating, and ease of mounting. Please refer to Table 19 and Figure 81 for nozzle design specifications. For further detail on the design process, please refer to VADL's Preliminary Design Review (PDR Section 6.2.3).

[15] Fortescue, Peter, Graham Swinerd, and John Stark. Spacecraft Systems Engineering. 4th ed. (301-306)
[16] Gurrisi, Charles, Raymond Seidel, Scott Dickerson, Stephen Didziulis, Peter Frantz, and Kevin Ferguson. "Space Station Control Moment Gyroscope Lessons Learned." Proceedings of the 40th Aerospace Mechanisms Symposium
[17] Fortescue, Peter, Graham Swinerd, and John Stark. Spacecraft Systems Engineering. 4th ed. (307)

Table 19: Nozzle Overview

Throat Diameter	1.5 mm
Exit Diameter	3 mm
Converging Half-Angle	30 degrees
Diverging Half-Angle	10 degrees
Length	19.05 mm

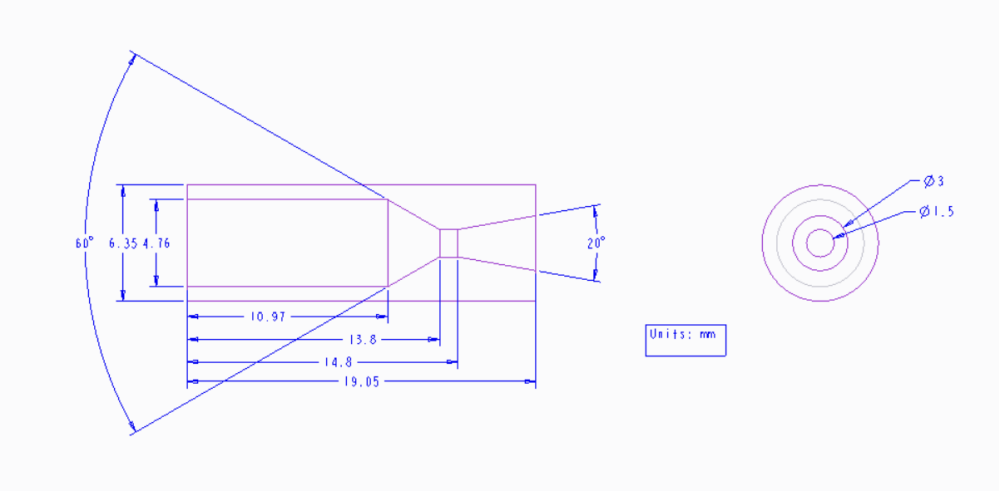

Figure 81: Nozzle Technical Drawing

One key difference from subscale in the operation of these nozzles is the choice of propellant. In order to obtain a greater thrust, VADL will be employing a mixture of air and nitrogen — specifically, 2000 psi of air and 2000 psi of N2 for a total tank pressure of 4000 psi. Since the specific volumes of nitrogen and air are quite similar (1.25 and 1.29 kg/m^3, respectively), a similar mass of each can be stored in the tank given equal volumes. However, nitrogen has a higher specific impulse than does air, giving the thrusters more thrust capability for the volume of propellant.

5.1.1.3 Payload Assembly and Rocket Integration

The payload thruster system as well as payload control electronics are located in the forward portion of the rocket body. As shown in Figure 82, the pressurized air tank rests in the nose cone, supported by expandable polyurethane high density foam. A centering bulkhead prevents lateral movement of the tank inside the nose cone and restrains the foam during the pouring and expansion phase of fabrication. The tank will be held rigidly in place by bulkheads 1 and 2 (BH1 and BH2, respectively) as shown in Figure 83, where bulkhead 1 is 3/8 plywood, and bulkhead 2 is 0.05 high strength stainless steel. Note that this dual bulkhead design was intended to hold the pressure regulator (see Figure 101) in tension and thus in a stable configuration without the support of the foam and nose cone. Also note that the regulator contains two burst discs — one protecting the regulator itself at 6 kpsi, and another protecting the outlet at around 750 psi.

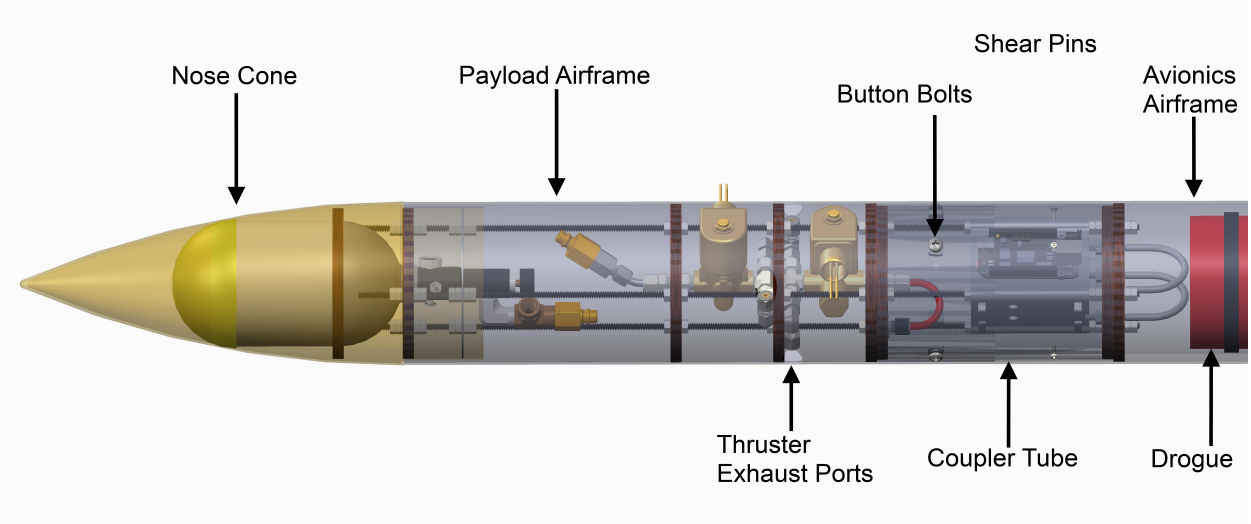

Figure 82: Payload Rocket Integration

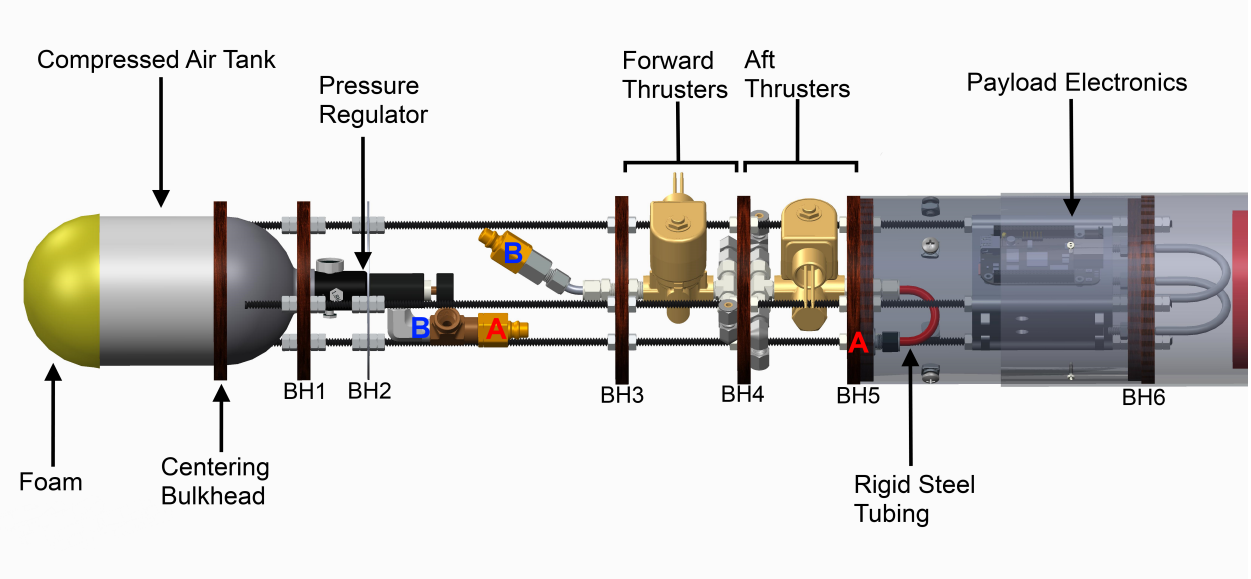

Figure 83: Payload Assembly

At the outlet of the regulator is a 1/8” male to 1/4” female NPT adapter, which will attach to an NPT pipe tee. From there, the propellant flow sees one of two routes depending on the active thruster couple. Only one route is open at any time. See Figure 84 for the two propellant routes and the sequence of components and fittings employed. Also shown in Figure 84 is the factor of safety for and set operating pressure seen by each component.

For actuation of the aft thruster couple (between bulkheads 4 and 5), the flow exits the pipe tee into a male NPT to Quick Disconnect hose coupling (red A in Figure 83) and then into a flexible hose (not shown) running through bulkheads 3 and 4 (BH3 and BH4, respectively). The hose is connected to female NPT threads into a through-wall Yor-Lok compression fitting adapter embedded in bulkhead 5, indicated by the red A (note that this bulkhead as well as bulkhead 6 consist of two pieces: an outer bulkhead and an inner centering bulkhead used to hold the coupler tube in place). The Yor-Lok based compression fitting design enables a modularity and interchangeability of components to the payload system as opposed to the rigidly welded thruster system in the 2015-2016 VADL project. From the

Yor-Lok fitting, a section of smooth bore steel tube is bent into a ”U”, diverting the flow back through bulkhead 5 into a Yor-Lok to male NPT through-wall fitting and then into the solenoid. The flow then passes through the open solenoid valve into a male NPT to Yor-Lok pipe tee fitting. The flow path then diverges into the two thrusters, which consist of a custom-machined converging-diverging steel nozzle held inside a Yor-Lok elbow.

Actuation of the forward thruster couple (between bulkheads 3 and 4) is similar. Flexible hose with male NPT fitting is connected to the female NPT orifice of the pipe tee, indicated by a blue B in Figure 83. The hose is then attached to the Quick Disconnect coupling (blue B), which is fixed to a female NPT to Yor-Lok adapter. From the Yor-Lok, a bent section of steel tube takes the flow to a through-wall Yor-Lok to male NPT adapter at bulkhead 3. The bent steel tube is used to offset the fittings in order to prevent interference with the regulator knob, allowing minimal space to be used in this section. From the through-wall fitting, the flow enters the forward solenoid and exits into the atmosphere through a thruster couple identical to that of the aft thruster couple.

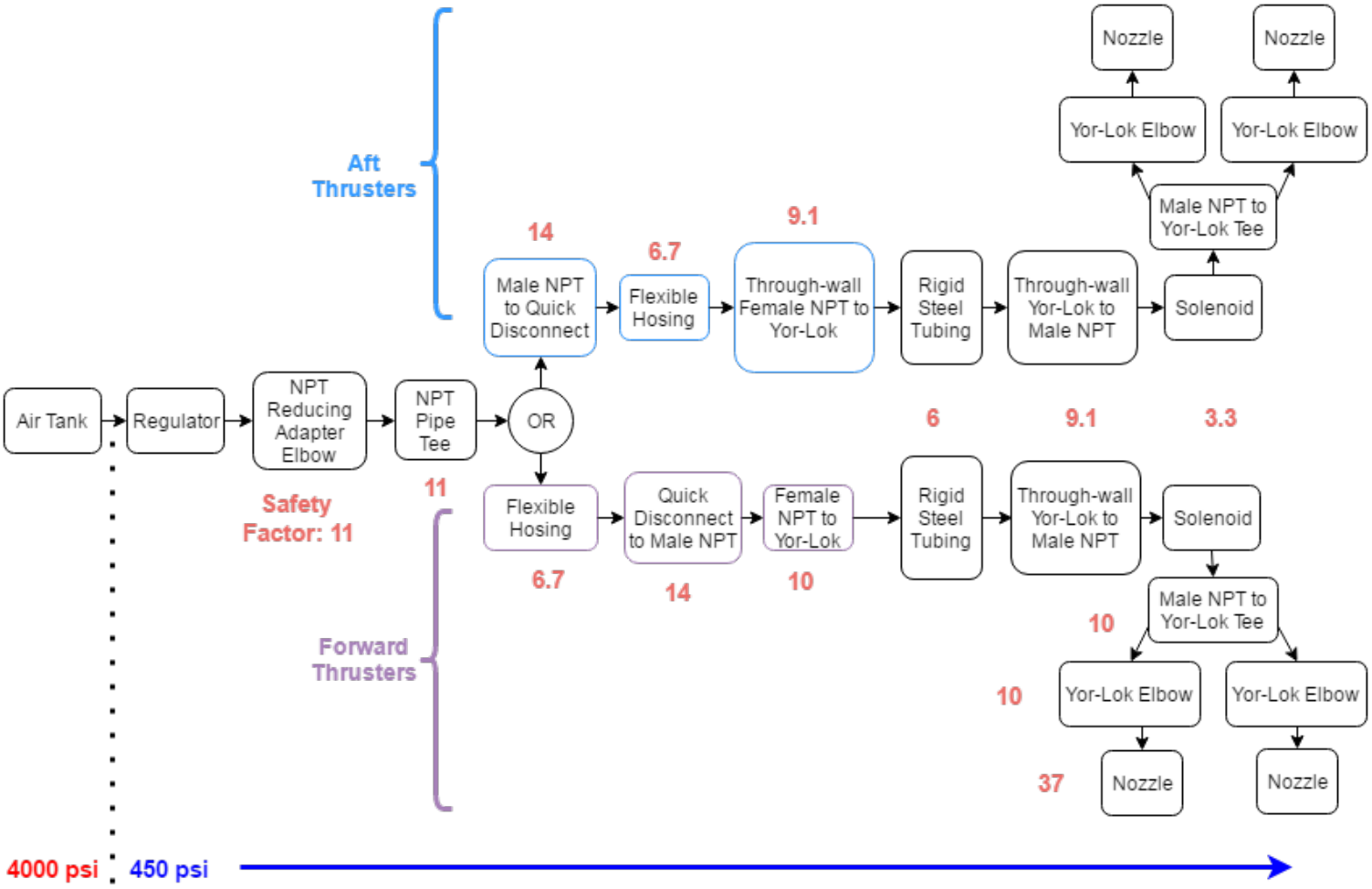

Figure 84: Payload Component Flowchart

Note that every Yor-Lok to Yor-Lok interface contains a segment of smooth-bore steel tubing. All components’ inner diameters are at least 1/4” (with the exception of the regulator outlet) in order to prevent any incident of choked flow.

The entire payload skeleton is held in place with three grade 8 steel threaded rods, a structural improvement over the 2015-2016 VADL design. When pressurizing the air tank at the launch pad, the entire payload body tube and nose cone will be removed, and the payload skeleton will remain free-standing through the coupling tube fixed to the avionics body tube. The coupling tube, which contains the payload electronics, is held in compression via bulkheads

5 and 6. Thus, the entire payload skeleton is supported by the threaded rods and coupler tube, and the coupler tube is fixed to the payload airframe by steel button bolts and to the avionics airframe by shear pins.

5.1.2 Payload Requirements and Risk Mitigation

5.1.2.1 NASA Derived Requirements

As described in the Payload Summary section (1.3.1), the selected scientific goal of VADL's payload is to induce and control post-MECO and pre-apogee roll about the rocket longitudinal axis. This objective entails several pertinent NASA derived requirements.

The entirety of the payload system is designed to accomplish the associated requirements with NASA's experimental objectives. Through computational analysis of thrusters and rigorous ground-based testing and flight testing, VADL will verify its ability to not only induce at least two rotations about the vehicle roll axis but also control vehicle roll post motor burnout. By implementing two sets of thruster couples pointed in opposite directions, the payload will have the ability to induce a roll as well as halt that rotation and induce counter roll. The very nature of the payload as well as the vehicle design guarantees that this objective is accomplished through mechanical devices and not through some passive roll effect.

Since the thruster system uses pressurized vessel, there is a need to meet the requirements that 1) the system employ a solenoid pressure relief valve that sees the full pressure of the tank, and that 2) the full pedigree of the tank shall be described, including the application for which the tank was designed, and the history of the tank, including the number of pressure cycles put on the tank, by whom, and when. In lieu of pressure relief valves, VADL has elected to use burst discs at regulator inlet and outlet (6 kpsi and 750 psi respectively). These single use pressure relief diaphragms will fully evacuate and vent into the atmosphere the gaseous propellant in the highly unlikely event of overpressurization. The tank itself is a Ninja carbon fiber wrapped aluminum air tank (SKU 40668; see Figure 85) manufactured for paintball purposes (note that the intended usage would subject the tank to much more frequent impacts than it would experience in VADL's payload). It was purchased solely for use in VADL's payload in July 2016. Since then, a detailed log of every refill cycle has been kept.

Figure 85: Ninja Air Tank and Regulator

Another key requirement is that the minimum factor of safety (Burst or Ultimate pressure versus Max Expected Operating Pressure) shall be 4:1. With an operating pressure of 450 psi, the minimum pressure rating of any payload component that sees should be 1800 psi. As indicated in Table 20, all components exceed this baseline pressure except for the solenoid, which was selected due to electrical and sizing constraints. VADL will apply for an exemption for this component.

Table 20: Payload Components and Pressure Ratings

Part	Supplier	P/N	Pressure Rating (psi)
Pressure Regulator	TBD	TBD	∼4500
NPT Male to Female Reducing Adapter	McMaster	50925K511	5000
Quick Disconnect Couplings	McMaster	5315K47	6500
Through-wall Yor-Lok to NPT fitting	McMaster	5182K196	4100
Steel Pipe Tee	McMaster	50925K197	5000
Yor-Lok to Female NPT Fitting	McMaster	5929K45	4900
Yor-Lok to Male NPT Tee Fitting	McMaster	5929K105	4900
Yor-Lok Elbow Fitting	McMaster	5929K213	4900
Female-female NPT Pipe Coupling	McMaster	50925K211	6000
Flexible Hose	TBD	TBD	∼3000
Steel Tubing	McMaster	9220K311	2700
Solenoid	Parker	73216BN2MT00	1500 (apply for exemption)
Air Tank	Ninja	40668	4500

5.1.2.2 Team Derived Requirements

In addition to NASA derived requirements, the payload system must meet requirements intrinsic to VADL's design. Through ground based testing, it has been verified that the each thruster is capable of delivering a minimum of 2.12 N of thrust. Through testing and inspection of specifications prior to purchase, it is verified that the solenoid is capable of actuating in under 30 ms and that all pressurized components upstream of the nozzle have an inner diameter of at least two times the throat area. By nature of the thorough design process, it is verified that the moment arm of the thrusters is maximized and that the custom-machined nozzle is machinable with respect to standard tool availability. Through rigorous ground based testing, it is verified that the pressure upstream of the nozzle is 450 psi and that the experimental thrust produced is within 15% of the ideal thrust. By nature of assembly, design, and selected components, it is verified that the payload is fully constrained and supported and that the system is modular in order to ensure interchangeability of components.

Requirements for the payload electronics system and their fulfillment are discussed in the following section.

5.1.3 Payload Electronics

5.1.3.1 System Level Design

The electrical system aboard VADL's full scale rocket will be composed of several main components - two solenoid valves, a microprocessor, an external circuit board, an IMU, a power supply, and a mounting sled. The system schematic (86) indicates signal paths through each component. The physical layout of the system is shown in 87. Although wires have not been included in 87, they will be routed through the internal cavity of the mounting sleds, with each component connected appropriately using 14-26AWG insulated copper wire and breakable high temperature terminals. In the following sections, each component will be analyzed more thoroughly with respect to design justification, requirements, and safety.

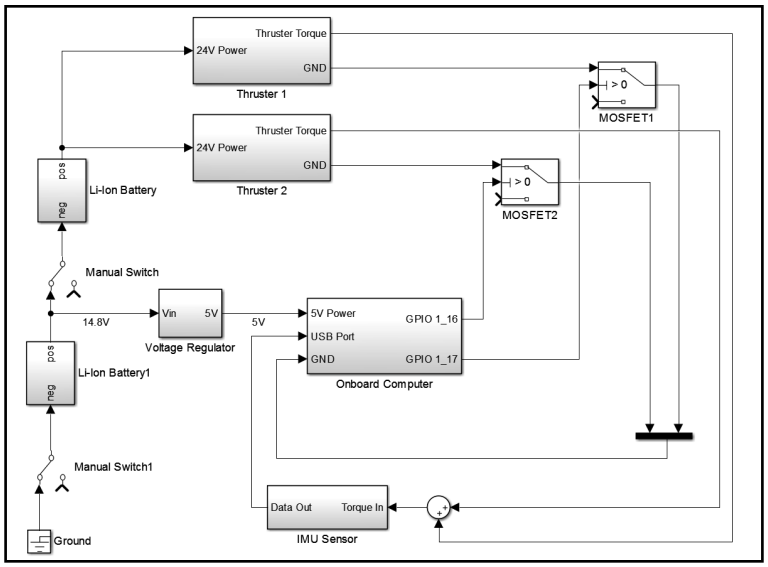

Figure 86: Payload Electronics System Schematic: Shows the payload electronics as a block diagram. Not all arrows represent electrical signals.

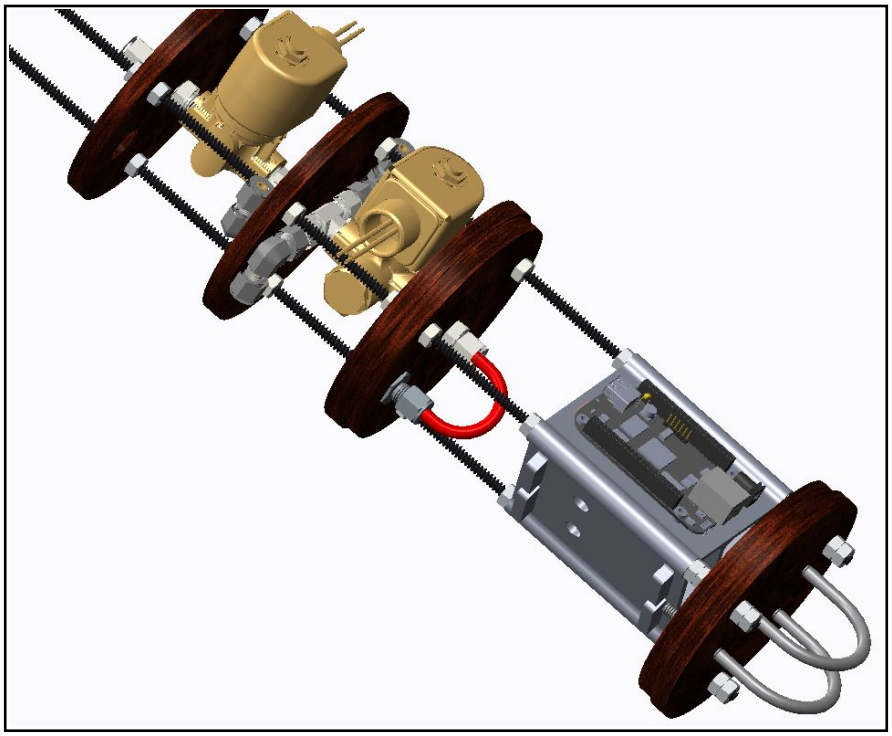

Figure 87: Payload Electronics System Layout: Connections will be made from the microprocessor (silver) to the solenoid valves (gold). Batteries are not depicted in this figure.

5.1.3.2 Electronics - Component Detail

Solenoid Valves Because the payload actuators use compressed gas as a pressure source, VADL will be using two normally-closed solenoid valves to control the flow of gas through two tangential thrusters. These solenoid valves

require approximately 0.75A at 24V for operation, already placing a major power requirement on the payload electronics. Solenoids also cause flyback, a large voltage spike that occurs when the solenoid's supply current is sharply reduced or cut off. A flyback diode placed in parallel with the solenoid allows the solenoid's inductive load to discharge safely when supply current is removed. A safety switch, which connects a high voltage terminal to the solenoids (this switch does NOT open the solenoids), is integrated into the external circuit board. This switch can be armed from outside the airframe after full assembly, preventing thruster misfire during assembly.

Heavy duty solenoids valves like these are relatively slow moving electromechanical devices. Therefore the opening and closing time of the solenoid is an important consideration for development of the control system, as pulse frequency could not exceed the sum of the opening and closing times of the solenoids, otherwise the solenoid will not fully open.

Microprocessor The microprocessor VADL chose to use is BeagleBoard's BeagleBone Black Wireless (BBB), a single-board computer equipped with a native Linux operating system. This particular microprocessor was chosen for its integrated wi-fi module, its large number of I/O ports, its compact size (85 x 50mm - slightly larger than a credit card), and because it has been used in the past for VADL projects.

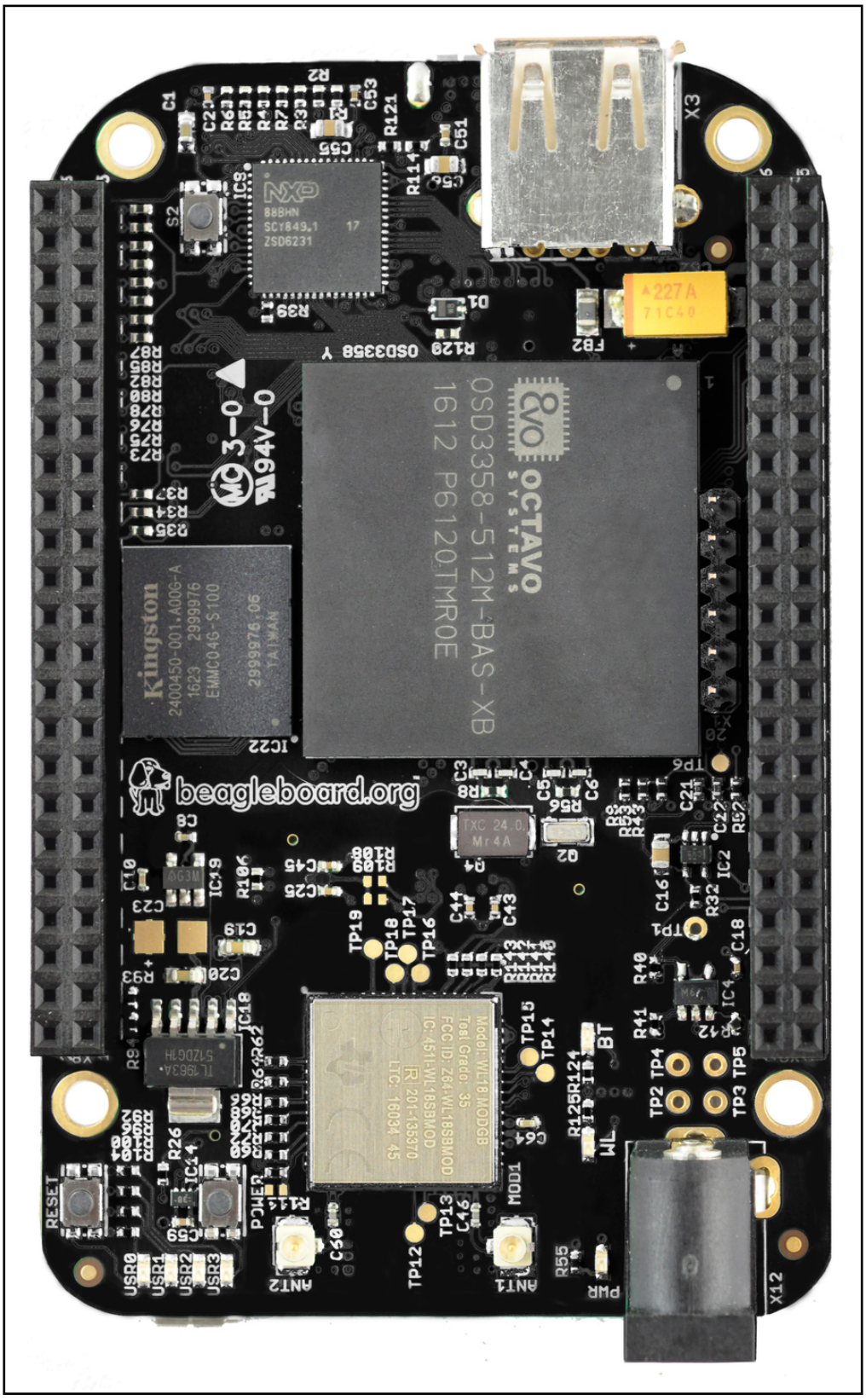

Figure 88: BeagleBone Black Wireless Single Board Computer

This particular microprocessor requires a power supply capable of delivering 2A at 5V, but draws 0.4A on startup, and settles to 0.25A idle. Since the solenoids require 24V for operation, a separate 5V circuit must be regulated from a higher voltage source, using a linear voltage regulator. An arming switch will connect the power supply to the BeagleBone, and can be activated from outside the air frame after full assembly.

During testing and launch procedures, the payload electronics bay is physically inaccessible, with the exception of two safety switches. Therefore, the BBB's integrated wi-fi module is an important design feature, because it allows for wireless communication between the microprocessor and ROSMOD's host servers, which are critical for software development, experiment compilation, launch initialization, and data storage.

Auxiliary Circuit Board An auxiliary circuit board is necessary for routing power and signals to and from the microprocessor. This circuit board was designed using Eagle Lite 7.6.0, and has been sent to Advanced Circuits for fabrication. Once the boards arrive back at Vanderbilt, they will be assembled with their components. Two previous circuit board prototypes were fabricated, one by hand-soldering components and jumpers to a protoboard specifically designed for the BBB, and another by milling a circuit board using Vanderbilt's in-house PCB mill. Complications arose from both of these earlier methods, so VADL chose a third-party fabrication house to avoid short circuits created during hand-soldering and manufacturing limitations of the in-house PCB mill. Components used in the auxiliary circuit board are rated above the voltage and current levels seen during normal operation. See layout (89), schematics (90 - 94), and bill of materials (95).

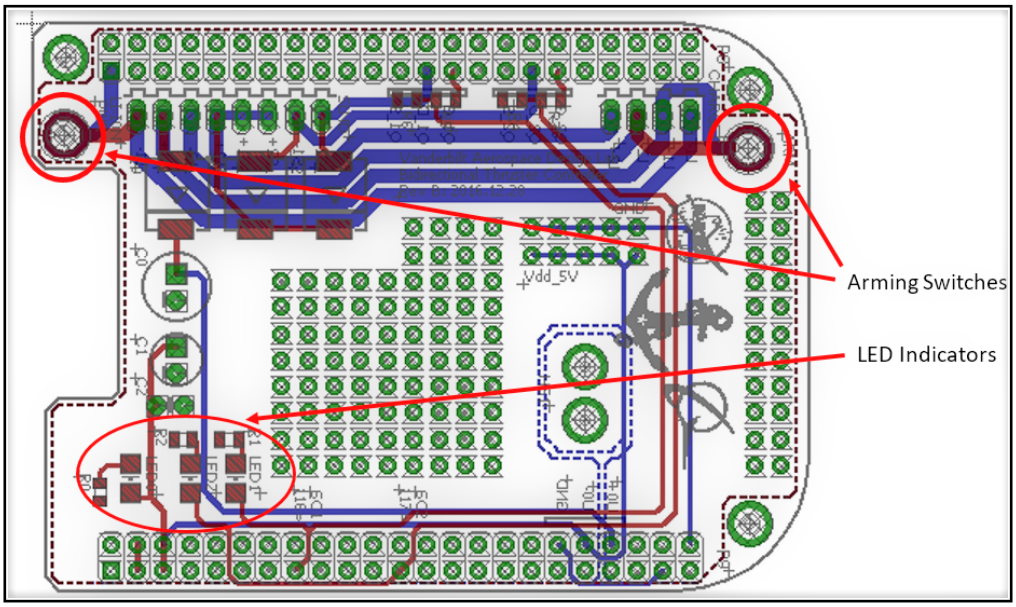

Figure 89: Auxiliary Circuit Board Layout: Switches and indicators are highlighted and labeled. Layout created using Eagle design software. Solid red traces represent the top copper layer. Solid blue traces represent the bottom copper layer. Green traces represent vias.

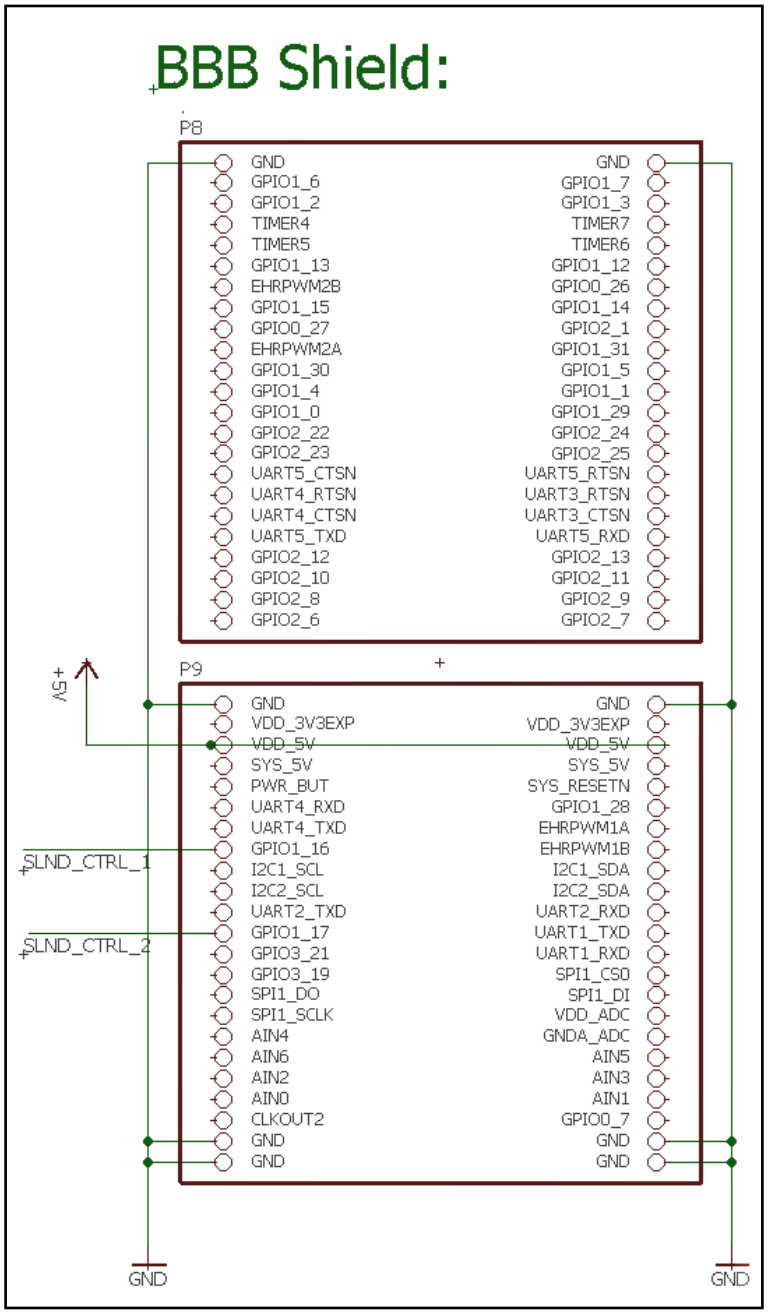

Figure 90: Auixiliary Circuit Board Schematic - BeagleBone Ports: This is a pinout of each input and output port of the BeagleBone Black. The nodes SLND-CTRL1 and SLND-CTRL2 are connected to pins GPIO 1-16 and GPIO 1-17, respectively. These pins are set to 3.3V (opens solenoid valve) or 0V (closes solenoid valve). 5V power is fed into the BB through the VDD-5V ports.

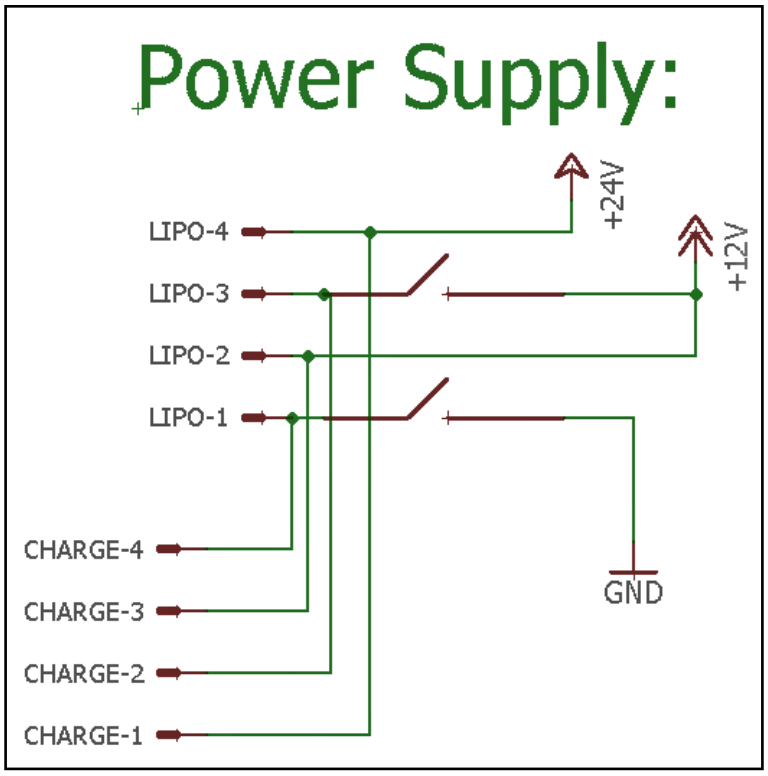

Figure 91: Auxiliary Circuit Board Schematic - Power Supply: LIPO1-4 represent the four leads of the two batteries. CHARGE1-4 represent the four leads that connect to a 3rd-party recharging circuit. Note the two switches that connect each battery's connection to ground. These are set-screw switches, and both must be closed to fully arm the payload. GND connects to the BeagleBone's ground node.

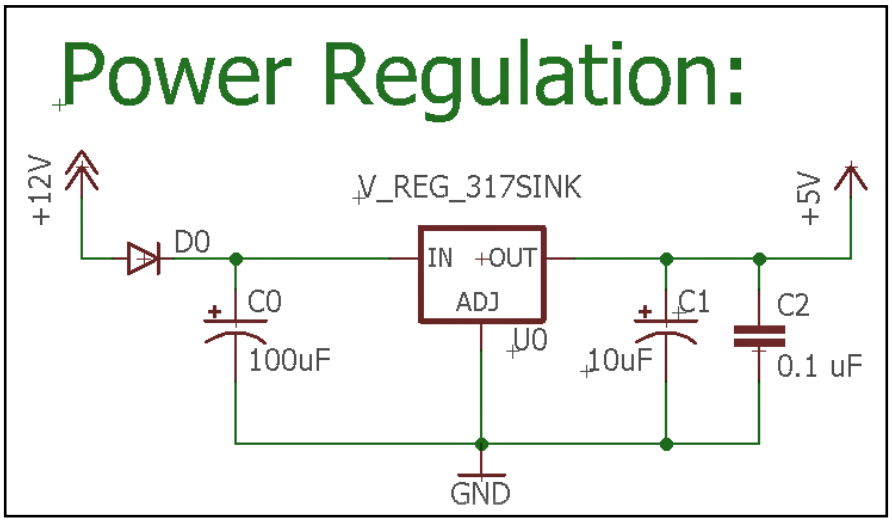

Figure 92: Auxiliary Circuit Board Schematic - Power Regulation: This circuit ensures that the BeagleBone Black is conncected to an appropriate voltage source. Capacitors provide power filtering, and a linear voltage regulator steps the voltage from 14.8V to 5V, dissapating power as thermal energy through a heatsink.

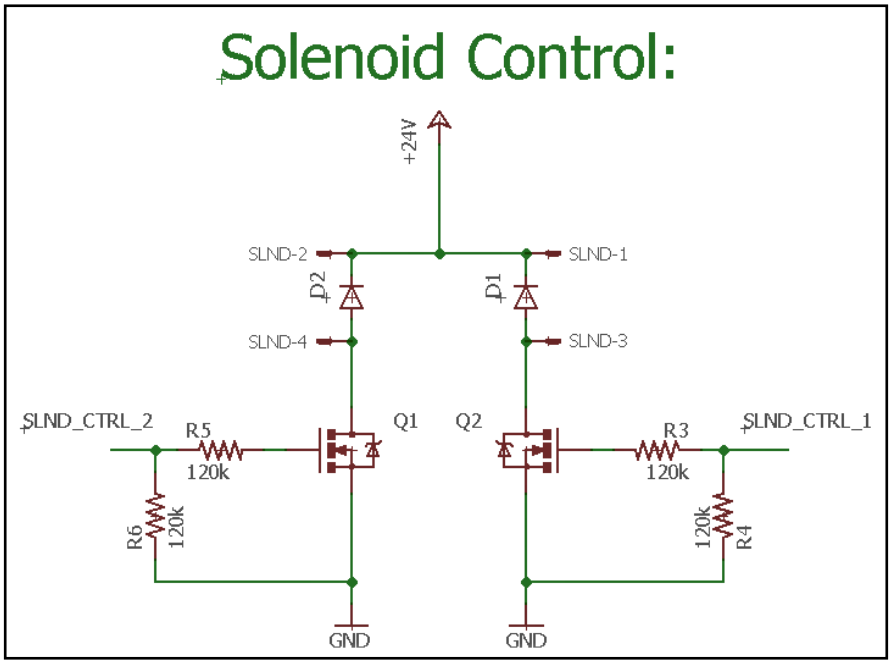

Figure 93: Auxiliary Circuit Board Schematic - Solenoid Control Circuit: This circuit uses N-channel MOSFETS switched by signals from the BeagleBone Black to transmit power to either solenoid. SLND1-4 are the four leads of the two solenoids. Flyback diodes allow the solenoids to discharge safely. The 24V node is connected to the output of the series connected batteries. Large resistors prevent leakage current, and hold the gate at 0V when the transistor is open.

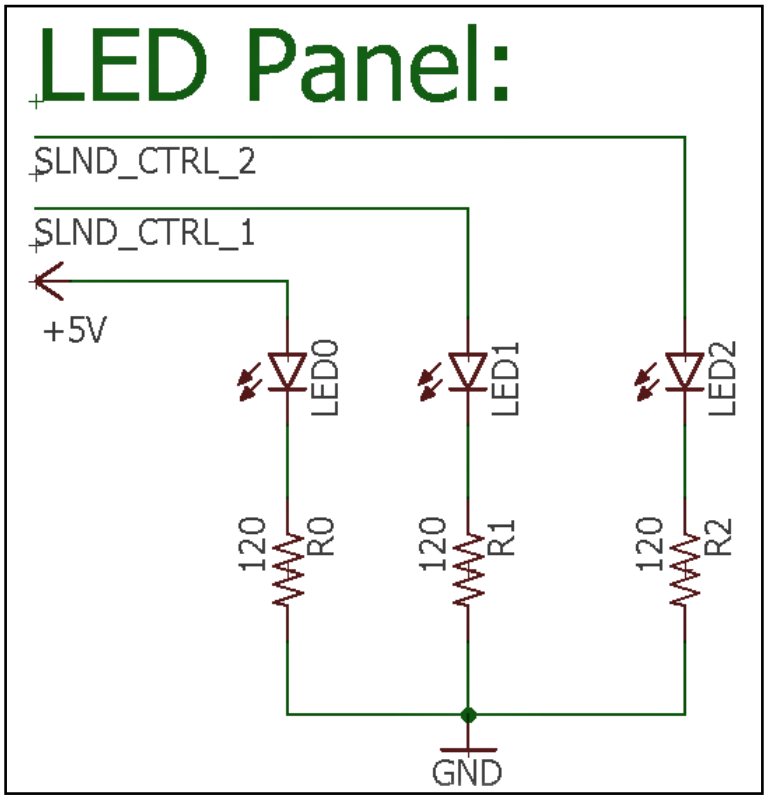

Figure 94: Auxiliary Circuit Board Schematic - LED Indicators: LED0 indicates 5V Power. LED1 and 2 indicate solenoid actuation.

Part Name	Manufacture	Description	Ratings/Value
LIPO, SLND	Molex	4 pin Connector @ PCB (Male) w contacts	24 AWG
LIPO, SLND	Molex	4 pin Connector @ PCB (Female)	24 AWG
D0, D1, D2	Vishay Semiconductor	Diode (smd)	3A, 600V
LED0, LED1, LED2	Lite-On, Inc.	LED (1206 smd, amber)	30mA
R0	Yageo	Resistor (0805 smd) - part of smd kit	200 Ω
R1, R2	Yageo	Resistor (0805 smd) - part of smd kit	120 Ω
R3, R4, R5, R6	Yageo	Resistor (0805 smd) - part of smd kit	120 kΩ
Q1, Q2	Fairchild Semiconductor	N-Channel MOSFET (through-hole)	60V, 32A
U0	STMicroelectronics	5V Regulator (through hole)	3A
C0	-	Polarized capacitor (through hole) - part of kit	100uF, 25V
C1	-	Polarized capacitor (through hole) - part of kit	10uF, 25V
C2	-	Ceramic capacitor (through hole) - part of kit	0.1uF, 50V
HS0	Aavid Thermalloy	T0-220 Heat Sink	2.5W @ 60C

Figure 95: Auxiliary Circuit Board Bill of Materials

The board features two integrated safety switches (highlighted in 89), designed to control power flow to the microprocessor and the solenoid valves, respectively. They are simple set-screw switches, closed by tightneing a screw into a nut soldered on the reverse side of the board. Once the screw head is in contact with the top surface of the board it will act as a via, connecting the switch contacts on either side of the board. Threads on the end of the screw will be fouled once inserted into the nut to prevent the screw from falling out.

The board also features an integrated charging port, so that the power supply can be recharged without detaching it from the board. This charging circuit will be tested and iterated upon if necessary, as it poses a risk of overheating the traces. However, these traces were thickened for high current transmission. Each battery is charged separatey on the manufacturer's charging circuit. The screw switches must be open during charging to ensure proper current flow from the charger to the batteries.

Another major component of the auxiliary board is the heat sink and the voltage regulator. Overheating was one of the major problems with early subscale prototypes, causing microprocessor power failures. The linear voltage regulator on the board was attempting to step 15V down to 5V, which requires a good bit of heat dissipation. If linear voltage regulators are not properly cooled, resistances inside the regulator will increase, generating even more heat, and reducing the output voltage. The regulator's thermal protection logic then momentarily forces the regulator to terminate power throughput, causing anything downstream to lose power. The voltage regulator will therefore require a heatsink, which has a fairly large footprint in all dimensions relative to other printed circuit board (PCB) components. To increase the clearance of the heatsink, its orthogonal fins will be bent wider.

There are three indicator LEDs on the external circuit board. LED0 indicates 5V power to the BBB. LED1 and LED2 indicate actuation of its corresponding solenoid. Each indicator draws approximately 20mA. However, the power draw of LED1 and LED2 is negligible, due to the low current consumption and extremely short duty cycle.

Inertial Measurement Unit VADL has chosen the VectorNav VN-100 IMU for onboard sensing (96). VADL has sourced the VectorNav VN-100 Rugged IMU as the primary on-board sensor from previous experimentation. This package exceeds all of the requirements in the payload requirements section above. It provides real-time data in nine axes comprised of a 3-axis gyroscope, 3-axis magnetometer, and 3-axis accelerometer. One of the strong points of the VN-100 is a built-in Kalman filter, which provides quaternion-based (gimbal-lock free) data in each axis at up to 300 Hz. This high speed and filtered data is critical for use in active control.

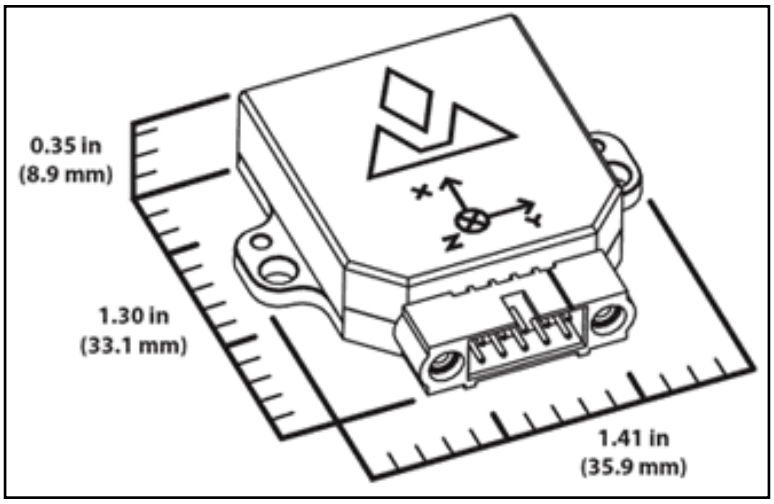

Figure 96: Dimensions of VN-100 IMU

Power Supply The payload's power supply must be at least 24V to operate the solenoid valves. 9V alkaline batteries were not a viable option because of their single power cycle and short lifetime. Since batteries must be secured to the rocket, it would be best if they could be attached once and recharged as needed, rather than having to replace or remove a dead battery. 9V batteries, even Li-Ion 9Vs, have fairly short lifetimes, around 600mAh. Since the BeagleBone Black, LEDs, and IMU pull 0.6A (worst-case) during steady-state operation, these batteries would last about an hour in the armed state.

To solve these issues, VADL chose to use two 14.8V rechargeable lithium-ion batteries, connected in series, to power the solenoids. Although large - each battery measures 73 x 71 x 18mm, and weighs 170g -these batteries are rechargeable. They are manufactured by Tenergy, have a capacity of 2200mAh, and are rated for a charge/discharge rate of up to 1C, or 2.2A. Since the BeagleBone Black, LEDs, and IMU pull 0.6A (worst-case) during steady-state opeation, the rocket, powered with these batteries, can be expected to power cycle at a little less than 4 hours. However, the solenoids require a large amount of power for operation, so the rocket should be launched within three hours of arming to prevent an airborne power failure. Together with the integrated chargine port, the entire payload can now be assembled once and recharged as a unit, rather than requiring a full disassembly of the rocket for recharging.

Large voltage sources present overheating issues for the the payload computer's voltage regulator, however. It is connected to the power source so that it sees the voltage across only one battery, instead of both. This prevents the voltage regulator from seeing the full series-connected voltage (29V), which would result in significantly increased heat generation. The heat sinking requirements that arise from this problem are detailed further in 5.1.3.2. Each battery is connected to the circuit board via low-profile locking connectors, and armed using safety switches highlighted in 89.

Mounting Sled VADL designed an innovatve mounting sled for the payload electronics, pictured below. It features a triangular shape, and an inner shelf, which allows the IMU to be mounted directly on the launch vehicle's longitudinal axis. Without this particular placement, roll data would be much more difficult to interpret. Wires are routed through the inner cavity of the sled, preventing accidental shorts during assembly. Batteries will be held to the sides of the sled using plastic zip-ties. The microprocessor will be secured to the sled with nylon 4-40 nuts and bolts.

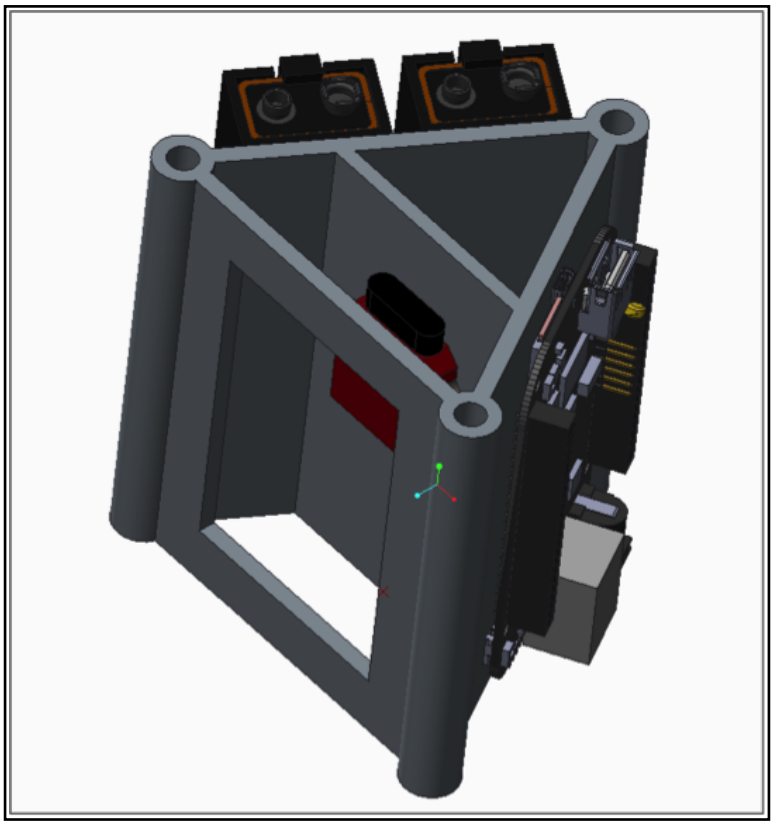

Figure 97: Payload Electronics Mounting Sled: This sled is made from ABS plastic a 3-D printer. Batteries pictured are 9V alkaline, but the actual power supply will consist of two Li-ion batteries, with one secured to each unoccupied face of the sled. The IMU is pictured in red on the center face of the sled. The sled will also feature cut outs for routing wires from the inside to the outsides of the triangular prism.

5.1.4 Control Schemes

The goal of the subscale flight was the successful actuation of the thruster system and IMU data collection to characterize the response of the system. Moving forward, the team must implement a control scheme to quickly and accurately achieve two rotations of both roll and counter-roll. This section will outline various control schemes that will be considered and tested on the FRAME to achieve this desired roll pattern.

5.1.4.1 System Dynamics

In order to apply an effective control scheme, the dynamics of the system must be fully characterized. The behavior of the system is described by a differential equation which is used to define the open-loop transfer function, an input-output relationship in the Laplace domain.

$$J\ddot{\theta} + B\dot{\theta} = T \tag{5.1}$$

In Equation (5.1), J is the moment of inertia about the rocket's main axis, B is the viscous damping coefficient, which is a function of the angular velocity, θ is the angular position, and T is the applied torque. Solving for the open-loop transfer function $H(s)$ results in Equation (5.2):

$$H(s) = \frac{\theta(s)}{T(s)} = \frac{1}{Js^2 + Bs} \tag{5.2}$$

Describing the output, $\theta(s)$, as a function of the input, $T(s)$ leads to Equation (5.3):

$$\theta(s) = \frac{\theta(s)}{T(s)} T(s) \tag{5.3}$$

A property of Linear Time Invariant (LTI) systems such as this one is that the response to any arbitrary input is a function of that arbitrary input convolved with the impulse response of the system. Plugging in an impulse as the input ($\delta(s) = 1$), Equation (5.3) becomes:

$$H(s) = \frac{\theta(s)}{T(s)} \delta(s) = \frac{\theta(s)}{T(s)} 1 \tag{5.4}$$

This shows that the impulse response is simply the transfer function of the system, which leads to the general dynamic response shown in Equation (5.5).

$$\theta(s) = H(s)T(s) \tag{5.5}$$

This is a second-order system with a characteristic equation given by Equation (5.6):

$$Js^2 + Bs = 0 \tag{5.6}$$

This shows that the system has poles at $s = 0, \frac{-B}{J}$. The lack of positive poles shows that the system is inherently stable. The response to a unit step torque input will result in an infinite output, which can be proven using the Final Value Theorem (FVT):

$$\begin{aligned}
\lim_{t\to\infty} f(t) &= \lim_{s\to 0} sF(s) \\
\lim_{t\to\infty} \theta(t) &= \lim_{s\to 0} sH(s)T(s) \\
&= \lim_{s\to 0} s \frac{1}{Js^2 + Bs} \frac{1}{s} \\
&= \lim_{s\to 0} \frac{1}{Js^2 + Bs} = \infty
\end{aligned}$$

5.1.4.2 Closed-Loop Response

Figure 98 shows the block diagram of the closed loop response, in which the present value of the controlled variable is compared to a reference input to allow the system to adjust accordingly.

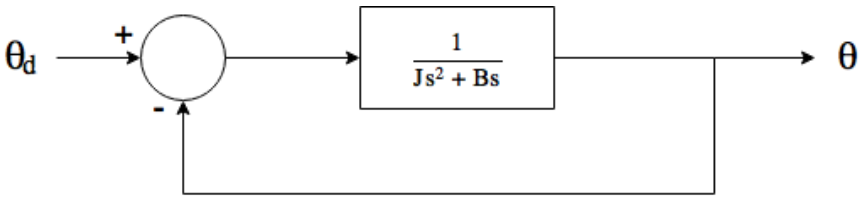

Figure 98: Closed-Loop Block Diagram

The FVT shows that a step input with a closed-loop leads to zero steady-state error. The closed-loop transfer function (CLTF) is derived as shown below:

$$\begin{aligned} CLTF &= \frac{H(s)}{1+H(s)} \\ &= \frac{\frac{1}{Js^2+Bs}}{1+\frac{1}{Js^2+Bs}} \\ &= \frac{1}{Js^2+Bs+1} \end{aligned}$$

Applying the FVT:

$$\begin{aligned} \lim_{s\to 0} s\frac{1}{Js^2+Bs+1}\frac{1}{s} &= \lim_{s\to 0}\frac{1}{Js^2+Bs+1} \\ &= 1 \end{aligned}$$

This result represents zero steady-state error, however says nothing about the speed of the response, which could be unacceptably slow. It is necessary to examine the damping ratio and the natural frequency of the system.

$$CLTF = \frac{\frac{1}{J}}{s^2+\frac{Bs}{J}+\frac{1}{J}} = \frac{\omega_n^2}{s^2+2\omega_n\xi s+\omega_n^2}$$

This results in a natural frequency of $\omega_n = \sqrt{\frac{1}{J}}$ and a damping ratio of $\xi = \frac{B}{2\sqrt{J}}$. A higher damping ratio will cause a slower response, however too low of a damping ratio can cause overshoot and oscillation.

To fully characterize the system, it is important to look at the step response and the impulse response of the plant in an open loop. The step response examines the output of the system to a continuous unit input at time $t > 0$. The impulse response is the output of the system to an instantaneous unit input at time $t = 0$. The impulse response is equal to the derivative of the step response. Equation (5.7) shows the transfer function in the Laplace domain of a step input.

$$H(s) = \frac{1}{s(Js^2+Bs)} \tag{5.7}$$

Using partial fractions expansion and the inverse Laplace transform, the step response is found (Equation (5.8)).

$$\theta(t) = \frac{J}{B^2}e^{-\frac{B}{J}t} + \frac{1}{B}t + -\frac{J}{B^2} \tag{5.8}$$

To plot these responses, values must be calculated for J and B. Initial calculations for the moment of inertia assumed the rocket to be a solid cylinder of mass $m = 11\ kg$ and radius $r = .057\ m$, which leads to a moment of inertia of $J = .018\ kg - m^2$. A more comprehensive analysis of the moment of inertia will be performed on the FRAME. The damping coefficient is a little more tricky, as this is a function of both the axial and angular velocity. A more complete discussion of this effect can be found in Section 3.4.3.2, however Equation (5.9) shows a brief derivation of the damping coefficient:

$$\frac{1}{2}C_d\rho v_d Z_{fin}\omega = (4)(0.5)(1.28)(1.2036)(100)(5.0404)(10^{-4})(\omega) = 0.155\omega \tag{5.9}$$

The axial velocity used in this calculation is 100 m/s, which is slightly above the velocity the rocket will be traveling during the experiment. The aggregate damping coefficient will therefore be a variable during flight rather than a constant, and must be estimated as well as possible. For the purposes of this analysis, a damping coefficient of $B = 0.2$ will be used. Figure 99 demonstrates the response of the system to a unit step input.

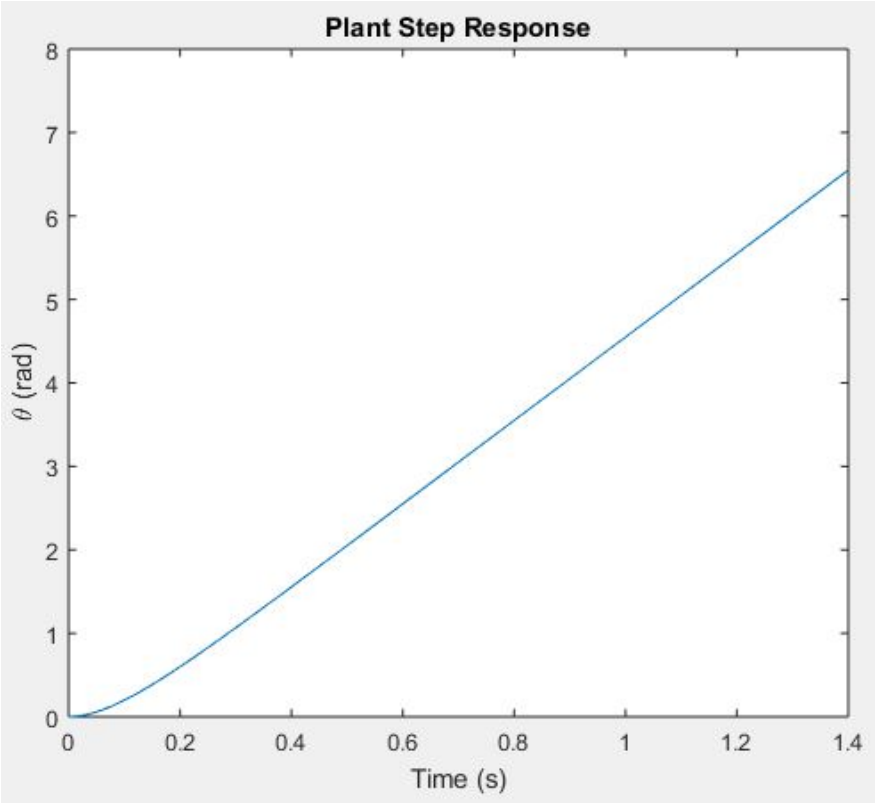

Figure 99: Step Response of Rocket

The angular position initially increases exponentially, which represents positive acceleration, however at a certain point the graph becomes linear, which represents a constant velocity. This shows the rocket reaching a terminal angular velocity due to the viscous damping force equaling the applied force. Equation (**??**) is the derivative of Equation (5.8) and represents the plant's impulse response. Figure 100 shows the reponse to an impulse. The rocket immediately begins to decelerate due to the damping.

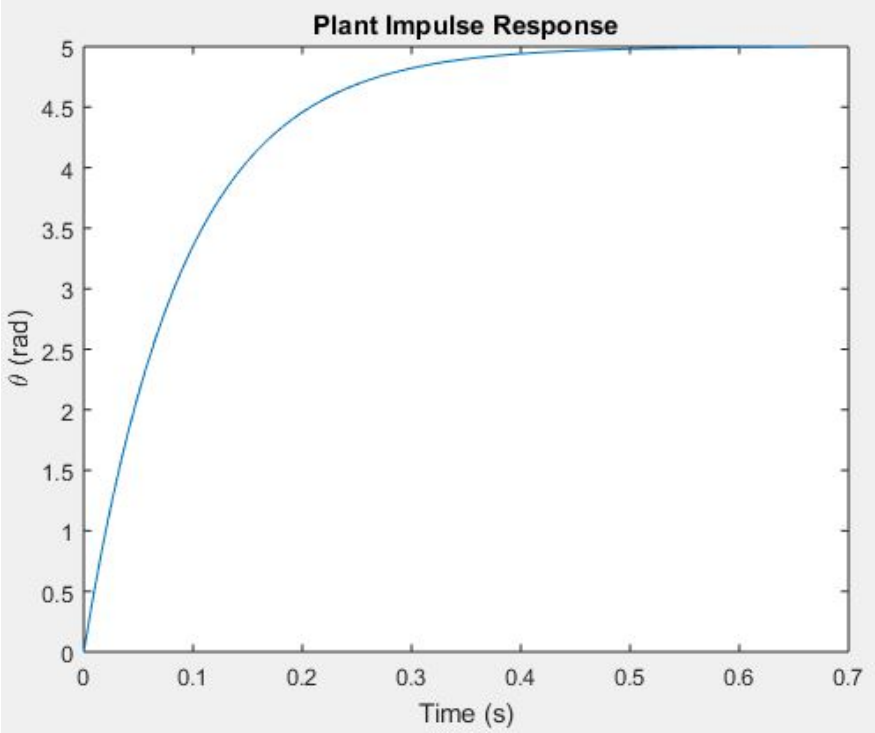

Figure 100: Impulse Response of Rocket

An analysis of these responsed under closed-loop control can be found in Section 5.1.4.3.

5.1.4.3 PID Control

Overview A PID controller is a feedback control mechanism that continuously calculates an error value based on the difference between a reference input and the measured control variable. The controller then applies a corrective action based on proportional, integral, and derivative terms of this error signla. The proportional term is based on the current error, the integral term is based on a summation of all past error, and the derivative term is based on a prediction of future error. Each term has its own effect on the system response, which must be analyzed to determine the appropriate scheme for this project.

In order to implement an effective PID controller, the system dynamics must be fully characterized (See Section 5.1.4.1). PID contrllers can be both stable and unstable. A stable PID controller is either an underdamped, critically damped, or overdamped system. Figure 101 shows the results of various damping conditions from a PID controller.

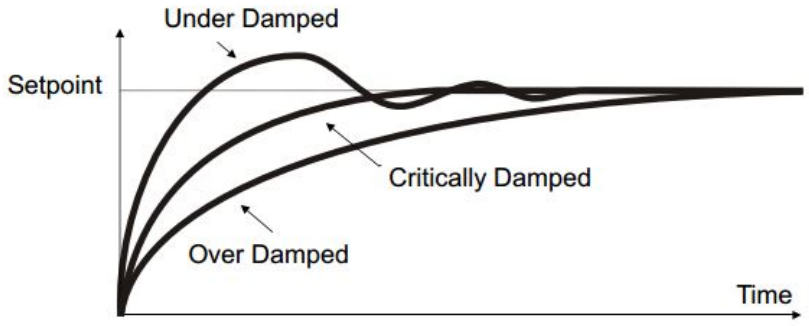

Figure 101: PID Damping Conditions

There are various values to examine when analyzing the performance of a PID controller, including overshoot, settling time, and steady-state error. Overshoot, which is seen in an underdamped system, is the distance past the reference input that the system travels. In the case of the roll-control system, the overshoot would be the the distance past 4π radians of revolution that the rocket travels. The rise time is the time it takes for the system to reach the reference input. In the case of this experiment, the time it takes for the rocket to reach 4π radians of revolution. Steady-state error occurs when the system settles at a point that is not equal to the setpoint. These values can be increased or decreased by changing the proportional, integral, and derivative gain terms.

A proportional (P) controller applies a corrective force that is proportional to the amount of error. Increasing the proportional gain value can decrease the steady-state error but can also lead to instability. An integral (I) controller applies a restoring force based on all of the past error values, which can reduce the steady-state error to zero and can also accelerate the process toward the setpoint, however it can also cause the system to overshoot the setpoint. Derivative (D) gain predicts system behavior which can improve settling time and stability of the system. Derivative controllers can never be used alone, as it can not improve steady-state error and also amplifies the effects of noise signals in the system.

Design Requirements The goal of the control system is to rotate the rocket exactly two rotations with minimal but positive overshoot while minimizing rise time, and then to repeat the process for counter-roll, returning the rocket to the predefined angular position defined after MECO. Table 21 shows the design requirements related to overshoot, rise time, and steady-state error for the two phases of the roll-control system.

Table 21: PID Design Requirements

PID Requirements		
Value	**Roll**	**Counter-Roll**
Overshoot	>0	0
Rise Time	Minimal	Minimal
Stead-State Error	>0	0

Once the system dynamics have been characterized, the next step is to decide which PID gain terms are to be included. Within PID control, each term (proportional, integral, derivative) affects the system in a different way. Based on the goals of the system controller, the gain values are either included or ignored to optimize the response. Section **??** lists the characteristics of various PID control schemes, and an analysis of the behavior under various gain values.

PID Analysis

Proportional Control Proportional control alone is incapable of stabilizing second-order systems like ours. Proportional control can also result in a steady-state error. As the proportional gain value is increased, the steady-state error will decrease, but will never be equal to zero. Although the elimination of steady-state error is not one of the goals of the control system, this control scheme is not ideal for our system. Figure 102 shows the Root Locus Plot of the proportional control open loop transfer function from Equation 5.2. A Root Locus Plot shows how variations in gain values effect the behavior of the system. The gain values begin on the poles when $K = 1$ and increase as the lines get farther away from the poles. Gain values on the horizontal axis in the left-hand plane represent overdamped systems, and values with non-zero y-coordinates are underdamped and see oscillation. Under proportional control, there is a location where the two poles meet, which represents the s value that corresponds to critical damping.

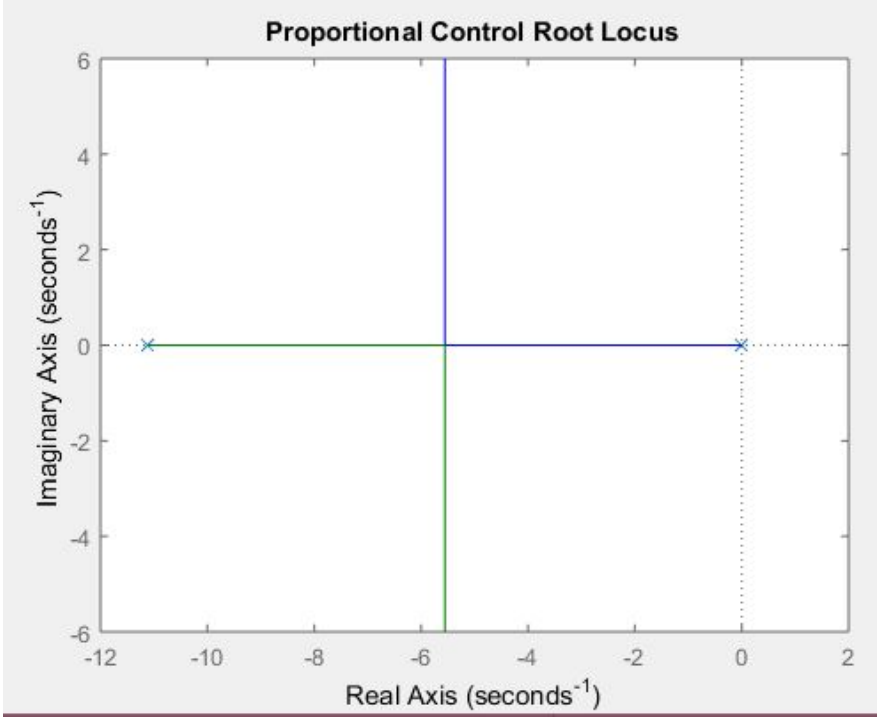

Figure 102: Root Locus Plot Under Proportional Control

The following derivation calculates the ideal gain value, K, under proportional control from the denominator of the closed-loop transfer function:

$$\begin{aligned} Js^2 + Bs + K &= 0 \\ (.018)s^2 + (.2)s + K &= 0 \\ (.018)(-5.5)^2 + (.2)(-5.5) + K &= 0 \\ K &= .56 \end{aligned}$$

Figure 103 shows the step response of the system under proportional control for various gain values.

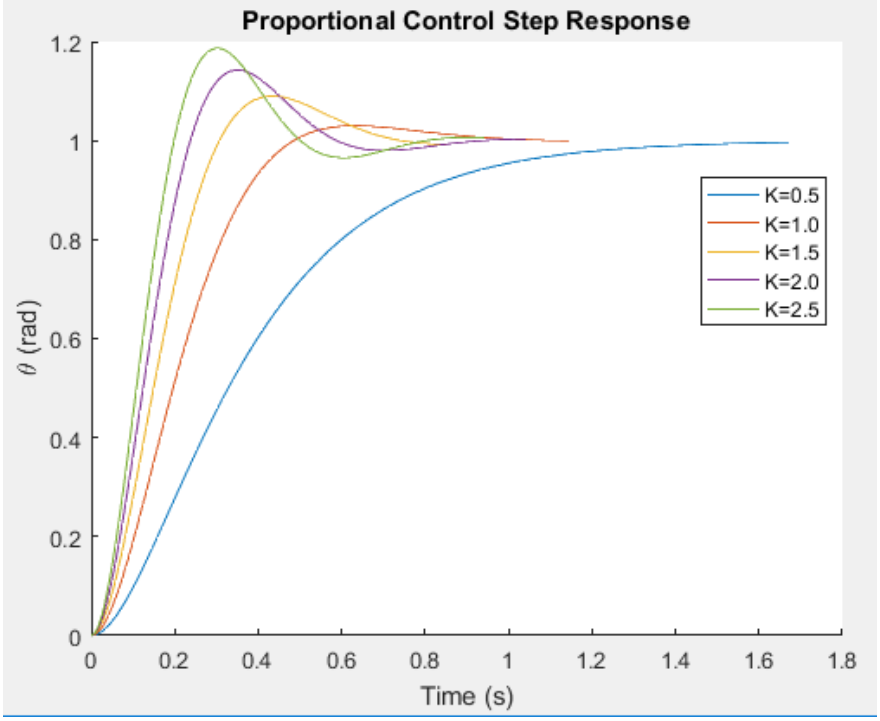

Figure 103: Step Response For Proportional Control

Increasing K_p beyond .56 will cause overshoot, however will also cause a faster rise time. Let's see what happens when we add in an integral controller.

Proportional-Integral Control The purpose of adding integral control to a proportional controller is to eliminate the steady-state error. However, in terms of speed of the response and stability of the system, integral control can be detrimental. PI control is most common in applications where the speed of the system response is not important, which could cause problems for our application. The open-loop transfer function for PI control is shown in Equation (5.10), and the closed-loop transfer function in Equation (**??**).

$$\frac{(1+\frac{\delta}{s})}{Js^2+Bs} \tag{5.10}$$

$$\frac{Ks(1+\frac{\delta}{s})}{Js^3+Bs^2+Ks+K\delta} \tag{5.11}$$

Where $\delta = \frac{K_p}{K_d}$. A similar analysis can be performed to optimize the gain values. The Root Locus Plot shown in Figure 104 provides the information necessary to calculate the gain value based on a specific gain ratio. The step response under PI control shown in Figure 105 shows the effect that altering the gain value has on the response of a system under a PI controller.

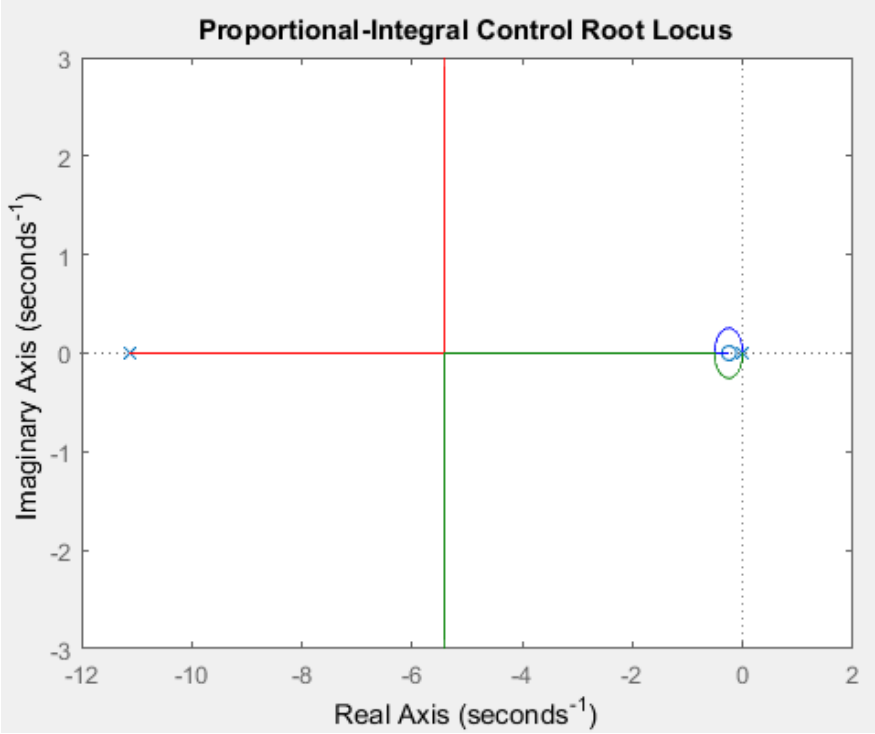

Figure 104: Root Locus Plot for Proportional-Integral Control

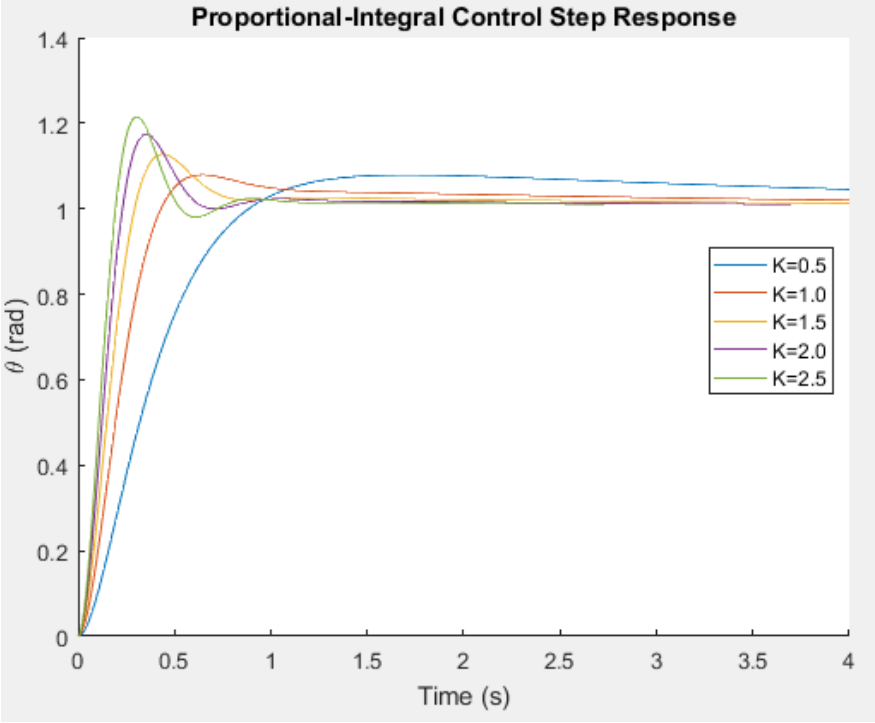

Figure 105: Step Response For Proportional-Integral Control

Although the response has an appropriate overshoot for our application, the rise time is quite slow compared even to proportional control. Integral control will most likely be deemed unnecessary for the roll-control system.

Proportional-Derivative Control The aim of using PD controller is to increase the stability of the system by improving control since it has an ability to predict the future error of the system response. PD control is common in high-speed applications such as satellite attitude control, and has all of the functionalities necessary to serve as the roll-control scheme. The open and closed loop transfer functions for a PD controller are shown in Equations (5.12) and (5.13):

$$\frac{1+\gamma s}{Js^2+Bs} \tag{5.12}$$

$$\frac{K(1+\gamma s)}{Js^2+(B+K\gamma)s+K} \tag{5.13}$$

Where $\gamma = \frac{K_d}{K_p}$. The Root Locus Plot (Figure 106) for the PD controller shows two points where there is critical damping. The step response (Figure 107) shows the effects of increasing the gain value past the critical damping value, introducing a small amount of overshoot into the response. The PD response has a very fast rise time and minimal overshoot, which are both criteria of the roll-control system.

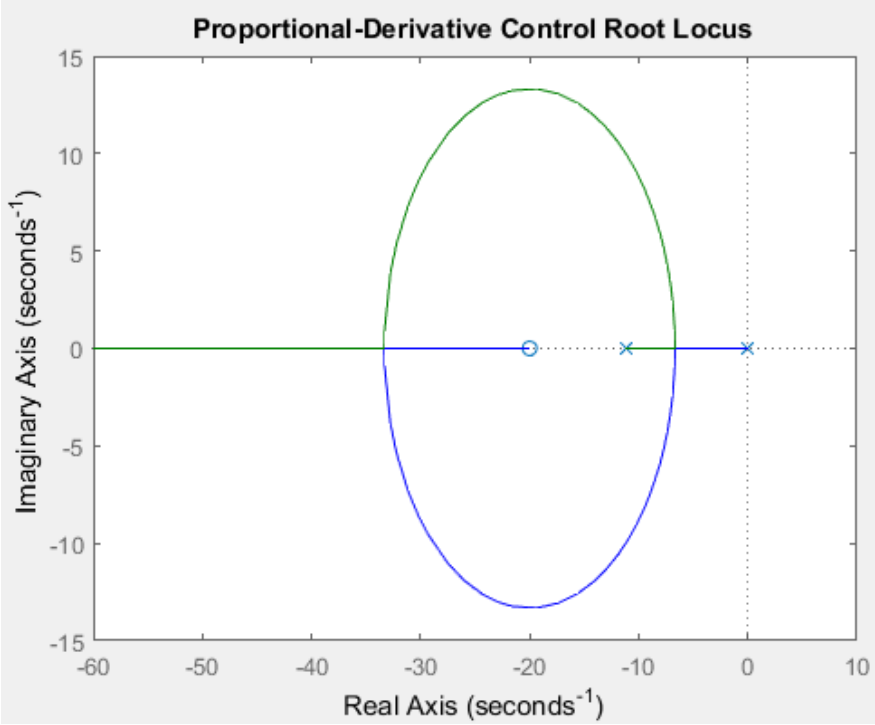

Figure 106: Root Locus Plot for Proportional-Integral Control

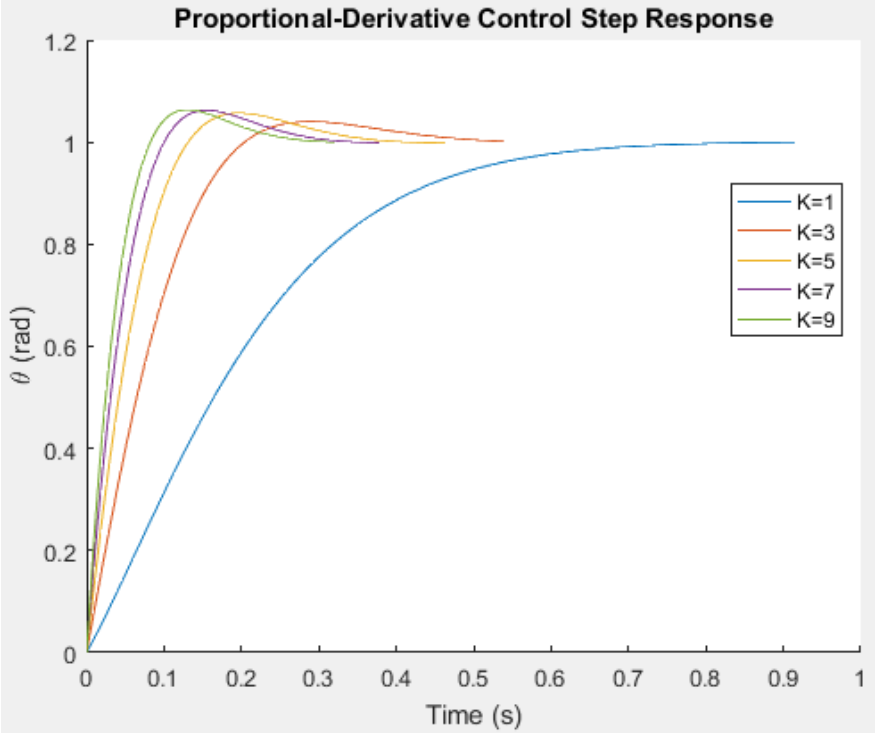

Figure 107: Step Response For Proportional-Integral Control

Proportional-Integral-Derivative Control PID control combines the effects of each individual gain term. This can allow for the optimization of the control system, however this combination can also be detrimental, adding unneeded complications in tuning and perfecting the system. The open and closed loop transfer functions for a PID control system are shown in Equations (5.14) and (5.15) respectively.

$$\frac{1+\gamma s+\frac{\delta}{s}}{Js^2+Bs} \tag{5.14}$$

$$\frac{K(1+\gamma s+\frac{\delta}{s})}{Js^2+(B+K\gamma)s+K+\frac{\delta}{s}} \tag{5.15}$$

The Root Locus Plot and the step response of the system are shown in Figures 108 and 109 show that the response of the system under PID control has a fairly quick rise time and an acceptable amount of overshoot and with the integral control applied, the steady-state error will be negligible.

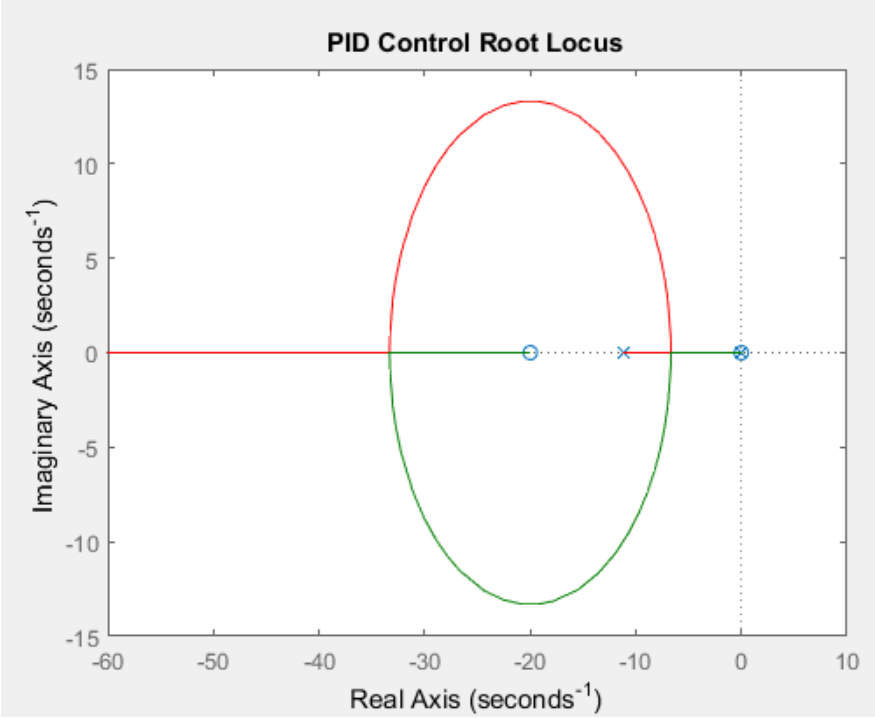

Figure 108: Root Locus Plot for PID Control

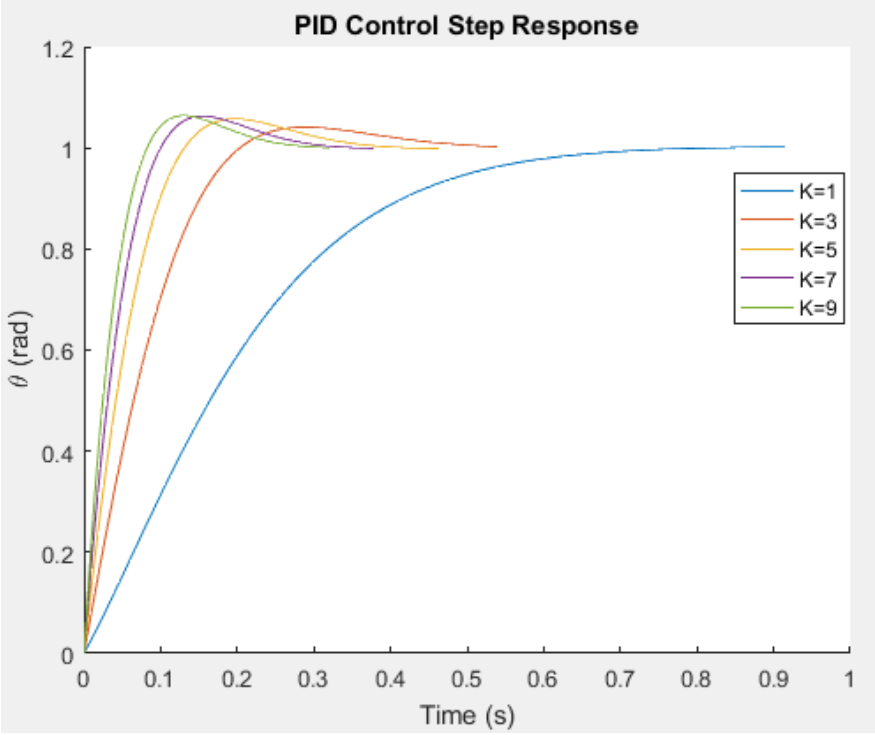

Figure 109: Step Response For PID Control

Although PID control would be an acceptable control system, PD control can accomplish the same with fewer room for error and a simpler tuning process. Tests on the FRAME will be performed for multiple control schemes, however

VADL is currently favoring a PD control scheme for the fullscale vehicle.

Advantages PID control is useful in a wide range of systems, especially second order systems, but use of PID control requires linearization of the system. Once the system's dynamics are linearized, the open loop transfer function can be found using the LaPlace Transform. From this point, a controller can be developed by setting design requirements for the closed loop transfer function, including rise time, settling time, and overshoot. In an electromechanical dynamic system, transfer functions are never empirical certainties, and therefore some experimentation will be necessary in order to produce an accurate control scheme. This experimentation will be conducted in the FRAME, where gain values will be tuned until the system meets the performance expectations of the team.

Disadvantages One disadvantage of PID control is that the tuning process requires the balancing of multiple gain values. Slight changes in these gain values can lead to an excess of overshoot, a loss of stability, sensitivity to disturbance, or a system that never reaches the setpoint. VADL believes that testing using the FRAME will allow for the gain values to be properly tuned and tested to ensure a reliable control system during flight. Another disadvantage to PID control is that it relies on a duty cycled pulse scheme, as the thrusters must be able to operate at a fraction of their maximum thrust, and this can only be accomplished via a duty cycle. This will require the software to sample and actuate at a higher frequency. The team must assess the capabilities of the hardware to ensure that this will not cause hardware failure during flight. This also means that the thrust will be produced immediately after the opening of the solenoid. Previous tests on the thruster test-stand have shown that the thrust immediate after the solenoid opens is greater than the normal thrust. The team must also assess the effects that this may have on the performance of the control scheme and the predictability of the dynamics. The team must determine whether a 50% duty cycle results in 50% of the thrust of a 100% duty cycle.

5.1.4.4 Bang-Bang Control

Overview A Bang-Bang controller is a feedback controller that switches abruptly between two states. It is a common control scheme for binary systems, where the state is either on or off. One example of Bang-Bang control is a thermostat, which maintains a household at a desired temperature by turning on and off a heating unit based on temperature feedback. This scheme was used in the VADL Hotbox as well.

Advantages The simplicity of this control scheme is definitely one of its main advantages. The system is also exactly the system in which a Bang-Bang controller is used, where the actuator exists between two discreet states, (roll thrusters on, or counter-roll thrusters on) and the rocket must be held between two thresholds. The simplicity of the system would allow for a lower operating frequency of the hardware, which would lead to more reliable data collection.

Disadvantages A main disadvantage to Bang Bang control is defining the thresholds where the switching event will occur. The goal of the roll induction is to achieve exactly two full rotations with minimal, yet positive, overshoot. If the switching event were set at exactly two rotations, there would be an unacceptable amount of overshoot. The dynamics must be fully characterized to identify the optimal location for this switching event, and a failsafe must be added to the software to ensure that the counter thrust does not cause failure to reach the full two rotations.

Bang-Bang Analysis A MATLAB simulation was performed to analyze the performance of a Bang-Bang controller (Figre 110. All forces were included in the model, including the damping caused by axial drag.

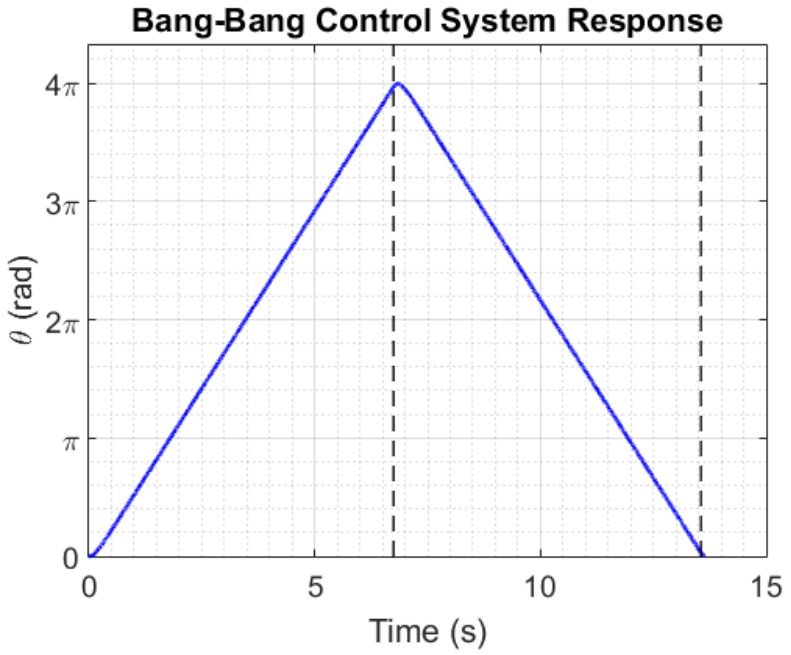

Figure 110: System Response Under Bang-Bang Control

For this simulation, a switching event was set slightly prior to the rocket reaching a full 4π radians of rotation. The result shows the almost immediate deceleration to zero velocity due to the counter-thrust activation and the damping forces of the axial flow. This leads VADL to consider whether a complex PID control scheme is necessary, or if the same task could be accomplished using the simplicity of a Bang-Bang controller. Software is being written to perform FRAME tests using this control scheme and the results will be compared to those from PID control.

5.1.4.5 Open-Loop Control

Overview An open-loop control system attempts to reach a setpoint without feedback from a sensor. The inputs are predetermined based on the dynamics of the system. For the VADL roll-control system, this would be a predefined pulse pattern for actuating the solenoids. In order for this control scheme to be effective, the system must be extremely well characterized and free of disturbances.

Advantages An open-loop control system does not require an IMU for active feedback and does not require a complicated software system which could introduce errors. In order to apply an open-loop control system, extensive testing must be performed on the FRAME, and the team may even elect to perform test launches or wind tunnel studies to examine and improve the pulse scheme.

Disadvantages One main disadvantage of an open-loop control system is the lack of a well-characterized dynamic system. Section **??** outlines the complicated effects that the axial drag has on the roll of the rocket. In addition to the complications that come with these resistive torques, a requirement of the control system is that it be robust to disturbances. A control system that can not sense its environment and adjust accordingly would fail under the intense conditions of flight and to attempt to characterize and perfect these dynamics using subscale or fullscale launches is costly and possibly hazardous. For these reasons an open-loop control system has been deemed incompatible with the requirements of the roll-control system.

5.1.5 Subscale Flight Software

The software is defined by the interfaces and the controls. The interfaces are the components that interact with the environment, such as the solenoid actuators and the IMU, and the controls decide whether or not the solenoid should

be actuated based on the IMU data. VADL uses a software modeling and execution framework called ROSMOD. All of the software is written, compiled, and executed using this environment. The goal of the subscale launch software is to detect takeoff and MECO and actuate the thrusters based on a predefined pulse pattern, all while collecting valuable IMU data. In addition, the software must be testable on the ground in order to verify its functionalities. Prior testing was required to determine the most appropriate pulse pattern. Even with this testing, the team was required to be prepared to alter the pulse pattern after the first test flight. For this reason, the software was to be modular and configurable. Due to the incredibly high speeds and short time frame of this experiment, the software was to be written succinctly and efficiently so as to not overlap tasks and waste valuable processing power.

The payload software was written in C++ using the ROSMOD modeling and execution environment developed by VADL alumni. ROSMOD is an excellent way to visualize the communication between components in a software integrated system. Figure 111 shows a high-level diagram showing the communication between the various components of the software.

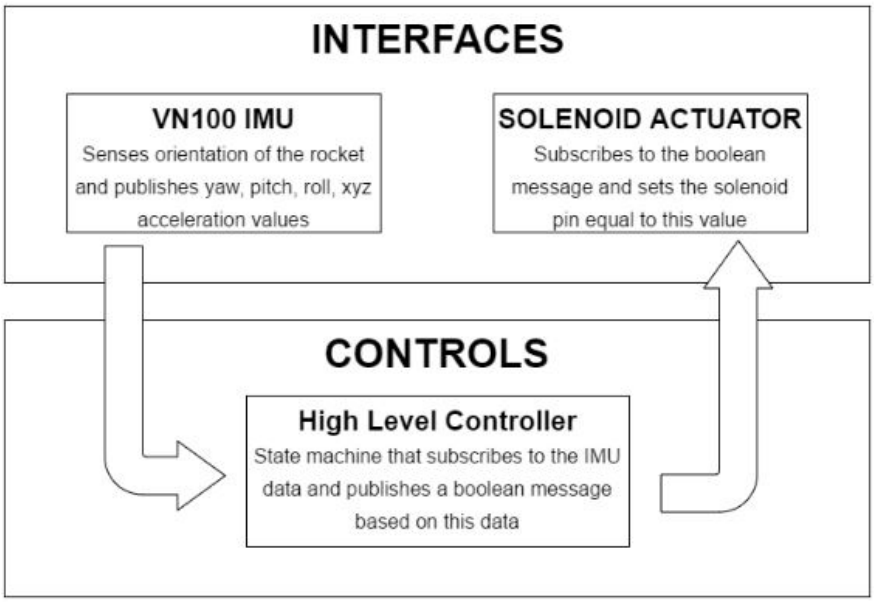

Figure 111: High-Level Diagram of Payload Software

The most important aspect of this software is the High Level Controller (HLC), which decides whether or not to fire the solenoid based on both elapsed time and IMU acceleration data. The HLC functions as a state machine that exits and enters various states based on past and current values. The HLC runs on a timer which checks for the state at 40 Hz and decides which phase of the flight the rocket is in. Each phase is associated with various operations. Figure 112 shows the various states and the conditions that cause a change of state.

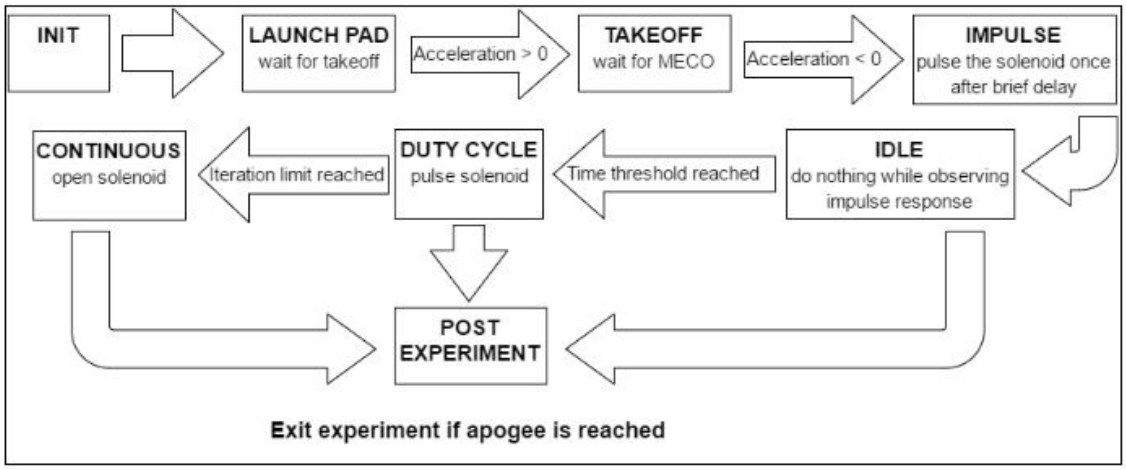

Figure 112: State Machine Flow Diagram

So 40 times a second the HLC receives IMU data and checks what state it is in to decide what to do. The INIT state verifies proper power up of the hardware and then sets the current state to LAUNCH PAD. The LAUNCH PAD state contains a conditional statement that sets the current state to TAKEOFF when the z acceleration surpasses 1 g of acceleration. The takeoff acceleration is about 16 gs so this is a reliable threshold to signal takeoff. The TAKEOFF state contains a conditional statement that sets the current state to IMPULSE when the the z acceleration becomes negative. After MECO the only forces will be gravity and drag which will cause the acceleration to be about -1.2 times the acceleration of gravity, so 0 is a reliable threshold. This state switch also defines a variable *beginTime* which will be compared to the current time in the IMPULSE state to determine how much time has elapsed since MECO. The IMPULSE state defines a variable *elapsedTime* which compares the current time (the time when the HLC timer activated to check the state) to the *beginTime*. Once the *elapsedTime* is greater than a certain time threshold, the solenoid boolean message is defined as True and this value is published to the solenoid actuator component which will then write the solenoid pin HIGH to release the compressed air. The team is only interested in learning about the impulse response of the rocket during this state, so the solenoid is very quickly shut off using another conditional statement that compares the *elapsedTime* to some predefined pulse length threshold. Once the solenoid has been closed, the current state is set to IDLE and the variable *beginTime* is redefined for use in the next state. The IDLE state is merely a brief delay to allow for the full characterization of the impulse response. It defines the *elapsedTime* and compares it to a predefined threshold. Once this threshold is surpassed, the current state is set to DUTY CYCLE and the variable *beginTime* is redefined. The DUTY CYCLE state uses a modulo operator to determine the state of the solenoid, shown in the code block below:

```
sol_msg.isOn = ((fmod(elapsedTime, P)) / (P) <= dutyCycle);
solenoid_publisher.publish(sol_msg);
```

fmod(a, b) finds the remainder of a/b. This remainder oscillates between 0 and P (period). By dividing it by P, this remainder is normalized. Then by comparing it to the *dutyCycle*, the boolean *isOn* will be True up until the duty cycle is reached and will then be False until the period is reached and will repeat until a predefined *dutyDuration* time threshold is reached. Once this threshold is reached, the current state is set to CONTINUOUS. The CONTINUOUS state will open the solenoid until apogee is reached.

The software is written to allow for a lot of user configuration and is also equipped with a few safety precautions. The goal for subscale launch was to launch twice with varying experiments. For this reason the IMPULSE, DUTY CYCLE, and CONTINUOUS states can be enabled or disabled in between launches. In addition, the duty cycling can be altered to experiment with various pulse lengths and periods. In each condition after MECO, there is a failsafe code that shuts off the solenoid if the apogee acceleration threshold is reached so as to not fire the thrusters while the parachute is being deployed.

6 Launch Operations Procedures

6.1 Hardware List

6.1.1 Vehicle Assembly

- ☐ X-frames (3)
- ☐ 4 x 1/4” button bolts for bolting forward body section to coupler tube (BRING EXTRAS)
- ☐ 1 x wood screw to constrain rotation of payload skeleton (BRING EXTRAS)
- ☐ Torx wrench for button bolts (check with bolt while packing)
- ☐ Larger Phillips screw driver (blue) for wood screw (check with screw while packing)
- ☐ 4-40 nylon shear pins for securing tail cone and coupler tube to tail section
- ☐ Black electrical tape to cover shear pins
- ☐ 1/4”-20 hex nuts (BRING BOX)
- ☐ Washers

6.1.2 Electronics

- ☐ Small Phillips head (grey/orange) for screw switches (check w/ screw while packing)
- ☐ Multimeter (yellow) to check voltage across battery
- ☐ 5/64” Allen wrench for VN100 IMU
- ☐ Spare Lipo battery
- ☐ Spare SD card with BBB image
- ☐ Spare connectors with leads
- ☐ Spare wire

6.1.3 Launch Pad Setup

- ☐ Launch pad
- ☐ Stakes for launch pad
- ☐ 2 x Resizable wrench for launch pad bolts
- ☐ Launch rail (12 ft)
- ☐ Vaseline for lubrication of launch rail
- ☐ Allen wrench (blue) to align launch lugs
- ☐ Level to check alignment of launch rail

6.1.4 Recovery Subsystem

- ☐ Parachute (8 ft Iris Ultra)
- ☐ Shock cords
- ☐ Quick-connects for shock cords
- ☐ Fireballs for anti-zippering
- ☐ Blast charges (pre-prepared)
- ☐ Blue 3M tape to tape blast charge wires to body tube interior

6.1.5 Motor Subsystem

- ☐ Motor retaining ring
- ☐ Motor refuel kit
- ☐ Igniter stick
- ☐ Launch electrics (in blue tub)

6.1.6 Payload Thruster Subsystem

- ☐ 7/16” Pittsburgh wrench for 1/4”-20 nuts on threaded rods
- ☐ 7/16” Craftsman wrench for 1/4”-20 nuts on threaded rods
- ☐ Air tank refiller (yellow)
- ☐ Refill regulator

6.1.7 General Field Supplies

- ☐ Tent (1)
- ☐ Tarps (2)
- ☐ Tables (2)
- ☐ Chairs (6)
- ☐ Garbage bags (2)
- ☐ Robins toolkit
- ☐ Dexters electronics box
- ☐ Dustins thruster box
- ☐ Pauls nuts and bolts bag
- ☐ Tape measure
- ☐ Wire cutters
- ☐ Needle nose pliers
- ☐ Shears
- ☐ Zip Ties

- ☐ Metal file
- ☐ Box cutter
- ☐ X-acto knife
- ☐ Gorilla tape
- ☐ Sealant tape (gray) for sealing bulkhead holes that contain wires
- ☐ Sealant putty (blue) for sealing all holes between payload and electronics
- ☐ Epoxy kit (5-minute epoxy resin and hardener, mixing cups, popsicle sticks)

6.2 Pre-Launch Checklist

- ☐ The pressurized air tank is stored in a protective, padded case on its journey to the launch site. Any refilling must be executed with safety mentor oversight. **WARNING!** Always handle pressurized tank with care.

6.2.1 Launch Location Setup

Required Personnel: Rocketry Mentor and Safety Officer

- ☐ Unload equipment and materials from van.
- ☐ Setup tent and secure with stakes.
- ☐ Assemble portable tables. **WARNING!** Ensure ground is level and clear from obstructions.
- ☐ Setup bags for trash collection. **WARNING!** Leaving trash behind is an environmental hazard.
- ☐ Place rocket stands for each section on tables.
- ☐ Place rocket sections on stands.
- ☐ Place all electronics and avionics on their own table.
- ☐ Verify that launch pad location will provide a sturdy base for launch. **WARNING!** If this is not the case, abort launch.
- ☐ If launch location is suitable, place launch pad components near desired location.

6.2.2 Launch Pad Setup

- ☐ Open launch pad legs fully and bolt them into place with the stainless steel bolts and lock nuts.
- ☐ With the mast in the horizontal position, slide the bottom half of the launch rail onto the carriage bolts on the mast so that the bottom of the rail is flush with the bottom of the mast and tighten the nuts.
- ☐ Slide the top portion of the launch rail over the steel joint and tighten bolts, ensuring a flush fit.
- ☐ Loosen the bolts on the launch rail stop and adjust to the appropriate height. Tighten bolts.
- ☐ **PPE Required:** Wear latex gloves. Apply Vaseline or another appropriate lube to the rail.
- ☐ After ensuring that there is a smooth transition from the lower to the upper rail sections, slide the rocket onto the rail. Both lug nuts should slide into the slot in the rail.
- ☐ Orient the launch rail into a vertical position and bolt the mast into the slotted hole at the desired launch angle.
- ☐ Use a level placed on the vertical surface of the launch rail to ensure that the desired angle is achieved in one direction and perpendicularity with the ground in the other direction.
- ☐ Fully inspect assembled launch pad to ensure it provides a sturdy base for the rocket during launch.**WARNING!** This step is imperative for a straight takeoff. **WARNING!** Inspect setup for damage - if damage exists, abort launch.

6.2.3 Tail Section Inspection and Assembly

- ☐ If the tailcone is not already installed, use shear pins to fasten it to the coupler tube.
- ☐ Tape over shear pins to make sure they dont fall out (black tape)
- ☐ Inspect the tail section for any damage from transportation and handling, specifically the structural integrity of the fins, body and motor tubes, and centering rings.
- ☐ Ensure the launch lugs are aligned vertically. If not, use Allen wrench to realign orientation. **WARNING!** Damage to the tail section is hazardous to all personnel. Abort launch if damage is found.

6.2.4 Avionics Assembly and Integration

Required Personnel: Recovery Lead and Safety Officer

- ☐ Inventory all avionics equipment.
- ☐ Inspect all avionics equipment for safety and security.
- ☐ Ensure the altimeters are secure and set for correct parachute deployment altitudes and that the connections are secure. **WARNING!** Double check the altitude settings, as errors in this step can cause recovery failure.
- ☐ Connect all charge ignition wires connecting altimeters to wire terminals outside the avionics bay. Seal interior holes on the bulkhead with putty. **WARNING!** Insufficient application of putty will alter blast dynamics and could cause recovery failure.
- ☐ Connect arming switches to each altimeter.
- ☐ Check the 9V battery terminals.
- ☐ Check voltage on new 9V batteries.
- ☐ Check that batteries are a compression fit with bulkhead.
- ☐ Verify correct wiring scheme for both altimeters.
- ☐ Place parachute charges in blast caps and secure with blue painters tape.
- ☐ Inspect all separation ignition wires.
- ☐ Seal wire passage holes into avionics bay with removable putty.
- ☐ Place putty over all wire terminals in parachute sections to ensure connections are maintained.
- ☐ Arm altimeters before launch. **WARNING!** Damaged equipment or improper wiring can cause recovery failure - hazard to the rocket, environment, and personnel.

6.2.5 Main Parachute Assembly and Integration

Required Personnel: Recovery Lead and Rocketry Mentor

- ☐ Take inventory of all recovery equipment.
- ☐ Inspect all Kevlar fiber shock cords, protective blankets, and anti-zipper devices for safety and security. **WARNING!** If damage is found, abort launch.
- ☐ Connect Fireballs to tail section bulkhead.
- ☐ Connect main shock cord to fireballs.
- ☐ Connect opposite end of shock cord to main parachute.

- ☐ Inspect parachute for hardware defects and security.
- ☐ Ensure all shock cord and parachute connections are in their proper locations.
- ☐ Visually inspect the deployment charges for secure connection.
- ☐ Visually verify that deployment charges are secured in their respective blast caps.
- ☐ Connect parachute to avionics bay bulkhead via shock cord.
- ☐ Load main parachute and shock cord, folded using a z-fold, into rocket below avionics bay.
- ☐ Align fireballs in bottom of tail section on either side of U-bolt.
- ☐ Join avionics section body tube to tail section via shear pins. **WARNING!** Failure to properly pack parachute can cause recovery failure - hazard to the rocket, environment, and personnel.

6.2.6 Drogue Parachute Assembly and Integration

Required Personnel: Recovery Lead and Rocketry Mentor

- ☐ Connect shock cord to top of payload section.
- ☐ Connect opposite end of shock cord to parachute.
- ☐ Place payload parachute charges in blast caps on rear of avionics bay and secure with blue painters tape.
- ☐ Inspect all separation ignition charges.
- ☐ Connect parachute to avionics bay rear bulkhead via a shock cord.
- ☐ Inspect payload parachute for hardware defects and security.
- ☐ Ensure all shock cord and parachute connections are in their proper locations.**WARNING!** Failure to properly connect drogue parachute will result in recovery failure.
- ☐ Visually inspect the deployment charges for secure connection.
- ☐ Visually verify that deployment charges are secured in their respective blast caps.
- ☐ Load drogue parachute and shock cord, folded using a z-fold, into forward section of rocket below avionics bay.
- ☐ Join forward section of rocket to the aft section via three 4-40 nylon shear pins. **WARNING!** Failure to properly pack parachute can cause recovery failure - hazard to the rocket, environment, and personnel.

6.2.7 Payload Skeleton and Electronics

Required Personnel: Electronics Lead

- ☐ With forward body section removed from rocket:
- ☐ Secure all bulkheads in flight location on threaded rods with nuts. (7 minus 1/16, 2 + 3/16)
- ☐ Verify air tank retention at the top of the payload section.
- ☐ Verify mounting of all thruster hardware. **WARNING!** Failure to secure payload hardware can result in a failed experiment and a risk of unstable flight.
- ☐ Slide coupler tube partially over payload electronics section of skeleton and install payload electronic sled, matching indices, attach electrical connections. Seal wires with putty.
- ☐ Fully slide on coupler tube, matching plus indices.

- ☐ Install avionics, matching indices.
- ☐ Attach avionics bulkhead and attach avionics connections to screw terminals, tighten bulkhead to compress blue tube coupler.
- ☐ Attach screw terminals to blast caps.
- ☐ Turn on BeagleBone using hole in coupler tube. **WARNING!** Ensure proper powerup - failure to do so will result in a failed flight experiment - no risk of recovery failure
- ☐ Load payload skeleton into tail section body tube and fasten with shear pins.

6.2.8 Software

Required Personnel: Software Lead

- ☐ Open Virtual Machine (VM) and connect to server
- ☐ Verify the most recent version of code is being used.
- ☐ Check User configurations to ensure proper launch experiment.
- ☐ Turn off *Time-Based Enable* and increase takeoff acceleration threshold. **WARNING!** Failure to do so can result in premature thruster firing - damage to personnel.
- ☐ Check system model to ensure proper hardware mapping
- ☐ **PPE Required:** safety goggles. Close compressed air tank valve and run experiment to ensure proper pulse scheme.
- ☐ Connect to BeagleBone via microUSB cable and deploy experiment.
- ☐ Disconnect from BeagleBone. **WARNING!** Experiment is now live, avoid inducing large vertical acceleration, as experiment could be triggered.

6.2.9 Forward Section

- ☐ Confirm that altimeter switches and payload electronics switches can be reached before installation of forward section.
- ☐ Bolt forward nose cone and body tube section to coupler tube around payload electronics.

6.2.10 Motor Installation

Required Personnel: Rocketry Mentor

- ☐ Motor should be stored in own container for transport and secured to avoid drops or impacts.
- ☐ Inspect the motor to ensure that no damage occurred during transportation or handling that could result in such failures. **WARNING!** If damage is identified, abort launch.
- ☐ Insert the Cesaroni J1520 motor into rocket motor tube and tighten the positive screw cap retention ring. Applying baby powder to the exterior of the motor can help facilitate installation.
- ☐ Verify that the positive screw cap retention ring is securely fastened to the rocket.

6.2.11 Igniter Installation

Required Personnel: Rocketry Mentor

- ☐ Insert igniter into the rocket motor.
- ☐ Attach leads that connect igniter to the ignition trigger.
- ☐ Ensure the ignition system is wired to the power source. **WARNING!** Always perform igniter installation under supervision of rocketry mentor.

6.2.12 Launch Vehicle Final Integration

- ☐ Carry rocket assembly to the launch pad.
- ☐ Line up the launch lugs that are attached with the rocket to the launch rail slots. Very slowly slide the launch lugs onto the rail guides making sure not to put a bending moment the rocket.

Arming Thruster System:

- ☐ Attach flexible hose from NPT fitting onto Quick Disconnect.
- ☐ **PPE Required:** safety goggles. Turn on the valve (twist pin depressor).
- ☐ Slide body tube and nose cone onto the payload skeleton, bolt it in with 4x button head bolts. Use Phillips head screwdriver to tighten wood screw that will constrain rotation
- ☐ Raise rocket.
- ☐ Arm the payload electronics and avionics using a through-wall screw switch. **WARNING!** Ensure proper booting of payload electronics - failure to do so will result in experiment failure.

Final Step:

- ☐ Once the launch vehicle is oriented so that the tail cone is placed one foot off the launch pad, slowly raise the launch rail back into a vertical configuration and bolt down the pad so that it will not pivot.

6.2.13 Troubleshooting

- ☐ Ensure all team members keep detailed notes on their respective subsystems.
- ☐ Approach problems with a composed and organized approach.
- ☐ Safely disarm rocket, close compressed air tank, and lower rocket from launch rail if problem arises on launch pad.
- ☐ Form systematic approach to troubleshooting - testing each possibility once at a time.

6.2.14 Post-Flight Inspection

- ☐ **PPE Required:** Wear appropriate shoes and clothing for retrieval of rocket. Locate rocket and safely retrieve it - avoid hazardous areas if possible, otherwise proceed with appropriate caution.
- ☐ Check parachutes and shock cords for damages.
- ☐ Properly dispose of any live black powder charges. **WARNING!** Risk to personnel if not done properly.
- ☐ Check compressed airframe for zippering.
- ☐ Connect to BeagleBone and stop experiment.
- ☐ Record apogee data from altimeters.

7 Project Plan

7.1 Testing

7.1.1 Thruster Testing

In order to conduct safe and controlled tests of each thruster, a ground-based test facility (further referred to as Thruster Test Stand) was designed. This test stand incorporates compressed propellant regulation capabilities allowing for continuous or pulsed operation of the thruster, and measures post-regulator pressure (with both a digital and analog sensor) and thrust delivered by the system. A schematic showing the flow of both air and power for the system can be seen in Figure 113 below.

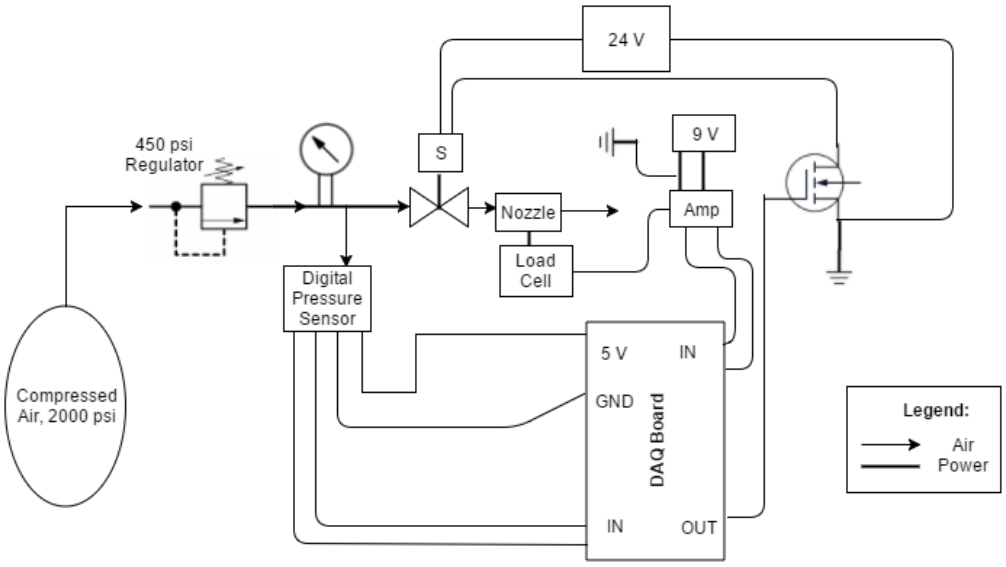

Figure 113: Test Stand Schematic

The thruster is integrated into the test stand by rigidly mounting the solenoid valve (and attached compression Yor-Lok fitting that retains the nozzle) to a plate of aluminum which is in turn suspended by two spring steel sheets. One end of each sheet is attached via L-brackets to the aluminum plate with the other end firmly attached to the roof of the outer structure of the test stand. This outer structure is made primarily of Aluminum 80/20 T-slot extrusions with a thick plate mounted on the rear two extrusions (orthogonal to the suspended solenoid mounting plate) which holds the load cell in place. This plate is also used as a surface to which the air tank is clamped with adjustable U-bolts. The load cell is set up so that a screw on the back side of the solenoid mounting plate will compress into it during thruster actuation, thus reading the reaction force felt from the thrust provided. Both the digital pressure sensor and load cell were calibrated before testing took place to ensure accurate results for each trial. For a more visual representation of the test stand, see Figures 114 and 115 below.

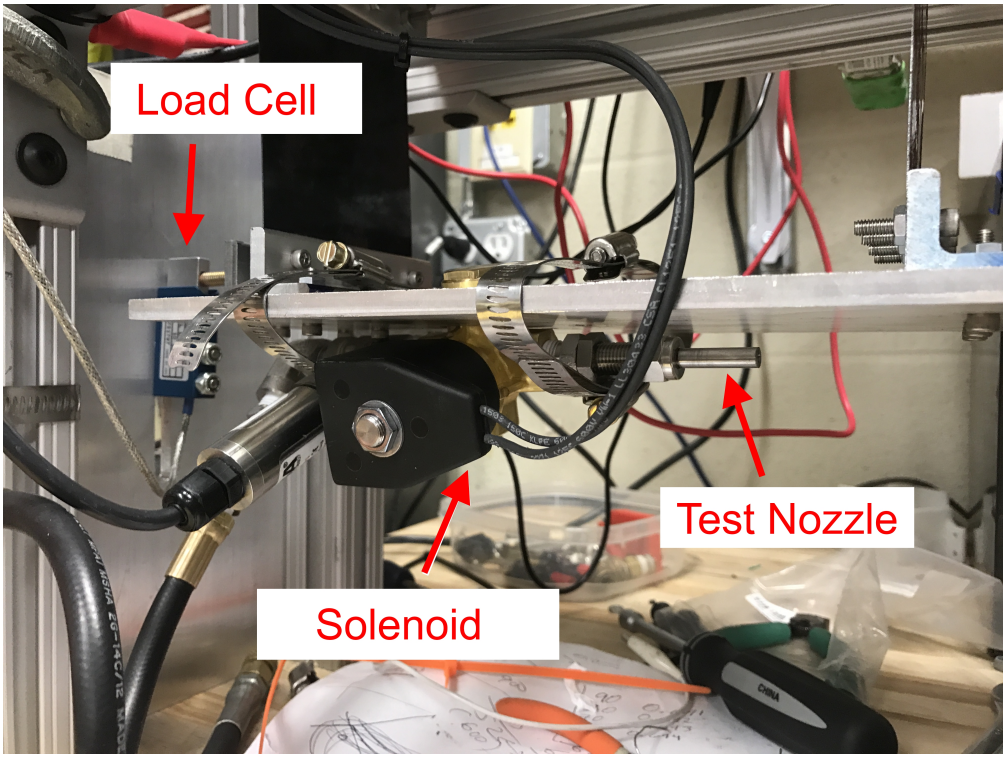

Figure 114: Test Stand Nozzle and Solenoid Mounting

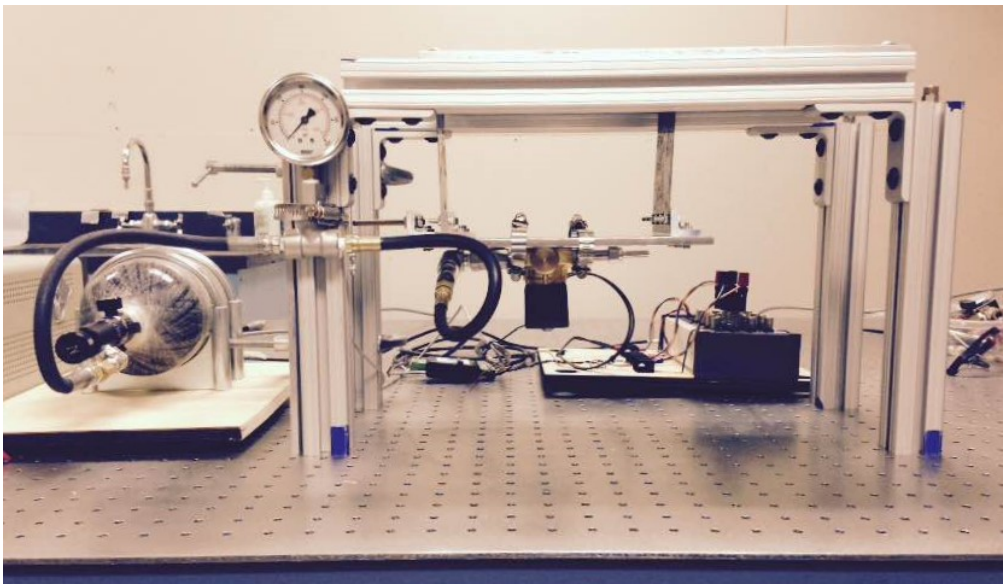

Figure 115: Test Stand Overview

The test stand was used to measure thrust for many different experimental setups, the results of which can be seen in Figures 116, 117, 118, and 119 below. The first figure shows the test results for running the thruster continuously to monitor thrust and pressure data over the time taken to empty the tank while Figures 117, 118,and 119 show pulsed conditions of various lengths. It should be noted that between each test, the tank was refilled to the same starting pressure of 2000 psi.

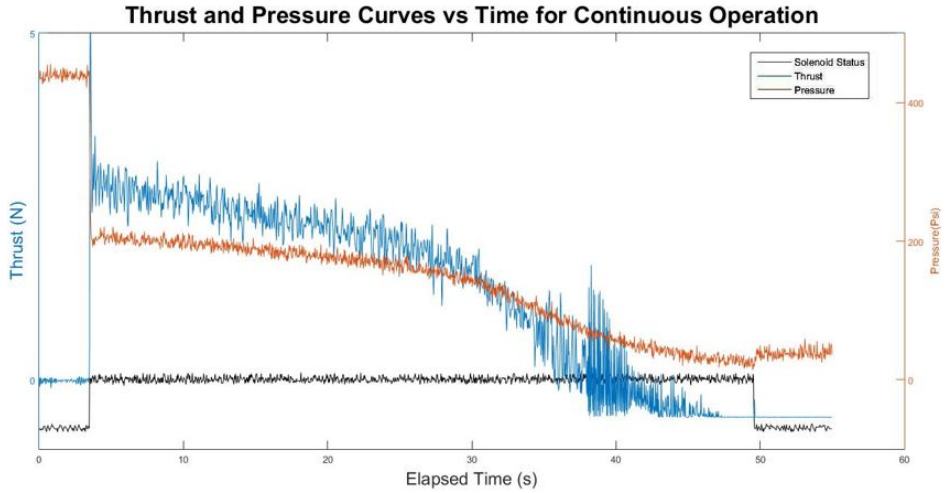

Figure 116: Thruster and Pressure vs Time, Continuous Run

The results of Figure 116 show that even with the tank pressurized only to 2000 psi (the tank pressure for all experiments listed below) a thrust value above the minimum needed thrust (2.12 N) was measured for roughly 30 seconds for one thruster. With two thruster firing simultaneously, the system runtime is reduced to 15 seconds, which is optimized for the experimental duration (10 seconds).

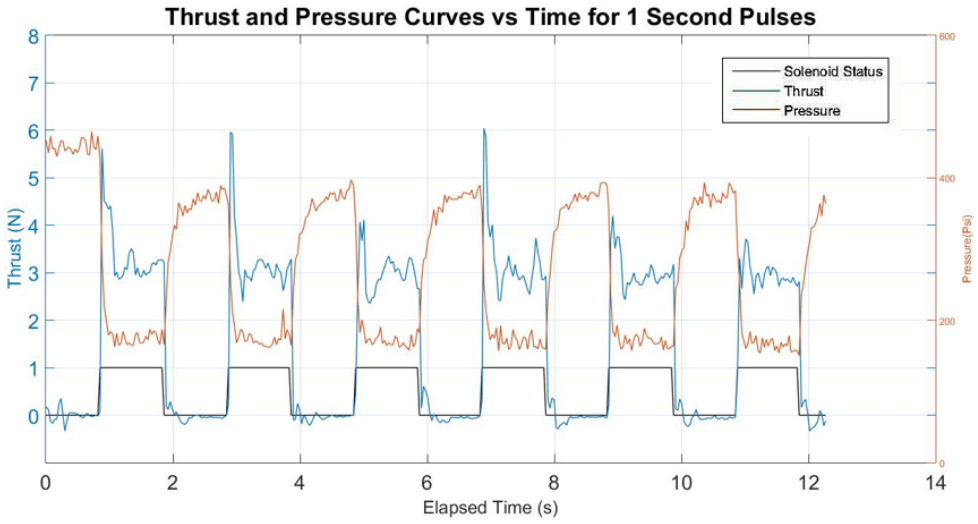

Figure 117: Thruster and Pressure vs Time, 1 Second Pulses

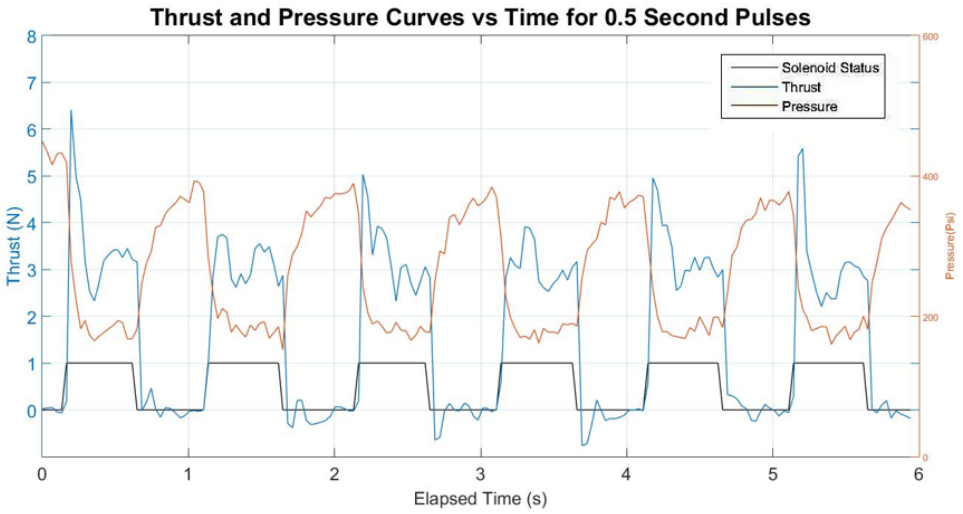

Figure 118: Thruster and Pressure vs Time, 0.5 Second Pulses

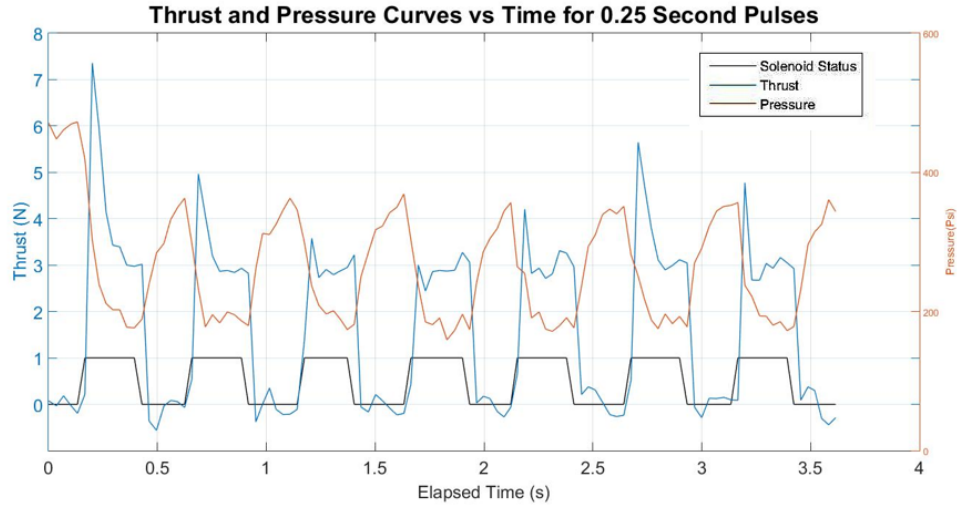

Figure 119: Thruster and Pressure vs Time, 0.25 Second Pulses

Analyzing the results of Figures 117, 118, and 119, a drop in static pressure was observed for each time stamp in which the solenoid was opened (from 450 psi tank conditions before the first pulse to approximately 200 psi during actuation). This can be explained in part by the fact that the pressure gauge just upstream of the solenoid reads static pressure; when the valve is closed, the air flow speed is essentially zero, and the static pressure reading is essentially equivalent to the stagnation, or total, pressure. When the valve is open, the air rushes out, and much of the static pressure is converted to dynamic pressure, which is not reflected in the pressure gauge reading. However, in order to achieve the desired thrust of 7.8 N (the 4X design thrust estimated by the team in PDR to allow our control scheme ample an operating range), consistent 450 psi static pressure is necessary at all stages of thruster operation.

Intuition points to an insufficient volumetric flow rate from the regulator as the culprit of this issue that in turn delivers an average thrust value that is less than half of the design value (3.2 N vs 7.9 N expected). However, it can also be seen by comparing the figures that regardless of the pulse length, the average thrust value of approximately 3.2 N was consistently provided for each pulse. This shows that the total pressure climb when the solenoid is closed

(which varies over the three figures due to the pulse length of time) does not drastically affect the thrust obtained from each subsequent pulse.

To resolve the low thrust value, a higher volumetric flow rate regulator was ordered and installed to the test stand. After repeating the one second pulse test with this new setup, a 5 N thrust was consistently measured with a pressure drop to 300 psi as opposed to 200 psi. The 5 N thrust matches exactly the design value for a 300 psi condition from the MATLAB design script written. The results of this test can be seen in Figure 120.

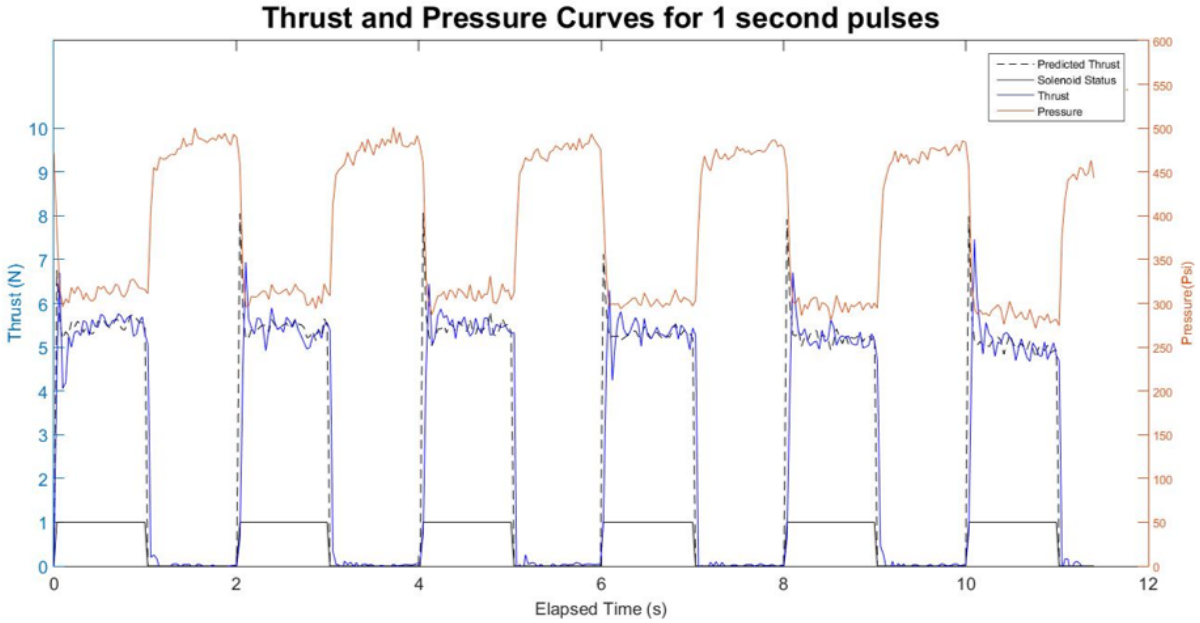

Figure 120: Thrust and Pressure vs Time, 1 Second Pulses, High Flow Regulator

Furthermore, this same test setup of single second pulses was performed with two thrusters. Figure 121 shows the two thruster arrangement while Figure 122 and Figure 123 show the pulsed thrust results and total impulse of this test respectively.

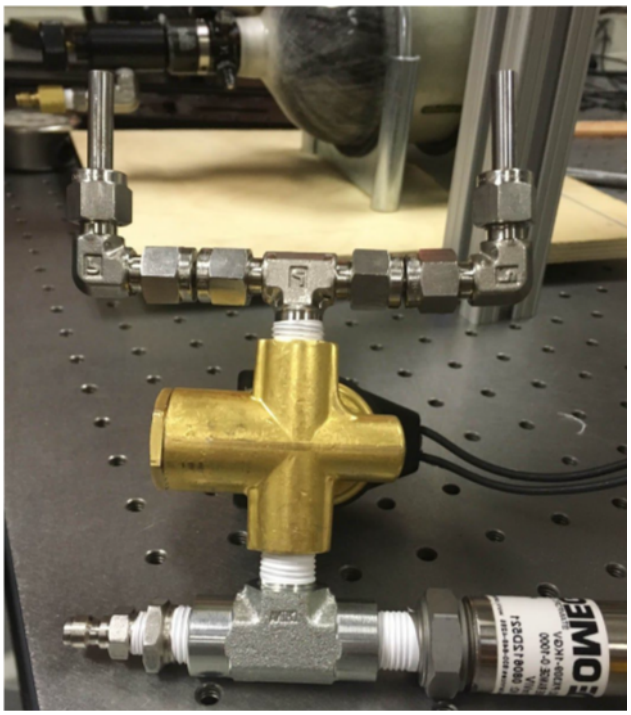

Figure 121: Two Thruster Arrangement

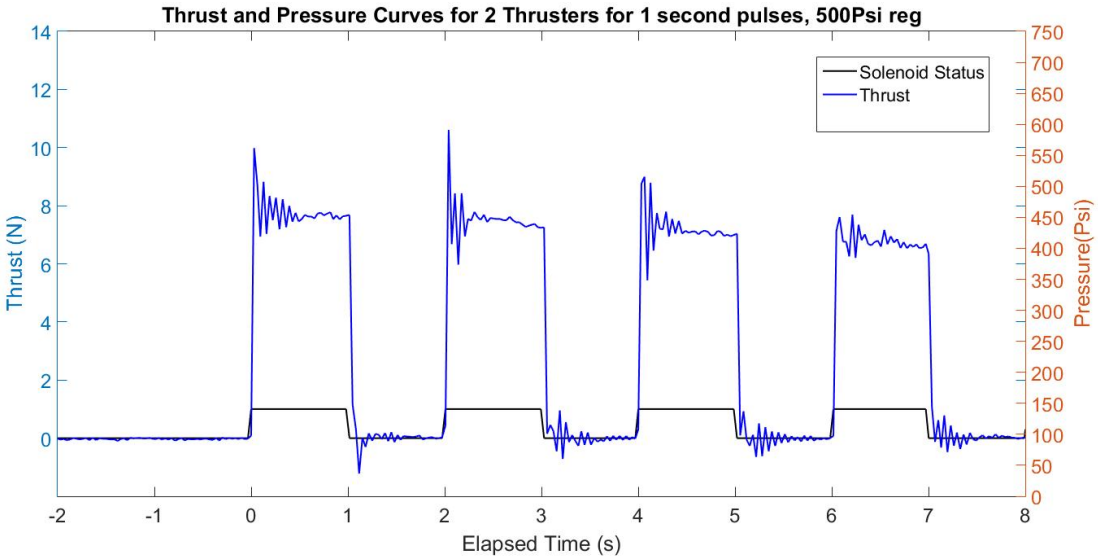

Figure 122: Thrust vs Time, 1 Second Pulses, Two Thrusters, High Flow Regulator

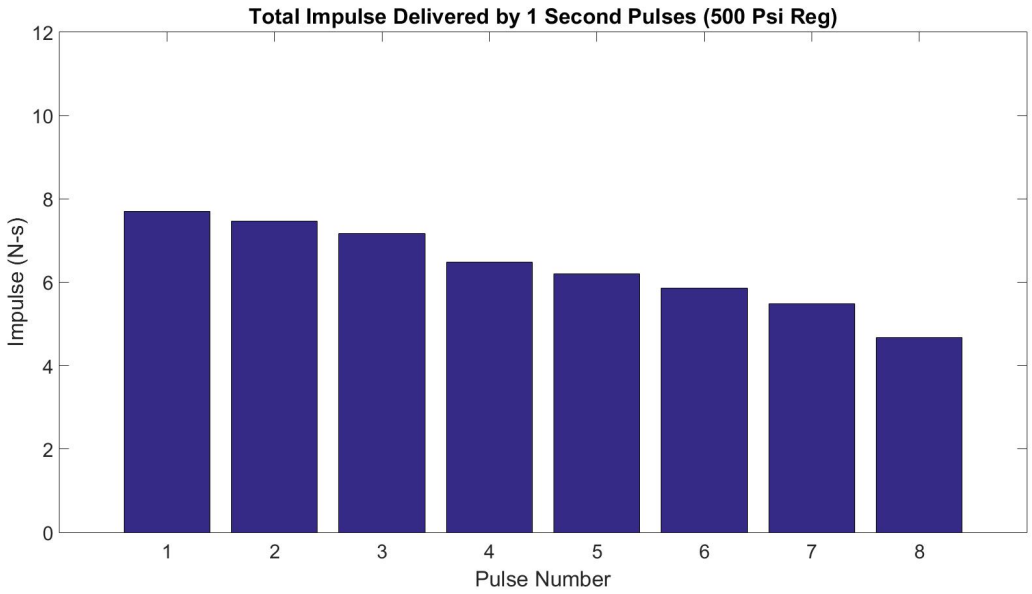

Figure 123: Total Impulse vs Pulse Number, 1 Second Pulses, Two Thrusters, High Flow Regulator

While adding a second thruster intuitively should have yielded double the thrust of a single nozzle, a value of approximately 7.5 N was measured for two thrusters (see Figure 122). After team research into flow characteristics of propellant tank regulators, VADL feels that this lower value is due to a pressure ”droop” inherent to many regulators where the delivery pressure decreases with increasing flow rate. By adding the second thruster, we increased the flow rate of air through the regulator, and this resulted in a corresponding decrease in delivery pressure. This decrease in pressure led to a lower mass flow rate through each thruster individually, and the results shown in Figure 122 show that each thruster in this dual-thruster arrangement achieved roughly 75% of the prior single thruster arrangement flow rate, giving a total of 150% of flow rate of the previous test (hence (1.5)*(5 N) = 7.5 N total thrust). It should be noted that this analysis assumes that the thrust from a given thruster is a function of flow rate alone, which VADL feels is a valid assumption given that we designed our nozzles for perfect expansion and have not modified the thruster geometry or stagnation temperature over the course of these tests.

To address this issue, further testing will be performed with the dual thruster arrangement on the VADL thruster test stand while increasing a few key variables including tank pressure and regulator delivery pressure.

7.1.2 Electronics Testing

7.1.2.1 Avionics Testing

Electronics testing comprises several processes over multiple systems. First, the more simple avionics system will be examined. The avionics system includes a rather intuitive single-board recording altimeter package powered by standard 9V batteries. A screw switch interrupts this power supply until the device is necessary for flight use. Two altimeters are used for redundancy. Each altimeter has leads to internal blast charges used for vehicle separation and parachute deployment as part of recovery operations. This system is pictured below in Figure 124.

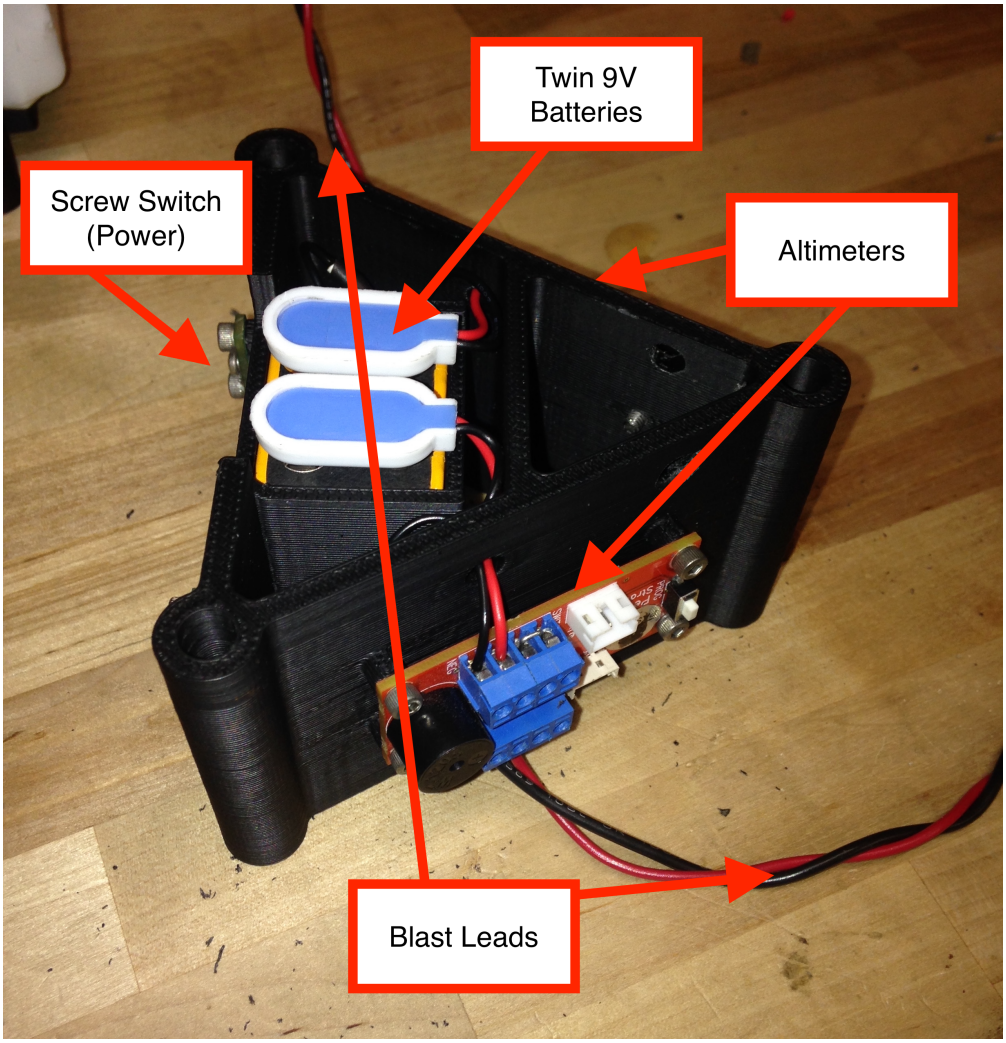

Figure 124: Avionics Bay Electronic Components

Testing this system requires validation of all electrical connections, calibration of altimeter units, and verification of altimeter blast charge detonation altitudes and function. Electrical connections are verified by turning on the altimeter units, observing for standard function, and conducting of a test electric match burn. After all hardware has been mounted into the launch vehicle battery and electronic match connections are tested again for continuity and proper voltage drop with a multimeter.
Altimeters were calibrated by testing in a vacuum chamber. Chamber pressure was lowered to atmospheric pressure for the range of altitudes relevant to USLI flight, and the altimeters calibrated according to this data. After setting the altimeters to their flight-ready detonation altitudes, they were again tested to validate proper setting of these altitudes, the audible indicator providing a post-experiment readout of ”detonation altitude.” Successful completion of these tests indicated flight readiness for the electronic portion of the avionics system.

7.1.2.2 Payload Electronics Testing

Assessing functionality of payload electronics required several tests: some purely electrical, and others electromechanical. The mission critical portion of the payload electronics system is the custom fabricated BeagleBone Black cape that can be seen in Figure 125 below. This cape required hours of work by way of surface mount component installation and through-hole soldering. The small workspace greatly increased the likelihood of a short. Extensive testing was done with a multimeter to ensure continuity where continuity was desired, and to ensure

no shorting where undesirable. Two iterations of board were required before a successful model was manufactured.

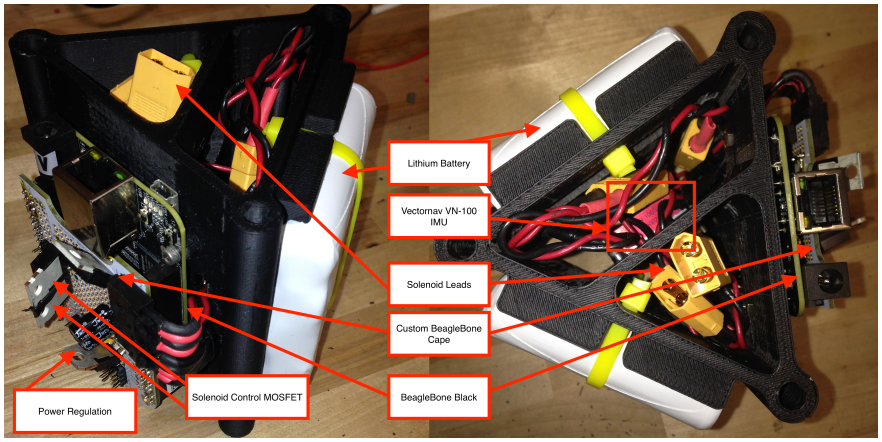

Figure 125: Payload Electronics Electronic Components

Plug connections for both batteries and solenoid control leads, as labeled in Figure 125, were checked for continuity after soldering. Solenoids were first checked for operational status by connection to a pulsed 27 V power source, and it was determined that voltage polarity was of no consequence in solenoid operation. This test is pictured in Figure 126 below. Proper eye and ear protection safety precautions were taken as pressurized air was being ejected in supersonic flow.

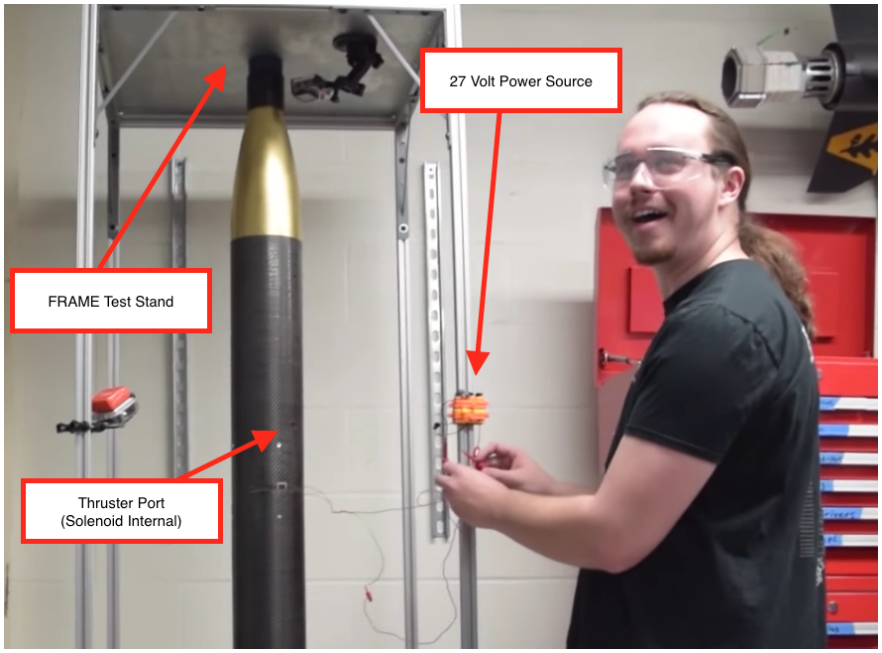

Figure 126: Testing of Solenoid Actuation by VADL Member

Software testing will be discussed in more detail below, but from an electronic function testing perspective, software played an integral role. Once a basic version of the flight software had been written to the point of being able to test electronic functionality, it was loaded onto the BeagleBone Black and the prototyped ”cape” was fitted along with all relevant battery and solenoid connections. A program directing pulsed actuation of the solenoid valves was run with an oscilloscope in the loop to visualize the duty cycle, allowing for analysis of rise time, overshoot, and steady state error in the system. With successful completion of solenoid pulse testing, full electronics integration testing was possible.

Before subscale flight, a full electronics integration test was completed on the FRAME. Kerbal Space Program was used to simulate the acceleration of the vehicle due to takeoff, as sensed by the software, which then prompted the electronic state machine to enter the experiment mode. The flight vehicle spun on the test stand as was expected of a successful test. This test was conducted multiple times, and thus the payload electronics were validated for flight.

7.1.3 Software Testing

Software reliability is one of the most essential aspects of this entire project. Without robust testing protocols we would be unable to confidently fly our rocket, actuate the solenoids, and receive usable IMU data. The testing protocol developed allowed us to individually test each aspect of the software and then combine it all together to test the HLC. First, the solenoid actuator was tested. A simple control component was written such that the user could input the number of pulses, the initial delay, the pulse length, and the delay length. This was deployed to the BeagleBone to light up an LED and was proven successful. As far as software is concerned, if this LED lit up, then it could be assumed that the solenoid would fire as well. Next, the IMU component was tested to verify its precision. For this test, the IMU simply plotted data for roll, pitch, yaw, and xyz acceleration. In testing the HLC, it was necessary to verify the triggering events that move the software from one state to another, as well as the activation of the solenoid. To do this, the IMU was connected to a BeagleBone and an LED was connected to the solenoid pin. Simply through a user-inputted upward acceleration of the IMU followed by a deceleration, all of these triggers could be verified. Once MECO is sensed and the experiment begins, everything is time based and not acceleration based, so it was only necessary to trigger the takeoff and MECO. By watching the LED and ensuring that its pulse pattern matches the user-inputted pulse pattern, it could again be assumed that the same would occur during flight. The output of the solenoid pin is automatically plotted in ROSMOD as seen in Figure 127. For incorporating this software into the full rocket integration tests on the FRAME, a time based enable feature was added to bypass the acceleration thresholds and begin the pulsing cycle after a user-defined initial delay. The goal of this was not to verify the software, but to use the software to verify the hardware, the FRAME, and the thruster system.

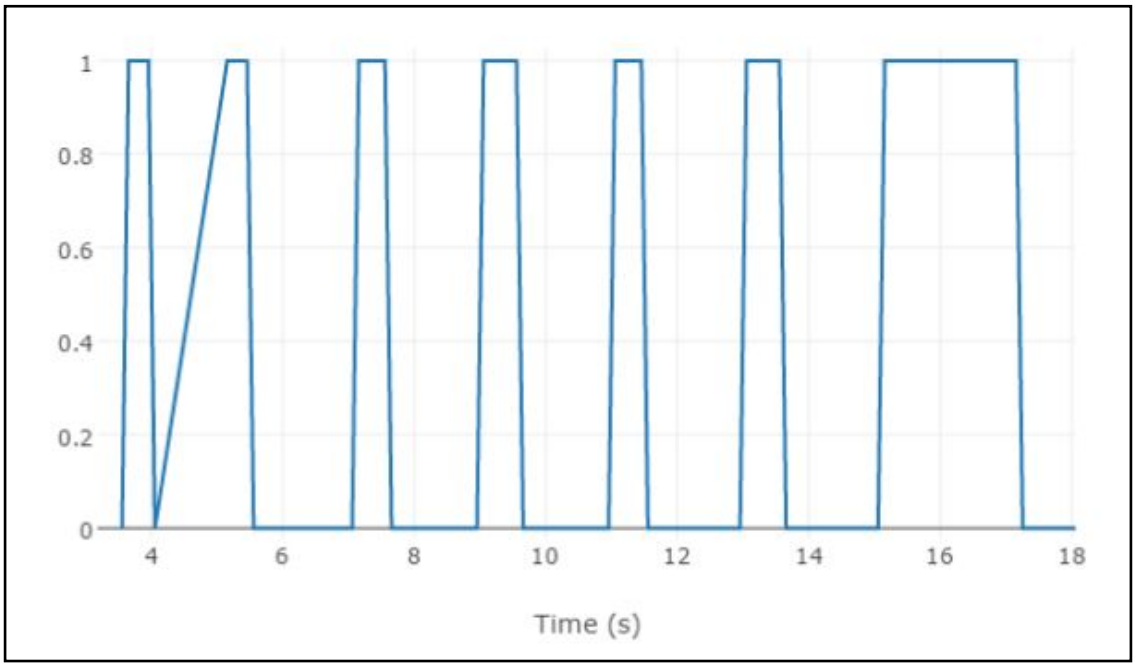

Figure 127: Solenoid Pin Value vs. Time

7.1.4 The FRAME

7.1.4.1 Introduction

In order to ensure a successful payload experiment, extensive testing is required to develop and refine the algorithms that control the attitude of the flight vehicle. Specifically, the payload must be able to precisely control the angular position of the rocket during flight such that it is able to complete two full rotations and then return to its initial angular position. This entire operation must occur in the eight seconds between MECO and apogee, necessitating a precise control algorithm to ensure efficient execution.

7.1.4.2 Purpose

The FRAME, seen in Figure 128 will allow for roll control algorithms to be developed and refined in the convenience of a laboratory setting. The algorithms will govern the actuation of two solenoids, which each activate a thruster couple to apply moments to rotate the flight vehicle. In order for the testing and refinement of these algorithms to be effective, the test and flight environments must be as similar to one another as possible. Accordingly, The FRAME must allow for flight conditions to be recreated in a ground-based laboratory setting.

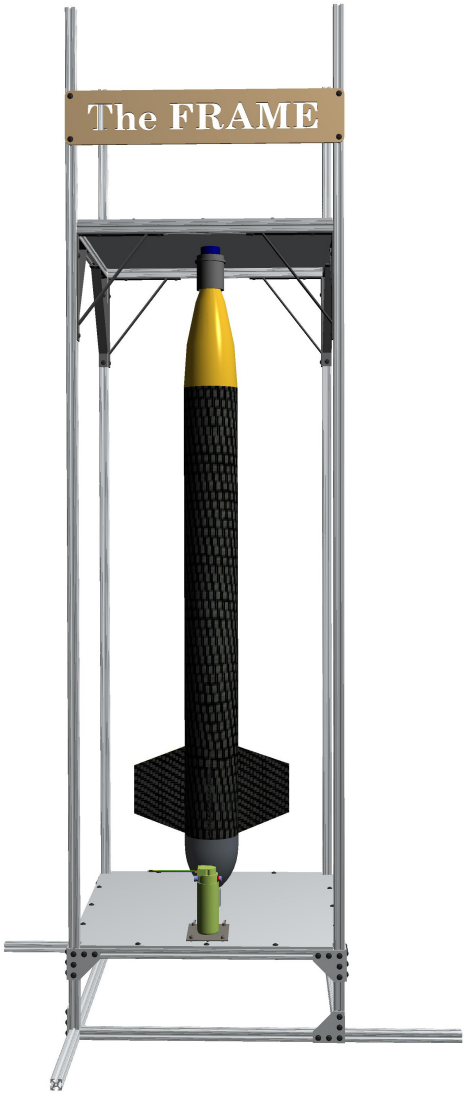

(a) CAD of the FRAME

(b) Picture of the Subscale Rocket Mounted for Testing in the FRAME

Figure 128: CAD and Picture of the FRAME

7.1.4.3 Advantages

Due to the apparent difficulty of modeling the dynamic flight environment of a rocket in a laboratory setting, it may seem more logical to conduct payload testing on practice flights. However, the cost, safety risks, and logistical difficulties associated with rocket launches make ground-based testing a much more attractive option. Specifically, it is estimated that a full rocket launch can cost as much as $500.00, with primary contributors being transportation to a remote launch location and the cost of the single-use motor. Additionally, a single launch can take as long as 6 hours to properly execute, as preparation, transportation, and careful launch operation each take a considerable amount of time. Furthermore, the considerable safety risks of handling blast charges and rocket motors must be taken into account.

Testing the payload in a controlled, ground-based laboratory environment solves all of these problems. The total cost of The FRAME is less than the cost of two launches, and each test can be performed in approximately 10 minutes. Furthermore, the safety hazards associated with the FRAME are negligible when compared to those associated with a

launch. Clearly, pursuing a ground-based testing solution for the payload is preferred, despite the difficulties associated with proper execution.

7.1.4.4 General Criteria For Success

While it is easy to talk about accurately replicating a rocket's flight environment in a ground-based laboratory setting, it is quite another matter to actually accomplish such a feat. In order to understand exactly what must occur in order to make this happen, it is important to get a sense of the important elements of the rocket's flight environment. The following list outlines the three most important criteria that were considered when designing the FRAME to ensure that it accurately modeled the flight environment.

1. Allow for frictionless rotation of the flight vehicle
2. Ensure a vertical orientation of the flight vehicle
3. Simulate the effects of aerodynamic damping on the rotation of the flight vehicle

Perhaps most importantly, the FRAME must allow for frictionless rotation about the main axis of the flight vehicle. This is a critical feature, as the roll control algorithms can only be monitored if the payload can cause the flight vehicle to rotate. The frictionless nature of this rotation is vital, as the flight vehicle will experience no opposition to its rotation during flight other than aerodynamic forces. Additionally, the flight vehicle must maintain a vertical orientation during testing, as it will throughout the payload experiment window of the flight. This vertical orientation during flight is ensured by the selection of a high impulse motor that burns for a short duration. Simulations and subscale flight have confirmed this expected flight path, and the FRAME must mirror this condition in order to properly model the flight environment. Finally, the aerodynamic forces that will act on the flight vehicle at high velocities must be properly understood and incorporated during testing. The FRAME must be able to accurately reproduce the rotational damping effect of air resistance. While there will be some inherent drag when testing in a ground-based laboratory setting, the tremendous airspeed experienced by the flight vehicle during the payload experiment significantly increases the rotational drag as discussed in Section **??**. Accordingly, this behavior must be modeled during testing in order to ensure that the roll control algorithms are optimized to function in a realistic flight environment.

7.1.4.5 Design Choices

Frictionless Rotation In order to ensure that the three primary criteria for successful tests are met, a number of design choices were made when building the FRAME. First, in order to ensure frictionless rotation, a bearing system was constructed using radial and thrust bearings. As can be seen in Figure 129, rotation about the main axis of the flight vehicle aligned with a vertical shaft, highlighted in blue. The shaft is supported by two radial bearings, which are highlighted in green. A thrust bearing, highlighted in red, supports vertical loads, ensuring smooth rotation even when supporting the full weight of the flight vehicle. The entire assembly is contained within a custom machined bearing cup, highlighted in yellow, which is bolted directly to the bottom plate of the FRAME to ensure stability.

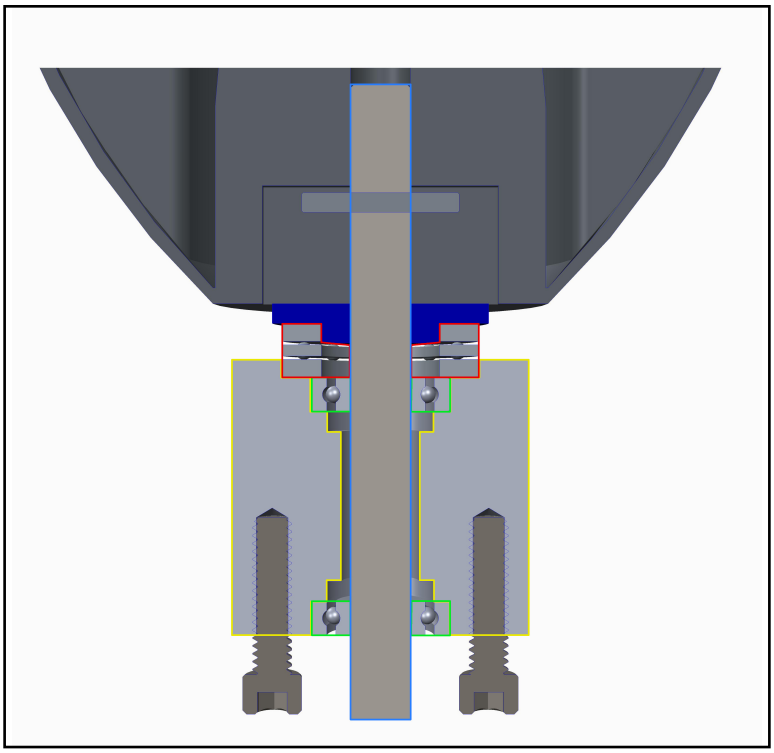

Figure 129: Cross Section View of Bearing System Enabling Frictionless Rotation

Vertical Orientation To preserve the vertical orientation of the flight vehicle during testing, a dual support system was implemented, constraining the nose cone and tail of the rocket. The top and bottom support systems can be seen in Figure 130. These independent supports are each aligned with the central axis of the flight vehicle and bolted to custom machined aluminum plates. Each of these plates features four identically placed holes that are accurate within hundredths of an inch, ensuring perfect vertical alignment of the two support systems. In order to ensure that the flight vehicle aligns precisely with each of the support systems, both were designed to specifically interface with components of the rocket.

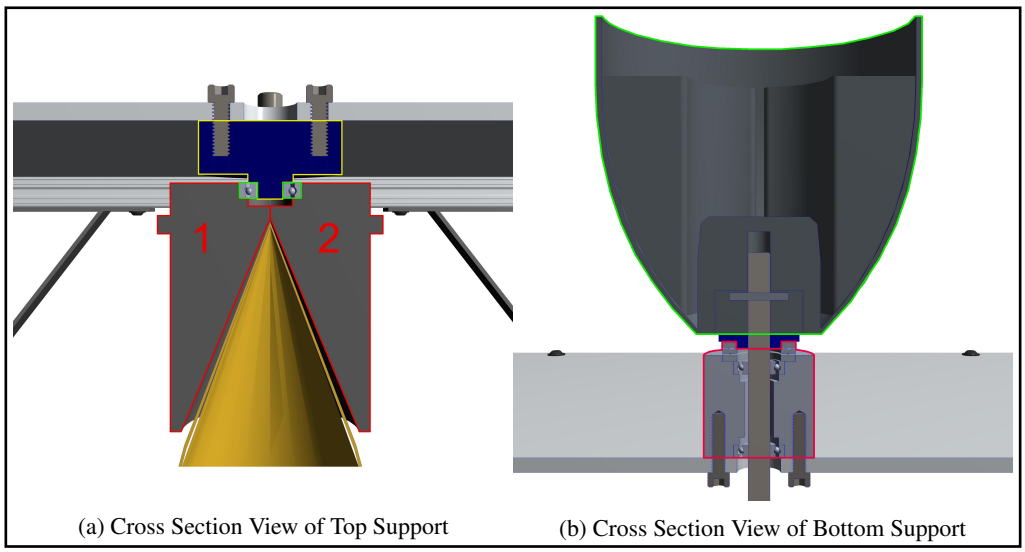

(a) Cross Section View of Top Support

(b) Cross Section View of Bottom Support

Figure 130: Top and Bottom Supports Enabling Vertical Orientation

The top support features a nose cone gripper, seen in Figure 130a. This two-part rapid prototyped component, highlighted in red, encloses the nose cone of the rocket, and is clamped into place during testing. It is clamped around a radial bearing, highlighted in green. The radial bearing is fit onto a rapid prototyped part, which is highlighted in yellow, and is bolted to the top plate of the FRAME to secure the top support in place. The conical interior of the nose cone gripper acts to center the tapered nose cone with the axis of rotation of the top support, while the clamp allows for easy assembly as well as a snug interface with the nose cone. Figure 130b shows the bottom support, which consists of a rapid prototyped fin gripper, highlighted in green, and aforementioned bearing assembly, highlighted in red. While the primary function of the fin gripper is to transmit torque to the rocket, it also serves to center the flight vehicle to ensure a vertical orientation. The central column of the fin gripper was specifically designed to fit snugly within the motor tube of the rocket. With the boat tail disassembled, the flight vehicle slides vertically down into the fin gripper, centering itself with the bottom support.

Aerodynamic Forces The third criteria for successful testing on the FRAME is that be able to model the aerodynamic damping present during flight. The effect of the flight aerodynamics that is pertinent to the roll control system is the rotational damping present at high airspeeds. Accordingly, aerodynamic influences can be considered based on their effect on the flight vehicle's rotation. These effects can then be applied to the rocket as a torque input via a DC motor, seen in Figure 131. The motor is coupled to the shaft of the bottom support via a timing belt with a gear ratio of 3:1 to allow for minimal power consumption while delivering the necessary torque. A picture of this linkage can be seen in Figure 132. The relevant motor specifications are pictured in Table 22.

Figure 131: Picture of DC Motor Used to Simulate Aerodynamic Damping via Torque Inputs

Table 22: DC Motor Specifications

Supplier	Ametek
Motor Type	Brushed
Supply Voltage	24 V
Power	100 W
Motor Torque Constant	.0706 Nm/A
Peak Current	41 A
Continuous Output Torque	.35 Nm

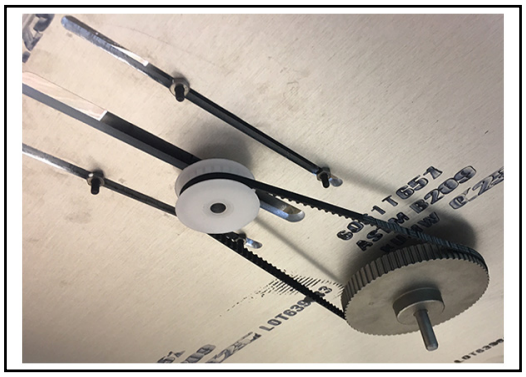

Figure 132: Picture of Pulley and Timing Belt Linkage Used to Transmit Torque from the DC Motor to the Shaft of the Bottom Support

The torque is transmitted from the motor through the timing belt to the vertical shaft. From there, the torque is transfered to the rapid prototyped fin gripper, which can be seen in Figure 133 highlighted in green. To facilitate torque transmission from the shaft to the fin gripper, a cross pin, highlighted in red in Figure 133a, was press fit through the top of the shaft, which is highlighted in yellow. In addition to serving the previously mentioned function of aligning the flight vehicle in a vertical orientation, the fin gripper was specifically designed to transmit torque from the shaft of the bottom support to the flight vehicle. Four slots were designed to snugly grip each of the four fins, through which torque can be transmitted. Figure 133b illustrates how the tail of the flight vehicle fits into the fin gripper. The dotted red lines show the path of the fins as they plunge into the fin gripper. It is important to note that the portion fo the fins that interface with the fin gripper are between the airframe and motor tube of the rocket. In order to access them, the boat tail of the flight vehicle must be removed during testing. Overall, the fin gripper facilitates the transmission of torque from the DC motor to the flight vehicle, which is needed in order to model the aerodynamic drag present during flight.

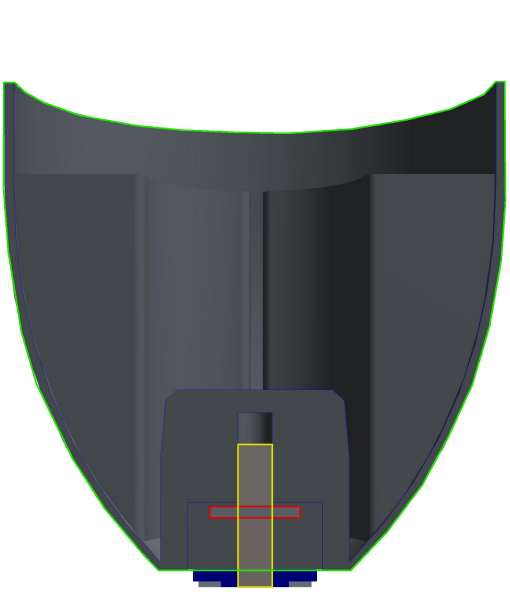

(a) Cross Section View of Fin Gripper and Shaft with Cross Pin

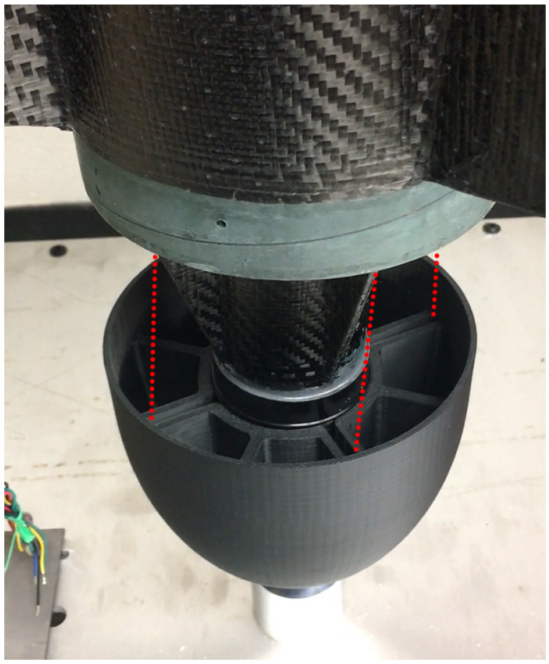

(b) Picture of Subscale Rocket Fins Meshing With Rapid Prototyped Fin Gripper

Figure 133: Fin Gripper Used to Transmit Torque to the Flight Vehicle

Using Kerbal Space Program for Real-Time Aerodynamic Modeling To produce the torque required to successfully emulate in-flight conditions, Kerbal Space Program (KSP) and ROSMOD are used. KSP is a flight simulation software with reliable physics that allows VADL to import CAD models of the rocket and assign empirically-derived material and aerodynamic properties to various parts. ROSMOD is the VADL-developed modeling and execution environment for software-integrated systems as discussed in Section 5.1.5.

The exact same software that was used to control the solenoid activation during flight, described in Section 5.1.5, is used during the FRAME testing The high level diagram of this system is shown in Figure 134a. However, a few modifications to this software are made for ground-based testing. First, instead of using acceleration to sense takeoff and initiate the roll control algorithm, KSP's accelerometer on the virtual rocket is used. Also, since the rocket on the frame obviously experiences no axial velocity, the motor has to be actuated to provide the correct damping torque. The high level controller (HLC) in ROSMOD is thus configured to receive vertical speed and atmospheric density input from KSP as well as rotation inputs from the IMU and calculate necessary damping torque. The HLC is then programmed to supply the necessary current to the motor to produce the equivalent torque, as well as apply point forces to the virtual rocket in KSP to make it spin synchronously with the real rocket. The high level diagram for the new software system for ground-based testing is shown in Figure 134b.

Equation 7.1, derived in Section **??**, shows how to calculate damping torque to rotation as the rocket ascends.

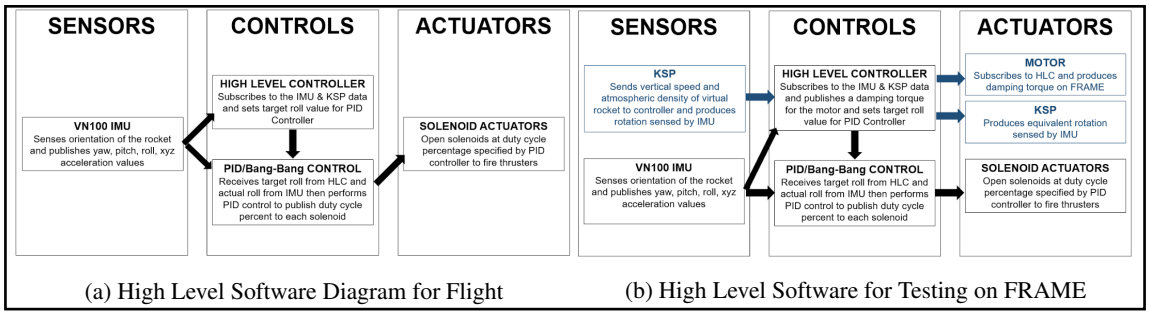

(a) High Level Software Diagram for Flight (b) High Level Software for Testing on FRAME

Figure 134: Comparison of High Level Software Diagrams between Testing and Flight

$$\tau_d = \tau_q + \tau_s + \tau_{jf} \approx F_{jf}(\tau_q + \tau_s) \tag{7.1}$$

$$\tau_q = \frac{1}{2} N C_{d,fin} Z_{fin} \rho v_d \omega$$

$$\tau_s = \frac{1}{2} C_f \rho A_{cyl} v_d \omega R$$

Where τ_q is the torque produced due to pressure drag, τ_s is the torque produced due to skin friction drag, and τ_{jf} is the torque produced due to jet-fin interaction, which is assumed to be zero for this purpose since it is much smaller than the other two and not currently computable in KSP. Table 23 defines the other variables used in Equation 7.1.

Table 23: Damping Torque Equations Symbol Definitions

Symbol	**Definition**
N	Number of fins
$C_{d,fin}$	Drag coefficient of fins
$C_{d,f}$	Skin friction drag coefficient of rocket cylinder
Z_{fin}	Fin geometry constant (m^4)
ρ	Atmospheric density of air (kg/m^3)
R	Radius of rocket (m)
A_{cyl}	Surface area of rocket cylinder (m^2)
ω	Angular velocity (rad/s)
v_d	Vertical speed (m/s)

As the real rocket is spinning on the FRAME, and the simulated rocket is flying in KSP, ROSMOD continuously calculated the damping torque that a real rocket would experience and applies that torque to the motor. The flow of information between the FRAME, ROSMOD, and KSP is shown in Figure 135.

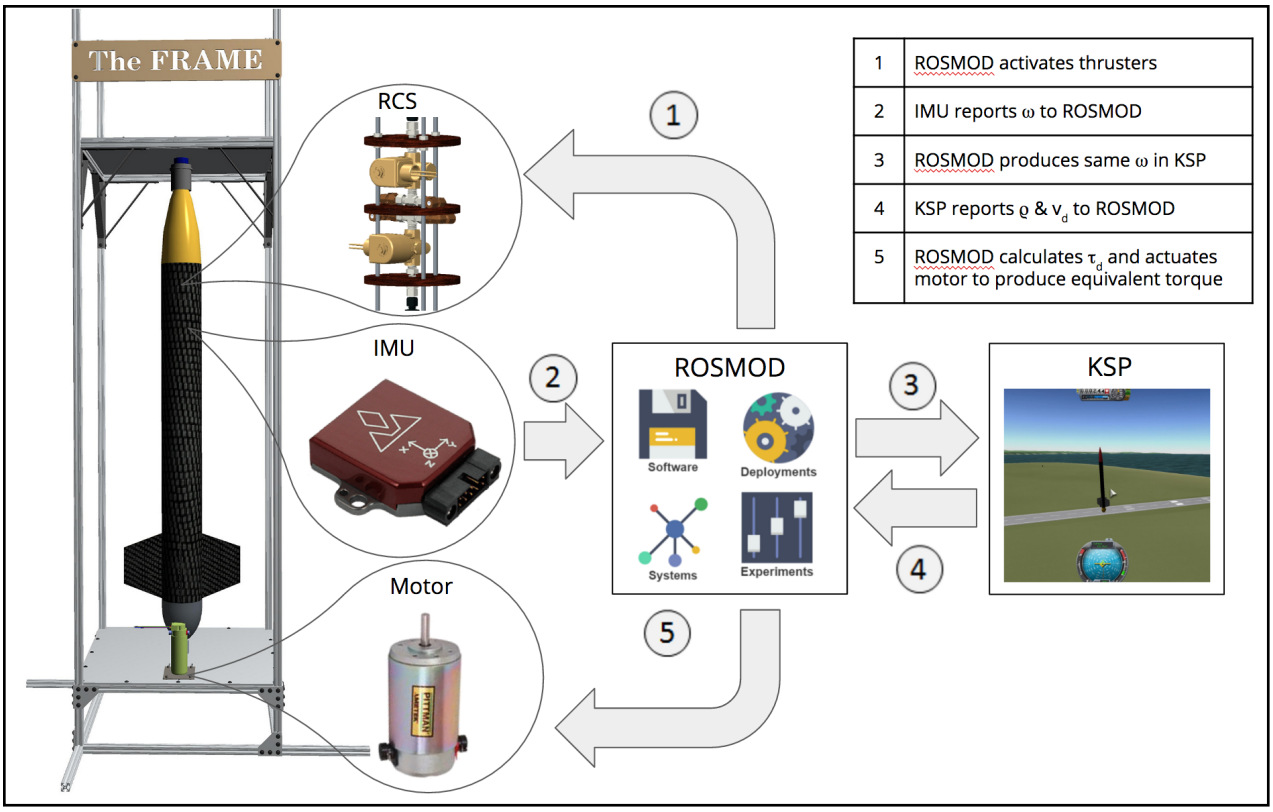

Figure 135: Information Flow Between FRAME, ROSMOD, and KSP during Ground-based Testing

The following list outlines what each of the numbers in Figure 135 represent after the simulated rocket is launched in KSP and reaches MECO.

1. ROSMOD activates thrusters
2. IMU reports ω to ROSMOD
3. ROSMOD produces same ω on KSP rocket
4. KSP reports ρ & v_d to ROSMOD
5. ROSMOD calculates damping torque and actuates motor to produce the equivalent torque

The four inputs in Equation 7.1 that are changing during the course of the flight are ω, ρ, v_d, and C_f. Rotational speed, ω, is obtained from the IMU aboard the real rocket on the FRAME. Atmospheric density, ρ and vertical speed, v_d are outputted by KSP. The skin friction drag coefficient of the cylinder, C_f, is calculated by Equation 7.2.

$$C_f = \frac{0.455}{[\log_{10}(Re)]^{2.58}}, 2 \times 10^5 < Re < 10^7 \tag{7.2}$$

As Equation 7.2 show, C_f is only dependent on Reynold's Number, which is a function of air density, flow speed, air viscosity, and characteristic length, all of which can be calculated in real time from KSP, so KSP can also be configured to output this number. The rest of the inputs remain constant and can just be plugged into ROSMOD to remember. Thus, ROSMOD can know in real time all variables needed to calculate the damping torque that should be produced by the motor, which is does so at 10 Hz. It is then programmed to supply the correct current to the motor to produce the necessary torque.

7.1.4.6 Testing

Overview Thus far, a number of tests have been successfully conducted on the FRAME, which has aided in design improvements of the payload as well as the FRAME itself. The tests have verified the payload's ability to perform its fundamental function, but have also validated the FRAME as a means of testing the payload. The following list shows the tests either already performed or planned to be performed as the roll control algorithm continues to be developed.

1. Open Loop Thruster Test
2. Subscale Integration
3. Flight Environment Comparison Test
4. Preliminary Roll Control Algorithm Development Testing
5. Fullscale Integration Test
6. Roll Control Algorithm Refinement with Atmospheric Damping
7. Roll Control Algorithm Robustness Test with Disturbance Input Torques

Open Loop Thruster Test

Objective

- Open solenoid to activate thrusters
- Validate thrusters' ability to rotate subscale flight vehicle

Success Criteria

- Solenoids open to actuate thrusters
- Thrusters fire with enough thrust to rotate subscale flight vehicle

Variables

- Angular Position
- Angular Velocity

Methodology

- Activate solenoid externally via 9V battery
- Use the FRAME to constrain the flight vehicle in a vertical orientation and allow for frictionless rotation
- Monitor variables visually

Results The open loop thruster test of the subscale payload was successful, as the solenoids were able to activate the thrusters. Furthermore, the thrust produced by the thruster couple was sufficient to cause the flight vehicle to rotate about its main axis.

Subscale Integration Test

Objective

- Use payload electronics to activate solenoid and pulse thrusters to cause vehicle to rotate
- Validate dynamic model of subscale flight vehicle

Success Criteria

- Payload electronics successfully activates thrusters to cause rotation
- IMU successfully records variables for analysis
- Impulse response of system obtained

Variables

- Angular Position
- Angular Velocity
- Angular Acceleration

Methodology

- Activate solenoid using onboard payload electronics
- Use the FRAME to constrain the flight vehicle in a vertical orientation and allow for frictionless rotation
- Monitor variables using onboard IMU and payload electronics

Results The subscale integration test was a success, as the payload electronics were able to activate the solenoid, which actuated the thruster couple and caused the subscale flight vehicle to rotate. Furthermore, the data obtained from the onboard IMU was compared to the dynamic model of the subscale flight vehicle. Figure 136 shows the dynamic model and IMU data plotted against one another. While the two data sets agree for the most part, a significant discrepancy occurs as the flight vehicle comes to a rest at around 15 seconds. The more rapid deceleration experienced by the physical frame test is likely due to the friction within the top support that is not accounted for in the dynamic model. Other than this minor detail, the two data sets largely agree, which validates the dynamic model.

Flight Environment Comparison Test

Objective

- Compare behavior of rocket in flight compared to mounted on The FRAME
- Use payload electronics to operate solenoid and actuate thrusters in identical scheme as subscale flight

Success Criteria

- Payload electronics successfully actuates thrusters to cause rotation
- IMU successfully records variables for analysis

Variables

- Angular Position
- Angular Velocity
- Angular Acceleration

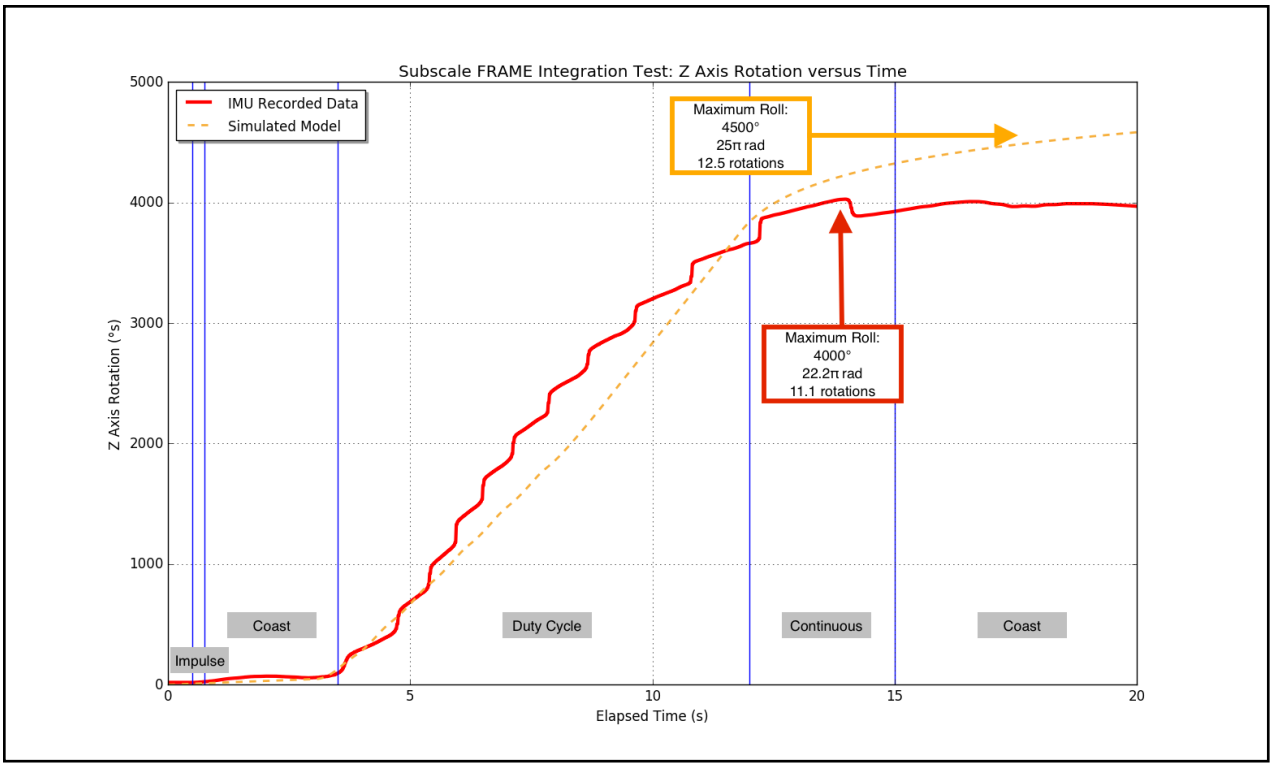

Figure 136: Dynamic Model and IMU Data Comparison

Methodology

- Compare data to subscale flight data to contrast test conditions of the FRAME and flight
- Operate solenoid using onboard payload electronics to actuate thrusters in identical scheme as subscale flight
- Use the FRAME to constrain the flight vehicle in a vertical orientation and allow for frictionless rotation
- Monitor variables using onboard IMU and payload electronics

Results The flight environment comparison test was a success, as it illustrated the differences between the test conditions of the FRAME and the flight environment. Figure 137 shows the angular position data gathered from the onboard IMU for each test. Clearly, the subscale flight vehicle performed many more rotations on the FRAME compared to the subscale launch. This is due to the lack of aerodynamic forces present on the FRAME. While this discrepancy is greater than anticipated, it validates the inclusion of a motor as part of the FRAME. Additionally, it has allowed the team to explore the phenomena of pressure drag and jet-fin interaction. Overall, this test represents an important step in the evolution of the FRAME, as it illustrated the need for real-time aerodynamic force modeling and transmission. Furthermore, this test highlighted the need for modifications to the payload design, as more thrust is needed to overcome the aerodynamic rotational damping.

Preliminary Roll Control Algorithm Development Testing

Objective

- Develop preliminary roll control control algorithms to cause flight vehicle to rotate to 4π radians and stop
- Use payload electronics to operate solenoid and actuate thrusters

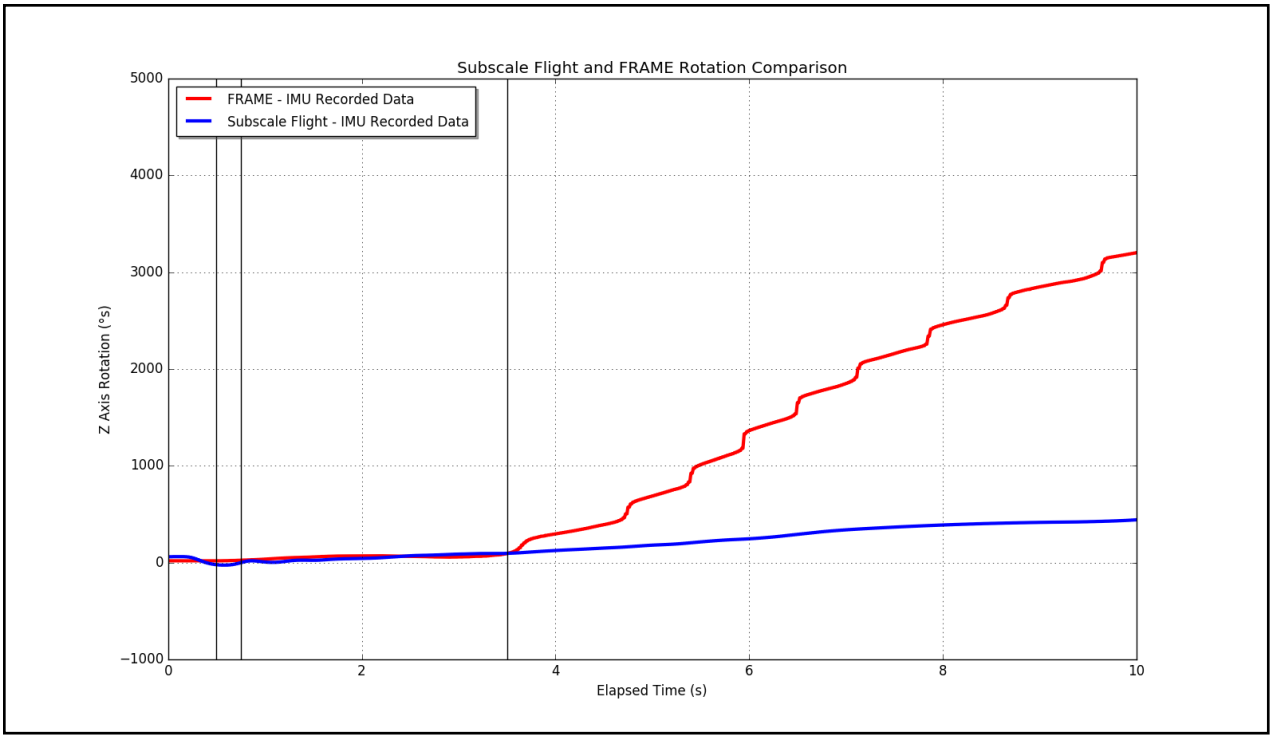

Figure 137: Subscale Flight and FRAME Angular Position Comparison

Success Criteria

- Payload electronics successfully activates thrusters
- Motor successfully arrests rotation at 4π radians
- IMU successfully records variables for analysis

Variables

- Angular Position
- Angular Velocity
- Angular Acceleration

Methodology

- Use DC motor to serve as reverse thruster couple, allowing subscale flight vehicle to be used to test preliminary roll control algorithms before full scale flight vehicle is constructed
- Operate solenoid using onboard payload electronics
- Use the FRAME to constrain the flight vehicle in a vertical orientation and allow for frictionless rotation
- Monitor variables using onboard IMU and payload electronics

Results This test has yet to be completed.

Full Scale Integration Test

Objective

- Use payload electronics to operate solenoids to pulse thrusters and cause vehicle to rotate
- Obtain impulse response of system on the FRAME

Success Criteria

- Payload electronics successfully activates thrusters to cause rotation
- IMU successfully records variables for analysis
- Impulse response of system obtained

Variables

- Angular Position
- Angular Velocity
- Angular Acceleration

Methodology

- Activate solenoids using onboard payload electronics
- Use the FRAME to constrain the flight vehicle in a vertical orientation and allow for frictionless rotation
- Monitor variables using onboard IMU and payload electronics

Results This test has yet to be completed.

Roll Control Algorithm Refinement with Atmospheric Damping

Objective

- Refine roll control algorithms so that precise roll control is possible with atmospheric damping
- Develop roll control algorithms so that at least 4π radians of roll and counter roll can be accomplished in eight seconds
- Use payload electronics to operate solenoids and activate thrusters and cause vehicle to rotate

Success Criteria

- roll control algorithm is able to overcome atmospheric damping to execute desired rotation within eight seconds
- Payload electronics successfully activates thrusters to cause desired rotation within eight seconds
- IMU successfully records variables for analysis

Variables

- Angular Position
- Angular Velocity
- Angular Acceleration

Methodology

- Use KSP to model atmospheric damping in real time during simulated rocket
- Use DC motor to input atmospheric damping torques to the rocket
- Activate solenoids using onboard payload electronics
- Use the FRAME to constrain the flight vehicle in a vertical orientation and allow for frictionless rotation
- Monitor variables using onboard IMU and payload electronics

Results This test has yet to be completed.

Roll Control Algorithm Robustness Test sith Disturbance Input Torques

Objective

- Improve robustness of roll control algorithms so that precise roll control is possible in a variety of conditions
- Develop roll control algorithms so that at least 4 π roll and counter roll can be accomplished in eight seconds
- Use payload electronics to operate solenoids and activate thrusters and cause vehicle to rotate

Success Criteria

- roll control algorithm is able to overcome disturbances to execute desired rotation within eight seconds
- Payload electronics successfully activates thrusters to cause desired rotation within eight seconds
- IMU successfully records variables for analysis

Variables

- Angular Position
- Angular Velocity
- Angular Acceleration

Methodology

- Use DC motor to input random disturbance torques to the rocket
- Activate solenoid using onboard payload electronics
- Use the FRAME to constrain the flight vehicle in a vertical orientation and allow for frictionless rotation
- Monitor variables using onboard IMU and payload electronics

Results This test has yet to be completed.

7.1.4.7 Conclusions

When considering the tests conducted thus far alongside the careful design choices made, it becomes clear that the FRAME offers a viable platform for testing the payload. It has been verified that the thrusters of subscale payload are capable of inducing rotation about the flight vehicle's main axis. Furthermore, it has been confirmed that the payload electronics are able to reliably activate the thrusters in various actuation patterns. Looking forward, the DC motor will be incorporated to take the flight environment modeling capabilities of the FRAME to the next level. roll control algorithms will be developed in a realistic flight environment and will be stress tested with various disturbance inputs. The convenience of testing in a ground-based laboratory setting will allow many tests to be run to refine roll control algorithms and verify the reliability of the payload. Overall, successful tests on the FRAME have thus far validated the design of both the payload and the FRAME itself. Looking forward, future tests will allow for robust roll control algorithms to be developed in an realistic flight environment.

7.1.5 Carbon Fiber Reinforced Blue Tube testing

The carbon fiber reinforced Blue Tube was tested both with holes and without holes, as described in 3.1.2. Future plans for body tube testing include a tear-out test to test the shear strength of the body tube. This test would be useful for any place where there are bolts in the airframe. The objective is to verify that bolts will not shear out of the airframe, and the test will be considered a success if the airframe can withstand three times the maximum expected load. The plan for this test is to place a blade along the top of the body tube and place the system in the load frame to complete a compression test.

7.2 Requirements Compliance

NASA Handbook Requirements To ensure a safe and successful flight as well as a rigorous design and experimental procedure for the VADL payload, the requirements of the NASA USLI competition must be satisfied. These requirements are separated into five system categories representing the entirety of the 2016-2017 USLI competition:

1. Vehicle Requirements
2. Recovery System Requirements
3. Experiment Requirements
4. Safety Requirements
5. General Requirements

Assigned to each requirement is one of (or a combination of) four methods of verification standard to systems engineering, in order of increasing time-consumption/expense:

- **Inspection**: The least expensive of verification methods, *inspection* is the verification of the requirement using the five senses. No exercising of the system is required; a simple observation can prove that the requirement is met.
- **Analysis**: By using simulations, calculations, models, or similarity, the requirement is verified by *analysis*. Often times it predicts the failure point of the system. Typical uses of *analysis* are CFD, structural analysis, rocket simulation, and mathematical calculations for shear pins, fin geometry, kinetic energy, center of mass, power draw, etc.
- **Test**: *Testing* is using a predefined series of inputs to ensure that the output will verify the requirement. It involves the testing of a particular subsystem as opposed to the full system. Common uses are deployment testing, hydrostatic testing, altimeter testing, tracking device testing, etc.
- **Demonstration**: The most expensive of verification methods, a *demonstration* is verification through the intended use of the system. In our case, *demonstration* involves a full flight test of the launch vehicle in subscale, fullscale, or competition flights.

The requirements, respective verification methods, and a description of the verification plan can be seen in the tables below.

Requirement	Method of Verification	Description of Verification Plan	Status	Document Section
1. Vehicle Requirements				
1.1. The vehicle shall deliver the science or engineering payload to an apogee altitude of 5,280 feet above ground level (AGL).	Analysis and Demonstration	The apogee altitude will be analyzed by simulation and demonstrated during fullscale test and competition flights using the altimeters.	In Progress - final verification will come from fullscale flight. Motor thrust and mass predictions, when fed into simulation, predict an altitude around 5,280 ft. AGL.	\ref{sec:mission_performance_predictions}
1.2. The vehicle shall carry one commercially available, barometric altimeter for recording the official altitude used in determining the altitude award winner. Teams will receive the maximum number of altitude points (5,280) if the official scoring altimeter reads a value of exactly 5280 feet AGL. The team will lose one point for every foot above or below the required altitude. The altitude score will be equivalent to the percentage of altitude points remaining after and deductions.	Inspection	*Inspection will verify that altimeters are onboard.*	In Progress - When full scale fabrication is finished, dual StratoLoggerCF altimeters will be included in the avionics bay.	\ref{sec:recovery_system}
1.2.1. The official scoring altimeter shall report the official competition altitude via a series of beeps to be checked after the competition flight.	Demonstration	*Competition flight demonstration will verify the official competition altitude. Full scale and subscale launches will test this capability.*	In Progress - subscale launch has verified the functionality of this system. Final verification will come from competition flight.	\ref{sec:recovery_system}
1.2.2. Teams may have additional altimeters to control vehicle electronics and payload experiment(s).	Inspection	*Inspection will verify the presence of a redundant altimeter.*	In Progress - When full scale fabrication is finished, dual StratoLoggerCF altimeters will be included in the avionics bay.	\ref{sec:recovery_system}
1.2.3. At the LRR, a NASA official will mark the altimeter that will be used for the official scoring.	Inspection	The official scoring altimeter will be inspected by a NASA official on launch day.	Incomplete - Verification will come on competition day.	\ref{sec:recovery_system}

1.2.4. At the launch field, a NASA official will obtain the altitude by listening to the audible beeps reported by the official competition, marked altimeter.	Inspection	An inspection of the audible beeps will verify the altitude reported by the marked altimeter.	In Progress - subscale launches have verified the functionality of this system. Final verification will come from competition flight.	\ref{sec:recovery_system}
1.2.5. At the launch field, to aid in determination of the vehicle's apogee, all audible electronics, except for the official altitude-determining altimeter shall be capable of being turned off.	Inspection	*An inspection of the audible electronics will verify they are turned off.*	In Progress - subscale launch has verified that no audible electronics are active besides the altimeters, which are activated via screw switches from outside the rocket.	\ref{sec:recovery_system}
1.2.6. The following circumstances will warrant a score of zero for the altitude portion of the competition:	Demonstration	Final competition flight demonstration will ensure that none of the circumstances are met.	Incomplete - Verification will come on competition day. Simulations show none	
1.2.6.1. The official, marked altimeter is damaged and/or does not report and altitude via a series of beeps after the team's competition flight.				\ref{sec:recovery_system}
1.2.6.2. The team does not report to the NASA official designated to record the altitude with their official, marked altimeter on the day of the launch.				
1.2.6.3. The altimeter reports an apogee altitude over 5,600 feet AGL.				
1.2.6.4. The rocket is not flown at the competition launch site.				

1.3. All recovery electronics shall be powered by commercially available batteries.	Test	A preflight test of the avionics subsystem will be performed to verify its functionality with commercially available batteries.	Complete	\ref{sec:recovery_system}
1.4. The launch vehicle shall be designed to be recoverable and reusable. Reusable is defined as being able to launch again on the same day without repairs or modifications.	Analysis and Demonstration	Simulation analysis and subscale/fullscale flight demonstrations will verify the recoverability and reusability of the launch vehicle.	Complete	*\ref{sec:Impacts On Full Scale Design}*
1.5. The launch vehicle shall have a maximum of four (4) independent sections. An independent section is defined as a section that is either tethered to the main vehicle or is recovered separately from the main vehicle using its own parachute.	Inspection	An inspection of the design plans for the fullscale flight vehicle shows three independent sections.	Complete	\ref{sec:vehicle_criteria)
1.6. The launch vehicle shall be limited to a single stage.	Inspection	An inspection of the design plans for the fullscale flight vehicle shows a single stage.	Complete	\ref{sec:vehicle_criteria)
1.7. The launch vehicle shall be capable of being prepared for flight at the launch site within 4 hours, from the time the Federal Aviation Administration flight waiver opens.	Demonstration	Fullscale flight demonstration will verify the ability of the flight vehicle to be prepared within 4 hours.	In Progress - pending fabrication and VADL's assembly experience	\ref{sec:vehicle_mission_statement}
1.8. The launch vehicle shall be capable of remaining in launch-ready configuration at the pad for a minimum of 1 hour without losing the functionality of any critical on-board component.	Analysis and Test	An analysis and subsequent test of the power draw of the electronic subsystems will verify the ability of the launch vehicle to remain in launch ready configuration for a minimum of one hour.	In Progress	\ref{sec:Payload_Electronics}

1.9. The launch vehicle shall be capable of being launched by a standard 12 volt direct current firing system. The firing system will be provided by the NASA-designated Range Services Provider.	Demonstration	The firing system used at the subscale flight demonstration and fullscale flight demonstration will verify the capability of being launched by a standard 12V DC firing system.	In Progress - subscale launch has verified the capability of launch by standard 12V firing system. No changes to launch capability will be incorporated into fullscale	\ref{sec:Payload_Electronics}
1.10. The launch vehicle shall require no external circuitry or special ground support equipment to initiate launch (other than what is provided by Range Services).	Inspection and Demonstration	An inspection of the design plans and demonstration during subscale and fullscale flights will verify that no external circuitry besides the 12V firing system will be required to initiate flight.	In Progress - subscale launch has verified the capability of launch by standard 12V firing system. No changes to launch capability will be incorporated into fullscale	\ref{sec:Payload_Electronics}
1.11. The launch vehicle shall use a commercially available solid motor propulsion system using ammonium perchlorate composite propellant (APCP) which is approved and certified by the National Association of Rocketry (NAR), Tripoli Rocketry Association (TRA), and/or the Canadian Association of Rocketry (CAR).	Inspection	An inspection of the design plans shows the planned motor meets the required specs.	Complete	\ref{sec:design_tail_section}
1.11.1. Final motor choices must be made by the Critical Design Review (CDR).	Inspection	An inspection of the CDR will indicate the final motor choice. Any changes before competition will be verified by the NASA RSO.	Complete	\ref{sec:launch_vehicle_summary)
1.11.2. Any motor changes after CDR must be approved by the NASA Range Safety Officer (RSO), and will only be approved if the change is for the sole purpose of increasing the safety margin.			In Progress - No motor changes are intended	\ref{sec:launch_vehicle_summary)
1.12. Pressure vessels on the vehicle shall be approved by the RSO and shall meet the following criteria:				

1.12.1. The minimum factor of safety (Burst or Ultimate pressure versus Max Expected Operating Pressure) shall be 4:1 with supporting design documentation included in all milestone reviews.	Inspection and Test	An analysis of the safety factor for components seeing pressure and a hydrostatic test of the custom subsystems under pressure will verify the 4:1 safety factor.	In Progress - VADL must apply for exemption for solenoid rated for 3.3:1	\ref{sec:Payload_Requirements_and_Risk_Mitigation}
1.12.2. The low-cycle fatigue life shall be a minimum of 4:1.			Complete	\ref{sec:Payload_Requirements_
1.12.3. Each pressure vessel shall include a solenoid pressure relief valve that sees the full pressure of the tank.			Complete	\ref{sec:Payload_Requirements_and_Risk_Mitigation}
1.12.4. Full pedigree of the tank shall be described, including the application for which the tank was designed, and the history of the tank, including the number of pressure cycles put on the tank, by whom, and when.	Inspection	An inspection of the log being kept for the tank will verify the full pedigree of the tank.	Complete	\ref{sec:Payload_Requirements_and_Risk_Mitigation}
1.13. The total impulse provided by a Middle and/or High School launch vehicle shall not exceed 5,120 Newton-seconds (L-class).				
1.14. The launch vehicle shall have a minimum static stability margin of 2.0 at the point of rail exit.	Analysis	An analysis (simulation) of the static stability margin (SSM) using the estimated mass and the real mass will be performed to ensure the minimum SSM.	Complete	\ref{sec:mission_performance_predictions}
1.15. The launch vehicle shall accelerate to a minimum velocity of 52 fps at rail exit.	Analysis and Demonstration	An analysis (simulation) and fullscale flight demonstration will verify the minimum velocity at rail exit.	Complete	\ref{sec:mission_performance_predictions}

1.16. All teams shall successfully launch and recover a subscale model of their rocket prior to CDR.	Demonstration	The subscale flight demonstration of launch and recovery will be performed prior to CDR submission.	Complete	\ref{sec:Flight Modeling and Recorded Data}
1.16.1. The subscale model should resemble and perform as similarly as possible to the fullscale model, however, the fullscale shall not be used as the subscale model.	Analysis	An analysis of the differences between subscale and fullscale will verify their similarities and differences.	Complete	\ref{sec:Scaling_ Factors}
1.16.2. The subscale model shall carry an altimeter capable of reporting the model's apogee altitude.	Inspection	A pre-flight inspection of the subscale model will verify that a capable altimeter is onboard.	Complete	\ref{sec:Flight Modeling and Recorded Data}
1.17. All teams shall successfully launch and recover their fullscale rocket prior to FRR in its final flight configuration. The rocket flown at FRR must be the same rocket to be flown on launch day. The purpose of the fullscale demonstration flight is to demonstrate the launch vehicle's stability, structural integrity, recovery systems, and the team's ability to prepare the launch vehicle for flight. A successful flight is defined as a launch in which all hardware is functioning properly (i.e. drogue chute at apogee, main chute at a lower altitude, functioning tracking devices, etc.). The following criteria must be met during	Inspection and Demonstration	An inspection of the rocket at competition demonstration will verify it is the same rocket recovered from fullscale demonstration.	Incomplete	\ref{sec:Timeline of Operations}
1.17.1. The vehicle and recovery system shall have functioned as designed.	Analysis and Demonstration	Proceeding the fullscale flight demonstration, an analysis will verify the functionality of the vehicle and recovery system.	Incomplete	N/A

1.17.2. The payload does not have to be flown during the fullscale test flight. The following requirements still apply:				
1.17.2.1. If the payload is not flown, mass simulators shall be used to simulate the payload mass.	Analysis	In the case that the payload is not flown, an analysis of estimated payload mass will verify the payload mass is simulated onboard.	Incomplete	N/A
1.17.2.1.1. The mass simulators shall be located in the same approximate location on the rocket as the missing payload mass.	Inspection	An inspection of the mass simulators will show their location is the same as the missing payload.	Incomplete	NA
1.17.3. If the payload changes the external surfaces of the rocket (such as with camera housings or external probes) or manages the total energy of the vehicle, those systems shall be active during the fullscale demonstration flight.	Demonstration	Any external surfaces will be demonstrated in the fullscale flight.	Incomplete	N/A
1.17.4. The fullscale motor does not have to be flown during the fullscale test flight. However, it is recommended that the fullscale motor be used to demonstrate full flight readiness and altitude verification. If the fullscale motor is not flown during the fullscale flight, it is desired that the motor simulate, as closely as possible, the predicted maximum velocity and maximum acceleration of the launch day flight.	Analysis and Demonstration	In the case that a different motor from that which is flown at competition is flown in the fullscale test flight, an analysis of the max velocity and acceleration from the demonstration will verify the similarity between the flights.	Incomplete	N/A

1.17.5. The vehicle shall be flown in its fully ballasted configuration during the fullscale test flight. Fully ballasted refers to the same amount of ballast that will be flown during the launch day flight.	Analysis and Demonstration	An analysis of the amount of ballast flown during fullscale flight demonstration will be used to verify the same amount of ballast will be flown at competition flight.	Incomplete	N/A
1.17.6. After successfully completing the fullscale demonstration flight, the launch vehicle or any of its components shall not be modified without the concurrence of the NASA Range Safety Officer (RSO).	Inspection	An inspection of the congruency between fullscale and competition flight vehicles will verify that any modifications were made with the concurrence of the RSO.	Incomplete	N/A
1.17.7. Full scale flights must be completed by the start of FRRs (March 6th, 2017). If the Student Launch office determines that a re-flight is necessary, than an extension to March 24th, 2017 will be granted. This extension is only valid for re-flights; not first time flights.	Inspection and Demonstration	An inspection of the FRR will verify the completeness of the full scale flight demonstration. In the In the case that a reflight is required, an inspection will verify that the re-flight demonstration will take place before March 24th.	Incomplete	\ref{sec:Timeline of Operations}
1.18. Any structural protuberance on the rocket shall be located aft of the burnout center of gravity.	Analysis	An analysis of the center of gravity (CG) will verify that any structural protuberances are located aft the CG.	In Progress	\ref{sec:fullscale_launch_vehicle_overview}
1.19. Vehicle Prohibitions				
1.19.1. The launch vehicle shall not utilize forward canards.				
1.19.2. The launch vehicle shall not utilize forward firing motors.				
1.19.3. The launch vehicle shall not utilize motors that expel titanium sponges (Sparky, Skidmark, MetalStorm, etc.)				

1.19.4. The launch vehicle shall not utilize hybrid motors.	Inspection	An inspection of the rocket design will verify that none of the prohibitions are used in the launch vehicle.	Complete	\ref{sec:fullscale_launch_vehicle_overview}
1.19.5. The launch vehicle shall not utilize a cluster of motors.				
1.19.6. The launch vehicle shall not utilize friction fitting for motors.				
1.19.7. The launch vehicle shall not exceed Mach 1 at any point during flight.				
1.19.8. Vehicle ballast shall not exceed 10% of the total weight of the rocket.				
Requirement	**Method of Verification**	**Description of Verification Plan**	**Status**	**Document Section**
2. Recovery System Requirements				
2.1. The launch vehicle shall stage the deployment of its recovery devices, where a drogue parachute is deployed at apogee and a main parachute is deployed at a much lower altitude. Tumble recovery or streamer recovery from apogee to main parachute deployment is also permissible, provided that kinetic energy during drogue-stage descent is reasonable, as deemed by the Range Safety Officer.	Analysis and Demonstration	The deployment events are controlled by the redundant altimeters. An analysis using simulation and demonstration of the deployment events during fullscale testing will verify their efficacy.	In Progress	\ref{sec:recovery_system}
2.2. Each team must perform a successful ground ejection test for both the drogue and main parachutes. This must be done prior to the initial subscale and full scale launches.	Test	A test of the deployment subsystem will verify its functionality prior to subscale and fullscale launch.	in Progress	\ref{sec:recovery_system}

2.3. At landing, each independent sections of the launch vehicle shall have a maximum kinetic energy of 75 ft-lbf.	Analysis and Demonstration	An analysis (simulation) to predict the maximum kinetic energy and results from the fullscale demonstration launch will verify the maximum kinetic energy is less than 75 ft-lbf.	in Progress	\ref{sec:recovery_system}
2.4. The recovery system electrical circuits shall be completely independent of any payload electrical circuits.	Inspection	An inspection of the design plan verifies the avionics to be completely independent of the payload electronics. The avionics are separated from the payload electronics by bulkheads and surrounding coupler tube.	Complete	\ref{sec:recovery_system}
2.5. The recovery system shall contain redundant, commercially available altimeters. The term “altimeters” includes both simple altimeters and more sophisticated flight computers.	Inspection and Demonstration	An inspection of the design plan verifies the presence of two PerfectFlite StratoLoggerCF altimeters, each altimeter will control the firing of independent ejection charges for both the drogue and main parachute. The altimeters will be demonstrated in the subscale and fullscale launches.	Complete	\ref{sec:recovery_system}
2.6. Motor ejection is not a permissible form of primary or secondary deployment.		Our launch vehicle will not use motor ejection.		

2.7. Each altimeter shall be armed by a dedicated arming switch that is accessible from the exterior of the rocket airframe when the rocket is in the launch configuration on the launch pad.	Inspection and Test	An inspection of the fullscale rocket verifies the presence of a dedicated arming switch accessible on the launch pad. Two independent screw-based switches, accessible from the exterior of the vehicle, are used to engage the pair of redundant altimeters. This will be tested in the laboratory and on the launch pad.	In Progress	\ref{sec:recovery_system}
2.8. Each altimeter shall have a dedicated power supply.	Inspection and Test	An inspection of the design plan verifies the presence of a redundant altimeter in addition to the scored altimeter. Laboratory and on-pad testing will verify the functionality of the independent, tested 9V batteries that will be wired to the arming switches.	In Progress	\ref{sec:recovery_system}
2.9. Each arming switch shall be capable of being locked in the ON position for launch.	Inspection and Test	An inspection of the screw-based switches show they are capable of being locked in the ON position. Laboratory and on-pad testing will verify this functionality.	In Progress	\ref{sec:recovery_system}
2.10. Removable shear pins shall be used for both the main parachute compartment and the drogue parachute compartment.	Analysis and Demonstration	The number and size of shear pins will be verified through mathematical analysis and demonstrated in subscale and fullscale flights.	In Progress	\ref{sec:recovery_system}

2.11. An electronic tracking device shall be installed in the launch vehicle and shall transmit the position of the tethered vehicle or any independent section to a ground receiver.	Test	Small radio transmitters that communicate with a base-station receiver track the location of the launch vehicle. The system's functionality will be tested on the ground and in subscale and fullscale flights. In the case that independent sections are added to the design plans, each section will have its own tracking device.	In Progress	\ref{sec:recovery_system}
2.11.1. Any rocket section, or payload component, which lands untethered to the launch vehicle, shall also carry an active electronic tracking device.			Complete	\ref{sec:recovery_system}
2.11.2. The electronic tracking device shall be fully functional during the official flight on launch day.			In Progress	\ref{sec:recovery_system}
2.12. The recovery system electronics shall not be adversely affected by any other on-board electronic devices during flight (from launch until	Inspection and Demonstration	An inspection of the recovery system electronics plans show they will be housed in an electrically shielded bay to prevent interference from transmitting devices. The recovery system will be demonstrated in subscale and fullscale	In Progress	*\ref{sec:recovery_system}* *\ref{sec:Payload_Electronics}*
2.12.1. The recovery system altimeters shall be physically located in a separate compartment within the vehicle from any other radio frequency transmitting device and/or magnetic wave producing device.			In Progress	\ref{sec:recovery_system}
2.12.2. The recovery system electronics shall be shielded from all onboard transmitting devices, to avoid inadvertent excitation of the recovery system electronics.			In Progress	\ref{sec:recovery_system}

2.12.3. The recovery system electronics shall be shielded from all onboard devices which may generate magnetic waves (such as generators, solenoid valves, and Tesla coils) to avoid inadvertent excitation of the recovery system.		flights in the presence of transmitting tracking devices to ensure unaffected functionality.	In Progress	\ref{sec:recovery_system}
2.12.4. The recovery system electronics shall be shielded from any other onboard devices which may adversely affect the proper operation of the recovery system electronics.			In Progress	\ref{sec:recovery_system}
Requirement	**Method of Verification**	**Description of Verification Plan**	**Status**	**Document Section**
3. Experiment Requirements				
3.1.1. Each team shall choose one design experiment option from the following list.				
3.1.2. Additional experiments (limit of 1) are encouraged, and may be flown, but they will not contribute to scoring.				
3.1.3. If the team chooses to fly additional experiments, they shall provide the appropriate documentation in all design reports so experiments may be reviewed for flight safety.		The design plan does not include an additional payload experiment.		
3.3. Roll induction and counter roll				

Requirement	Method of Verification	Description of Verification Plan	Status	Document Section
4. Safety Requirements				
3.3.1. Teams shall design a system capable of controlling launch vehicle roll post motor burnout.	Analysis and Test	A computational analysis of the thrusters and ground-based testing will verify their ability to control vehicle roll post motor burnout. The payload's control ability will also be verified through fullscale flight.	In Progress	\ref{sec:payload_criteria}
3.3.1.1. The systems shall first induce at least two rotations around the roll axis of the launch vehicle.	Analysis and Test	Cold-gas thrusters, tangential to the rocket body, will be actively controlled to induce rolling. A simulation analysis, ground-based testing, and fullscale flight will verify the ability of the payload to induce at least two rotations and halt all rolling motion.	In Progress	\ref{sec:payload_criteria}
3.3.1.2. After the system has induced two rotations, it must induce a counter rolling moment to halt all rolling motion for the remainder of launch vehicle ascent.			In Progress	\ref{sec:payload_criteria}
3.3.1.3. Teams shall provide proof of controlled roll and successful counter roll.			Complete	\ref{sec:payload_criteria}
3.3.2. Teams shall not intentionally design a launch vehicle with a fixed geometry that can create a passive roll effect.			Complete	\ref{sec:payload_criteria}
3.3.3. Teams shall only use mechanical devices for rolling procedures.			Complete	\ref{sec:payload_criteria}

4.1. Each team shall use a launch and safety checklist. The final checklists shall be included in the FRR report and used during the Launch Readiness Review (LRR) and any launch day operations.	Inspection	The PDR includes a preliminary checklist. An inspection of the FRR will verify the presence of the final checklist to be used during LRR and launch day operations.	In Progress	\ref{sec:launch_operations}
4.2. Each team must identify a student safety officer who shall be responsible for all items in section 4.3.	Inspection	An inspection of the proposal verifies the designation of a student safety officer.	Complete	*\ref{sec:team_members}*
4.3. The role and responsibilities of each safety officer shall include, but not limited to:	Inspection	An inspection of the design reports verifies the presence of current safety documentation. The Student Safety Officer will oversee the overall safety and launch procedures of the team and will work to fulfill the safety requirements.		
4.3.1. Monitor team activities with an emphasis on Safety during:				
4.3.1.1. Design of vehicle and launcher			In Progress	*\ref{sec:safety}*
4.3.1.2. Construction of vehicle and launcher			In Progress	*\ref{sec:safety}*
4.3.1.3. Assembly of vehicle and launcher			In Progress	*\ref{sec:safety}*
4.3.1.4. Ground testing of vehicle and launcher			In Progress	*\ref{sec:safety}*
4.3.1.5. Sub-scale launch test(s)			Complete	*\ref{sec:launch_operations}*
4.3.1.6. fullscale launch test(s)			Incomplete	*\ref{sec:launch_operations}*
4.3.1.7. Launch day			Incomplete	*\ref{sec:launch_operations}*
4.3.1.8. Recovery activities			Incomplete	*\ref{sec:launch_operations}*
4.3.1.9. Educational Engagement Activities			In Progress	*\ref{sec:safety}*

4.3.2. Implement procedures developed by the team for construction, assembly, launch, and recovery activities			In Progress	*\ref{sec:launch_operations}*
4.3.3. Manage and maintain current revisions of the team's hazard analyses, failure modes analyses, procedures, and MSDS/chemical inventory data			In Progress	*\ref{subsec:hazard_analysis}*
4.3.4. Assist in the writing and development of the team's hazard analyses, failure modes analyses, and procedures.			In Progress	*\ref{subsec:hazard_analysis}*

4.4. Each team shall identify a "mentor." A mentor is defined as an adult who is included as a team member, who will be supporting the team (or multiple teams) throughout the project year, and may or may not be affiliated with the school, institution, or organization. The mentor shall maintain a current certification, and be in good standing, through the National Association of Rocketry (NAR) or Tripoli Rocketry Association (TRA) for the motor impulse of the launch vehicle, and the rocketeer shall have flown and successfully recovered (using electronic, staged recovery) a minimum of 2 flights in this or a higher impulse class, prior to PDR. The mentor is designated as the individual owner of the rocket for liability purposes and must travel with the team to launch week. One travel stipend will be provided per mentor regardless of the number of teams he or she supports. The stipend will only	Inspection	A self-imposed inspection shows that the necessary requirements are met by our designated mentor.	Complete	*\ref{sec:team_members}*

4.5. During test flights, teams shall abide by the rules and guidance of the local rocketry club's RSO. The allowance of certain vehicle configurations and/or payloads at the NASA Student Launch Initiative does not give explicit or implicit authority for teams to fly those certain vehicle configurations and/or payloads at other club launches. Teams should communicate their intentions to the local club's President or Prefect and RSO before attending any NAR or TRA	Inspection	A self-imposed inspection will verify that the rules and guidance provided by our RSO, including the NAR high power rocket safety code, and our ability to launch our particular payload, will be followed.	In Progress	*Safety - launch operations and operational procedures*
4.6. Teams shall abide by all rules set forth by the FAA.	Inspection	A self-imposed inspection will verify that the FAA regulations, included in the safety binder of the VADL and our design reports, will be abided by.	In Progress	*Safety - launch operations and operational procedures*
Requirement	**Method of Verification**	**Description of Verification Plan**	**Status**	**Document Section**
5. General Requirements				
5.1. Students on the team shall do 100% of the project, including design, construction, written reports, presentations, and flight preparation with the exception of assembling the motors and handling black powder or any variant of ejection charges, or preparing and installing electric matches (to be done by the team's	Inspection	A self-conducted inspection will verify that only students on the team work on the project, with the exception of operations handled by the team's mentor.	In Progress	NA

5.2. The team shall provide and maintain a project plan to include, but not limited to the following items: project milestones, budget and community support, checklists, personnel assigned, educational engagement events, and risks and mitigations.	Inspection	An inspection of our operations shows the Vanderbilt Student Launch meets weekly to discuss these aspects of the competition. Our design reports include budgeting, project milestones, checklists, personnel specialties, and risks and mitigations in our design reports, while educational engagement events are submitted using the proper form.	Complete	NA
5.3. Foreign National (FN) team members shall be identified by the Preliminary Design Review (PDR) and may or may not have access to certain activities during launch week due to security restrictions. In addition, FN's may be separated from their team during these activities.		Our team does not involve any FN participants.	NA	NA
5.4. The team shall identify all team members attending launch week activities by the Critical Design Review (CDR). Team members shall include:	Inspection	A self-conducted inspection of team members, mentors, and educators will identify all team members attending launch week.	Complete	\ref{sec:team_members}
5.4.1. Students actively engaged in the project throughout the entire year.			Complete	\ref{sec:team_members}
5.4.2. One mentor (see requirement 4.4).			Complete	\ref{sec:team_members}
5.4.3. No more than two adult educators.			Complete	\ref{sec:team_members}

5.5. The team shall engage a minimum of 200 participants in educational, hands-on science, technology, engineering, and mathematics (STEM) activities, as defined in the Educational Engagement Activity Report, by FRR. An educational engagement activity report shall be completed and submitted within two weeks after completion of an event. A sample of the educational engagement activity report can be found on page 28 of the	Inspection	An inspection of our Educational Engagement Activity Reports and final summary will show our engagement meets the required specifications.	In Progress	\ref{sec:Timeline of Operations}
5.6. The team shall develop and host a Web site for project documentation.	Inspection	An inspection of the team's website, https://www.vanderbilt.edu/usli/ will verify our development and presence of documentation throughout the competition cycle.	Complete	*\ref{sec:Team_Summary}*
5.7. Teams shall post, and make available for download, the required deliverables to the team Web site by the due dates specified in the project timeline.	Inspection	An inspection of our website after each due date will show that deliverables are posted before the required due dates.	In Progress	*\ref{sec:Team_Summary}*
5.8. All deliverables must be in PDF format.	Inspection	An inspection of our deliverables shows they are all in .pdf format.	In Progress	*\ref{sec:Team_Summary}*
5.9. In every report, teams shall provide a table of contents including major sections and their respective sub-sections.	Inspection	An inspection of our design reports show they all include a table of contents with sections and subsections.	In Progress	*\ref{sec:Team_Summary}*
5.10. In every report, the team shall include the page number at the bottom of the page.	Inspection	An inspection of our design reports will verify that page numbers are included.	In Progress	*\ref{sec:Team_Summary}*

5.11. The team shall provide any computer equipment necessary to perform a video teleconference with the review board. This includes, but not limited to, a computer system, video camera, speaker telephone, and a broadband Internet connection. If possible, the team shall refrain from use of cellular phones as a means of speakerphone capability.	Inspection	An inspection shows that VADL provides the necessary equipment perform a video teleconference.	In Progress	*\ref{sec:Team_Summary}*
5.12. All teams will be required to use the launch pads provided by Student Launch's launch service provider. No custom pads will be permitted on the launch field. Launch services will have 8 ft. 1010 rails, and 8 and 12 ft. 1515 rails available for use.	Demonstration	The launch vehicle will be designed to use the launch pads provided by the service provider at the competition demonstration flight.	In Progress	*\ref{sec:launch_pad}*
5.13. Teams must implement the Architectural and Transportation Barriers Compliance Board Electronic and Information Technology (EIT) Accessibility Standards (36 CFR Part 1194) Subpart B-Technical Standards (http://www.section508.gov): §1194.21 Software applications and operating systems.§1194.22 Web-based intranet and Internet information and applications.	Inspection	An self-conducted inspection of our operations will prove that we will follow the proper standards outlined in 5.13.	In Progress	*\ref{sec:Team_Summary}*

Team Derived Requirements Deriving team-specific requirements outside the boundaries of the competition is an essential step to ensure program success. The VADL has derived requirements for our launch vehicle and operations in five categories:

1. Thruster System Requirements
2. Control System Requirements
3. Ground Based Test Facility Requirements
4. Vehicle Requirements
5. Safety Requirements

Assigned to each requirement is a method of verification (the same four methods defined in 7.2) and thorough verification plan. The team derived requirements can be found in the tables below:

The requirements, respective verification methods, and a description of the verification plan can be seen in the tables below.

Requirement	Method of Verification	Description of Verification Plan	Status	Document Section
1. Thruster System Requirements				
1.1 System shall deliver a minimum of 2.12 N per thruster.	Analysis and Test	Our isentropic gas dynamic analysis will verify the ideal thrust from our nozzle geometry. The thruster stand shall be used to test the real thrust received given both continuous and pulsed conditions of the solenoid actuation.	Complete	\ref{sec:Payload_Requirements_and_Risk_Mitigation}
1.2 Solenoid should actuate in under 30 ms.	Inspection	Manufacturers should be contacted to verify all specifications before purchase. An inspection of the accompanying spec sheets will verify the actuation time.	Complete - solenoid tested to actuate within 30ms.	\ref{sec:Payload_Requirements_and_Risk_Mitigation}
1.3 Orifice of all pressurized components upstream of the nozzle shall have 2X the area of the nozzle .	Inspection	An inspection of all component dimensions prior to purchase will verify their flow area.	Complete	\ref{sec:Payload_Requirements_and_Risk_Mitigation}
1.4 Nozzles should be mounted on an inner bulkhead in such a manner as to maximize moment arm.	Analysis	A CAD-based analysis of our mounts and fittings will verify that the moment arm approaches the bulkhead diameter of 5.35".	Complete	\ref{sec:Payload_Requirements_and_Risk_Mitigation}
1.5 Nozzle will have machinable geometry: standard diameter throat and exit, no smaller than 1.5 mm based on machining tool availability.	Analysis	The isentropic gas dynamic analysis shall be run recursively to verify standard nozzle dimensions.	Complete	\ref{sec:Payload_Requirements_and_Risk_Mitigation}

1.6 System should provide an upstream pressure of 450 psi to the nozzle during solenoid actuation.	Test	The analog and digital pressure sensors present on the thruster test stand will be used to verify the upstream pressure during solenoid actuation.	Complete	\ref{sec:Payload_Requirements_and_Risk_Mitigation}
1.7 Thrust produced should be within 15% of the calculated ideal thrust.	Test	The thruster test stand will verify the accuracy of our custom-machined thrusters.	In progress	\ref{sec:Payload_Requirements_and_Risk_Mitigation
1.8 Payload will be rigidly supported as to not shift within rocket body during flight.	Inspection	Inspection will ensure team uses three threaded rods and fixed bulkheads to constrain the movement of the payload skeleton within the rocket body before the top body tube is assembled.	In progress	\ref{sec:Payload_Requirements_and_Risk_Mitigation}
1.9 The system shall be modular to enable troubleshooting and interchangeability.	Inspection	The skeleton payload system will be designed with sliding bulkheads and Yor-Lok compression fittings to allow ease of assembly and modification of thruster system for simple troubleshooting.	Complete	\ref{sec:Payload_Requirements_and_Risk_Mitigation}
Requirement	**Method of Verification**	**Description of Verification Plan**	**Status**	**Document Section**
2. Control System Requirements				
2.1 The roll simulated in KSP should be consistent within 10% of the data obtained from the IMU.	Analysis and Test	The KSP analysis and the ground-based test facility shall be used to verify the synching of KSP and physical IMU output.	Complete	\ref{sec:Control}
2.2 The control system shall activate the first thruster pair within 2 seconds of MECO.	Demonstration	Data from the subscale and fullscale demonstration will verify the actuation time delay.	In Progress	\ref{sec:Control}

2.3 The IMU shall define a zero-point initial rotational orientation after MECO and the control system shall return the rocket to this position after the roll period.	Test	The ground-based test facility shall be used to verify that the rocket will return to original orientation.	In Progress	\ref{sec:Control}
2.4 The control system shall determine the response necessary to complete the roll.	Test	The ground-based test facility will verify the ability of the control system to predict an underdamped or overdamped response in accordance with the input.	In Progress	\ref{sec:Control}
2.5 The control system should keep rocket at fixed rotational orientation from time roll stops until apogee.	Test	The ground-based test facility shall be used along with pre-competition launch data to verify the post-roll angular position control capabilities.	In Progress	\ref{sec:Control}
2.6 The control system shall be robust enough to respond to atmospheric disturbances	Test and Demonstration	The motor input on the ground based test facility will simulate atmospheric disturbances and be correlated to data collected from subscale and fullscale demonstrations.	In Progress	\ref{sec:Control}
2.7 The Hotbox shall use ROSMOD and BeagleBone Black to help the team build familiarity with the payload electronic hardware and software	Inspection	An inspection of our hotbox assembly will show the use of ROSMOD and BBB and their relation to our launch vehicle.	Complete	\ref{sec:Control}
Requirement	**Method of Verification**	**Description of Verification Plan**	**Status**	**Document Section**
3. Payload Electonics Requirements				
3.1 All electronics, except for solenoids, must fit within the upper coupler tube section, and allow for safe assembly with no damage to any team member or the rocket itself.	Analysis and Demonstration	Use of CAD software will ensure all components integrate in the space provided.	Complete	\ref{sec:Payload_ Electronics}

3.2 The payload must be powered by rechargeable batteries, chargeable from outstide the coupler tube section.	Demonstration	Integrate charging port, and extend leads outside top bulkheads for each battery	In Progress	\ref{sec:Payload_Electronics}
3.3 The payload must be able to remain armed on the launchpad for at least 3 hours.	Analysis	Calculate normal use-case battery life for both testing and launch environments, then compare to battery capacity	Complete	\ref{sec:Payload_Electronics}
3.4 The payload must be armable from the exterior of the airframe while on the launch rail.	Test and Demonstration	Install and integrated screw switch, assemble airframe and drill access holes	In Progress	\ref{sec:Payload_Electronics}
3.5 No electrical components will experience levels of voltage or current for which they are not rated.	Analysis	Check ratings on components before finalizing design, simulate circuit	Complete	\ref{sec:Payload_Electronics}
3.6 Solenoid valve leads will be connected to a flyback diode to prevent current spikes.	Test	Operate solenoids using a flyback diode, verifying continuity of power to BeagleBone	Complete	\ref{sec:Payload_Electronics}
3.10 The payload computer will have wirless communication capabilities.	Test and Demonstration	Connect to BeagleBone Wireless while payload is both inside and outside of the airframe.	In Progress	\ref{sec:Payload_Electronics}
Requirement	**Method of Verification**	**Description of Verification Plan**	**Status**	**Document Section**
4. Ground Based Test Facility Requirments				
4.1 Test stand should simulate torque on the rocket to simulate in-flight wind disturbances.	Test	The ground-based test facility shall be equipped with a motor with enough torque to simulate the resistive response of wind effects.	In Progress	\ref{sec:the_frame}
4.2 Yaw, pitch, and roll data will be collected by the IMU and plotted in real-time via ROSMOD.	Test	Ground-based test facility shall be used to verify the data delivery and graphic representation.	In Progress	\ref{sec:the_frame}

4.3 Test facility will be able to transmit the peak torque output of the motor via the fin gripper system.	Test	This load-bearing capability of the fin gripper system will be verified by the first test.	In Progress	\ref{sec:the_frame}
4.4 Test facility shall have a motor capable of inducing torques equal to or greater than that of the thrusters system.	Test	The motor capability will be analyzed by comparing experimental data of the rocket rotation in the test facility with the thruster actuation to data with motor actuation but without thruster actuation.	In Progress	\ref{sec:the_frame}
4.5 Test facility should be able to operate at angular velocities up to 240 RPM.	Analysis and Test	An analysis of the motor specs and mass properties of the rocket will be verified by fullscale rocket experiments on the test facility.	In Progress	\ref{sec:the_frame}
4.6 Test facility axial constraint system shall be able to support rocket during dynamic loading from thruster fire at maximum thrust.	Analysis and Test	Analysis using free body diagram of stand while thrusters are being fired will be verified by preliminary tests.	In Progress	\ref{sec:the_frame}
4.7 KSP visualization shall use hardware-in-the-loop simulation to visualize the rocket's current angular position during flight.	Test	This visualization will be refined and verified during experimentation after fullscale rocket integration onto the test facility.	In Progress	\ref{sec:the_frame}
Requirement	**Method of Verification**	**Description of Verification Plan**	**Status**	**Document Section**
5. Vehicle Requirements				
5.1 Carbon fiber wrapped blue tube will offer twice the strength of standalone blue tube.	Test	Compression testing will be conducted for both materials to compare yield strength values.	Complete	\ref{sec:fullscale_launch_vehicle_overview}
5.2 The launch vehicle should weigh less than 40 lb	Inspection	The weights of all components will be summed to verify total vehicle weight is less than 40 lbs.	In Progress	\ref{sec:fullscale_launch_vehicle_overview}

5.3 The launch vehicle should be capable of being prepared at launch site within 2 hours.	Demonstration	This will be verified and demonstrated at launch site.	In Progress	\ref{sec:vehicle_mission_statement}
5.4 The tail section shall be capable of withstanding temperatures of over 200°F due to recirculation of hot air during initial launch phase.	Analysis and Test	An analysis of material properties and testing Hotbox will ensure capability of withstanding hot temperatures.	In Progress	\ref{sec:fullscale_launch_vehicle_overview}
5.5 Average drag coefficient of entire rocket in upwards orientation should be known to the nearest 0.01 before launch.	Analysis	Computational fluid dynamic (CFD) analysis will be performed on a CAD version of the rocket to compute drag.	Complete	\ref{sec:Flight Modeling and Recorded Data}
5.6 Center of pressure of launch shall be known to nearest 1" before launch.	Analysis	Mathematical pressure analysis and CFD will be performed to calculate and verify the placement of the COP.	Complete	\ref{sec:launch_operations}
5.7 The descent speed of the rocket after the drogue parachute is released should be greater than 60 ft./s to minimize drift.	Analysis and Demonstration	A simulation analysis and the onboard sensors will monitor speed during flight demonstration and verify the descent speed after release of the drogue parachute.	Complete	\ref{sec:Flight Modeling and Recorded Data}
5.8 The lengths of parachute cord will be sized such that no two independent sections will be able to hit each other during deployment.	Analysis and Demonstration	Inspection and mathematical analysis considering lengths of rocket airframe sections will be performed.	In Progress	\ref{sec:launch_operations}
Requirement	**Method of Verification**	**Description of Verification Plan**	**Status**	**Document Section**
6. Safety Requirements				
6.1 All VADL members involved in fabrication shall wear latex or vinyl gloves when handling chemicals, allergens, or carbon fiber layup.			In Progress	*\ref{sec:safety}*
6.2 All personnel present at machining operations will wear eye protection.		A self-imposed inspection by our	In Progress	*\ref{sec:safety}*

6.3 All personnel will wear close-toed shoes in the lab.	Inspection	student safety officer will verify our use of proper equipment during operations.	In Progress	\ref{sec:safety}
6.4 At least two team members will be present for hazardous operations such as machining and carbon fiber layup.			In Progress	\ref{sec:safety}
6.5 All team members operating or present around heavy machinery will wear hearing protection.			In Progress	\ref{sec:safety}
6.6 Internal cavities in the launch vehicle shall be kept at atmospheric pressure.	Inspection	Inspection of the launch vehicle design will show proper venting throughout the payload bay to the atmosphere.	In Progress	\ref{subsubsec:payload_control_failure_modes}
6.7 Black powder charges will be isolated from all components excluding parachutes.	Inspection	Launch vehicle will be inspected to ensure black powder charges are not in contact with any other components.	In Progress	\ref{subsubsec:recovery_system_failure_modes}
6.8 All parachutes will be covered with a fire retardant blanket so as to mitigate fire exposure during deployment events.	Inspection	Inspection will ensure fire retardant blankets will be placed to cover all parachutes when assembling rocket.	In Progress	\ref{subsubsec:recovery_system_failure_modes}
6.9 When particulates are released during cutting operations, an air filter shall be used.	Inspection	A self-imposed inspection will verify our use of the air filter during cutting operations.	In Progress	\ref{sec:safety}
6.10 The hotbox shall have a control algorithm to prevent reaching excess temperatures.	Analysis and Test	An analysis and test of the control algorithm used on the hotbox will verify its ability to prevent excess temperatures.	Complete	\ref{sec:Electronics Testing}
6.11 The hotbox shall be wired according to electric code to reduce the risk of fire.	Inspection	An inspection of the wiring plan for the hotbox will show its compliance with electric codes.	Complete	\ref{sec:Electronics Testing}
6.12 The hotbox will have a protective box over the control panel that prevents exposure to high voltage.	Inspection	An inspection of the design plan for the hotbox will show the use of a protective box.	Complete	\ref{sec:Electronics Testing}

6.13 The solenoids selected will be normally closed to prevent venting in the case of power loss.	Inspection	An inspection of the solenoid spec sheet will verify it is normally closed in the case of power loss to the system.	In Progress	*\ref{subsubsec:payload_control_failure_modes}*
6.14 Heating elements in the hotbox will be deactivated if the BeagleBone is deactivated	Inspection	An inspection of the schematic for the hotbox will show its ability to turn off heating elements if the BeagleBone is deactivated.	In Progress	*\ref{subsubsec:personnel_hazard_analysis}*
6.15 All components exposed to heat in the Hotbox shall be rated to above 200F.	Inspection	An inspection of the manufacturer spec sheet for hotbox components will show their rating to be above the required amount.	Complete	*\ref{subsubsec:personnel_hazard_analysis}*
6.16 An anti-zippering device shall be used to prevent damage to the rocket body during deployment.	Inspection	An inspection of the deployment plans will shows the use of an antizippering device.	In Progress	\ref{sec:launch_operations}
6.17 The chosen air tank shall contain burst discs to prevent excess pressure from flooding the thruster system.	Inspection	An inspection of the regulator used on the air tank will show the presence of properly rated burst disks.	In Progress	*\ref{subsubsec:payload_control_failure_modes}*
6.18 Li-ion batteries will be safely recharged using the manufacturer's charging circuit.	Inspection	Batteries will be monitored during charging periods and will only be charged with the manufacturer's charger.	In Progress	\ref{sec:Payload_Electronics}
6.19 Payload electronics will not present an electrical hazard by way of fire, heat, or ground fault.	Inspection and Test	Wires will be routed to prevent shorts, and components will be cooled appropriately.	In Progress	\ref{sec:Payload_Electronics}

7.3 Budgeting and Timeline

7.3.1 Budget

VADL receives funding from multiple sources, including NASA, Boeing, and Vanderbilt University. These funding sources and amount are listed in the Table 24.

Table 24: Funding Source

Funding Source	**Amount**
Boeing	2750
NASA	5000
Vanderbilt	12250
Total	20000

Figures 138, 139, 140, 141, 142, 143, 144, 145 and 146 show the categorized purchases to this point in the project.

Company	Item	Part cost	Quantity	Total Cost	Order cost	Category
Sparkfun	Resistor Kit - 1/4 W	$7.95	1	$7.95		Electronics
Sparkfun	LED- Assorted 20 pack	$2.95	1	$2.95		Electronics
Sparkfun	Discrete Semiconductor Kit	$8.95	1	$8.95		Electronics
Sparkfun	Solid State Relay- 40A	$9.95	1	$9.95		Electronics
Sparkfun	Screw Terminals 3.5mm Pitch	$0.95	10	$9.50		Electronics
Sparkfun	Molex Jumper 2 Wire Assembly	$0.95	20	$19.00		Electronics
Sparkfun	DC Barrel Jack Adapter- Breadboard Compatible	$0.95	5	$4.75		Electronics
SparkFun	Triple Axis Accelerometer and Gyro Breakout - MPU-6050	$39.95	1	$39.95		Electronics
SparkFun	SparkFun OpenLog	$14.95	1	$14.95		Electronics
SparkFun	P-Channel MOSFET 60V 27A	$0.95	1	$0.95		Electronics
SparkFun	Arduino ProtoShield - Bare PCB	$4.95	1	$4.95		Electronics
SparkFun	Arduino Stackable Header Kit	$1.50	1	$1.50		Electronics
Sparkfun	Shipping	$21.96	1	$37.30	$162.65	Electronics
Sparkfun	Sparkfun Electronics	$15.15	1	$15.15	$15.15	Electronics
Amazon	Wick	$5.95	1	$5.95		Electronics
Amazon	Soldering Paste	$17.95	1	$17.95		Electronics
Amazon	Soldering Station	$250.52	1	$250.52		Electronics
Amazon	16 GB MicroSD cards	$7.11	5	$35.55		Electronics
Amazon	AC Fan (Heavy Duty Aluminum)	$18.99	2	$37.98		Electronics
Amazon	Shipping	$7.23	1	$7.23	$355.18	Electronics
Amazon	Digital Multimeter	$17.99	1	$17.99	$17.99	Electronics
Amazon	Drone Connectors	$2.99	4	$11.96	$11.96	Electronics
Adafruit	Element 12 BeagleBone Black	$55.00	5	$275.00		Electronics
Adafruit	Stacking Header Set for Beagle Bone Capes	$4.95	5	$24.75		Electronics
Adafruit	Half-size Breadboard	$5.00	5	$25.00		Electronics
Adafruit	Thermistors	$4.00	4	$16.00		Electronics
Adafruit	Miniature Wifi (802.1b/g/n) Module	$11.95	3	$35.85		Electronics
Adafruit	SMT/SMD 0805 Resistor and Capacitor Book	$39.96	1	$39.96		Electronics
Adafruit	Shipping	$16.68	1	$16.68	$433.24	Electronics
Adafruit	5V 2.4A Switching Power Supply	$7.95	2	$15.90		Electronics
Adafruit	Adafruit Proto Cape Kit for Beagle Bone Black	$9.95	5	$49.75		Electronics
Adafruit	5V 2A Switching Power Supply	$7.95	2	$15.90		Electronics
Adafruit	Shipping	$9.97	1	$9.97	$91.52	Electronics

Figure 138: Categorized Purchases

Company	Item	Part cost	Quantity	Total Cost	Order cost	Category
Southern Fluid Power	Solenoid Coil	$75.07	2	$150.14		Rocket Fab
Southern Fluid Power	Valve Body	$114.20	2	$228.40	$378.54	Rocket Fab
Loftis Steel & Aluminum	1/4" Alum Plate 6061-T6	$68.36	2	$136.72		FRAME
Loftis Steel & Aluminum	1/4" Alum Plate 6061-T6 Saw Cut	$46.00	1	$46.00	$182.72	FRAME
Loftis Steel & Aluminum	Water jet cutting of carbon fiber material for sub-scale fins	$100.00	1	$100.00	$100.00	FRAME
Loftis Steel & Aluminum	Custom Cutting	$250.00	1	$250.00	$250.00	FRAME
McMaster Carr	1" Aluminum T-Slotted Framing Extrusion - 2 ft	$8.35	8	$66.80		FRAME
McMaster Carr	1" Aluminum T-Slotted Framing Extrusion - 3 ft	$11.53	4	$46.12		FRAME
McMaster Carr	1" Aluminum T-Slotted Framing Extrusion - 8 ft	$26.38	4	$105.52		FRAME
McMaster Carr	90° Plate for Aluminum T-Slotted Framing Extrusion	$8.47	24	$203.28		FRAME
McMaster Carr	Pack of 4 Steel End-Feed Fastener for 1" Aluminum T-Slotted Framing Extrusion	$2.30	35	$80.50		FRAME
McMaster Carr	Brace for 1" Aluminum T-Slotted Framing Extrusion	$5.51	6	$33.06		FRAME
McMaster Carr	Thrust Bearing	$5.11	2	$10.22		FRAME
McMaster Carr	Radial Bearings	$5.59	4	$22.36		FRAME
McMaster Carr	3 ft Carbon Steel 3/8" Diameter Rod	$8.25	1	$8.25		FRAME
McMaster Carr	1/8" Diameter 1/2" long alloy steel dowel (pack of 100)	$10.01	1	$10.01		FRAME
McMaster Carr	1/4" 20, 1" Long Socket Head Cap Screws pack of 50	$7.84	1	$7.84		FRAME
McMaster Carr	Large Diameter Radial Bearing	$11.89	2	$23.78	$617.74	FRAME
McMaster Carr	Multipurpose 6061 Aluminum with Certification Rod, 1' Long	$12.92	2	$25.84		Rocket Fab
McMaster Carr	High-Speed Steel Metric Size Chucking Reamer 1.5mm Dia	$16.27	2	$32.54		Rocket Fab

Figure 139: Categorized Purchases

Company	Item	Part cost	Quantity	Total Cost	Order cost	Category
McMaster Carr	Carbide Chamfer End Mill Four Flute	$29.56	2	$59.12		Rocket Fab
McMaster Carr	1/4" 316 Stainless Steel Yor-Lok Tube Fitting Through-Wall	$23.32	2	$46.64		Rocket Fab
McMaster Carr	1/4" 316 Stainless Steel Yor-Lok Tube Fitting Tee	$34.98	2	$69.96		Rocket Fab
McMaster Carr	1/4" 316 Stainless Steel Yor-Lok Tube Fitting Elbow	$19.55	4	$78.20		Rocket Fab
McMaster Carr	Smooth-Bore Seamless Stainless Steel Tubing 1 ft	$7.83	3	$23.49		Rocket Fab
McMaster Carr	1/4", 12L14 Carbon Steel Tight-Tol. Rod 1 ft	$2.17	3	$6.51		Rocket Fab
McMaster Carr	Power Strip (15' cord, 4 outlets)	$31.17	1	$31.17		Rocket Fab
McMaster Carr	GFIC Outlet (Duplex)	$20.00	3	$60.00		Rocket Fab
McMaster Carr	Power Cord Whips (NEMA)	$11.82	2	$23.64		Rocket Fab
McMaster Carr	Ceramic Lightbulb Sockets (4.5" dia)	$3.68	6	$22.08		Rocket Fab
McMaster Carr	Flex Connectors	$1.11	20	$22.20		Rocket Fab
McMaster Carr	Electrical Boxes (4")	$1.96	6	$11.76	$513.15	Rocket Fab
McMaster Carr	1/4"-20, 1" Long stainless bolt	$5.24	1	$5.24		Misc
McMaster Carr	1/4"-20, 3" Long stainless bolt	$8.99	1	$8.99		Misc
McMaster Carr	1/2"-13, 3.5" Long stainless partial threaded bolt	$1.97	9	$17.73		Misc
McMaster Carr	1/4" Stainless washer	$8.25	1	$8.25		Misc
McMaster Carr	1/4" Lock washers	$5.12	1	$5.12		Misc
McMaster Carr	1/2" Stainless washers	$9.71	1	$9.71		Misc
McMaster Carr	1/4"-20 Stainless nuts	$4.21	1	$4.21		Misc
McMaster Carr	1/2"-13 Stainless nuts	$5.10	1	$5.10		Misc
McMaster Carr	1/2"-13 Stainless lock nuts	$5.82	1	$5.82	$70.17	Misc
McMaster Carr	Yor Lok to 1/4" NPT Female Adapter	$14.11	1	$14.11		Rocket Fab
McMaster Carr	Reducing 1/8" to 1/4" NPT Elbow	$8.38	1	$8.38		Rocket Fab
McMaster Carr	Stainless Steel Cable Tie	$11.44	1	$11.44		Rocket Fab
McMaster Carr	Brass Snap-Tite H-Shape Hose Coupling	$12.37	1	$12.37		Rocket Fab
McMaster Carr	Grade 8 Steel Fully Threaded Rod	$3.60	3	$10.80		Rocket Fab
McMaster Carr	Extreme-Strength Steel Hex Nut (50)	$11.46	1	$11.46		Rocket Fab
McMaster Carr	Aligning Weld Nut (20 pk)	$15.81	1	$15.81		Rocket Fab
McMaster Carr	Snap-in Nut	$9.09	1	$9.09		Rocket Fab

Figure 140: Categorized Purchases

Company	Item	Part cost	Quantity	Total Cost	Order cost	Category
McMaster Carr	Galvanized Steel U-Bolt 1/4"20 Thread	$0.97	3	$2.91		Rocket Fab
McMaster Carr	Sleeves for 1/4" Tube OD Stainless Steel Yor Lok	$3.53	5	$17.65		Rocket Fab
McMaster Carr	Nut for 1/4" Tube OD Steel Yor Lok	$0.87	5	$4.35		Rocket Fab
McMaster Carr	High Strength Stainless Steel Sheet (6" x 6")	$16.41	1	$16.41		Rocket Fab
McMaster Carr	Large Clamping U-Bolt	$6.42	1	$6.42		Rocket Fab
McMaster Carr	0.055" bit	$2.29	3	$6.87	$148.07	Rocket Fab
McMaster Carr	Compact Extreme-Pressure Steel Thrd Fitting 1/4 Pipe Size, Female X Male X Female Tee	$6.02	1	$6.02		Rocket Fab
McMaster Carr	Compact Extreme-Pressure Steel Thrd Fitting 1/4" Male X 1/8" Fem Pipe Size, Hex Head Bushing	$1.60	3	$4.80		Rocket Fab
McMaster Carr	Liquid-Filled Gauge Plastic Case, 2-1/2" Dial, 1/4 Bottom, 1000 PSI	$19.72	1	$19.72		Rocket Fab
McMaster Carr	Rubber Edge Trim, 10 ft. Length	$8.80	1	$8.80		Rocket Fab
McMaster Carr	Grade 8 Steel Fully Threaded Rod 1/4"-20 Thread, 2 ft Long	$6.93	5	$34.65	$73.99	Rocket Fab
McMaster Carr	Pan Head Drilling Screw for Metal 410 SS, 6-20 Thread, Packs of 100	$5.40	2	$10.80		Rocket Fab
McMaster Carr	Indoor Steel Enclosure with Knockouts Hinged Cover	$24.38	1	$24.38	$35.18	Rocket Fab
McMaster Carr	Smooth-Bore Seamless 304 SS Tubing 1/4" OD, 0.028" Wall Thickness, 3 ft. Long	$13.53	3	$40.59		Rocket Fab
McMaster Carr	Clamping U-Bolt Znc-Pltd STL, 5/16"-18 Thrd Sz, 2" ID	$1.84	3	$5.52		Rocket Fab
McMaster Carr	Steel Yor-Lok Tube Fitting Straight Adapter for 1/4" Tube OD X 1/4 NPT Male	$4.86	4	$19.44		Rocket Fab
McMaster Carr	Steel Yor-Lok Tube Fitting Straight Adapter for 1/4" Tube OD X 1/8 NPT Male	$4.61	2	$9.22		Rocket Fab

Figure 141: Categorized Purchases

Company	Item	Part cost	Quantity	Total Cost	Order cost	Category
McMaster Carr	Compact Extreme-Pressure Steel Pipe Fitting Tee Connector, 1/4 NPTF Female	$6.13	1	$6.13		Rocket Fab
McMaster Carr	Compact Extreme-Pressure Steel Pipe Fitting Right-Angle Tee Adapter, 1/4 NPTF Female X Male	$6.38	1	$6.38		Rocket Fab
McMaster Carr	Medium-Strength Steel Thin Hex Nut Grade 5, Zinc-Plated, 5/16"-18 Thread Size, Packs of 100	$5.53	1	$5.53		Rocket Fab
McMaster Carr	General Purpose 1074/1075 Spring Steel Sheet .050" Thick, 8" X 24"	$36.04	1	$36.04		Rocket Fab
McMaster Carr	Compact Extreme-Pressure Steel Pipe Fitting 90 Degree Elbow Adapter, 1/4 NPTF Female X Male	$4.14	2	$8.28		Rocket Fab
McMaster Carr	Compact Extreme-Pressure Steel Pipe Fitting Straight Connector, 1/4 NPTF Male	$1.29	4	$5.16	$142.29	Rocket Fab
McMaster Carr	Timing Belt Pulley XL Series, 4.564" OD	$49.87	1	$49.87		FRAME
McMaster Carr	XL Series Lightweight Timing Belt Pulley 1.75" OD	$8.20	1	$8.20		FRAME
McMaster Carr	XL Series Timing Belt, Trade NO. 290XL025	$5.55	1	$5.55		FRAME
McMaster Carr	XL Series Timing Belt, Trade NO. 250XL025	$5.01	1	$5.01		FRAME
McMaster Carr	Black-Oxide Steel U-Bolt W/Mounting Plate,	$1.73	1	$1.73		FRAME
McMaster Carr	18-8 Stainless Steel Hex Nut Black-Oxide, 5/16"-18 Thread Size	$5.89	1	$5.89	$76.25	FRAME
McMaster Carr	T0-220 Heat Sink	$0.25	10	$2.50		Electronics
McMaster Carr	4 pin Connector PCB (Female)	$1.13	15	$16.95		Electronics
McMaster Carr	4 pin Connector PCB (Male)	$1.05	5	$5.25	$24.70	Electronics
McMaster Carr	18-8 SS Hex Drive Rounded Head Screw 1/4"-20 Thread Size	$7.06	1	$7.06		Electronics
McMaster Carr	Extreme-Strength Steel Hex Nut Grade 9	$11.46	1	$11.46		Electronics

Figure 142: Categorized Purchases

Company	Item	Part cost	Quantity	Total Cost	Order cost	Category
McMaster Carr	Button/Coin Cell Battery Alkaline, Size LR44	$1.44	1	$1.44		Electronics
McMaster Carr	Button/Coin Cell Battery Lithium, Size CR2032	$1.92	2	$3.84		Electronics
McMaster Carr	TICN-Coated Carbide End Mill Two Flute	$14.17	2	$28.34		Electronics
McMaster Carr	J-B Weld Adhesive 8265-S, 2 Ounce Tube	$6.17	1	$6.17		Electronics
McMaster Carr	Sanding Sheet for Alum, Soft Metal, & Nonmetal Waterproof, 600 Grit	$16.82	1	$16.82		Electronics
McMaster Carr	Sanding Sheet for Alum, Soft Metal, & Nonmetal Waterproof, 1000 Grit	$15.87	1	$15.87		Electronics
McMaster Carr	Plastic Syringe with Taper Tip, 4.7 oz Capacity	$12.50	1	$12.50		Electronics
McMaster Carr	Grade 8 Steel Washer Black Ultra-Corrosion-Rst,	$7.47	1	$7.47	$110.97	Electronics
McMaster Carr	18-8 SS Hex Drive Rounded Head Screw 1/4"-20 Thread Size, 3/4" Long, Packs of 50	$7.06	1	$7.06		Electronics
McMaster Carr	Extreme-Strength Steel Hex Nut Grade 9, Cadmium Ylw-Chromate Pltd, 1/4"-20 Thrd Sz, Packs of 50	$11.46	1	$11.46		Electronics
McMaster Carr	Button/Coin Cell Battery Alkaline, Size LR44	$1.44	1	$1.44		Electronics
McMaster Carr	Button/Coin Cell Battery Lithium, Size CR2032	$1.92	2	$3.84		Electronics
McMaster Carr	TICN-Coated Carbide End Mill Two Flute, 1/8" Mill Dia, 1/8" Shank Dia	$14.17	2	$28.34		Electronics
McMaster Carr	J-B Weld Adhesive 8265-S, 2 Ounce Tube	$6.17	1	$6.17		Electronics
McMaster Carr	Sanding Sheet for Alum, Soft Metal, & Nonmetal Waterproof, 600 Grit, 4-1/2" X 11", Packs of 25	$16.82	1	$16.82		Electronics
McMaster Carr	Sanding Sheet for Alum, Soft Metal, & Nonmetal Waterproof, 1000 Grit, 4-1/2" X 11", Packs of 25	$15.87	1	$15.87		Electronics

Figure 143: Categorized Purchases

Company	Item	Part cost	Quantity	Total Cost	Order cost	Category
McMaster Carr	PVC Tubing for Chemicals, 1/4" ID, 3/8" OD, 25 ft. Length	$8.50	1	$8.50		Electronics
McMaster Carr	Plastic Syringe with Taper Tip, 4.7 oz Capacity	$12.50	1	$12.50	$112.00	Electronics
McMaster Carr	Nut for 1/4" Tube OD Type 316 Stainless Steel Yor-Lok Tube Fitting	$2.42	10	$24.20		Electronics
McMaster Carr	Front & Back Sleeve for 1/4" Tube OD Type 316 Stainless Steel Yor-Lok Tube Fitting	$3.53	10	$35.30		Electronics
McMaster Carr	Steel Yor-Lok Tube Fitting Straight Adapter for 1/4" Tube OD X 1/8 NPT Female	$6.37	2	$12.74	$72.24	Electronics
McMaster Carr	Side-Mount External Retaining Ring (E-Style) Stainless Steel	$4.45	1	$4.45		Tools
McMaster Carr	Chipbreaking Cutoff Blade for Steel, Alum, Brass	$12.96	1	$12.96		Tools
McMaster Carr	Swivel Leveling Mount	$5.95	4	$23.80	$41.21	Tools
MSC Industrial Supply Co	Carbide Tapered End Mill	$63.14	2	$126.28		Electronics
MSC Industrial Supply Co	3/16" Chamfer End Mill, 60 degree	$59.40	1	$59.40	$185.68	Electronics
Mouser	Inrush Current Limiter (NTC Thermistor)	$2.49	3	$7.47		Electronics
Mouser	DC Fan	$9.35	1	$9.35		Electronics
Mouser	100uF Capacitor	$0.55	5	$2.75		Electronics
Mouser	10uF Capacitor	$0.48	5	$2.40		Electronics
Mouser	0.1uF Capacitor	$0.10	5	$0.50		Electronics
Mouser	5V Regulator	$1.49	5	$7.45		Electronics
Mouser	NPN Transistor	$0.13	20	$2.60	$32.52	Electronics
Newegg	SSR/Heatsink Assembly	$18.78	1	$18.78	$18.78	Electronics
Newegg	Digital Thermistor	$26.04	1	$26.04	$26.04	Rocket Fab
Newark	High Current Terminal Block	$5.90	5	$29.50	$29.50	Electronics
Lowes	2 x 4 x 8 Laboratory Supplies	$2.64	8	$21.12		Rocket Fab
Lowes	Top Choice 1/2-in Common Birch/Blondewood Plywood	$34.27	4	$137.08		Rocket Fab
Lowes	The Hillman Group 100-Count Wood Screws	$14.99	1	$14.99		Rocket Fab

Figure 144: Categorized Purchases

Company	Item	Part cost	Quantity	Total Cost	Order cost	Category
Digikey	Fans	$9.36	3	$28.08	$28.08	Rocket Fab
Digikey	12V 36W AC/DC External Wall Mount Adapter Fixed Blade Input	$20.27	1	$20.27	$20.27	Electronics
Digikey	TO-220 Heat sink	$0.21	10	$2.10		Electronics
Digikey	4 pin Connector PCB (Female)	$1.23	5	$6.15		Electronics
Digikey	4 pin Connector PCB (Male)	$1.05	10	$10.50		Electronics
Digikey	Shottkey Diode	$1.38	10	$13.80	$32.55	Electronics
Digikey	IC OPAMP INSTR 800KHZ 8DIP	$15.44	5	$77.20		Rocket Fab
Digikey	IC OPAMP GP 14KHZ RRO 8DIP	$0.80	10	$8.00		Rocket Fab
Digikey	IC REG LDO 5V 1.5A TO220-3	$1.45	10	$14.46		Rocket Fab
Digikey	IC REG LDO 1.8V 0.5A TO220-3	$1.16	8	$9.28		Rocket Fab
Digikey	IC OPAMP INSTR 800KHZ RRO 8DIP	$7.47	3	$22.41		Rocket Fab
Digikey	RES KIT 10K-97.6K 1/4W 480PCS	$29.95	1	$29.95		Rocket Fab
Digikey	CAP CER 10000PF 100V NP0 RADIAL	$3.64	6	$21.84		Rocket Fab
Digikey	POT 10K OHM 0.15W CARBON LINEAR	$1.55	3	$4.65		Rocket Fab
Digikey	POT 1K OHM 0.15W CARBON LINEAR	$1.55	3	$4.65	$192.44	Rocket Fab
Fibre Glast	3K, 2 x 2 Twill Weave Carbon Fiber Fabric, 60" Wide, 5 Yard Roll	$299.95	1	$299.95		Rocket Fab
Fibre Glast	System 2000 Epoxy Resin - Gallon (8lbs)	$104.95	1	$104.95		Rocket Fab
Fibre Glast	Epoxy Hardener 60 Minute Pot Life - Quart	$44.95	1	$44.95		Rocket Fab
Fibre Glast	Gray Sealant Tape - Single Roll	$10.95	4	$43.80		Rocket Fab
Fibre Glast	5 yd. Low Temperature Release Film - Perforated, 60" Wide Sheet	$29.95	1	$29.95		Rocket Fab
Fibre Glast	5 yd. Low Temperature Release Film - Non-Perforated, 60" Wide Sheet	$14.95	1	$14.95		Rocket Fab
Fibre Glast	1" Flash Tape	$29.95	1	$29.95		Rocket Fab
Fibre Glast	6 lb Polyurethene Mix and Pour Foam	$34.95	1	$34.95		Rocket Fab
Fibre Glast	Shipping	$79.90	1	$79.90	$683.35	Rocket Fab
AMETEK	Brush DC Motor	$375.67	1	$375.67		FRAME
AMETEK	Shipping	$27.35	1	$27.35	$403.02	FRAME

Figure 145: Categorized Purchases

Company	Item	Part cost	Quantity	Total Cost	Order cost	Category
A-L Compressed Gases	Cylinder of compressed air	$15.00	1	$15.00	$15.00	Rocket Fab
Drop Zone Extreme Sports	Air Tank	$69.95	1	$69.95		Misc
Drop Zone Extreme Sports	Shipping	$19.54	1	$19.54	$89.49	Misc
All-battery.com	Tenergy TLP-2000 Smart Charger for Li-Ion/LiPo Battery Packs: 3.7V - 14.8V	$14.99	1	$14.99		Electronics
All-battery.com	Tenergy Li-Ion 14.8V 2200mAh Rechargeable Battery Pack w/ PCB (4S1P, 32.56Wh, 4A Rate)	$28.40	3	$85.20		Electronics
All-battery.com	Shipping	$14.97	1	$14.97	$115.16	Electronics
Featherwieght Altimeters	Screw Switch	$5.00	3	$15.00		Electronics
Featherwieght Altimeters	Shipping	$10.00	1	$10.00	$25.00	Electronics
Technical Training Aids	Black Build Material	$130.00	3	$390.00		Tools
Technical Training Aids	Shipping	$11.70	1	$11.70	$401.70	Tools
Enterprise	Vans	$170.38	2	$340.76	$340.76	Travel
McMaster Carr	Spring-Loaded Ball Fastener	$1.12	40	$44.80		FRAME
McMaster Carr	1/4" Stainless Steel Washer 100pk	$3.37	1	$3.37	$48.17	FRAME
RiteAid	Soft Drinks & Water	$16.27	1	$16.27	$16.27	Travel

Figure 146: Categorized Purchases

VADL organizes all orders through the budget officer and one mentor to ensure that all items are ordered promptly and the budget remain accurate and up to date. As discussed in **??**, the budget has been modified according to the spending trends throughout subscale launch. Figure 147 shows the new breakdown of this year's budget by category.

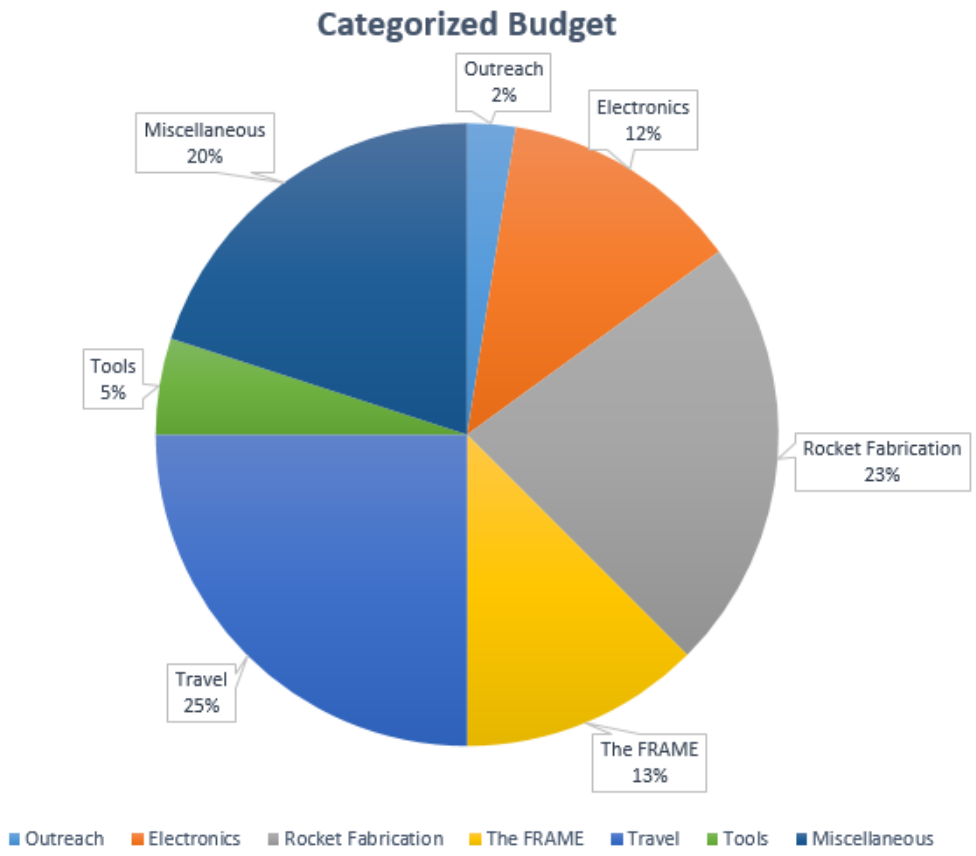

Figure 147: Budget by Category

The largest items in the budget are travel and housing for the competition launch, rocket fabrication, and miscellaneous expenses that may come up during the year. Examples of miscellaneous spending include launchpad materials, a new air filtration unit for the lab, and air tanks. The large allocation for miscellaneous expenses also mediates the risk of unexpected events that may require large purchases. So far, about $1200 has been spent on electronics, $3400 on rocket fabrication supplies, $1600 on the ground-based test facility, $360 on travel, $570 on tools, and $180 on miscellaneous purchases. Figure 148 shows the team's current status.

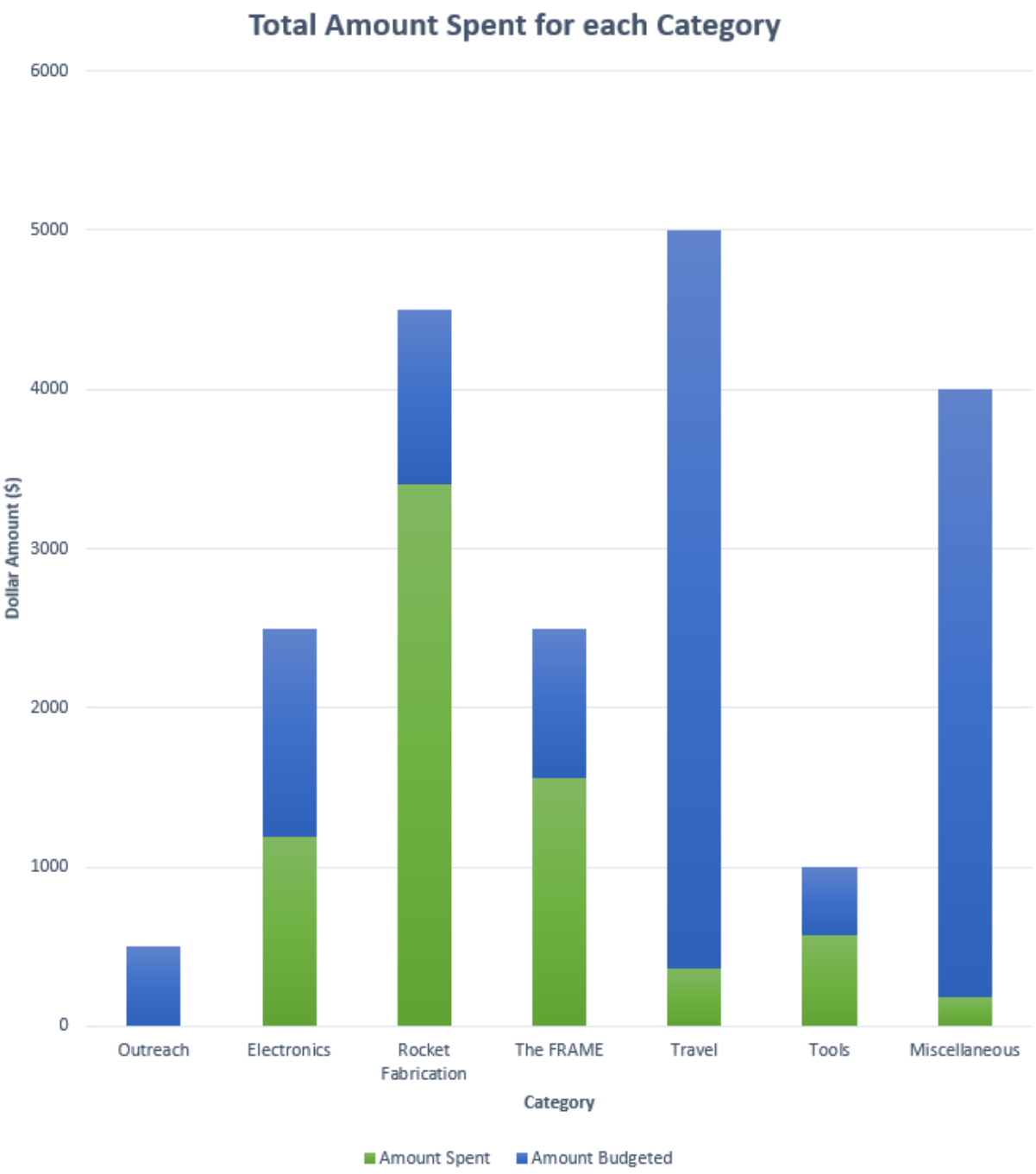

Figure 148: Budget and Present Expenditures

The team tries to be as material efficient as possible and always considers cost in the decision making process. The budget officer will continue to create budget projections and monitor the team's spending as the year progresses.

7.4 Timeline of Operations

A Gantt Chart (Figures 149, 150, 151, 152, and 153) was used to illustrate the team's timeline. A text version is shown following the visual representation. Since PDR, we have added a full scale flight window and outreach events,

and have refined various event dates.

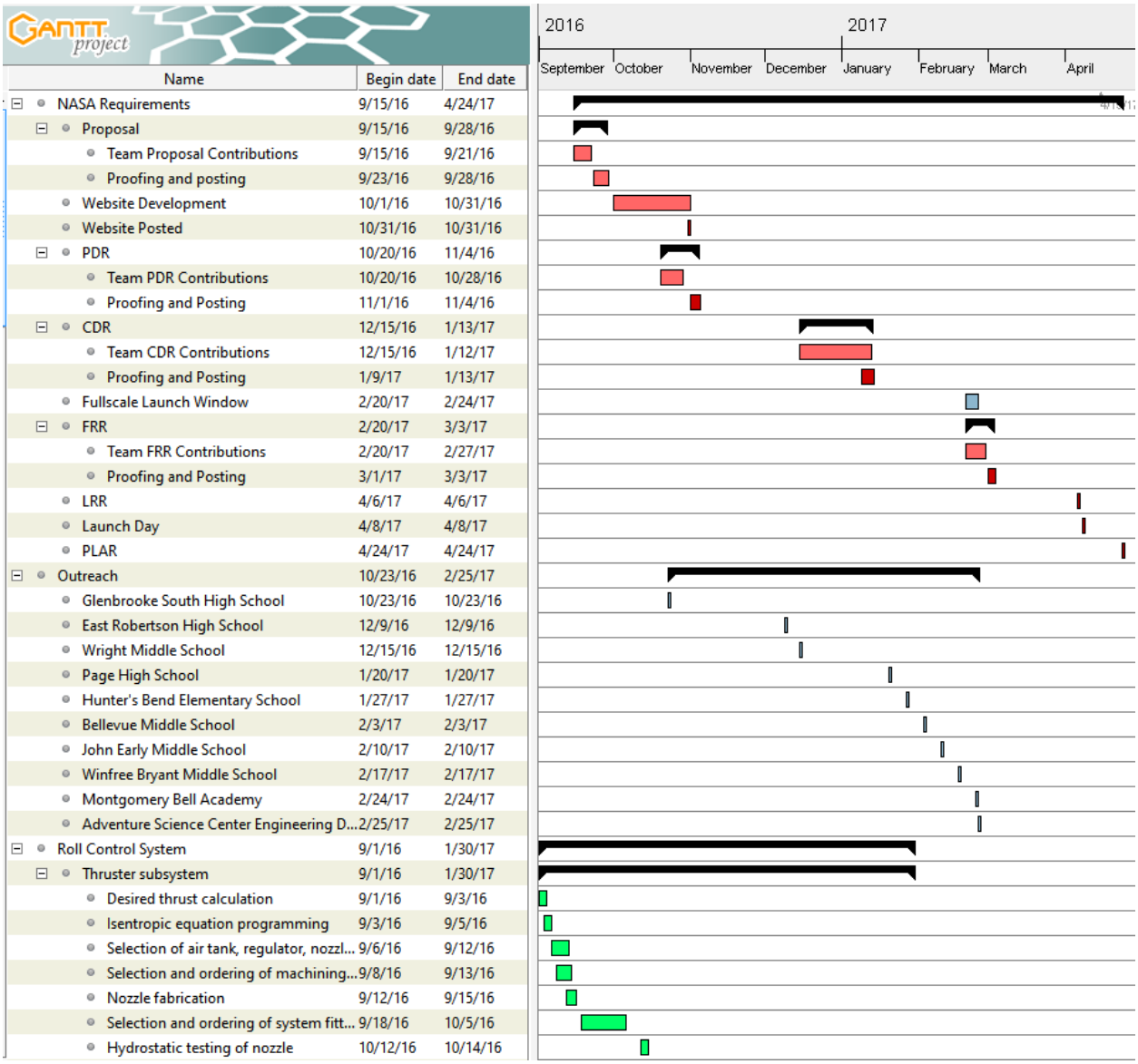

Name	Begin date	End date
NASA Requirements	9/15/16	4/24/17
Proposal	9/15/16	9/28/16
Team Proposal Contributions	9/15/16	9/21/16
Proofing and posting	9/23/16	9/28/16
Website Development	10/1/16	10/31/16
Website Posted	10/31/16	10/31/16
PDR	10/20/16	11/4/16
Team PDR Contributions	10/20/16	10/28/16
Proofing and Posting	11/1/16	11/4/16
CDR	12/15/16	1/13/17
Team CDR Contributions	12/15/16	1/12/17
Proofing and Posting	1/9/17	1/13/17
Fullscale Launch Window	2/20/17	2/24/17
FRR	2/20/17	3/3/17
Team FRR Contributions	2/20/17	2/27/17
Proofing and Posting	3/1/17	3/3/17
LRR	4/6/17	4/6/17
Launch Day	4/8/17	4/8/17
PLAR	4/24/17	4/24/17
Outreach	10/23/16	2/25/17
Glenbrooke South High School	10/23/16	10/23/16
East Robertson High School	12/9/16	12/9/16
Wright Middle School	12/15/16	12/15/16
Page High School	1/20/17	1/20/17
Hunter's Bend Elementary School	1/27/17	1/27/17
Bellevue Middle School	2/3/17	2/3/17
John Early Middle School	2/10/17	2/10/17
Winfree Bryant Middle School	2/17/17	2/17/17
Montgomery Bell Academy	2/24/17	2/24/17
Adventure Science Center Engineering D...	2/25/17	2/25/17
Roll Control System	9/1/16	1/30/17
Thruster subsystem	9/1/16	1/30/17
Desired thrust calculation	9/1/16	9/3/16
Isentropic equation programming	9/3/16	9/5/16
Selection of air tank, regulator, nozzl...	9/6/16	9/12/16
Selection and ordering of machining...	9/8/16	9/13/16
Nozzle fabrication	9/12/16	9/15/16
Selection and ordering of system fitt...	9/18/16	10/5/16
Hydrostatic testing of nozzle	10/12/16	10/14/16

Figure 149: Gantt Chart, part 1.

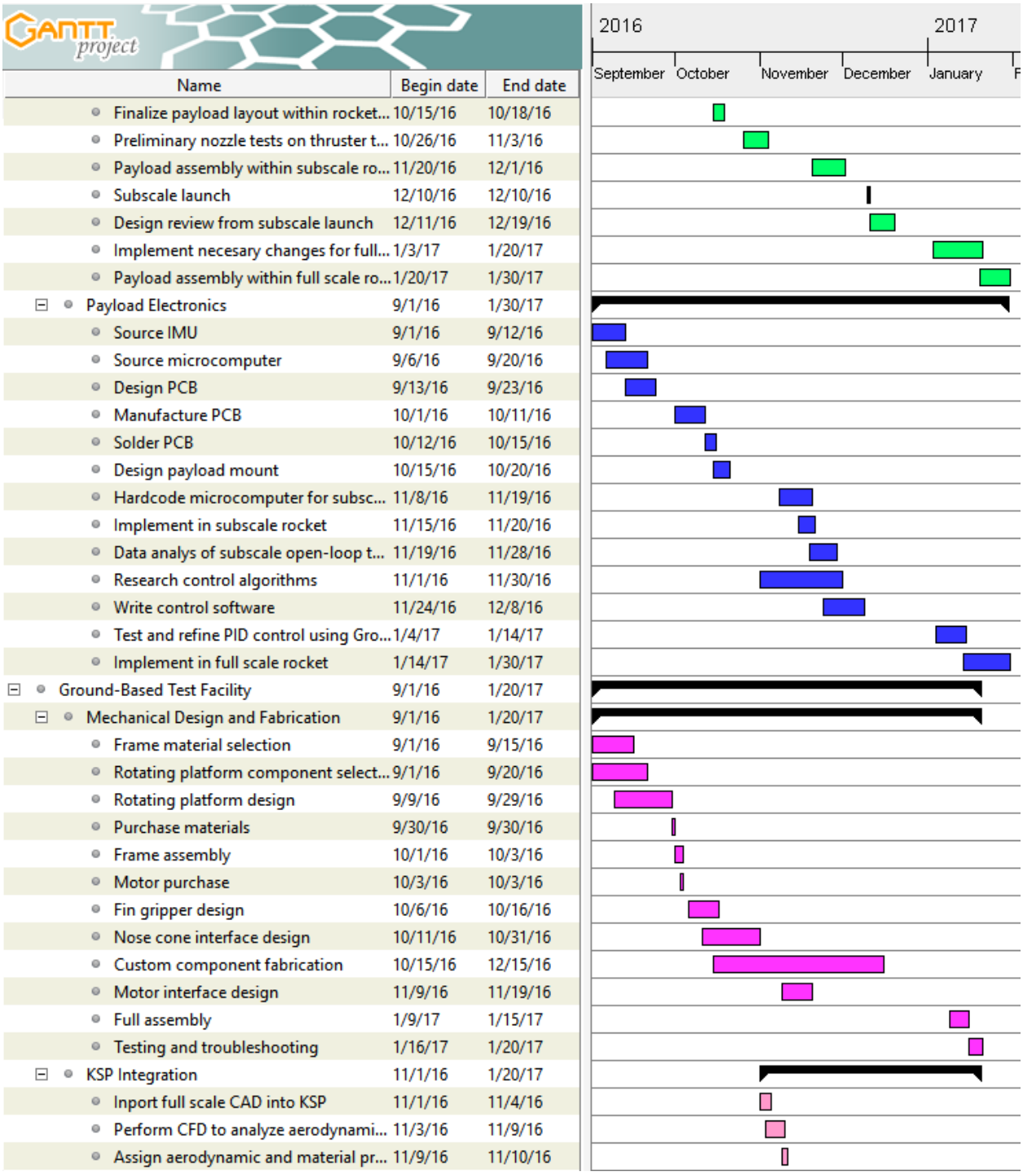

Name	Begin date	End date
Finalize payload layout within rocket...	10/15/16	10/18/16
Preliminary nozzle tests on thruster t...	10/26/16	11/3/16
Payload assembly within subscale ro...	11/20/16	12/1/16
Subscale launch	12/10/16	12/10/16
Design review from subscale launch	12/11/16	12/19/16
Implement necesary changes for full...	1/3/17	1/20/17
Payload assembly within full scale ro...	1/20/17	1/30/17
Payload Electronics	9/1/16	1/30/17
Source IMU	9/1/16	9/12/16
Source microcomputer	9/6/16	9/20/16
Design PCB	9/13/16	9/23/16
Manufacture PCB	10/1/16	10/11/16
Solder PCB	10/12/16	10/15/16
Design payload mount	10/15/16	10/20/16
Hardcode microcomputer for subsc...	11/8/16	11/19/16
Implement in subscale rocket	11/15/16	11/20/16
Data analys of subscale open-loop t...	11/19/16	11/28/16
Research control algorithms	11/1/16	11/30/16
Write control software	11/24/16	12/8/16
Test and refine PID control using Gro...	1/4/17	1/14/17
Implement in full scale rocket	1/14/17	1/30/17
Ground-Based Test Facility	9/1/16	1/20/17
Mechanical Design and Fabrication	9/1/16	1/20/17
Frame material selection	9/1/16	9/15/16
Rotating platform component select...	9/1/16	9/20/16
Rotating platform design	9/9/16	9/29/16
Purchase materials	9/30/16	9/30/16
Frame assembly	10/1/16	10/3/16
Motor purchase	10/3/16	10/3/16
Fin gripper design	10/6/16	10/16/16
Nose cone interface design	10/11/16	10/31/16
Custom component fabrication	10/15/16	12/15/16
Motor interface design	11/9/16	11/19/16
Full assembly	1/9/17	1/15/17
Testing and troubleshooting	1/16/17	1/20/17
KSP Integration	11/1/16	1/20/17
Inport full scale CAD into KSP	11/1/16	11/4/16
Perform CFD to analyze aerodynami...	11/3/16	11/9/16
Assign aerodynamic and material pr...	11/9/16	11/10/16

Figure 150: Gantt Chart, part 2.

Name	Begin date	End date
Write ROSMOD control software for ...	11/7/16	11/17/16
Interface with motor and rocket IMU	1/10/17	1/10/17
Troubleshoot	1/11/17	1/20/17
Perform RCS testing	11/1/16	11/1/16
Launch Vehicle	9/1/16	1/30/17
Fins	9/1/16	1/30/17
Examine legacy fin designs	9/1/16	9/7/16
Research fin designs	9/1/16	9/10/16
Determine fin number and geometry	9/11/16	9/16/16
Calculate center of pressure	9/18/16	9/18/16
Verify center of pressure with CFD a...	9/20/16	9/25/16
Calculate stability margin	9/25/16	9/25/16
Order fin material	9/26/16	9/26/16
Subscale	10/15/16	11/24/16
Cut fins	10/15/16	10/17/16
Attach to motor tube using jig, e...	10/18/16	10/28/16
Fins, motor tube, and tail section...	11/4/16	11/24/16
Full scale	1/6/17	1/30/17
Cut fins	1/6/17	1/8/17
Attach to motor tube using jig, e...	1/9/17	1/15/17
Fins, motor tube, and tail section...	1/25/17	1/30/17
Nose Cone	9/1/16	1/18/17
Examine legacy nose cones	9/1/16	9/8/16
Research nose cone geometries	9/5/16	9/15/16
Determine nose cone geometry	9/11/16	9/15/16
Purchase nose cone	9/19/16	9/19/16
Implement nose cone in subscale	11/12/16	11/12/16
Implement nose cone in full scale	1/18/17	1/18/17
Tail Cone	9/1/16	1/21/17
Examine legacy tail cone	9/1/16	9/11/16
Subscale	11/1/16	11/26/16
Create mold	11/1/16	11/5/16
Carbon fiber layup on mold	11/6/16	11/8/16
Cure layup in Hotbox	11/9/16	11/11/16
Assemble with subscale	11/14/16	11/26/16
Full Scale	12/15/16	1/21/17
Design review of subscale tail co...	12/15/16	12/23/16
Create mold	1/10/17	1/12/17
Carbon fiber layup on mold	1/13/17	1/14/17

Figure 151: Gantt Chart, part 3.

Name	Begin date	End date
Cure layup in Hotbox	1/15/17	1/16/17
Assemble with full scale	1/20/17	1/21/17
Airframe	9/1/16	1/20/17
Examine legacy airframe	9/1/16	9/9/16
Research airframe materials	9/12/16	10/12/16
Determine subscale airframe geome...	10/12/16	10/18/16
Subscale	10/19/16	11/18/16
Purchase blue tube	10/19/16	10/19/16
Purchase carbon fiber	10/19/16	10/19/16
Prepare blue tube for epoxy	11/4/16	11/6/16
Carbon fiber layup on blue tube ...	11/7/16	11/9/16
Cure top section in Hotbox	11/10/16	11/11/16
Carbon fiber layup on blue tube ...	11/10/16	11/11/16
Assemble subscale airframe	11/12/16	11/18/16
Full scale	1/7/17	1/20/17
Purchase blue tube	1/7/17	1/7/17
Purchase carbon fiber	1/7/17	1/7/17
Prepare blue tube for epoxy	1/15/17	1/17/17
Carbon fiber layup on blue tube ...	1/17/17	1/19/17
Cure top section in Hotbox	1/19/17	1/20/17
Carbon fiber layup on blue tube ...	1/17/17	1/20/17
Cure mid section in Hotbox	1/19/17	1/20/17
Carbon fiber layup on blue tube ...	1/16/17	1/18/17
Cure tail section in Hotbox	1/18/17	1/19/17
Hotbox	10/1/16	11/3/16
Design structure	10/1/16	10/10/16
Order structural components	10/5/16	10/5/16
Fabricate structure	10/12/16	10/18/16
PCB design	10/14/16	10/19/16
Order PCB components	10/19/16	10/19/16
PCB fabrication	10/20/16	10/25/16
PCB soldering	10/25/16	10/27/16
High power wiring	10/27/16	10/28/16
Electronics assembly	10/28/16	10/29/16
Write control software	10/25/16	10/31/16
Test control software	11/1/16	11/3/16
Avionics	10/1/16	1/18/17
Examine legacy avionics bay	10/1/16	10/8/16
Research new components	10/9/16	10/16/16

Figure 152: Gantt Chart, part 4.

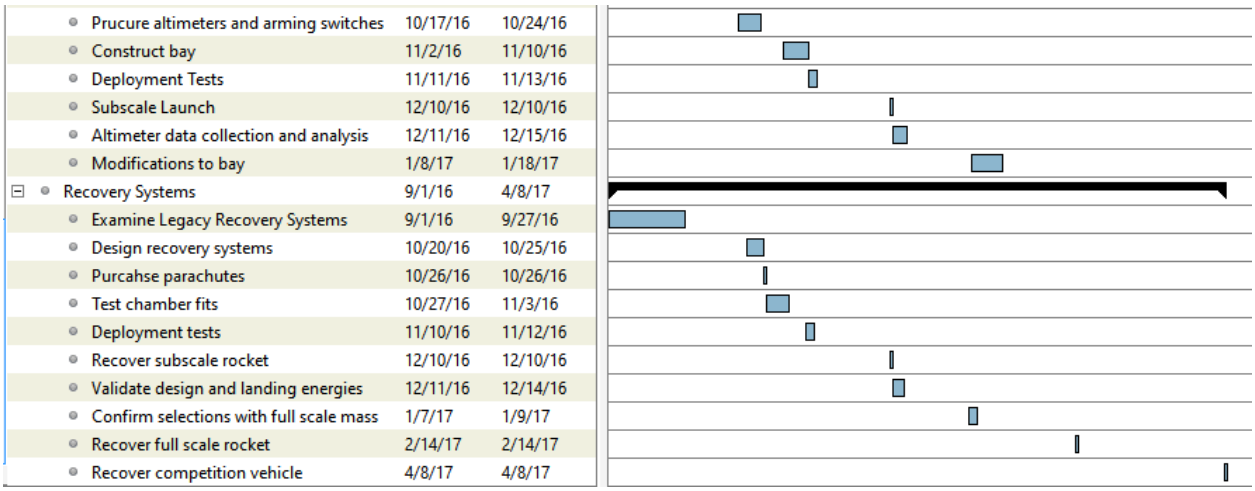

Prucure altimeters and arming switches	10/17/16	10/24/16
Construct bay	11/2/16	11/10/16
Deployment Tests	11/11/16	11/13/16
Subscale Launch	12/10/16	12/10/16
Altimeter data collection and analysis	12/11/16	12/15/16
Modifications to bay	1/8/17	1/18/17
Recovery Systems	9/1/16	4/8/17
Examine Legacy Recovery Systems	9/1/16	9/27/16
Design recovery systems	10/20/16	10/25/16
Purcahse parachutes	10/26/16	10/26/16
Test chamber fits	10/27/16	11/3/16
Deployment tests	11/10/16	11/12/16
Recover subscale rocket	12/10/16	12/10/16
Validate design and landing energies	12/11/16	12/14/16
Confirm selections with full scale mass	1/7/17	1/9/17
Recover full scale rocket	2/14/17	2/14/17
Recover competition vehicle	4/8/17	4/8/17

Figure 153: Gantt Chart, part 5.

Tasks

Name	Begin date	End date
NASA Requirements	9/15/16	4/24/17
Proposal	9/15/16	9/28/16
Team Proposal Contributions	9/15/16	9/21/16
Proofing and posting	9/23/16	9/28/16
Website Development	10/1/16	10/31/16
Website Posted	10/31/16	10/31/16
PDR	10/20/16	11/4/16
Team PDR Contributions	10/20/16	10/28/16
Proofing and Posting	11/1/16	11/4/16
CDR	12/15/16	1/13/17
Team CDR Contributions	12/15/16	1/12/17
Proofing and Posting	1/9/17	1/13/17
Fullscale Launch Window	2/20/17	2/24/17
FRR	2/20/17	3/3/17
Team FRR Contributions	2/20/17	2/27/17
Proofing and Posting	3/1/17	3/3/17
LRR	4/6/17	4/6/17
Launch Day	4/8/17	4/8/17
PLAR	4/24/17	4/24/17
Outreach	10/23/16	2/25/17
Glenbrooke South High School	10/23/16	10/23/16
East Robertson High School	12/9/16	12/9/16
Wright Middle School	12/15/16	12/15/16
Page High School	1/20/17	1/20/17
Hunter's Bend Elementary School	1/27/17	1/27/17
Bellevue Middle School	2/3/17	2/3/17
John Early Middle School	2/10/17	2/10/17
Winfree Bryant Middle School	2/17/17	2/17/17
Montgomery Bell Academy	2/24/17	2/24/17
Adventure Science Center Engineering Day	2/25/17	2/25/17
Roll Control System	9/1/16	1/30/17
Thruster subsystem	9/1/16	1/30/17
Desired thrust calculation	9/1/16	9/3/16
Isentropic equation programming	9/3/16	9/5/16
Selection of air tank, regulator, nozzle size	9/6/16	9/12/16
Selection and ordering of machining tools	9/8/16	9/13/16
Nozzle fabrication	9/12/16	9/15/16
Selection and ordering of system fittings and couplings	9/18/16	10/5/16
Hydrostatic testing of nozzle	10/12/16	10/14/16
Finalize payload layout within rocket envelope	10/15/16	10/18/16
Preliminary nozzle tests on thruster test stand	10/26/16	11/3/16
Payload assembly within subscale rocket	11/20/16	12/1/16

Tasks

Name	Begin date	End date
Subscale launch	12/10/16	12/10/16
Design review from subscale launch	12/11/16	12/19/16
Implement necesary changes for full scale	1/3/17	1/20/17
Payload assembly within full scale rocket	1/20/17	1/30/17
Payload Electronics	9/1/16	1/30/17
Source IMU	9/1/16	9/12/16
Source microcomputer	9/6/16	9/20/16
Design PCB	9/13/16	9/23/16
Manufacture PCB	10/1/16	10/11/16
Solder PCB	10/12/16	10/15/16
Design payload mount	10/15/16	10/20/16
Hardcode microcomputer for subscale data collection	11/8/16	11/19/16
Implement in subscale rocket	11/15/16	11/20/16
Data analys of subscale open-loop thruster actuation	11/19/16	11/28/16
Research control algorithms	11/1/16	11/30/16
Write control software	11/24/16	12/8/16
Test and refine PID control using Ground-Based Test Facility	1/4/17	1/14/17
Implement in full scale rocket	1/14/17	1/30/17
Ground-Based Test Facility	9/1/16	1/20/17
Mechanical Design and Fabrication	9/1/16	1/20/17
Frame material selection	9/1/16	9/15/16
Rotating platform component selection	9/1/16	9/20/16
Rotating platform design	9/9/16	9/29/16
Purchase materials	9/30/16	9/30/16
Frame assembly	10/1/16	10/3/16
Motor purchase	10/3/16	10/3/16
Fin gripper design	10/6/16	10/16/16
Nose cone interface design	10/11/16	10/31/16
Custom component fabrication	10/15/16	12/15/16
Motor interface design	11/9/16	11/19/16
Full assembly	1/9/17	1/15/17
Testing and troubleshooting	1/16/17	1/20/17
KSP Integration	11/1/16	1/20/17
Inport full scale CAD into KSP	11/1/16	11/4/16
Perform CFD to analyze aerodynamic properties	11/3/16	11/9/16
Assign aerodynamic and material properties	11/9/16	11/10/16
Write ROSMOD control software for KSP	11/7/16	11/17/16
Interface with motor and rocket IMU	1/10/17	1/10/17
Troubleshoot	1/11/17	1/20/17
Perform RCS testing	11/1/16	11/1/16
Launch Vehicle	9/1/16	1/30/17
Fins	9/1/16	1/30/17

Tasks

Name	Begin date	End date
Examine legacy fin designs	9/1/16	9/7/16
Research fin designs	9/1/16	9/10/16
Determine fin number and geometry	9/11/16	9/16/16
Calculate center of pressure	9/18/16	9/18/16
Verify center of pressure with CFD analysis	9/20/16	9/25/16
Calculate stability margin	9/25/16	9/25/16
Order fin material	9/26/16	9/26/16
Subscale	10/15/16	11/24/16
Cut fins	10/15/16	10/17/16
Attach to motor tube using jig, epoxy	10/18/16	10/28/16
Fins, motor tube, and tail section assembled	11/4/16	11/24/16
Full scale	1/6/17	1/30/17
Cut fins	1/6/17	1/8/17
Attach to motor tube using jig, epoxy	1/9/17	1/15/17
Fins, motor tube, and tail section assembled	1/25/17	1/30/17
Nose Cone	9/1/16	1/18/17
Examine legacy nose cones	9/1/16	9/8/16
Research nose cone geometries	9/5/16	9/15/16
Determine nose cone geometry	9/11/16	9/15/16
Purchase nose cone	9/19/16	9/19/16
Implement nose cone in subscale	11/12/16	11/12/16
Implement nose cone in full scale	1/18/17	1/18/17
Tail Cone	9/1/16	1/21/17
Examine legacy tail cone	9/1/16	9/11/16
Subscale	11/1/16	11/26/16
Create mold	11/1/16	11/5/16
Carbon fiber layup on mold	11/6/16	11/8/16
Cure layup in Hotbox	11/9/16	11/11/16
Assemble with subscale	11/14/16	11/26/16
Full Scale	12/15/16	1/21/17
Design review of subscale tail cone	12/15/16	12/23/16
Create mold	1/10/17	1/12/17
Carbon fiber layup on mold	1/13/17	1/14/17
Cure layup in Hotbox	1/15/17	1/16/17
Assemble with full scale	1/20/17	1/21/17
Airframe	9/1/16	1/20/17
Examine legacy airframe	9/1/16	9/9/16
Research airframe materials	9/12/16	10/12/16
Determine subscale airframe geometry	10/12/16	10/18/16
Subscale	10/19/16	11/18/16
Purchase blue tube	10/19/16	10/19/16
Purchase carbon fiber	10/19/16	10/19/16
Prepare blue tube for epoxy	11/4/16	11/6/16
Carbon fiber layup on blue tube for top section	11/7/16	11/9/16

Tasks

Name	Begin date	End date
Cure top section in Hotbox	11/10/16	11/11/16
Carbon fiber layup on blue tube for tail section	11/10/16	11/11/16
Assemble subscale airframe	11/12/16	11/18/16
Full scale	1/7/17	1/20/17
Purchase blue tube	1/7/17	1/7/17
Purchase carbon fiber	1/7/17	1/7/17
Prepare blue tube for epoxy	1/15/17	1/17/17
Carbon fiber layup on blue tube for top section	1/17/17	1/19/17
Cure top section in Hotbox	1/19/17	1/20/17
Carbon fiber layup on blue tube for mid section	1/17/17	1/20/17
Cure mid section in Hotbox	1/19/17	1/20/17
Carbon fiber layup on blue tube for tail section	1/16/17	1/18/17
Cure tail section in Hotbox	1/18/17	1/19/17
Hotbox	10/1/16	11/3/16
Design structure	10/1/16	10/10/16
Order structural components	10/5/16	10/5/16
Fabricate structure	10/12/16	10/18/16
PCB design	10/14/16	10/19/16
Order PCB components	10/19/16	10/19/16
PCB fabrication	10/20/16	10/25/16
PCB soldering	10/25/16	10/27/16
High power wiring	10/27/16	10/28/16
Electronics assembly	10/28/16	10/29/16
Write control software	10/25/16	10/31/16
Test control software	11/1/16	11/3/16
Avionics	10/1/16	1/18/17
Examine legacy avionics bay	10/1/16	10/8/16
Research new components	10/9/16	10/16/16
Prucure altimeters and arming switches	10/17/16	10/24/16
Construct bay	11/2/16	11/10/16
Deployment Tests	11/11/16	11/13/16
Subscale Launch	12/10/16	12/10/16
Altimeter data collection and analysis	12/11/16	12/15/16
Modifications to bay	1/8/17	1/18/17
Recovery Systems	9/1/16	4/8/17
Examine Legacy Recovery Systems	9/1/16	9/27/16
Design recovery systems	10/20/16	10/25/16
Purcahse parachutes	10/26/16	10/26/16
Test chamber fits	10/27/16	11/3/16
Deployment tests	11/10/16	11/12/16
Recover subscale rocket	12/10/16	12/10/16
Validate design and landing energies	12/11/16	12/14/16

Tasks

Name	Begin date	End date
Confirm selections with full scale mass	1/7/17	1/9/17
Recover full scale rocket	2/14/17	2/14/17
Recover competition vehicle	4/8/17	4/8/17